

Nonlinear Analysis of Rectangular Concrete-Filled Steel Tubular Columns at Elevated Temperatures

by

Ghanim Mohammed Kamil, MSc



Thesis submitted in fulfilment of the requirement for the degree of

Doctor of Philosophy

College of Engineering and Science, Victoria University, Australia

April 2019

ABSTRACT

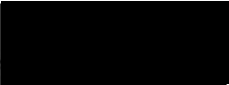
Rectangular thin-walled concrete-filled steel tubular (CFST) slender columns under axial and eccentric loads may undergo local and global interaction buckling when exposed to fire. Computational studies on the fire and post-fire behavior of rectangular short and slender CFST columns including local buckling effects have been extremely limited. This thesis presents new computational models for predicting the responses of rectangular and square CFST short and slender columns under fire exposure and after being exposed to fire. The models incorporate important features, which include local and global interaction buckling, air gap between the steel tube and concrete, concrete moisture content, emissivity of exposure surfaces, initial geometric imperfections, second-order, and material nonlinearities at elevated temperatures.

Computational models are formulated by using the fiber approach for simulating the fire resistance, fire behavior and post-fire performance of rectangular CFST short and slender columns loaded concentrically and eccentrically. The progressive local buckling of steel tube walls at elevated temperatures is included in the formulation by using the local and post-local buckling models proposed. Computer simulation procedures sequentially coupling the nonlinear thermal and stress analyses are developed. The temperature distribution within a CFST column exposed to fire is determined by the thermal analysis. The modeling procedures capture the axial load-strain behavior, axial load-deflection responses, and fire-resistance of loaded CFST columns exposed to fire. Numerical solution algorithms implementing Müller's method are developed to solve the nonlinear equilibrium equations of loaded CFST columns under fire exposure.

The existing experimental and numerical results are utilized to validate the fiber-based computational models, which are employed to study the fire and post-fire responses of CFST short and slender columns with various important parameters. It is shown that the computational models are capable of predicting well the responses of rectangular CFST short and slender columns exposed to fire and after being exposed to fire. The computed results on the fire resistance and fire and post-fire behaviors of CFST rectangular columns with local buckling effects are given in the thesis for the first time. The research findings presented provide a better understanding of the fire and post-fire performance of short and slender CFST columns incorporating local buckling, and are valuable to structural designers and composite code writers.

DECLARATION

I, Ghanim Mohammed Kamil, declare that the PhD thesis by Publication entitled *Nonlinear Analysis of Rectangular Concrete-Filled Steel Tubular Columns at Elevated Temperatures* is no more than 100,000 words in length including quotes and exclusive of tables, figures, appendices, bibliography, references and footnotes. This thesis contains no material that has been submitted previously, in whole or in part, for the award of any other academic degree or diploma. Except where otherwise indicated, this thesis is my own work.

Signature 

Date: 15/04/2019

ACKNOWLEDGEMENTS

First and foremost is the recognition and the gratefulness towards the great right of the Creator, GOD almighty, ALLAH, the most compassionate and the merciful, for his kindness and blessings. His peace and blessings are upon the prophet Mohammed and his infallible family and all the prophets and messengers and their successors, and all the righteous people.

The author would like to express his thanks to his principal supervisor Associate Professor Qing Quan Liang for his dedicated supervision, useful discussions and valuable suggestions throughout the period of the research project. The author would also like to thank his associate supervisor Associate Professor Muhammad N.S. Hadi of the University of Wollongong for his helpful comments.

The author would like to express his sincere gratitude to his great country, Iraq, and to the sincere sacrifices and efforts of the martyrs and the Iraqi people to defend it. The scholarship program of the Ministry of higher education and scientific research in Iraq is greatly appreciated, and the author would also like to thank all staff in the Ministry, the Scholarship department, Thi-Qar University, the College of Engineering and the Iraqi cultural Attaché in Australia for their assistance.

The author would like to thank all staff in the College of Engineering and Science, Victoria University library, the Office for Researcher Training, Quality & Integrity and the international team for their assistance. The author would like to thank his friends and colleagues for their support.

Last, but not least, the author would like to thank deeply and sincerely his family and relatives for being supported and passionate during the whole time.

LIST OF PUBLICATIONS

Based on the research work, the candidate has written the following papers, which have been published or submitted for publication in international journals.

1. **Kamil, G. M.**, Liang, Q. Q. and Hadi, M. N. S. (2018) Local buckling of steel plates in concrete-filled steel tubular columns at elevated temperatures, *Engineering Structures*, 168: 108-118.
2. **Kamil, G. M.**, Liang, Q. Q. and Hadi, M. N. S. (2019) Numerical analysis of axially loaded rectangular concrete-filled steel tubular short columns at elevated temperatures, *Engineering Structures*, 180: 89-102.
3. **Kamil, G. M.**, Liang, Q. Q. and Hadi, M. N. S. (2019) Interaction behavior of local and global buckling of axially loaded rectangular thin-walled concrete-filled steel tubular slender columns under fire exposure, *Thin-Walled Structures* (currently under review).
4. **Kamil, G. M.**, Liang, Q. Q. and Hadi, M. N. S. (2019) Fire-Resistance of Eccentrically Loaded Rectangular Concrete-Filled Steel Tubular Slender Columns Incorporating Interaction of Local and Global Buckling, *International Journal of Structural Stability and Dynamics*, 2019; 19(8):1950085.
5. **Kamil, G. M.**, Liang, Q. Q. and Hadi, M. N. S. (2019) Nonlinear post-fire simulation of concentrically loaded rectangular thin-walled concrete-filled steel tubular short columns accounting for progressive local buckling, *Thin-Walled Structures* (currently under review).

PART A:
DETAILS OF INCLUDED PAPERS: THESIS BY PUBLICATION

Please list details of each Paper included in the thesis submission. Copies of published Papers and submitted and/or final draft Paper manuscripts should also be included in the thesis submission.

Item/ Chapter No.	Paper Title	Publication Status (e.g. published, accepted for publication, to be revised and resubmitted, currently under review, unsubmitted but proposed to be submitted)	Publication Title and Details (e.g. date published, impact factor etc.)
3	Local buckling of steel plates in concrete-filled steel tubular columns at elevated temperatures.	Published	<i>Engineering Structures</i> , 2018; 168: 108-118. SCImago Journal Rank: Q1(1.690) Impact Factor: 2.755 (Year of 2017)
4	Numerical analysis of axially loaded rectangular concrete-filled steel tubular short columns at elevated temperatures.	Published	<i>Engineering Structures</i> , 2019; 180: 89-102. SCImago Journal Rank: Q1(1.690) Impact Factor: 2.755 (Year of 2017)
5	Interaction behavior of local and global buckling of axially loaded rectangular thin-walled concrete-filled steel tubular slender columns under fire exposure.	Currently under review	<i>Thin-Walled Structures</i> , 2019. SCImago Journal Rank: Q1(1.672) Impact Factor: 2.881 (Year of 2017)

	Fire-Resistance of Eccentrically Loaded Rectangular Concrete-Filled Steel Tubular Slender Columns Incorporating Interaction of Local and Global Buckling.	Accepted	<i>International Journal of Structural Stability and Dynamics</i> , 2019. SCImago Journal Rank: Q1 (1.005) Impact Factor: 2.082 (Year of 2017)
6	Nonlinear post-fire simulation of concentrically loaded rectangular thin-walled concrete-filled steel tubular short columns accounting for progressive local buckling.	Currently under review	<i>Thin-Walled Structures</i> , 2019. SCImago Journal Rank: Q1(1.672) Impact Factor: : 2.881 (Year of 2017)

Declaration by [candidate name]:

Signature:

Date:

Ghanim Mohammed Kamil



15/04/2019

CONTENTS

	Page No.
Title	i
Abstract	ii
Declaration	iv
Acknowledgements	v
List of Publications	vi
Details of Included Papers: Thesis by Publication	vii
Contents	ix
Chapter 1 Introduction	1
1.1 Concrete-Filled Steel Tubular Columns	1
1.2 Significance of Research	5
1.3 Aims of This Research Project	6
1.4 Layout of This Thesis	8
Chapter 2 Literature Review	11
2.1 Introduction	11
2.2 Local and Post-Local Buckling of Steel Plates	12
2.2.1 Thin Steel Plates at Ambient Temperature	12

2.2.2 Thin Steel Plates at Elevated Temperatures	15
2.3 CFST Columns at Ambient Temperatures	18
2.3.1 Experimental Works on CFST Columns	18
2.3.2 Nonlinear Analysis of CFST Columns	23
2.4 CFST Columns at Elevated Temperatures	29
2.4.1 Standard Fire Tests on CFST Columns	29
2.4.2 Nonlinear Analysis and Design of CFST Columns Exposed to Fire	35
2.5 Post-Fire Behavior of CFST Columns	45
2.5.1 Post-Fire Tests on CFST column	45
2.5.2 Post-Fire Response Simulations	48
2.6 Concluding Remarks	52
Chapter 3 Local and Post-Local Buckling of Steel Plates at Elevated	
Temperatures	53
3.1 Introduction	53
3.2 Declarations	55
3.3 Local Buckling of Steel Plates in Concrete-Filled Steel Tubular Columns at	
Elevated Temperatures	57
3.4 Concluding Remarks	68
Chapter 4 CFST Short Columns at Elevated Temperatures	69

4.1 Introduction	69
4.2 Declarations	71
4.3 Numerical Analysis of Axially Loaded Rectangular Concrete-Filled Steel Tubular Short Columns at Elevated Temperatures	73
4.4 Concluding Remarks	87
Chapter 5 CFST Slender Columns under Fire Exposure.....	88
5.1 Introduction	88
5.2 Declarations	90
5.3 Interaction Behavior of Local and Global Buckling of Axially Loaded Rectangular Thin-Walled Concrete-Filled Steel Tubular Slender Columns under Fire Exposure.....	94
5.4 Fire-Resistance of Eccentrically Loaded Rectangular Concrete-Filled Steel Tubular Slender Columns Incorporating Interaction of Local and Global Buckling.....	143
5.4 Concluding Remarks	183
Chapter 6 Performance of CFST Columns after Being Exposed to Fire	184
6.1 Introduction	184
6.2 Declarations	186
6.3 Nonlinear Post-Fire Simulation of Concentrically Loaded Rectangular Thin-Walled Concrete-Filled Steel Tubular Short Columns Accounting for Progressive Local Buckling... ..	188

6.4 Concluding Remarks	226
Chapter 7 Conclusions	227
7.1 Summary.....	227
7.2 Achievements	229
7.3 Further Research.....	230
References	231

Chapter 1

INTRODUCTION

1.1 CONCRETE-FILLED STEEL TUBULAR COLUMNS

Concrete-filled steel tubular (CFST) columns are constructed by filling concrete into hollow steel tubular columns. The most commonly used CFST columns are illustrated in Figure 1.1, which include circular, rectangular and square cross-sections. The applications of CFST columns in buildings, sport stadia, bridges, industrial buildings and offshore structures have been widespread. In the last two decades, CFST columns were used to construct many high-rise buildings around the world. Some of the practical applications of CFST columns in tall buildings are listed in Table 1.1.

The widespread applications of CFST columns are attributed to their structural and construction advantages over reinforced concrete and steel columns. Filling concrete into a steel tubular hollow rectangular column significantly improves not only the strength and stiffness but also the fire resistance of the steel tubular hollow column. When a rectangular CFST column is compressed, the concrete prevents the inward local-buckling of thin-walled steel tube and forces it buckles locally outward (Liang 2014). This unilateral local buckling mode considerably improves the resistance of the steel tube to local buckling and thereby the ultimate strength of the CFST column (Liang et al. 2007;

Liang 2014). In a rectangular CFST column, the concrete is encased by the steel tube completely, which increases the concrete ductility. Moreover, the steel tube is utilized as the permanent formwork as well as longitudinal steel reinforcement for the concrete. This remarkably reduces not only the material and labor costs and but also the construction time. The thermal conductivity of concrete is low when compared to steel so the concrete infill markedly improves the fire-resistance of the hollow tubular steel column. Owing to their high strength performance, the cross-sections of CFST columns can be reduced to increase the space usage in a composite building. In the composite construction of a tall building, hollow steel tubes and floor systems are usually erected several stories ahead of pumping the wet concrete into the steel tubes at the ground level. This significantly speeds up the construction process and thus reduces the construction time.

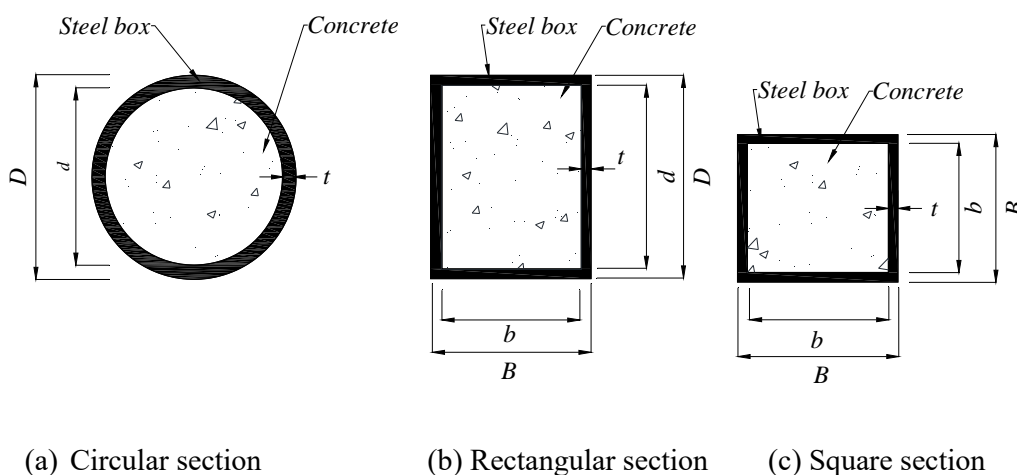


Figure 1.1. Different ordinary shapes of concrete filled steel tubular beam-columns.

Table 1.1. High-rise buildings with CFST columns

Building Name	City	Architectural height (m)	Completion Year
Bank of China Tower	Hong Kong	367	1990
Casselden Place	Melbourne	166	1992
CITIC Plaza	Guangzhou	390	1996
Shun Hing Square	Shenzhen	384	1996
Petronas Twin Tower 1	Kuala Lumpur	452	1998
TAIPEI 101	Taipei	508	2004
Shanghai World Financial Center	Shanghai	492	2008
Bank of America Tower	New York City	366	2009
International Commerce Centre	Hong Kong	484	2010
Guangzhou International Finance Center	Guangzhou	439	2010
Shanghai Tower	Shanghai	632	2015
Guangzhou CTF Finance Centre	Guangzhou	530	2016
Ping An Finance Center	Shenzhen	599	2017
Wilshire Grand Center	Los Angeles	335	2017
Lotte World Tower	Seoul	555	2017
Comcast Technology Center	Philadelphia	342	2018
Merdeka PNB118	Kuala Lumpur	644	2021 (under construction)

The CFST columns of rectangular sections in tall buildings may be subjected to fire effects in their intended design life. Fire is one of the most detrimental risks that threaten the sustainability of CFST columns. The fire generates high temperatures that significantly degrade the material properties of steel and concrete in terms of stiffness and strength and induces nonlinear responses in CFST columns (Wang 2002). Consequently, the fire effects greatly reduce the load-carrying capacities of CFST columns. Thin-walled high-strength steel tubes are increasingly utilized to fabricate CFST columns in order to achieve economical designs. However, this gives rise to the local buckling of steel tubes, which markedly decreases the load-carrying capacities of CFST columns (Liang et al. 2007). Standard fire tests on the responses of CFST columns indicated that square short columns failed by the unilateral local-buckling of steel tubes while slender square and rectangular columns failed by the local-global interaction buckling (Lie and Chabot 1992;

Sakumoto et al. 1994; Han et al. 2003; Lu et al. 2009; Espinos et al. 2015a; Rodrigues and Laim 2017). Test results showed that the local-global interaction buckling remarkably reduced the resistance to fire as well as the strength of CFST slender rectangular columns under fire exposure. It would appear that the influences of local buckling as well as interaction local-global buckling must be incorporated in computational models to accurately predict structural behavior of CFST columns of rectangular sections subjected to fire effects.

After CFST columns were exposed to fire, they were damaged in some degrees by the fire effects but might not collapse. The post-fire repair of fire-damaged CFST columns requires the evaluation of their residual strength and stiffness in order to develop a cost-effective solution. Post-fire tests on the structural behavior of CFST columns demonstrated that short columns failed by the outward local buckling whereas slender columns failed by the local and global interaction buckling (Han et al. 2002, 2003; Han and Huo 2003; Jiang et al. 2020; Rush et al. 2015). Although the residual strengths of CFST columns could be assessed by post-fire tests, the tests are not only highly time-consuming but also expensive. Moreover, it is impossible to conduct the destructive post-fire tests on CFST columns in real buildings to ascertain their residual stiffness and strength. Therefore, nonlinear post-fire computer models including local buckling need to be developed to ascertain the post-fire responses of loaded CFST rectangular columns.

1.2 SIGNIFICANCE OF RESEARCH PROJECT

Rectangular CFST columns including square ones are efficient and important structural members, which have been frequently incorporated in frame systems in tall buildings to transfer loads from upper floor systems to the foundations. This is owing to not only their high strength, ductility and fire resistance performance but also their aesthetic appearance and ease of connection with steel beams. Although a number of mathematical models have been developed for the predictions of the fire and post-fire behaviors of CFST columns, the effects of important features, such as local buckling, interaction local-global buckling, air gap at the steel-concrete interface, concrete tensile behavior and deformations induced by preloads, have not been taken into consideration in these existing models (Lie and Irwin 1995; Han et al. 2002; Han and Huo 2003; Yang et al. 2008; Yin et al. 2006; Chung et al. 2008; Schaumann et al. 2009; Ibanez et al. 2013). There are lacks of accurate and efficient computational models using the approach of fiber element analysis for the simulations of the fire and post-fire responses of CFST rectangular columns loaded concentrically and eccentrically including local buckling effects. These have hindered the development of economical and safe composite buildings and infrastructure. These lacks have become much more important due to the climate changes, which demand low costs, lightweight, high performance and sustainable construction of composite buildings. Therefore, there is an urgent need for developing computationally efficient and accurate mathematical models, which can predict the fire and post-fire behavior of CFST columns of rectangular sections.

The interaction local-global buckling response of CFST slender rectangular columns under fire exposure and after being exposed to fire is highly complicated and is a challenging problem in structural mechanics. This research project develops

mathematical models based on the method of fiber analysis, which can accurately predict the fire and post-fire responses of CFST columns of rectangular sections incorporating local-global interaction buckling. The important features, which have not been taken into account in other existing theoretical models, are also taken into account in the formulations. The anticipated outcomes of the project will significantly advance the present state of knowledge and lead to accurate and robust computer simulation technologies, which will be widely used by international researchers, practicing engineers and code writers. The industry and communities can be benefited by employing advanced technologies developed to design more economical, safe and sustainable composite buildings and infrastructure and to evaluate the residual strength and stiffness of CFST columns after fire exposure.

1.3 AIMS OF THE RESEARCH PROJECT

This research mainly aims at developing accurate and efficient computational models that can simulate the fire responses of rectangular CFST short and slender columns at high temperatures and the post-fire residual strengths of CFST columns after fire exposure. The computational models consider the influences of local buckling, interaction local-global buckling, air gap at the steel-concrete interface, tensile concrete behavior and deformations induced by preloads. The computer software ANSYS is utilized to simulate the nonlinear behavior of local and post-local buckling in steel plates of rectangular CFST columns exposed to fire. Expressions for calculating the critical local-buckling stresses in addition to the strengths of post-local buckling of steel plates subjected to high temperatures are developed and implemented in the mathematical models to consider

local buckling influences on the fire and post-fire behavior of CFST columns. The available test results as well as numerical solutions are employed to verify the numerical models. The verified mathematical models are utilized to demonstrate the significance of important parameters on the fire and post-fire responses of CFST columns.

Specific aims are to:

- Develop design equations for quantifying the critical stresses at the onset of local-buckling in addition to the post-local buckling strengths of steel plates in CFST rectangular columns exposed to fire.
- Develop a computational model that can compute the fire resistance of short CFST columns loaded axially exposed to high temperatures.
- Develop a computational model for fire-response nonlinear analysis of slender CFST columns loaded concentrically exposed to high temperatures.
- Develop a mathematical modeling technique for quantifying the fire responses of eccentrically loaded CFST slender columns exposed to fire loads.
- Develop a computer model for predicting the post-fire behavior of CFST shot columns after being exposed to high temperatures generated by fire.
- Verify the computational models developed by existing experimental and numerical results.
- Use computer models developed to demonstrate the significance of geometric and material parameters on the fire and post-fire performance of CFST short and slender columns.

1.4 LAYOUT OF THE THESIS

This thesis contains seven chapters. **Chapter 2** provides a literature review on the most relevant studies on the behavior of CFST columns at ambient and high temperatures. Firstly, a review on the publications on the initial local buckling as well as post-local buckling of thin steel plates exposed to ambient and high temperatures is presented. Numerical works in addition to experiments on the structural performance of CFST columns at ambient temperature are then discussed. Extensive reviews are devoted to experimental and computational investigations on CFST columns under fire exposure. Finally, research work on the post-fire structural behavior of CFST columns is highlighted.

Chapter 3 is devoted to the material and geometric nonlinear analysis of steel plate elements subjected to non-uniform stresses in rectangular CFST columns exposed to fire. Finite element models are created using the program ANSYS to determine the critical local buckling in addition to the post-buckling responses of steel plates exposed to high temperatures. The finite element models consider the initial geometric imperfection of plates as well as residual stresses in addition to the temperature-dependent material properties of steel. Formulas are proposed that can be used to quantify the critical local-buckling stresses and the post-local buckling strengths of steel plates subjected to stress gradients and exposed to high temperatures. Effective width expressions that determine the post-local buckling strength of steel plates at different levels of temperatures are also proposed. The equations proposed are verified by means of comparisons with independent solutions. These equations can be implemented in computational techniques

to include local-buckling effects on the structural responses of CFST columns exposed to fire.

In **Chapter 4**, a computational model for thermal and stress nonlinear analysis of concentrically loaded CFST short columns exposed to fire loading considering local buckling is developed. A sequentially coupled analysis procedure is proposed for the thermal and stress analyses. The model uses the method of fiber analysis to discretize the column cross-section. In the thermal analysis, the finite difference approach is utilized to ascertain the temperature distribution in cross-sections. The temperature-dependent stress-strain relations of concrete and steel are employed in the formulation of the computational model. The expressions, which are used to estimate the critical stresses of local-buckling and the strength of post-local buckling of steel plates presented in Chapter 3 are incorporated in the computer modeling procedure to consider their influences on the fire behavior of CFST columns. Parametric studies are carried out by means of employing the computational modeling technique developed to ascertain the influences of important features, such as section geometry, loading ratio in addition to local buckling on the strength and fire resistance of CFST short columns exposed to elevated temperatures.

Chapter 5 describes the computational models developed for the simulations of the fire resistance and behavior of CFST slender columns loaded concentrically and eccentrically considering local-global interaction buckling. The temperature fields in cross-sections are determined by the thermal analysis. The formulation of the computer model accounts for the effects of air gap at the concrete-steel interface, temperature-dependent material behavior, concrete tensile strength, initial geometric imperfection, second order,

deformations caused by preloads, and local-global interaction buckling. The computer procedure is proposed and described, which can calculate the interaction local-global buckling responses and fire resistance of CFST slender columns loaded concentrically and eccentrically under fire exposure. The accuracy of the computational model is established by means of comparisons with experimental results and employed to examine the structural responses of loaded CFST columns to fire loading.

A nonlinear post-fire computational model including local buckling effects for quantifying the residual stiffness and strengths of CFST stub columns loaded concentrically to failure and after being exposed to fire is presented in **Chapter 6**. The mathematical model implements the post-fire material constitutive relations of steel and concrete. The gradual post-local buckling of steel tubes is modeled by using the concept of effective widths. The established experimental data is utilized to validate the nonlinear post-fire computer model. The significance of local buckling, material strengths and width-to-thickness ratio on the post-fire performance of CFST short columns is demonstrated by the post-fire computer simulation technique.

Chapter 7 highlights the most important remarks concluded from the research study. The remarkable achievement are summarized, and the further research studies are recommended.

Chapter 2

LITERATURE REVIEW

2.1 INTRODUCTION

Structural fire engineering research is to quantify the performance of structural systems under fire exposure and has been an important and active research area for a few decades. The research findings are utilized to propose design guides for the structural fire engineering design of structural systems. During fire exposure, structural members and systems experience ambient temperature, heating by fire, cooling and post-fire. The heating and cooling process significantly alters material properties and induces nonlinear responses in structural members. The behavior of structural members at different temperatures during fire exposure is significantly different and can be evaluated by both experimental and numerical methods. This thesis focuses on numerical studies on the fire and post-fire responses of thin-walled rectangular concrete-filled steel tubular (CFST) columns where thin-walled steel tubes buckle locally outward.

This chapter presents a literature review on structural and structural fire engineering research studies on CFST columns. Although this thesis focuses on the fire performance and post-fire behavior of CFST rectangular columns, research investigations on the structural behavior of circular and rectangular CFST columns at ambient temperature are

also reviewed in order to understand important issues associated with CFST columns. Several books and design guides have been published on steel-concrete composite structures and CFST columns (Wang 2002; Zhao et al. 2010; Liang 2014; Liew and Xiong 2015; Patel et al. 2015a; Patel et al. 2018; Han et al. 2018). Published work dealing with the critical local buckling as well as post-local buckling of thin steel plates at ambient and high temperatures is firstly reviewed. This is followed by discussions on experimental and numerical studies of CFST columns at ambient temperature. Extensive reviews are devoted to publications on CFST columns at elevated temperatures, including standard fire testes on CFST columns and their nonlinear analyses under fire exposure. Finally, published papers on the post-fire structural behavior of CFST columns are discussed.

2.2 LOCAL AND POST-LOCAL BUCKLING OF STEEL PLATES

2.2.1 Thin steel plates at ambient temperature

There have been many studies on the critical local and post-local buckling behavior of steel plates at ambient temperature (Timoshenko and Gere 1963; Bulson 1970). Usami (1982) derived effective width expressions for estimating the post-buckling strengths of rectangular plates subjected to in-plane bending and compression. Usami (1993) extended the previous study by performing elastic-plastic large displacement finite element analyses considering residual stresses and initial imperfection to introduce a set of formulas to predict the effective width of simply supported steel plates. Azhari and Bradford (1991) utilized the method of semi-analytical finite strip to quantify the elastic local buckling loads of steel I-sections where the webs were stiffened longitudinally

subjected to bending. The study was to optimize the location of the longitudinal stiffeners for obtaining higher buckling resistances.

Wright (1993, 1994) presented a theoretical investigation into the elastic local buckling characteristics of thin steel plates that were restrained by concrete. The theoretical model was formulated on the basis of the energy method presented by Timoshenko and Gere (1963). The initial imperfection of the plate was considered in the analysis while residual stresses were explicitly included by applying a safety factor to the yield strength of steel plates. The width-to-thickness limits on steel plates restrained by concrete against local buckling were derived for the design of such plates in steel-concrete composite members with various boundary conditions.

Liang and Uy (1998, 2000) investigated numerically the critical local and post-local buckling responses of clamped thin steel plates in rectangular CFST columns loaded concentrically. The steel plates under investigation were subjected to uniform in-plane stresses. They utilized the finite element analysis system STRAND 6.1 to develop finite element models to simulate the nonlinear critical local and post-local buckling behavior of steel plates with clamped boundary conditions. The significance of width-to-thickness ratios, residual stresses and geometric imperfections on the post-local buckling strengths of thin plates was studied. Liang et al. (2004) employed the finite element software STRAND7 to quantify the critical local buckling stresses as well as the post-local buckling strengths of steel skins in double-skin steel-concrete composite panels subjected to in-plane shear and biaxial compression. The initial imperfection was taken as $0.003b$, where b stands for the plate element width. The four edges of a steel plate element

between stud connectors were clamped, which reflected the restraint offered by the rigid concrete in real construction.

Liang et al. (2007) performed numerical investigations into the critical local and post-local buckling responses of steel plates that formed a CFST column of rectangular cross-section that were loaded biaxially. The steel tube walls of the CFST rectangular column were restrained rotationally by the rigid concrete infill so that square steel plates with clamped edge conditions were considered based on the suggestion given by Liang and Uy (2000). The finite element model was developed for the nonlinear inelastic analysis of thin steel plates that accounted for the influences of residual stresses in addition to geometric imperfection. Steel plates under investigations were subjected to gradient stresses, which included non-uniform and uniform edge compressive stresses and bending stresses. Mathematical expressions for the determination of the initial local buckling stresses of clamped steel plates subjected to stress gradients were developed based on finite element results. The effective strength and width equations were also derived for thin steel tube walls of CFST columns loaded biaxially. These analytical models proposed can be incorporated in computer modeling procedures to consider the influences of local and post-local buckling on the structural behavior of thin-walled CFST columns.

Bedair (2009) investigated the effects of the interaction of flanges and web on the critical local buckling stresses and the post-local buckling strengths of steel H-shape columns. The restraints on the edges of the plate accounted for the influence of the geometry of flanges and web and its effect on the local buckling and ultimate strength of steel columns was included in the analytical method. Ragheb (2010) employed an analytical model to

investigate the local buckling behavior of pultruded fiber-reinforced polymer (FRP) columns loaded eccentrically. The model ignored the geometry imperfection. Although this model could be applied to other sections, the parametric study was conducted on I-section columns only. Ragheb (2015) presented an inelastic stability model considering residual stresses for determining the local-buckling loads of flanges and web in steel I-beams taking the interaction of flange and web into account. It was shown that the predicted results differed from the calculations by the codified methods. The width-to-thickness ratios of flanges and web were found to have a remarkable influence on the local buckling of web and flange plate elements.

2.2.2 Thin steel plates at elevated temperatures

Knobloch and Fontana (2006) proposed a strain-based method of effective widths for estimating the post-local buckling strengths of stiffened and unstiffened plate elements in steel sections exposed to high temperatures. The method accounted for the influences of plastic strain, distribution of plastic stress and material nonlinear strain-dependent properties of steel at high temperatures. The method of effective width underlying the strain principle does not require the classification of steel cross-sections and can be used directly in the design of unstiffened and stiffened plates in steel cross-sections under fire exposure. It was reported that there was a good correlation between calculations by the strain-based effective width method and finite element analysis results.

Heidarpour and Bradford (2007) employed the method of semi-analytical finite strip to investigate the local buckling behavior of flange outstands in steel beams exposed to high

temperatures. The cubic functions were used to describe the buckling displacements of flange outstands exposed to high temperatures. The formulation considered residual stresses presented in the flange outstands in steel beams. Based on the finite strip analysis results, the limits of slenderness on flange outstands subjected to high temperatures were proposed, which recognized the degradation in material properties at high temperatures. The analysis was used to obtain the critical local buckling temperatures for flange outstands with pinned or clamped edge supports. It was shown that residual stresses had an insignificant influence on the buckling strength of flange outstands.

The finite element software SAFER was used by Quiel and Garlock (2010) to undertake nonlinear analyses on steel plates exposed to high temperatures. It was assumed that the unloaded edges of the steel plate were either fixed or simply-supported whereas the loaded edges were simply-supported. The finite element model of steel plates did not include residual stresses. The plate geometric imperfections of $b/200$ and $0.1t$, where b stands for the width of the plate and t its thickness, were considered in the nonlinear analysis. Steel plates subjected to uniform compressive stresses and stress gradients were analyzed to determine their ultimate strengths when exposed to high temperatures. Expressions for effective widths were developed based on AISC specifications (2005) and Eurocode (EC3 2003 & 2004) for steel plates subjected to high temperatures.

Couto et al. (2014) conducted finite element analyses on the local buckling responses of steel plates with simply-supported edge conditions under exposure to high temperatures. The finite element software SAFER was utilized in the investigations. Rectangular steel plates with an aspect ratio of 4 under either compressive edge stresses or in-plane bending

were analyzed. The local buckling model of steel plates subjected to high temperatures incorporated the residual stress pattern at room temperature. The geometric imperfection of a steel plate was specified as its first buckling mode determined by the linear buckling analysis. Effective width equations were derived for the estimation of the post-local buckling strengths of plates with simply-supported edges exposed to high temperatures.

Experiments on the local-buckling behavior of axially-loaded short steel columns exposed to high temperatures were performed by Wang et al. (2014). Twelve welded steel H-section columns with two different yield strengths were fabricated and tested. It was observed that all specimens tested at ambient temperature failed by local buckling before attaining their section capacities. Under exposure to high temperatures, the strength of steel columns with higher yield strength decreased rapidly and they were more vulnerable to local buckling. The comparison of experiment with results computed by the design approach given in Eurocode 3 (2004) indicated that the codified method generally overestimated the strengths of short steel columns. The finite element program ABAQUS was utilized to simulate the experimental behavior of short steel columns at elevated temperatures accounting for residual stresses at ambient temperatures as well as geometric imperfection of $0.01t$.

Ragheb (2016) presented an inelastic stability model for ascertaining the critical local buckling loads of I-section columns exposed to fire that ignored the effect of residual stresses. Expression were given for the estimation of the critical local buckling loads of the web and flanges in terms of the critical strain at which local buckling occurs. The study showed that there was no difference in the critical strain in the steel plate element

at different temperatures. The local buckling load of steel plate elements was sensitive to the geometry of the flanges and web but not to the steel yield strength at elevated temperatures. The study confirmed that the approach specified in AISC (2005) overestimated the critical local buckling load of steel flanges and web in I-section steel columns under exposure to high temperatures.

2.3 CFST COLUMNS AT AMBIENT TEMPERATURE

2.3.1 Experimental works on CFST columns

Research into the behavior of CFST columns has been undertaken since the early time of the last century. Experiments on the strengths of CFST columns were pioneered by Kloppel and Goder (1957). Furlong (1967) undertook tests to study the responses of CFST short columns having circular and square sections loaded eccentrically. The experimental program examined the significance of the width-to-thickness ratio as well as the confinement offered by the steel tube on the ultimate strengths of CFST columns. The width-to-thickness ratios of tested specimens varied from 29 to 98. It was found that the concrete infill was confined by the circular steel tube so that the compressive strength and ductility of concrete improved while the square steel tube exerted little confinement to the concrete. Knowles and Park (1969) undertook experiments on square and circular CFST columns to ascertain the effects of the confinement and column slenderness on the column ductility and strength. Local buckling was not observed in the tested columns owing to their small section slenderness ratios.

Bridge (1976) conducted an experimental research into the structural behavior of pin-ended square CFST slender beam-columns subjected to biaxial bending and axial compression. The tested columns had the cross-sectional dimensions of 300×300 mm and the width-to-thickness ratio of 20 so that the steel sections were compact. The sensitivities of the ultimate strengths of CFST slender columns to the angle of applied loads, column slenderness, and the loading eccentricity were examined in the experimental program. It was observed that increasing either the column slenderness or the loading eccentricity markedly reduced the ultimate strengths of biaxially loaded CFST columns of square sections. However, the loading angle was found to have an insignificant influence on the column ultimate strength. The evaluations of composite design rules for CFST columns against experimental measurements were undertaken. It was reported that the simplified design method underlying the equivalent pin-ended column model with moment amplifications yielded un-conservative results for CFST columns. However, the design method could produce satisfactory results if the effective flexural stiffness of composite columns was used in the calculations.

Sahkir-Khalil and Zeghiche (1989) performed tests on seven full-scale slender rectangular CFST beam-columns. One of the columns was loaded concentrically to failure while every two other columns were loaded eccentrically about the strong axis, the weak axis and both axes. The column cross-sections had the depth-to-thickness ratio of 24 and width-to-thickness ratio of 16, which were considered compact. Sahkir-Khalil and Mouli (1990) undertook further experiments on uniaxially loaded CFST slender rectangular columns with the depth-to-thickness ratios of 24, 30 and 40. The study investigated the influences of concrete and steel strengths and the cross-sectional sizes in

addition to the column slenderness ratio on the behavior of CFST columns. The aforementioned tests showed that the cause for the failure of all tested columns was the overall buckling without local plate buckling owing to small section slenderness ratios.

Experiments on the load-axial strain performance of square, circular and rectangular CFST short columns under axial compression were undertaken by Schneider (1998). The study investigated the significance of cross-sectional shape and depth-to-thickness ratio on the performance of CFST columns. The depth-to-thickness ratios of these columns ranged from 17 to 50. Circular CFST columns were shown to have higher initial axial stiffness, ultimate strength and local buckling strength compared to other shapes. With increasing the depth-to-thickness ratio, the ultimate strength of CFST columns decreased significantly. It was observed that the strain-hardening behavior occurred in circular CFST columns, but it occurred only in rectangular and square sections that had the depth-to-thickness ratio less than 20.

Bridge and O'Shea (1998) studied experimentally the effect of the concrete filling on the performance of CFST columns with width-to-thickness ratios ranging from 37 to 131 subjected to concentric loads. Test results showed that the unilateral local buckling of the square steel tubes caused the failure of CFST square columns while inward local buckling was effectively prevented by the concrete infill. It was evident that the ultimate axial strengths of CFST columns were markedly reduced by local buckling. O'Shea and Bridge (2000) also undertook experimental studies on the responses of short circular CFST columns loaded axially. The diameter-to-thickness ratios of these circular columns ranged from 60 to 220, which were relatively large. It was clearly shown that the unilateral local

buckling of circular sections had a considerable effect on the column ultimate strengths. It was concluded that the results predicted by the approach provided in Eurocode 4 (1992) were conservative for eccentrically loaded CFST columns constructed by normal strength concrete when compared with experimentally measured values.

Uy (2000) undertook experimental programs to study the local and post-local buckling behavior of CFST columns with square thin-walled steel sections subjected to eccentric loads. The width-to-thickness ratios of the 30 tested specimens varied from 40 to 50, 60, 80 and 100. It was reported that the failure modes of these square CFST columns having large plate element slenderness ratios were the unilateral local buckling of steel tubes coupling with concrete crushing.

The influences of the depth-to-width ratio and constraining factors on the structural responses of rectangular CFST columns loaded axially were examined by Han (2002) by means of conducting experiments. A confinement factor was proposed, which reflected the composite action in composite section. The performance of short CFST columns of rectangular sections under sustained loading was reported by Han and Yang (2003). The parameters examined in the experiment were the steel ratio, preload load level, column slenderness ratio, material properties, and the depth-to-thickness ratio. Design formulas for estimating the ultimate strength of short CFST columns that were under long-term sustained loads were proposed. Zhang et al. (2003) investigated the influences of the steel ratio, load eccentricity and column slenderness ratio on structural behavior by testing eight square CFST columns constructed with high strength concrete. The ultimate axial

load of CFST beam-columns was decreased remarkably by the increase in the column slenderness, load eccentricity and width-to-thickness ratio.

Fujimoto et al. (2004) determined the responses of high-strength short CFST columns of square and circular sections subjected to eccentric loads by the experimental method. The tested column sections had the depth-to-thickness ratios varying from 27 to 101. It was found that the ductility of square CFST columns decreased with increasing the concrete strength. With smaller diameter-to-thickness ratios, circular CFST columns could exhibit very ductile behavior. The study highlighted the importance of incorporating the effect of the unilateral local-buckling of steel tubes with large width-to-thickness ratios.

Reports on the structural behavior of CFST rectangular columns made of high strength concrete that were loaded eccentrically to failure were given by Liu (2006). Both short and slender steel columns filled 60 MPa concrete were considered in the experimental investigations. It was observed that thin-walled steel tubes underwent the outward local buckling owing to the restraint of the concrete infill. Test results were compared with those predicted by the design method given in Eurocode 4 (2004). The comparison showed that the codified approach estimated well the measured responses of CFST columns under axial loading, but the margin of conservatism of the strength estimations of uniaxially loaded columns increased with increasing the eccentricity ratio. Lue et al. (2007) studied the performance of slender rectangular tubular steel columns having the depth-to-thickness ratio of 33 that were filled with concrete having different strengths. It was reported that the local buckling of steel tubes with thin-walled sections occurred in tested columns constructed by higher strength concrete.

Qu et al. (2013) performed experiments on the structural responses of 17 rectangular stub CFST columns that were loaded eccentrically to failure. The cross-sections under investigations had the depth-to-thickness ratios of 36, 45 and 52. The study aimed to examine the significance of several parameters on the column performance, which included material strengths, cross-sectional dimensions and loading eccentricity. The columns were under axial compression and either uniaxial bending or biaxial bending. The outward local buckling occurred on three tube walls in compression zones in columns under uniaxial bending while it took place on the two adjacent tube walls in columns loaded biaxially. A steel enhancing factor was introduced to consider the concrete contribution to the steel tube resistance against the unilateral local buckling.

More recently, Li et al. (2018) presented an experimental study on the performance of high strength stub CFST square columns that were constructed with high strength concrete and loaded eccentrically. The width-to-thickness ratios of specimens were 25, 30 and 38, and eccentric loads with the eccentricity ratios of 0.133, 0.233, 0.333 and 0.433 were applied to the columns. The effects of loading eccentricity and steel ratio on the strength and ductility of CFST columns were examined. Experimental observations showed that local buckling took place in the compression zones of all specimens.

2.3.2 Nonlinear analysis of CFST columns

In comparison with experimental methods, nonlinear analysis techniques are cost-effective alternatives that could be used to ascertain the structural behavior of short and slender CFST columns made of circular, square and rectangular sections that are

subjected to either concentric or eccentric loads. Generally, researchers have used either commercial finite element programs, fiber-based numerical models or analytical models to predict the structural behavior of CFST columns. Papers dealing with numerical modeling of CFST columns subjected to mechanical loads are reviewed in this section.

Schneider (1998) presented a nonlinear three-dimensional model of the behavior of CFST short columns with rectangular and circular sections. The model was created by utilizing the finite element software ABAQUS. The inelastic behavior of materials was considered in the simulation. The results obtained showed that the model of finite element was capable of reproducing the measured responses of CFST columns with reasonable accuracy. An analytical procedure was given by Vrcelj and Uy (2002), which calculated the strengths of high-strength CFST square columns. However, the analytical procedure ignored the effects of confinement on concrete ductility and local buckling of steel tubes.

Hu et al. (2003) utilized the ABAQUS package to simulate the responses of nonlinear circular and square short CFST columns. The nonlinearities of concrete and steel materials in addition to the interaction of concrete and steel components were taken into consideration in the modeling. Confining pressure models and strength degradation factors that were applied to confined concrete in CFST columns were developed by means of the finite element simulations of measured responses of CFST columns. The proposed constitutive laws of confined concrete can be implemented in computer modeling techniques for the nonlinear simulations of CFST columns.

Liang et al. (2006) developed a computational model utilizing the approach of fiber analysis for quantifying the strength and behavior of stub CFST columns of square and

rectangular sections loaded concentrically to failure. The fiber model incorporated the post-local buckling effect on the structural behavior of CFST short columns under axial compression by means of employing the effective width equations developed by Liang and Uy (2000). The developed model was verified by the established experimental data. The model was employed to examine the sensitivities of the strengths of CFST columns to important parameters, such as material strengths as well as the width-to-thickness ratios. It was demonstrated that the unilateral local-buckling of thin-walled sections had a marked influence on the ultimate axial loads of CFST columns.

Liang (2009a) developed a performance-based analysis (PBA) model for the simulation of short rectangular CFST columns fabricated with thin-walled sections that are subjected to biaxial bending and axial compression. The PBA technique was formulated by using the method of fiber analysis. The critical local and post-local buckling models derived by Liang et al. (2007) were implemented in the PBA procedure to taken into account the influences of the gradual post-local buckling of steel tubes on structural behavior. For this purpose, a numerical modeling scheme was specially developed that gradually redistributed the in-plane stresses from the heavily buckled region to the edge strips in the steel tube wall in accordance with the concept of effective widths. Computational procedures were proposed for the predictions of the load-axial strain behavior and axial load-moment-curvature responses of CFST columns considering local buckling. Numerical solution algorithms were developed that implemented the secant method to solve the dynamic nonlinear equilibrium equations generated in the incremental-iterative analysis process. The developed PBA model was verified through available test results with good accuracy by Liang (2009b). A computer program implementing the PBA

models was written and employed to study the structural behavior of CFST columns considering various parameters. Numerical results obtained formed the basis of the fundamental behavior of CFST thin-walled columns subjected to biaxial loads. The PBA technique can be employed to design and analyze biaxially loaded stub square and rectangular CFST columns with slender, non-compact or compact steel sections.

A three-dimensional finite element model was described by Tao et al. (2011) by utilizing ABAQUS package, which simulated the structural behavior of short concrete-filled stainless-steel tubular (CFSST) columns loaded concentrically. The geometric imperfection was considered using the formula presented by Tao et al. (2009), which had the value of 0.01 times the width of the section for columns made of carbon steel. Residual stresses were assumed to have an insignificant influence so that they were ignored in the analysis. The width-to-thickness ratios of cross-sections varying from 18 to 54 were considered in the parametric study. Investigations on the significance of the stainless-steel grade, initial imperfection, enhanced strength of corners, concrete compressive strength, proof strength and width-to-thickness ratio on structural performance were undertaken. It was shown that stainless-steel composite columns possessed better ductility and strength compared with the ones fabricated by carbon steel tubes. This was owing to the strain-hardening characteristics of stainless-steel. A simple equation was proposed for estimating the ultimate axial loads of short CFSST columns.

Liang (2011a) proposed a mathematical modeling technique for the predictions of the structural responses of slender CFST circular beam-columns constructed by high-strength materials loaded eccentrically to failure. The formulation of the mathematical model was

based on the approach of fiber analysis. The mathematical model accounted for the influences of concrete confinement that was provided by the circular steel tube, second order induced by the interaction of axial load and deformations and initial deflections. The part-sine wave displacement function was used to represent the deformed shape of slender pin-ended CFST beam-columns. Computer simulation procedures were developed that calculated the deflections and axial load-moment interaction envelopes of slender CFST columns that were subjected to combined bending and axial load. In accordance with the secant method, computer algorithms were programmed to produce converged solutions to the dynamic nonlinear incremental equilibrium functions for slender CFST beam-columns. The algorithms iteratively adjusted the depth of neutral axis in the cross-section to satisfy the equilibrium of moment at the column mid-length in the load-deflection analysis, and the curvature to meet the force and moment equilibrium conditions at the column mid-length in the analysis of load-moment interaction strength. Liang (2011b) used the established experimental results to verify the computer model proposed with good accuracy. The verified computer model was then employed to undertake extensive parametric studies on the structural behavior of slender CFST columns. The influence of concrete confinement on the column strength curves was demonstrated by using the theoretical model.

Liang et al. (2012) developed a multiscale computational model for the predictions of the structural responses of rectangular slender CFST pin-ended beam-columns made of high-strength materials subjected to biaxial bending and axial load. The mesoscale model was formulated by the method of fiber analysis that simulated the inelastic nonlinear behavior of cross-sections under biaxial loads. The influence of the gradual post-local buckling of

steel tubes made of thin-walled sections was taken into account in the formulation at the mesoscale level. Expressions derived by Liang et al. (2007) were adopted to compute the critical local-buckling stresses, post-local buckling strengths and effective widths of thin steel plates that were subjected to stress gradients. The numerical simulation scheme programmed by Liang (2009a) was adopted to model the gradual post-local buckling of steel tube that formed a CFST column based on the concept of effective widths. The macroscale model was developed for the simulation of strength envelopes and deflection responses of slender CFST columns that were loaded biaxially. Computer algorithms underlying Müller's numerical method were programmed to solve dynamic nonlinear equilibrium functions of biaxially-loaded slender columns. Numerical modeling procedures for computing strength envelopes as well as deflection responses of slender CFST beam-columns were given. Patel et al. (2015b) verified the multiscale mathematical model presented by Liang et al. (2012) by comparisons with independent experimentally measured data. The multiscale model was used to demonstrate the significance of important parameters on the axial strength, strength reduction factor and steel and concrete contribution ratios of high-strength CFST slender columns.

Patel et al. (2012a) presented a nonlinear fiber modeling technique for analyzing high-strength CFST rectangular beam-columns that were under axial load and uniaxial bending. The models of local and post-local buckling derived by Liang et al (2007) were utilized to take into account the local buckling effect of clamped steel plates in CFST columns. The nonlinear inelastic material behavior was adopted in the simulations. Müller's method was implemented in computational algorithms to solve the stability equations of pin-ended slender CFST beam-columns. Computer algorithms for the

predictions of the axial load-lateral deflection and strength interaction curves were developed. Patel et al. (2012b) examined the accuracy of the mathematical model by means of comparing computations with experimentally measured data on slender CFST beam-columns. The agreement between theory and experiment was shown to be good. An extensive parametric study was undertaken to highlight the influences of local buckling, loading eccentricity and geometric properties and material strengths on the nonlinear behavior of high-strength CFST columns subjected to uniaxial bending.

2.4 CFST COLUMNS AT ELEVATED TEMPERATURES

2.4.1 Standard fire tests on CFST columns

Lie and Chabot (1992) carried out standard fire tests to ascertain the fire resistance of full-scale CFST slender columns of circular and square sections constructed by plain concrete. In a standard fire test, the CFST column was exposed to heating in a furnace that was specially constructed for testing columns loaded concentrically and eccentrically. The temperatures generated by heating in the furnace were controlled so that the average temperatures followed the standard temperature-time curve defined in ASTM-E119 (1985) or CAN/ULC-S101 (1982). The sensitivities of fire responses of CFST columns to the sectional dimension, section type, the applied load ratio, the column slenderness, and loading eccentricity were investigated. Six square CFST columns were loaded axially with the B / t_s ratios varying from 24 to 48. The compressive strengths of concrete varied from 46.5 MPa to 58.3 MPa while steel tubes had a yield strength of 350 MPa. The tested columns had either fixed or pinned support conditions. The length of all

tested columns was 3810 mm. The test results indicated that slender CFST columns failed by local and global interaction buckling or compression depending on the column slenderness. The fire resistance of slender CFST columns made of circular steel sections and fiber-reinforced concrete was studied experimentally by Kodur and Lie (1995). Six full-scale specimens with a length of 3810 mm were tested in a furnace where the temperatures created by heating followed the standard fire curve given in ASTM E199-88 (1990). The columns tested had the depth-to-thickness ratios varying from 51 to 56. Only one column failed by global buckling.

Fire tests on the fire behavior of square CFST slender columns fabricated by either fire-resistant steel tubes of steel tubes or without protections loaded eccentrically were conducted by Sakumoto et al. (1994). These columns had a length of 3500 mm and width-to-thickness ratio of 33. It was confirmed that slender CFST columns failed by the local-global interaction buckling and concrete crushing.

Han et al. (2003a) determined the fire behavior of CFST slender columns with and without fire protected materials subjected to either axial or eccentric loading by means of conducting standard fire tests. The experiment examined the significance of fire exposure time, cross-sectional area, columns slenderness, load eccentricity and material strengths of concrete and steel on the fire performance of CFST columns. Eleven columns with a length of 3810 mm and pinned support conditions were tested in a furnace where the average temperatures followed the standard fire curve defined in ISO-834 (1975). The study showed that material properties, loading eccentricity and steel ratio had a moderate effect on the fire resistance. However, the fire resistance of CFST columns was

significantly affected by the protection thickness, column slenderness and cross-sectional area. The failure of square slender CFST columns was caused by the local and global interaction buckling.

The fire performance of slender CFST square columns loaded axially was reported by Choi et al (2005). The specimens made of normal strength concrete and steel had the width-to-thickness ratios of 33.3 and 38.9. The columns were tested under pin-ended support conditions that had a length of 3500 mm. However, only part of the CFST column was heated in the furnace during exposure to high temperatures. The heated length of the columns varied from 2400 mm to 3000 mm.

Experimental investigations into the structural responses of short CFST columns with square and rectangular sections under fire exposure have been extremely limited. Lu et al. (2009) conducted experimental studies on the fire behavior of square CFST stub columns constructed with self-consolidation concrete. These columns were subjected to constant loads during fire exposure that simulated the standard fire temperature-time curve give in ISO-834 (1980). Two of the six columns were loaded eccentrically while others were under axial compression. Other variables examined were section size and loading level. The cross-sections of these columns had the width-to-thickness ratios of 30 and 33. It was reported that CFST short columns exhibited ductile performance and the integrity of the columns was maintained during fire exposure. Short CFST columns of square sections failed by the unilateral local buckling in addition to concrete crushing.

Romero et al. (2011) undertook experimental research into the fire behavior of sixteen concentrically loaded CFST slender circular columns made of either fiber-reinforced concrete, steel rebar-reinforced concrete or plain concrete. The columns, which had a length of 3810 mm and D/t_s ratio of 26.5, were under an axial load with the load ratios of 0.2 and 0.4. It was confirmed that using steel rebar-reinforced concrete markedly improved the fire resistance of CFST columns. The tested results were utilized to verify a design model proposed previously by the authors and it was extended to CFST column with high strength concrete. It was shown that the simplified design approach given in Eurocode 4 (2005) needed to be revised in order to yield realistic predictions of the fire resistance of CFST columns under concentric loads.

Han et al. (2013) presented a report on the experimental results of CFSST columns under fire exposure. Five square and circular full-scale CFSST slender columns subjected to constant axial loads were tested in a furnace to investigate the influences of sectional shape, cross-sectional dimension, and the axial load level on the structural responses to fire effects. The depth-to-thickness ratios of sections were 60 and 63. The experiments showed that the section dimensions as well as axial load levels had remarkable effects on the fire performance of CFSST columns.

The fire behavior of elliptical and rectangular slender pin-ended CFST columns that were loaded concentrically and eccentrically under standard fire exposure specified in ISO-834 was investigated experimentally by Espinos et al. (2015a). The width-to-thickness ratios of rectangular cross-sections were 15, 25 and 35. The constant load applied to the columns with a length of 3180 mm was equal to 20% of the column ultimate axial load at ambient

temperature. The structural responses and fire resistance of six elliptical columns and twelve rectangular columns subjected to fire effects were measured. The significance of the percentage of reinforcement, cross-sectional shape as well as loading eccentricity on the fire resistance was examined. Test results indicated that the failure of all circular columns was caused by global buckling while rectangular columns failed by local and global interaction buckling. It was found that the addition of reinforcing bars improved the strengths of slender CFST columns and the loading eccentricity had a remarkable effect on their fire resistance.

Espinos et al. (2015b) conducted standard fire tests on steel tubular slender columns made of square and circular sections filled with rebar-reinforced concrete subjected to large eccentricities. The parameters examined were section shape, section dimensions, and reinforcement ratio as well as loading eccentricity. The loads with the eccentricity ratios of 0.5 and 0.75 were applied to columns before heating and were maintained constant during fire exposure. Square sections had the width-to-thickness ratios of 18.75 and 22. The columns with a length of 3180 mm were pinned at both ends. It was found that the failure of all columns tested was global buckling. The fire performance of circular columns in terms of strength and fire resistance was higher than that of square ones. Increasing the loading eccentricity remarkably reduced the fire resistance. However, increasing the percentage of reinforcement markedly improved the fire resistance as well as the column strength.

Experimental investigations on the structural responses of concentrically loaded CFSST slender square and circular columns with pin-ended conditions to fire effects were undertaken by Tao et al. (2016). All six columns tested had the section depth of 200 mm

and a length of 1870 mm. The axial load ratios ranged from 0.28 to 0.48, which was defined as the ratio of the axial load applied to the column to its ultimate axial strength calculated in accordance with Eurocode 4 (2005). The significance of the reinforcement ratio, sectional shape and axial load ratio on the fire performance was evaluated by standard fire tests. Test observations indicated that all square and circular CFSST columns under fire exposure failed by local and overall interaction buckling. Circular CFSST columns had higher fire resistance than square columns. The fire resistance of CFSST columns was increased by adding longitudinal steel reinforcement in the concrete.

Yang et al. (2017) conducted an experimental work on the fire behavior of square steel tubular slender columns filled with recycled aggregate concrete. Standard fire tests on nine specimens under concentric loading were undertaken to ascertain the influences of the axial load ratio, the replacement ratio of recycled aggregate as well as the fire protection thickness on the fire performance of CFST columns. Square steel sections had the width-to-thickness ratio of 50.8. The length of specimens was 2750 mm and their effective length taking into account the pin-ended supports was 3810 mm. The percentage replacement of recycled aggregate ranged from 0.0% to 100%. The ratios of the axial loads were 0.2, 0.3, 0.4 and 0.5, which were considered in the tests. The fire protection thickness was taken as 0.0 mm, 3 mm, 6 mm and 9 mm, respectively. It was reported that all slender columns failed by local and global interaction buckling in addition to concrete crushing. The more serious local buckling occurred in unprotected steel tubes than protected ones. The recycled aggregate replacement of 50% had an insignificant influence on the resistance of CFST columns to fire effects. It was confirmed that the fire-resistance

time of slender CFST columns was increased by either increasing the fire protection thickness or reducing the axial load ratio.

The fire behavior of CFST slender columns made of reinforced concrete restrained axially and rotationally by surrounding structures was experimentally investigated by Rodrigues and Laím (2017). The parameters examined in the experimental program were the axial and rotational restraints, sectional shape as well as column slenderness. Different cross-sections were considered, which included circular, square, rectangular and elliptical shapes with the depth-to-thickness ratios ranging from 15 to 35. The study demonstrated that the stiffness of the surrounding structure had an insignificant influence on the fire resistance. In addition, the section shape and the column slenderness had a remarkable effect on the fire resistance. It was highlighted that the failure of slender rectangular CFST columns with depth-to-thickness ratio of 35 was induced by local and global interaction buckling with multiple local buckling half-waves along the column.

2.4.2 Nonlinear analysis and design of CFST columns exposed to fire

Mathematical models for calculating the temperatures, fire resistance and load-deflection responses of slender rectangular and circular CFST columns made of fiber-reinforced concrete, bar-reinforced concrete and plain concrete under fire exposure have been proposed by Lie (1984, 1994), Lie and Chabot (1990), Kodur and Lie (1995), and Lie and Irwin (1995). The models used the approach of fiber elements to mesh the cross-section of a CFST column. The temperatures on the surface of a CFST column under fire exposure were calculated by means of the standard temperature-time curve described in

ASTME119 (1990). The method of finite difference was employed to compute the temperature distribution within the column cross-section. For a specific time or temperature, the analysis procedure for load-deflections was proposed to predict the ultimate strength of the CFST slender column. The fire resistance of the column was calculated by gradually increasing the fire time and repeating the above computation process. The water content was considered in the thermal analysis. However, the limitations of the mathematical models were that the concrete tensile strength, deformations caused by preloads and the local buckling of rectangular thin-walled steel sections on the fire resistance were not considered.

Wang and Kodur (1999) evaluated the accuracy of the design approach given in Eurocode 4 Part 1.2 (1994) for estimating the ultimate axial strength and flexural stiffness of concentrically loaded CFST columns exposed to fire. For this purpose, the fire test results on CFST columns made of fiber-reinforced concrete, bar-reinforced concrete and plain concrete reported by Lie and Chabot (1992) were used. The comparisons showed that the use of column buckling curve “c” and concrete models given in Eurocode 4 Part 1.2 yields conservative predictions of structural behavior of CFST columns at elevated temperatures. A simplified approach was proposed that estimated the resistance of CFST columns to axial loading exposed to fire. The temperature distribution in column cross-sections was evaluated by an approximate method derived using the results computed by the heat transfer analysis in one-dimension.

A simple design formula was proposed by Kodur (1999) for estimating the fire resistance of CFST columns having circular and square sections made of various types of concrete

at elevated temperatures. The design formula incorporated the most important features that affect the fire responses of CFST columns, including the loading eccentricity, type of aggregate, concrete strength, column slenderness, axial load, cross-sectional dimension, and type of concrete. The comparison with test results indicated that the simple design formula yielded conservative fire resistances of CFST columns under standard fire exposure.

Yin et al. (2006) described a theoretical model for calculating the fire resistance of short CFST columns of square and circular sections under fire exposure and axial loading. The standard fire curve given in ISO-834 (1980) was used to express the temperature-fire time relationship for columns under fire exposure. The concrete model at elevated temperatures given by Anderberg and Thelandersson (1976) was adopted while Han's model (2001) for steel was used. The parametric study conducted demonstrated that the circular CFST column had a slightly higher fire resistance than square one for the same material strengths as well as steel and concrete area. However, the theoretical model did not consider concrete moisture content and local buckling of square steel tubes.

Ding and Wang (2008) developed finite element models by utilizing the ANSYS package to quantify the thermal and structural responses of square and circular CFST slender columns under fire exposure. In the thermal analysis, 2D finite element model was created to ascertain the distribution of temperatures within the cross-section of the CFST column that was exposed to fire defined by the standard temperature-time curve provided in ISO-834 (1980). The temperature-dependent stress-strain laws and thermal properties of concrete and steel suggested in Eurocode 4 (2005) were used in the thermal and structural

analyses. Important features that influenced the fire behavior were considered in the finite element modeling, which included the air gap at the steel-concrete interface, slip between concrete and steel components, initial deflection and concrete tensile behavior. The results obtained confirmed that the slip between concrete and steel components was so small that its influence on the fire resistance was minor and could be ignored. The inclusion of an air gap at the concrete-steel interface improved the predictions of both structural and thermal responses of CFST columns. The concrete tensile strength had an insignificant influence on the fire resistance. The fire resistance of slender CFST columns was considerably affected by the initial deflection. It was recommended that an initial deflection of $L/1000$ at the mid-height of the column should be used in numerical simulations. The numerical investigations presented provided useful remarks on the realistic modeling of CFST slender columns exposed to fire, but the local buckling of square thin-walled steel tubes was not taken into account.

A numerical model implementing the approach of fiber analysis was described by Chung et al (2008) that predicted the fire behavior of CFST slender columns with square steel cross-sections subjected to constant axial load. The method of finite difference was used to quantify the distribution of temperatures in column cross-sections. It was assumed that the thermal and stress analyses were uncoupled. The nonlinear stress analysis of CFST columns was based on structural mechanics considering equilibrium and compatibility equations. The numerical model was validated by experimentally measured data and was employed to examine the influences of the available material models on the fire-resistance of square CFST slender columns. The evaluations of material constitutive laws given by Lie (1992), Yin et al. (2006), Eurocode 4 (2003) and AIJ code (1997) were conducted.

The comparative studies showed that the material model specified in Eurocode 4 (2003) produced reasonable predictions of the responses of CFST columns to fire effects. The thermal properties and constitutive laws of concrete had a more significant effect on the fire performance than those of structural steels. It was confirmed that the fire resistance was markedly affected by the concrete compressive strength. The main drawbacks of the numerical model described were: (a) the initial geometric imperfection was not included; (b) the local buckling of steel tubes with square thin-walled sections was not considered; (c) and the air gap and moisture content were not incorporated in the thermal analysis.

Chung et al. (2009) described a numerical model for determining the fire responses of slender CFST square columns loaded eccentrically under fire exposure. The model used the fiber element technique to discretize cross-sections in the thermal and stress analyses as described by Chung et al. (2008). The numerical model was proposed to generate the moment-curvature relationships as well as axial load-moment envelopes of eccentrically-loaded CFST columns at elevated temperatures. Material models for steel and concrete recommended in Eurocode 4 (2003) were adopted in the formulation of the theoretical model. Numerical studies indicated that the steel tube had a remarkable influence on the fire performance of CFST columns loaded eccentrically. After 30 minutes fire exposure, the stiffness and ultimate moment capacity of CFST columns decreased rapidly. It was confirmed that increasing the loading eccentricity decreased the fire resistance. However, the limitations of the numerical model presented were that the effects of local buckling, tensile strength of concrete, initial geometric imperfection and air gap between concrete and steel components were not taken into consideration.

Numerical models were developed by Hong and Varma (2009) for modeling the fire behavior of slender square CFST columns loaded axially and eccentrically. A sequentially uncoupled analysis procedure was used to conduct the fire response analysis of CFST columns. The temperature-time curves applied to the surfaces of square CFST columns were determined by using the available computer program Fire Dynamic Simulator. The finite element program ABAQUS was employed to carry out the heat transfer analysis on the CFST column to ascertain the temperature distribution within its cross-section. The concrete moisture content of 7% was taken into account in the heat transfer analysis. Three-dimensional models using ABAQUS were created to simulate the structural responses of loaded CFST columns to fire effects determined from the heat transfer analysis. The numerical models were employed to examine the sensitivities of the fire behavior to important parameters, which included the material models for steel and concrete, concrete tensile behavior, thermal expansion model, geometric imperfection, composite interaction and local buckling. The sensitivity analysis indicated that the temperature-dependent material laws of steel and concrete had significant influences on the predicted fire performance. The continuum finite element model could not accurately simulate the concrete tension cracking behavior. The fire responses of CFST slender columns were considerably affected by the geometric imperfection. Since the analyzed CFST columns had small width-to-thickness ratios that were in the range from 32 to 48, the effect of local buckling on the fire behavior was not significant in these cases.

The finite element analyses were carried out by Lu et al. (2009) to investigate the fire responses of square CFST short column that were constructed by high-strength steel tubes and high-strength self-consolidating concrete. The sequentially coupled procedure of

thermal and stress analysis in the finite element program ABAQUS was employed. The temperature-dependent material model for concrete given by Han et al. (2003b) was used in the analysis. The influences of concrete moisture content, concrete tensile behavior and heat contact conductance at the steel-concrete interface were accounted for in the finite element model. It was confirmed that the unilateral local buckling of the thin-walled steel tubes took place before the CFST columns failed. The unilateral local-buckling and crushing of concrete reduced the capacity of the CFST column.

Schaumann et al. (2009) employed BoFIRE a finite element software to study the structural responses of circular and square CFST slender columns made of high-strength concrete under fire exposure. The finite element model took the second order theory and concrete moisture content of 10% into account. The effects of section size, cross-section shape, column slenderness and the yield strength of steel on the structural performance of CFST columns made of bar-reinforced concrete, fiber-reinforced concrete and plain concrete under standard fire exposure were examined by the computer model. It was pointed out that local buckling effects have not been incorporated in most computer simulation techniques including BoFIRE, which might result in exaggerated results of square CFST columns.

Three-dimensional models were developed by Espinos et al (2009, 2010) by means of employing ABAQUS the finite element software for the simulations of the fire responses of CFST columns of circular sections under axial loads and fire exposure. The temperature-dependent stress-strain model for concrete proposed by Lie (1994) was used together with concrete thermal properties at high temperatures suggested in Eurocode 2

(2004). The computer model adopted the material constitutive relations as well as thermal properties at elevated temperatures for structural steels specified in Eurocode 3 (2005). A sequentially coupled procedure of thermal and stress analysis was employed in the simulations of CFST columns under fire exposure that followed the standard fire curve provided in ISO-834 (1980). The comparison of numerical results with fire test data was reasonably good. The sensitivities of the fire responses of circular CFST columns to several important parameters were investigated by Espinos et al. (2010) using the finite element models, which included the slip between the steel and concrete, air gap at the concrete-steel interface, geometric imperfection, material models at elevated temperatures and moisture contents.

Dai and Lam (2012) presented numerical studies on the sensitivities of the fire behavior of axially loaded CFST stub columns to various sectional shapes, including square, rectangular, circular and elliptical sections. The ABAQUS software package was used to develop 3D finite element models for the simulation of the fire behavior of stub CFST columns under standard fire exposure. The CFST square columns had the width-to-thickness ratios of 24.6, 23.78, 25.18 while rectangular sections had the depth-to-thickness ratios of 33.8, 31.7, 35.8 and width-to-thickness ratios of 16.9, 15.86, 17.9. The material constitutive laws of steel and concrete at high temperatures as well as thermal properties given in Eurocodes 3 (1993) and Eurocode 4 (1994) were used in the analysis. Comparisons of the temperature distribution within cross-sections, critical temperatures in steel tubes and fire resistances of CFST columns with different shapes were made. Circular CFST columns were demonstrated to have higher fire resistance than other

sections. However, local buckling was not incorporated in the modeling of CFST columns with square and rectangular thin-walled sections under fire exposure.

A fiber-based finite element beam-column model was developed by Ibanez et al. (2013) by means of utilizing the FedeaLab platform and MATLAB toolbox for the predictions of the fire performance of circular CFST slender columns loaded concentrically to failure. The cross-section of a circular CFAT column was meshed by fiber elements while the column along its length was discretized into finite elements. The steel tube and concrete components were modeled separately as individual elements in the longitudinal direction but linked at the nodes by link elements longitudinally and transversely. Mixed formulation was employed to formulate the concrete and steel tube components. The concrete model proposed by Lie (1994) and thermal properties of concrete given in Eurocode 2 (2004) were adopted for normal strength concrete. The concrete model of Kodur et al. (2004) and concrete thermal properties given by Kodur and Sultan (2003) were used for high-strength concrete. The material laws for structural steel at high temperatures recommended in Eurocode 3 (2005) was employed. The fiber-based model used a sequentially coupled procedure of thermal and stress analysis to quantify the structural behavior of CFST columns under fire exposure defined in ISO-834 (1980). The temperature distribution within the cross-section was determined by the method of finite difference. The gap conductance at the concrete-steel interface was considered in the thermal analysis as well as the water content. In the nonlinear structural analysis, the initial deflection of columns was included. It was reported that the finite element model generally predicted well the measured fire responses of circular CFST slender columns but could not be able to capture the responses at the last stages of fire exposure. It was

also pointed out that further research should be focused on developing more accurate concrete constitutive models that could be implemented in numerical simulations.

Wang and Young (2013) studied the fire performance of slender CFST circular columns numerically. The ABAQUS package was utilized to create a three-dimensional model to perform both nonlinear thermal and stress analyses of CFST columns. In the thermal analysis, a 3D model was employed to determine the temperature distribution in cross-sections. The thermal properties of concrete given in Eurocode 2 (2004) were adopted while the steel thermal properties suggested in Eurocode 3 (2005) were used in the thermal analysis. The moisture content, geometric imperfection, and air gap and slip between the concrete and steel components were incorporated in the finite element analysis. The columns were loaded with different load ratios ranged from 0.24 to 0.54. A parametric study was undertaken to ascertain the significance of high-strength steel on the fire behavior of CFST columns loaded axially to failure. It was reported that the column diameter and concrete strength had more significant effects on the fire-resistance than steel strength. If the same load ratio was applied to the column, the fire resistance decreased by increasing the steel yield strength.

The fire responses of slender CFST columns fabricated by circular steel sections under eccentric loads were studied numerically by Yao et al. (2016). Three-dimensional finite element models were created by employed the ABAQUS package for the sequentially coupled thermal and stress analyses of circular slender CFST columns under standard fire exposure specified in ISO-834 (1980). The thermal analysis took into account an air gap at the concrete-steel interface with a conductance of $150\text{W/m}^2\text{K}$. The finite element

analysis employed the thermal properties of concrete and steel provided by Lie and Irwin (1995), the temperature-dependent constitutive laws for concrete suggested by Han et al. (2003b), and the temperature-dependent constitutive model for steel by Lie and Stringer (1994). In the stress analysis, the concrete tensile strength was considered. The models of finite elements were used to examine the significance of material strengths, reinforcement ratio and loading eccentricity on the fire performance of CFST columns loaded eccentrically and exposed to fire. It was shown that the concrete tensile strength had a significant influence on the fire-resistance and the effect of stirrup ratio could be ignored.

2.5 POST-FIRE BEHAVIOR OF CFST COLUMNS

2.5.1 Post-fire tests on CFST columns

Han et al. (2002, 2005) conducted post-fire tests on twenty-six rectangular CFST short columns and two square CFST stub columns loaded axially after being exposed to temperatures ranging from 20 °C to 900 °C to study their post-fire performance. The rectangular columns had the depth-to-thickness ratios of 35 and 45.5 while the square ones had the depth-to-thickness ratios of 41.4. Before testing, a CFST column was exposed to heat in an electric heating furnace at specific temperatures. After the column had been cooled down to the room temperature of 20 °C, the column was tested under axial compression to failure to determine its load-axial strain behavior, residual strength and stiffness. It was found that the unilateral local buckling was the failure mode of short CFST columns tested, which occurred in all tested specimens. In addition, the steel tube local buckling exposed to higher temperatures occurred earlier and severer than those

exposed to lower temperatures. Local buckling markedly reduced the residual stiffness and strength of CFST columns. Specimens exposed to higher temperatures exhibited strain-hardening behavior while those exposed to lower temperatures demonstrated strain-softening behavior.

Post-fire experiments on twelve slender circular and square CFST columns with or without fire protection after being exposed to fire were undertaken by Han and Huo (2003). Square CFST columns had the depth-to-thickness ratios of 34. All columns before testing were exposed to standard fire in a furnace where the average temperatures followed the temperature-time curve defined in ISO-834 (1980). The fire exposure time were 90 min for the unprotected specimens and 180 min for the protected ones. After the specimen had been cooled down to the room temperature, it was tested under either axial compression or eccentric loading to failure at room temperature. It was discovered that all columns failed by the overall buckling coupling with rupture of steel tube in the tension zone and unilateral local-buckling of steel tube in the compression zone. There was an interaction of local and global buckling in these slender CFST columns.

Huo et al. (2009) undertook an experimental investigation to highlight the influences of the cooling phase and preload on the residual stiffness and strength of CFST short columns with circular sections loaded axially. The circular columns having the diameter-to-thickness ratios of 36 and 37.5 subjected to constant axial load were heated to specific temperatures in an electrical furnace and cooled down to the room temperature. The short columns were loaded axially to failure at room temperature. The experimental program examined the significance of the sectional dimensions, axial load level and the maximum

exposure temperatures on the post-fire behavior of CFST stub columns. It was reported that the preload and cooling phase had an insignificant effect on the residual strength of fire-damaged CFST stub columns, but they had a noticeable influence on the residual stiffness and deformations of CFST columns and should be considered in the assessment of fire-damaged CFST columns.

Post-fire tests on fourteen short and slender CFST columns of rectangular sections loaded biaxially were conducted by Jiang et al. (2010) to investigate their residual ductility and strength after exposure to fire. The column cross-sections had the depth-to-thickness ratios of 21.6, 32.4 and 43.2. Parameters under investigations included the loading angle, column slenderness ratio, depth-to-width ratio of the sections and exposure temperatures. Before testing, the columns were exposed to heating in a furnace where the targeted temperatures were 20 °C, 400 °C, 600 °C and 800 °C. Test results demonstrated that the failure of all columns was caused by global buckling in addition to local buckling of the steel tube walls in compression at the column mid-height. It was found that the concrete crushed at places where the tube wall buckled. It was observed that biaxially loaded CFST columns after exposed to high temperatures still had good ductility.

Rush et al. (2015) performed post-fire experiments on the post-fire structural behavior of circular and square CFST slender columns including or excluding fire protection and were loaded eccentrically. The with-to-thickness ratios of square sections were 12 and 24, which were relatively small and considered compact sections at ambient temperature. The significance of important parameters on the residual strengths of CFST columns was assessed in the experimental program, which included the coating thickness, concrete age,

fire protection, type of concrete infill, tube thickness and sectional shape. The failure of all square columns was caused by either local buckling or global buckling. Local buckling occurred even in columns without being exposed to fire. The residual strength of slender square CFST columns was more sensitive to the exposure of elevated temperature compared with that of circular ones.

Post-fire tests on the behavior of reinforced concrete short columns confined by circular steel tubes loaded axially and eccentrically were reported by Liu et al. (2014, 2016). The specimens were heated in a furnace in which the temperatures were controlled by the standard temperature-time curve defined in ISO-384 (1980). During the heating process, the specimens were not loaded. In the post-fire tests, the load was applied to the reinforced concrete column only and the circular steel tube was not loaded directly with the role of providing confinement to the concrete. It was found that all columns loaded concentrically failed by shear and the local buckling of steel tubes did not occur before the columns attained their ultimate loads. However, the failure of all columns loaded eccentrically was due to the local buckling of steel tubes in addition to concrete crushing.

2.5.2 Post-fire response simulations

Han et al. (2002) proposed an analytical model for calculating the post-fire residual strengths of rectangular CFST stub columns loaded concentrically to failure after exposure to high temperatures. The analytical model incorporated the post-fire nonlinear stress-strain laws with strain-hardening for structural steels given by Cheng (2001) and constitutive relations of confined concrete suggested by Han et al. (2001). The post-fire

residual concrete compressive strength and its corresponding strain were estimated by the equations provided by Li and Guo (1993). The slip between the concrete and steel tube was not considered while force equilibrium and deformation compatibility in the longitudinal direction were ensured. The analytical model predicted the post-fire load-axial strain responses of CFST short columns, which were in reasonable agreement with measurements. However, the unilateral local buckling of steel tubes with thin-walled sections observed in post-fire tests (Han et al. 2002) was not incorporated in the formulation of the theoretical model.

An analytical model was proposed by Han and Huo (2003) that predicted the post-fire axial load-deflection behavior of slender CFST columns having square and circular sections under uniaxial bending and axial compression. The post-fire material constitutive laws for structural steels presented by Cheng (2001) and for concrete given by Han et al. (2001) and Li and Guo (1993) were adopted. The part-sine wave function was used to describe the deflected shape of the slender columns. The analysis included an initial deflection of $L/1000$ at the column mid-height. After verification, the analytical model was employed to demonstrate the significance of various factors on the post-fire structural behavior. However, the tensile behavior of concrete and local-global interaction buckling were not incorporated in the nonlinear analyses of slender CFST square thin-walled columns.

Yang et al. (2008) developed a fiber-based finite element model for determining the post-fire responses of square and circular CFST slender columns that were loaded eccentrically after being exposed to standard fire. The column cross-section was meshed into fiber

elements while finite elements were employed to discretize the column along its length. The expressions of Cheng (2001) were employed to model the post-fire stress-strain relationship of structural steels while the concrete models by Han et al. (2001) and Li and Guo (1993) were utilized. The proposed finite element model generated load-deflection responses of eccentrically-loaded CFST columns after being exposed to fire, which were in good correlations with post-fire experimental measurements. The parametric study indicated that the cross-sectional dimensions, column slenderness and axial load ratio had the most remarkable effects on the post-fire structural behavior. The limitations of the finite element model proposed were that it did not incorporate the effects of tensile concrete behavior and local and post-buckling.

Song et al. (2010) described a finite element model created by employing ABAQUS for analyzing the post-fire performance of stub CFST columns constructed by rectangular circular and square sections under axial compression at different stages of fire exposure including heating, cooling and post-fire. The post-fire material models used by Yang et al. (2008) were employed in the nonlinear analysis. The model was utilized to predict the post-fire resistance of tested CFST short columns without initial loads and after being exposed to high temperatures. However, the local buckling of square and rectangular CFST columns was not included in the simulation of the post-fire structural behavior.

Yao and Hu (2015) presented an interaction approach to model the post-fire residual strength of square and circular CFST columns after being subjected to different temperatures cases including the standard fire curve ISO-834, the natural fire curve and steady state temperatures. A 3D model was created by utilizing the ABAQUS package

that employed the post-fire material models described by Han et al. (2002). The model of finite elements was utilized to study the influence of material properties, load ratio and cross-sectional dimensions on the structural responses. An analytical approach was proposed for simple calculations of the residual capacities of CFST short columns after being exposed to fire. It was observed that the local buckling of steel tubes was not included in the finite element analysis.

Ibanez et al. (2018) extended the fiber-based finite element beam-column model proposed by Ibanez et al. (2013) for the nonlinear modeling of loaded slender CFST circular columns under fire exposure to the simulation of their post-fire structural behavior. The method of fiber elements was employed to divide the column cross-section into fiber elements while finite elements were used to mesh the column along its length. The CFST column was simulated by means of modeling the hollow steel tubular column and concrete column separately but they were connected at the nodes by link elements transversely as well as longitudinally. The gap conductance at the concrete-steel interface and concrete moisture content were taken into consideration in the finite element formulation. After verification against post-fire test data, the finite element model was utilized to examine the post-fire structural performance by means of conducting a parametric study. It was pointed out that it was important to include the preload on the CFST slender columns in their post-fire simulations in order to yield realistic results.

2.6 CONCLUDING REMARKS

This chapter has presented a review on publications that are most relevant to the current research project. These included experimental and computational investigations on the critical local-buckling as well as post-local buckling of thin steel plates at ambient and high temperatures, axially and eccentrically loaded CFST columns exposed to ambient and high temperatures, and the post-fire structural responses of CFST columns after being exposed to fire.

The literature review has identified the following areas that need further research:

- (1) Analytical models have not been developed for computing the critical local-buckling stresses as well as post-local buckling strengths of thin-walled steel tubes in rectangular CFST columns under fire exposure;
- (2) Local and post-local buckling has not been incorporated in most of the existing numerical techniques for the fire and post-fire simulations of square and rectangular CFST stub columns;
- (3) The local-global interaction buckling has not been incorporated in computational models using the method of fiber analysis for the predictions of the fire performance of CFST slender columns;
- (4) The air gap at interface of steel and concrete has not been included in most of the existing fiber models for the thermal simulation of CFST columns; and
- (5) The deformations induced by preloads have not been accounted for in the fiber-based numerical models for slender CFST columns exposed to fire.

Chapter 3

LOCAL AND POST-LOCAL BUCKLING OF STEEL PLATES AT ELEVATED TEMPERATURES

3.1 INTRODUCTION

This chapter presents the nonlinear inelastic finite element analyses of clamped steel plates subjected to non-uniform in-plane compressive stresses in CFST columns exposed to elevated temperatures. The finite element software ANSYS is used to develop a finite element model for the nonlinear analysis of steel plates at high temperatures incorporating residual stresses and initial geometric imperfections. The thermal and mechanical properties of steel at high temperatures recommended in Eurocode 3 is utilized in the finite element model. The model is validated by comparisons with solutions provided by other researchers. The local and post-local buckling behavior and strength of thin steel plates with various parameters exposed to various high temperatures is investigated by the finite element model. Based on the numerical results, equations are proposed for predicting the initial local buckling stresses, post-local buckling strength and effective widths of steel plates under high temperature exposure.

This chapter includes the following paper:

Kamil, G. M., Liang, Q. Q. and Hadi, M. N. S. (2018) Local buckling of steel plates in concrete-filled steel tubular columns at elevated temperatures, *Engineering Structures*, 168: 108-118.

GRADUATE RESEARCH CENTRE

DECLARATION OF CO-AUTHORSHIP AND CO-CONTRIBUTION: PAPERS INCORPORATED IN THESIS BY PUBLICATION

This declaration is to be completed for each conjointly authored publication and placed at the beginning of the thesis chapter in which the publication appears.

1. PUBLICATION DETAILS (to be completed by the candidate)

Title of Paper/Journal/Book:	Kamil, G. M., Liang, Q. Q. and Hadi, M. N. S. (2018) Local buckling of steel plates in concrete-filled steel tubular columns at elevated temperatures, Engineering Structures, 168:108-118.		
Surname:	Kamil	First name:	Ghanim
College:	College of Engineering & Science	Candidate's Contribution (%):	70
Status:			
Accepted and in press:	<input type="checkbox"/>	Date:	
Published:	<input checked="" type="checkbox"/>	Date:	1 August 2018

2. CANDIDATE DECLARATION

I declare that the publication above meets the requirements to be included in the thesis as outlined in the HDR Policy and related Procedures – policy.vu.edu.au.

	28/02/2019
Signature	Date

3. CO-AUTHOR(S) DECLARATION

In the case of the above publication, the following authors contributed to the work as follows:

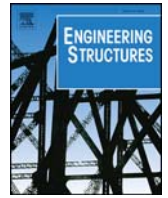
The undersigned certify that:

1. They meet criteria for authorship in that they have participated in the conception, execution or interpretation of at least that part of the publication in their field of expertise;
2. They take public responsibility for their part of the publication, except for the responsible author who accepts overall responsibility for the publication;
3. There are no other authors of the publication according to these criteria;
4. Potential conflicts of interest have been disclosed to a) granting bodies, b) the editor or publisher of journals or other publications, and c) the head of the responsible academic unit; and

5. The original data will be held for at least five years from the date indicated below and is stored at the following location(s):

Location: College of Engineering and Science, Victoria University, Melbourne, Victoria, Australia.

Name(s) of Co-Author(s)	Contribution (%)	Nature of Contribution	Signature	Date
Ghanim Mohammed Kamil	70	Developed and verified the model Conducted the parametric study Drafted the manuscript	[Redacted Signature]	28/02/ 2019
Qing Quan Liang	20	Provided initial concepts Provided critical revision of the article Final approval and submitting the manuscript	[Redacted Signature]	28/02/ 2019
Muhammad N. S. Hadi	10	Provided critical revision of the article Final approval of the manuscript	[Redacted Signature]	28/2/ 2019



Local buckling of steel plates in concrete-filled steel tubular columns at elevated temperatures

Ghanim Mohammed Kamil^a, Qing Quan Liang^{a,*}, Muhammad N.S. Hadi^b

^a College of Engineering and Science, Victoria University, PO Box 14428, Melbourne, VIC 8001, Australia

^b School of Civil, Mining and Environmental Engineering, University of Wollongong, Wollongong, NSW 2522, Australia

ARTICLE INFO

Keywords:

Concrete-filled steel tubes
Effective width
Elevated temperatures
Finite element analysis
Local buckling
Post-local buckling

ABSTRACT

Local buckling remarkably reduces the strength of steel plates in rectangular thin-walled concrete-filled steel tubular (CFST) columns at ambient temperature. This effect is more remarkable at elevated temperature. However, there have been very limited experimental and numerical investigations on the local and post-local buckling behavior of steel plates in CFST columns at elevated temperatures. This paper presents numerical studies on the local and post-local buckling behavior of thin steel plates under stress gradients in rectangular CFST columns at elevated temperatures. For this purpose, finite element models are developed, accounting for geometric and material nonlinearities at elevated temperatures. The initial geometric imperfections and residual stresses presented in steel plates are considered. Based on the finite element results, new formulas are proposed for determining the initial local buckling stress and post-local buckling strength of clamped steel plates under in-plane stress gradients at elevated temperatures. Moreover, new effective width formulas are developed for clamped steel plates at elevated temperatures. The proposed formulas are compared with existing ones with a good agreement. The effective width formulas developed are used in the calculations of the ultimate axial loads of rectangular CFST short columns exposed to fire and the results obtained are compared well with the finite element solutions provided by other researchers. The initial local buckling and effective width formulas can be implemented in numerical techniques to account for local buckling effects on the responses of rectangular thin-walled CFST columns at elevated temperatures.

1. Introduction

Filling concrete into a rectangular thin-walled steel tubular column as shown in Fig. 1 results in a significant increase in its ultimate strength and fire resistance as reported by Schneider [1], Sakino et al. [2], Liang et al. [3] and Dundu [4]. However, the thin steel tube walls of a rectangular concrete-filled steel tubular (CFST) column under applied loads may undergo outward local buckling, which remarkably reduces the strength of the column as discussed by Liang [5]. In a fire condition, the strength and stiffness of steel plates decrease significantly with an increase in the elevated temperature [6,7]. As a result, the local buckling of thin steel plates at elevated temperatures is more likely to occur than the ones at ambient temperatures. In addition, the local and post-local buckling strengths of a thin steel plate at elevated temperature are much lower than those of the plate at ambient temperature. It is assumed that the steel tube walls of a rectangular CFST column under axial load and bending have a clamped boundary condition that recognizes the restraint provided by the rigid concrete core and are subjected to in-plane stress gradients [5]. The CFST

columns have been widely used in high-rise composite buildings that could be exposed to fire. The behavior of CFST columns at elevated temperatures has been investigated by researchers [8–11]. However, little attention has been devoted to the study of the local and post-local buckling problem of clamped steel plates under stress gradients in CFST columns at elevated temperatures. Therefore, this paper addresses this challenging problem.

The local and post-local buckling behavior of steel plates under edge stresses at ambient temperature has been investigated by many researchers [12–17]. Shanmugam et al. [16] presented an analytical study on the post-local buckling strengths of steel plates in thin-walled steel box columns under biaxial loads. The steel plates of the hollow steel box column were assumed to be simply-supported. Effective width expressions were proposed by Shanmugam et al. [16] for calculating the post-local buckling strengths of simply-supported steel plates under stress gradients. Uy and Bradford [18] and Uy [19] conducted experiments to examine the local buckling characteristics of thin steel plates in rectangular CFST columns. Liang et al. [20] developed nonlinear finite element models to study the critical local and post-local buckling

* Corresponding author.

E-mail address: Qing.Liang@vu.edu.au (Q.Q. Liang).

<https://doi.org/10.1016/j.engstruct.2018.04.073>

Received 30 October 2017; Received in revised form 19 March 2018; Accepted 20 April 2018
0141-0296/ © 2018 Elsevier Ltd. All rights reserved.

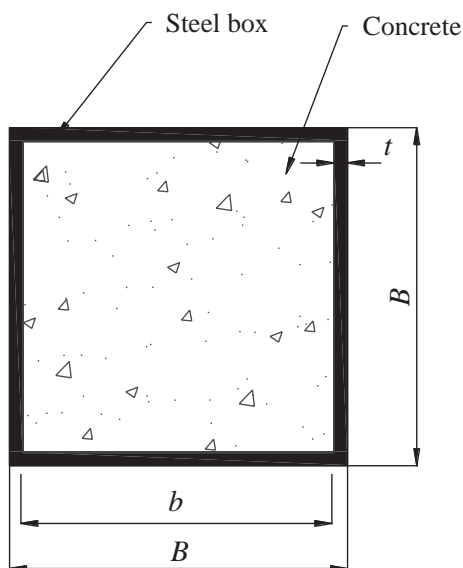


Fig. 1. Cross-section of square CFST beam-column.

strengths of steel plates in biaxially loaded CFST columns where the steel tube walls could be subjected to stress gradients. They proposed design formulas for computing the critical local and post-local buckling strengths of clamped steel plates under stress gradients. Moreover, effective width formulas were developed by Liang et al. [20] and implemented in numerical models by Liang [21,22] to account for local buckling effects on the strength and ductility of rectangular CFST columns.

Thin steel plates at elevated temperatures are more susceptible to local buckling because the elevated temperatures significantly reduce their stiffness and strength [7,23]. Heidarpour and Bradford [24] used a spline finite strip method of buckling analysis to investigate the local buckling of flange outstands subjected to elevated temperatures and proposed the plasticity and yield slenderness limits. The local buckling temperatures of plates under certain boundary conditions were also anticipated. Knoblock [7] investigated the local buckling behavior of steel sections at elevated temperatures. He suggested that the methods commonly used for calculating the strength of steel sections and for section classification subjected to elevated temperatures should be revised. Couto et al. [25] used a finite element analysis software to study the local buckling of simply-supported steel plates at elevated temperatures. These steel plates were subjected to in-plane bending or compressive edge stresses. The residual stress pattern at ambient temperatures was assumed for the plates at elevated temperatures. A constant initial geometric imperfection at the plate center was considered regardless of the plate thickness. Design formulas were proposed for determining the ultimate strength of simply-supported plates at elevated temperatures. Quiel and Garlock [26] utilized the computer program SAFIR to determine the local buckling strengths of steel plates exposed to fire. The loaded edges of the steel plate were assumed to be simply-supported while the unloaded edges were either simply-supported or fixed. However, the effect of residual stresses was not considered in their study. They proposed expressions for estimating the ultimate strengths of steel plates with various boundary conditions.

However, none of the studies reported in the literature investigated the local and post-local buckling behavior of clamped steel plates under stress gradients in CFST columns at elevated temperatures. There is a lack of effective width formulas for steel plates that could be incorporated in numerical models to account for local buckling effects on the strength of rectangular thin-walled CFST columns at elevated temperatures. Therefore, to bridge the knowledge gap, this paper utilizes the finite element program ANSYS 16 [27] to study the local and

post-local buckling behavior of clamped steel plates under stress gradients in rectangular CFST columns at elevated temperatures. The effects of residual stresses and initial geometric imperfections presented in the steel plates are taken into account. Based on the results obtained from the nonlinear finite element analyses, design formulas are proposed for determining the initial local and post-local buckling strengths of clamped steel plates under stress gradients at elevated temperatures and verified by comparisons with the ones proposed by other researchers and with finite element results on rectangular CFST short columns at elevated temperatures.

2. Nonlinear finite element analysis of plates

2.1. General

The finite element analysis program ANSYS 16 [27] was employed in the present study to investigate the critical local and post-local buckling strengths of steel plates in CFST columns at elevated temperatures. The steel tube walls of a rectangular CFST column under compression can only buckle locally outward due to the restraint provided by the concrete core. This restraint effect was considered in the finite element model by incorporating an initial geometric imperfection caused by the lateral pressure applied on the plate. This implies that the steel plate can only buckle locally outward in the nonlinear analysis. The local and post-local buckling of steel plates in CFST columns at ambient temperatures has been studied by Liang et al. [20] and the effective width formulas proposed by them have been incorporated in the fiber element models to accurately account for local buckling effects on the behavior of CFST columns by Liang [21,22]. As suggested by Liang et al. [20], the four edges of the steel tube wall were treated as clamped due to the restraint provided by the rigid concrete core. The boundary conditions of the clamped plate are schematically depicted in Fig. 2. A square steel plate was chosen to simulate the webs and flanges of a CFST column at elevated temperatures. The von Mises yield criterion was used in the material models to treat the material plasticity. The four-node shell/plate element SHELL 181 in ANSYS 16 was used to discretize the steel plate into a 20×20 mesh. The sensitivity analysis of the element size was conducted and the results obtained are shown in Fig. 3, which indicates that the 20×20 mesh is suitable in terms of the computational time and the accuracy of the results.

2.2. Applied edge stresses on steel plates

The two adjacent steel tube walls of a rectangular CFST columns under axial load and biaxial bending may be subjected to non-uniform compressive stresses while the other two adjacent walls are under in-

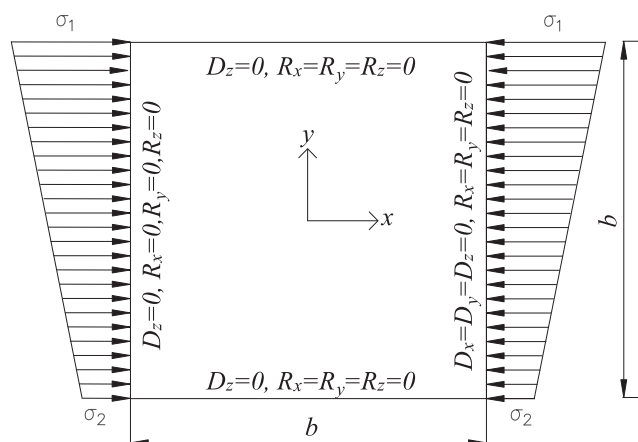


Fig. 2. Boundary conditions of clamped steel plate under compressive edge stresses.

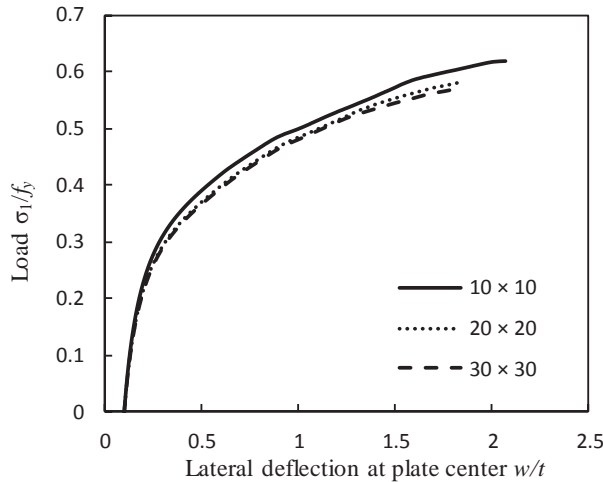


Fig. 3. Sensitivity analysis of element size on the load-deflection curves of square steel plate under uniform edge compression.

plane bending stresses as discussed by Liang et al. [20], Liang [21,22] and Liang [5]. Fig. 2 illustrates a steel plate under non-uniform edge compressive stresses. For a rectangular CFST column under axial compression, its four steel tube walls are subjected to uniform compressive stresses. The top flange of the CFST column under uniaxial bending is in uniform compression while other steel tube walls are subjected to either tension or in-plane bending stresses. The stress gradient coefficient is used to define the stress ratio of the non-uniform compressive stresses on the steel plate. The stress gradient is maintained by the applied edge stresses on the plate as shown in Fig. 2. Only steel plates under compressive edge stresses are considered in the present study.

2.3. Geometric imperfections

The initial geometric imperfections have a significant effect on the local buckling of thin steel plates. Feng et al. [28] conducted numerical analyses to examine the effect of initial geometric imperfections on the ultimate strengths of rectangular cold-formed hollow steel columns exposed to uniform elevated temperatures. They concluded that the magnitude of the initial imperfection had a remarkable effect on the strength of the hollow steel columns. Liang et al. [20] used an initial geometric imperfection of $0.1t$ (where t is the plate thickness) at the plate center in the nonlinear local and post-local buckling analyses of steel plates at ambient temperatures. Quiel and Garlock [26] examined the effects of initial geometric imperfections of $0.1t$ and $b/200$ (where b is the plate width) on the buckling strengths of steel plates at elevated temperatures. The numerical results obtained indicated that there were not much differences between the buckling strengths predicted using these two initial geometric imperfections. Couto et al. [25] considered an initial geometric imperfection of $80\% b/t$ for the steel plates in their models. In the present study, the initial geometric imperfection at the plate center was taken as $0.1t$. A lateral uniform pressure was applied to the plate to induce the required initial geometric imperfection. The value of the lateral pressure was determined by a trial-and-error method and by conducting a nonlinear analysis on the plate until the $0.1t$ deflection at the plate center was obtained.

2.4. Residual stresses

The residual stress pattern depicted in Fig. 4 was applied to the steel plate as suggested by Liang et al. [20] and Abambres and Quach [29]. The tensile residual stresses were presented at the welds while the rest of the plate was subjected to the compressive residual stresses. The compressive residual stress was taken as 25% of the steel yield strength.

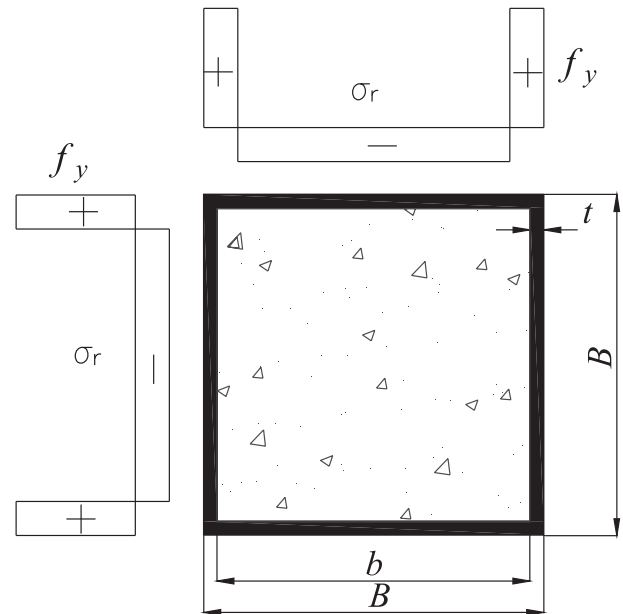


Fig. 4. Residual stress pattern in CFST beam-column.

In the finite element model, the residual stresses were applied to the steel plate by prestresses. Research studies indicated that the residual stresses locked in the steel plate were released at a temperature above $400\text{ }^\circ\text{C}$ [30–34]. Therefore, the residual stresses were not considered for steel plates at temperatures above $400\text{ }^\circ\text{C}$ in the present study.

2.5. Stress-strain relationships for steels at elevated temperatures

The stress-strain relationships given in Eurocode 3 [35] were adopted in the finite element model to simulate the material behavior of steel plates at elevated temperatures. Fig. 5 depicts the stress-strain curve for structural steels without strain hardening at elevated temperatures, which is expressed by

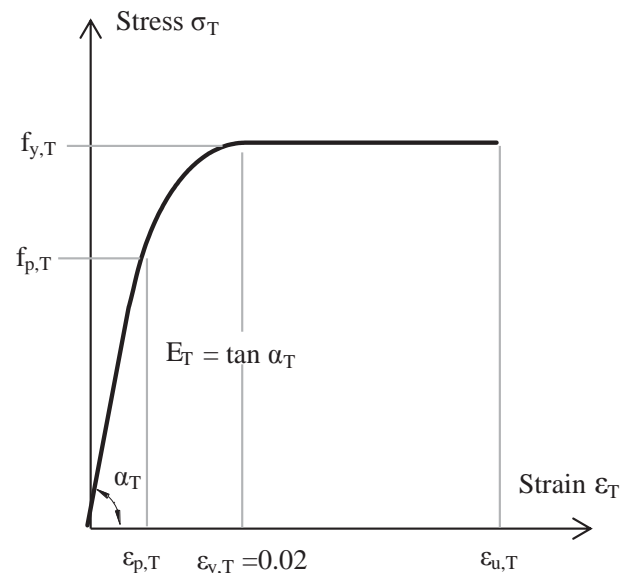


Fig. 5. Typical strain-stress curve of structural steel at elevated temperatures based on Eurocode 3 [35].

$$\sigma_T = \begin{cases} E_T \varepsilon_T & \text{for } \varepsilon_T \leq \varepsilon_{p,T} \\ (f_{p,T} - h_3) + \frac{h_2}{h_1} \sqrt{h_1^2 - (\varepsilon_{y,T} - \varepsilon_T)^2} & \text{for } \varepsilon_{p,T} \leq \varepsilon_T \leq \varepsilon_{y,T} \\ f_{y,T} & \text{for } \varepsilon_{y,T} \leq \varepsilon_T \leq \varepsilon_{u,T} \end{cases} \quad (1)$$

where

$$h_1^2 = (\varepsilon_{y,T} - \varepsilon_{p,T})(\varepsilon_{y,T} - \varepsilon_{p,T} + h_3/E_T) \quad (2)$$

$$h_2^2 = E_T(\varepsilon_{y,T} - \varepsilon_{p,T})h_3 + h_3^2 \quad (3)$$

$$h_3 = \frac{(f_{y,T} - f_{p,T})^2}{E_T(\varepsilon_{y,T} - \varepsilon_{p,T}) - 2(f_{y,T} - f_{p,T})} \quad (4)$$

where E_T is the elastic modulus of steel, $f_{p,T}$ is the proportional limit, $f_{y,T}$ is the effective yield strength, $\varepsilon_{p,T}$ is the strain corresponding to $f_{p,T}$, $\varepsilon_{y,T}$ is the yield strain, and $\varepsilon_{u,T}$ is the ultimate strain at elevated temperatures.

The strain hardening is considered for structural steels at temperatures less than 300 °C using the following equation [35]:

$$\sigma_T = [(f_{u,T} - f_{y,T})/0.02]\varepsilon_T - f_{u,T} + 2f_{y,T} \quad \text{for } 0.02 < \varepsilon_T < 0.04 \quad (5)$$

For $\varepsilon_T \geq 0.04$, σ_T equals to the ultimate tensile strength of the steel at elevated temperature.

Elevated temperatures significantly reduce the material properties of structural steels. The reduction factors applied to the material properties of structural steels at elevated temperatures given in Eurocode 3 [35] are shown in Fig. 6, where $k_{p,T}$ is the reduction factor of the proportional limit, $k_{y,T}$ is the reduction factor of the yield strength, $k_{0.2p,T}$ is the reduction factor of the proof stress, $k_{E,T}$ is the reduction factor of the Young’s modulus, $k_{u,T}$ is the reduction factor of the ultimate tensile strength.

2.6. Verification of the finite element model

Before utilizing the finite element model to investigate the local and post-local buckling behavior of steel plates at elevated temperatures, comparisons have been made to verify the finite element model at both ambient and elevated temperatures. A rectangular simply-supported steel plate with an initial imperfection of $0.1t$ at ambient temperature reported by Quiel and Garlock [26] was analysed. The ultimate strength curve of the steel plate obtained by the finite element analysis is compared with that given by Quiel and Garlock [26] in Fig. 7. The figure shows that a good agreement between these two solutions is obtained. A nonlinear finite element analysis on a simply-supported rectangular steel plate with a/b ratio of 5 (where a is the plate length)

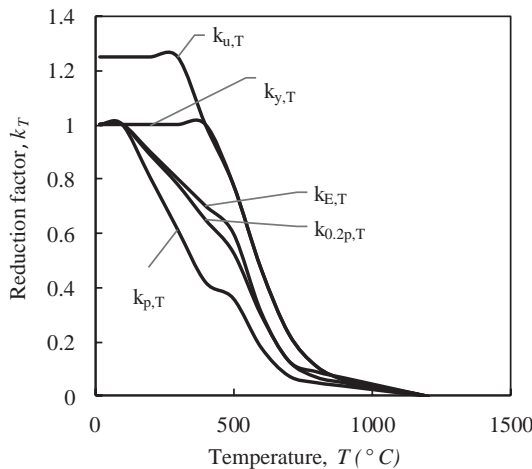


Fig. 6. Reduction factors k_T for stress-strain relationships allowing for strain-hardening of structural steel at elevated temperatures based on Eurocode 3 [35].

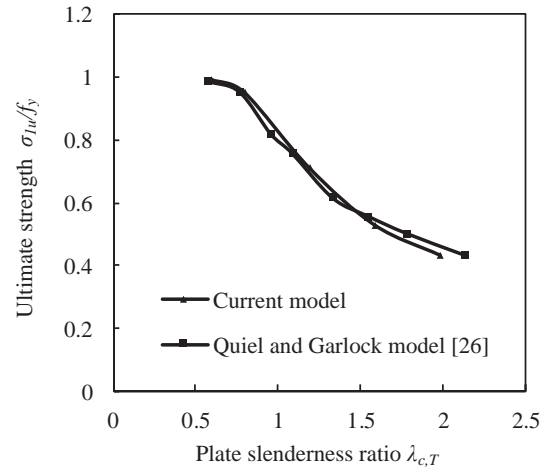


Fig. 7. Comparison of plate strength curves at ambient temperature predicted by the current model and Quiel and Garlock model [26].

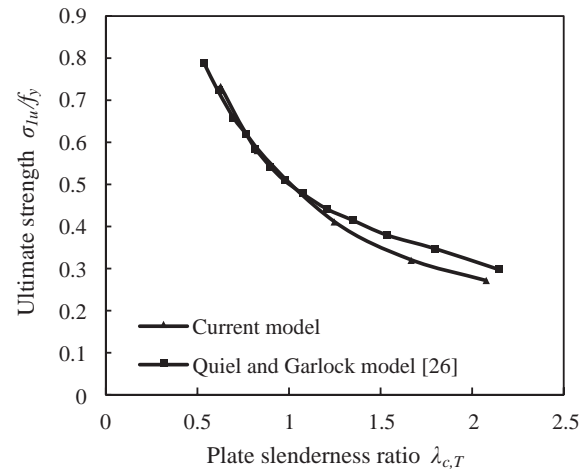


Fig. 8. Comparison of plate strength curves at temperature 700 °C predicted by the current model and Quiel and Garlock model [26].

and initial geometric imperfection of $0.1t$ and no residual stresses at an elevated temperature of 700 °C was performed. It can be seen from Fig. 8 that the finite element model predicts well the performance of the steel plates with various slenderness ratios at elevated temperature.

3. Post-local buckling behavior at elevated temperatures

The nonlinear finite element model developed was employed to investigate the local and post-local behavior of clamped steel plates at temperatures ranging from 20 to 700 °C and subjected to in-plane stress gradients as shown in Fig. 2. Four temperature levels were considered in addition to the ambient temperature, which were 200, 400, 600, and 700 °C. The square steel plates of 500 × 500 mm with initial geometric imperfections of $0.1t$ and b/t ratios ranging from 30 to 110 with an increment of 10 were considered. The stress gradient coefficient (α) is defined as the ratio of the minimum edge stress to the maximum edge stress. The stress gradient coefficient (α) varied from 0.0 to 1.0 with an increment of 0.2. The yield strength of steel plates at ambient temperature was 300 MPa and the Young’s modulus was 210 GPa. At elevated temperatures, the reduction coefficients for the material properties given in Eurocode 3 [35] were used. The typical local and post-local buckling modes of steel plates under uniform edge compressive stresses at elevated temperatures are shown in Fig. 9.

Figs. 10 and 11 show the load-lateral deflection curves for the steel

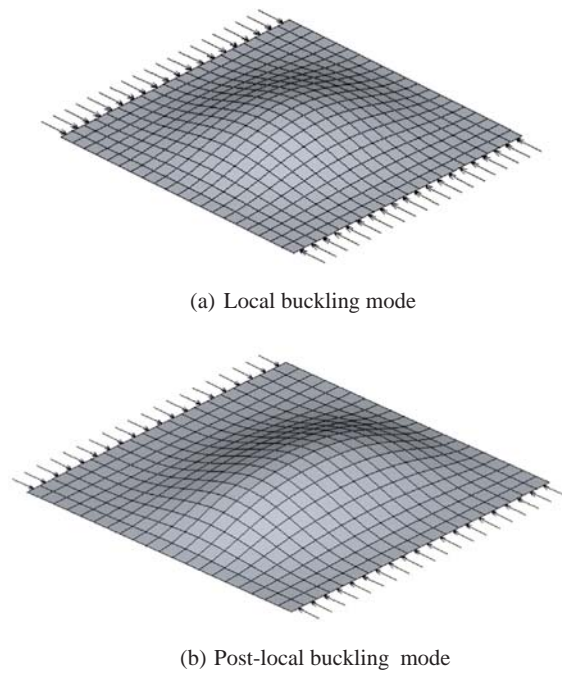


Fig. 9. Buckling modes of clamped square steel plate under uniform edge compression at elevated temperatures.

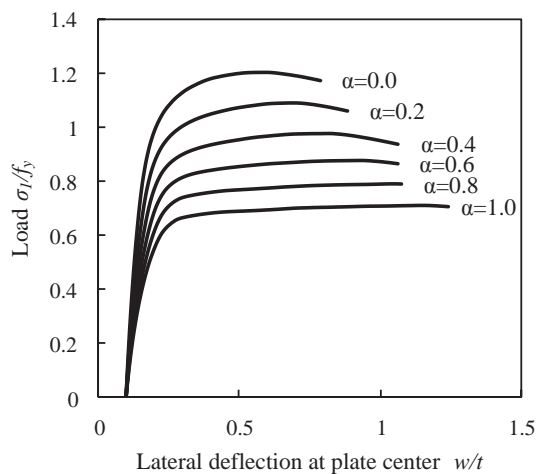


Fig. 10. Load-deflection curves for steel plates with $b/t = 70$ under stress gradients at ambient temperature.

plate with a b/t ratio of 70 subjected to stress gradients at ambient temperature and 600 °C, respectively. It appears that the post-local buckling strength or the ultimate strength of the steel plate decreases with an increase in the stress gradient coefficient α regardless of the temperature levels. However, for the plate under the same stress gradient, increasing the temperature significantly reduces its post-local buckling strength. It can be observed from Figs. 10 and 11 that at both temperature levels, the steel plate under uniform edge stresses ($\alpha = 1.0$) could not attain its yield strength due to the effects of initial geometric imperfection, residual stresses and the deterioration of material properties at elevated temperatures. When the stress gradient coefficient is small and the temperature is low, the post-local buckling strength of the steel plate with a small b/t ratio may be higher than its yield strength. This is attributed to the strain hardening of the steel material as reported by Usami [14,15] and Liang et al. [20].

Fig. 12 shows load-lateral deflection curves for steel plates with $b/t = 80$ subjected to uniform edge stresses at different temperatures. It

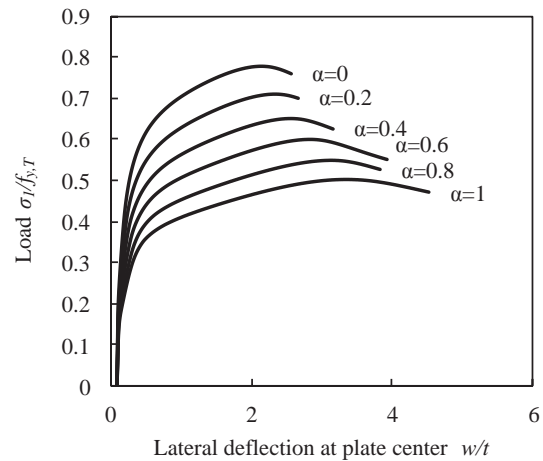


Fig. 11. Load-deflection curves for steel plates with $b/t = 70$ under stress gradients at temperature 600 °C.

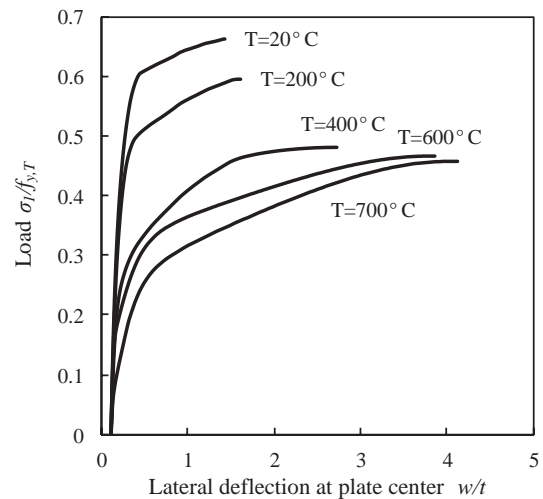


Fig. 12. Effect of temperatures on the load-deflection curves for steel plates with $b/t = 80$ under uniform edge compression.

can be seen from the figure that the post-local buckling strength of steel plates decreases significantly with an increase in the temperature level. Moreover, increasing the temperature remarkably reduces the flexural stiffness of the steel plate. The ultimate strength curves of steel plates at ambient temperature and temperatures of 200 °C, 400 °C and 700 °C are shown in Figs. 13–17, respectively. It appears that the post-local buckling strength of clamped steel plates generally decreases with increasing their slenderness ratios regardless of the temperature levels and stress gradients. Under the same temperature level, increasing the stress gradient coefficient significantly reduces the post-local buckling strength of the steel plate. Furthermore, for a steel plate with the certain b/t ratio and stress gradient, its post-local buckling strength is shown to be reduced by increasing the temperature. When the temperature level increases from 20 °C to 700 °C, the ultimate strength of steel plates decreases from $0.804f_y$ to $0.55f_{y,T}$.

4. Critical local buckling strengths at elevated temperatures

As shown in Figs. 10–12, it is obvious that there is no way to determine the initial local buckling stress of a steel plate because of geometric imperfections. The method presented by Liang et al. [20] was utilized to predict the initial local buckling stress of steel plates with imperfections. In this method, the non-dimensional central lateral deflection versus the ratio of the deflection to the applied load is plotted

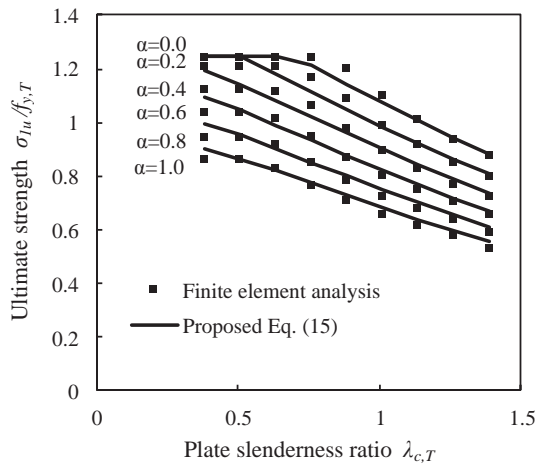


Fig. 13. Ultimate strengths of steel plates at ambient temperature.

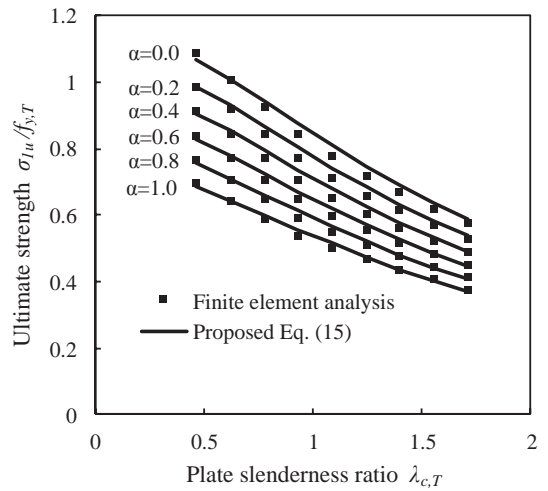


Fig. 16. Ultimate strengths of steel plates at temperature of 600 °C.

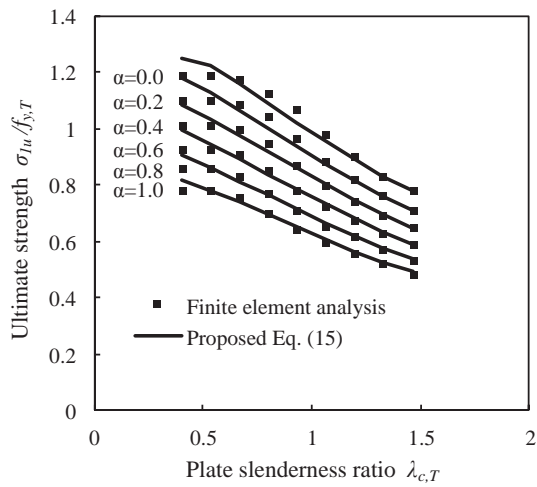


Fig. 14. Ultimate strengths of steel plates at temperature of 200 °C.

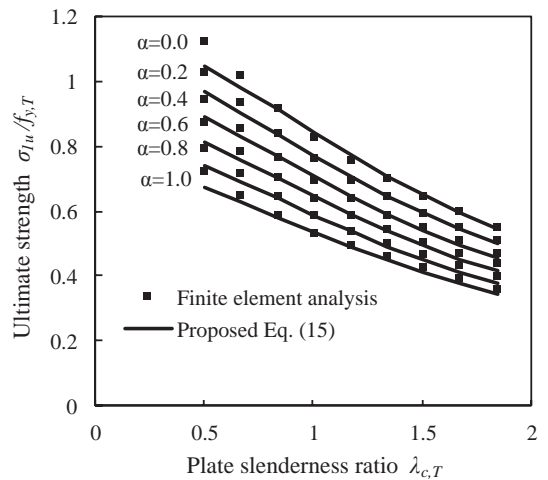


Fig. 17. Ultimate strengths of steel plates at temperature of 700 °C.

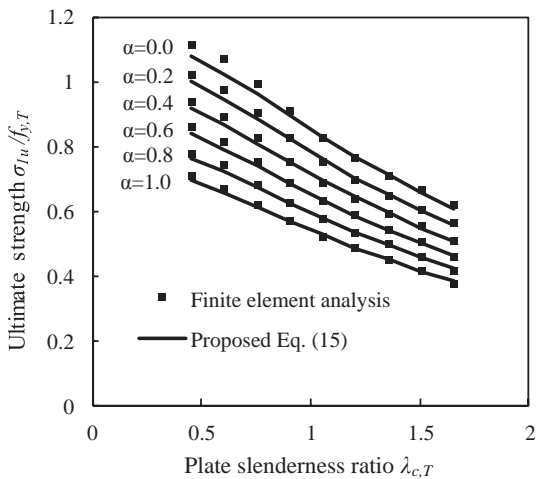


Fig. 15. Ultimate strengths of steel plates at temperature of 400 °C.

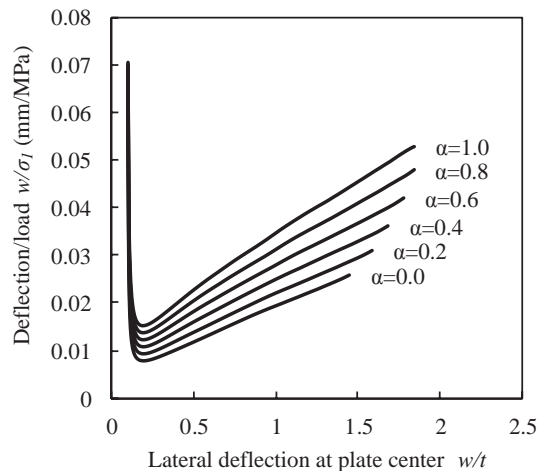


Fig. 18. Load-deflection curves for determining the critical local buckling strengths of steel plates with b/t ratio of 100 at ambient temperature.

as shown in Figs. 18 and 19 for steel plates with a b/t ratio of 100 at ambient temperature and at 600 °C, respectively. The minimum value on the curve represents the onset of the critical local buckling of the plate. It can be observed from Figs. 18 and 19 that the general trend of the curves is that the w/σ_1 ratio of the plate decreases with an increase in its lateral deflection at the plate center. This is because the lateral

deflection of the plate at the initial loading stages is small before initial local buckling. After reaching the minimum, however, the w/σ_1 ratio increases significantly with increasing the lateral deflection. This is attributed to the fact that after the onset of the plate local buckling, the plate undergoes large deflections under the load increments. It appears

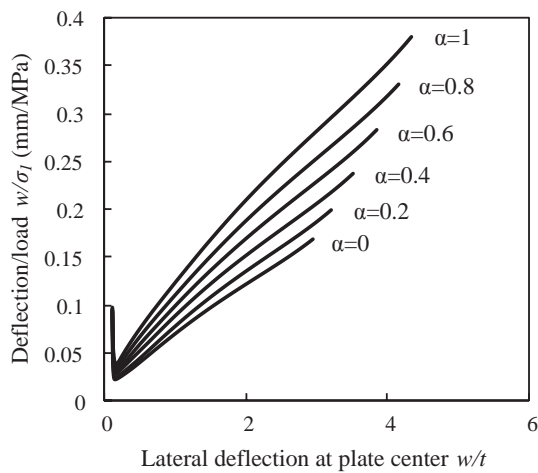


Fig. 19. Load-deflection curves for determining the critical local buckling strengths of steel plates with b/t ratio of 100 at temperature of 600 °C.

that the minimum w/σ_1 ratio indicates the onset of local buckling. For a steel plate under the same stress gradient and lateral deflection, the w/σ_1 ratio at elevated temperature is higher than that at ambient temperature. This means that at the same deflection the critical local buckling stress of the plate decreases with increasing the temperature level. This is reasonable because increasing the temperature reduces the material properties and strength.

The critical local buckling strengths of steel plates subjected to various temperature levels as a function of the relative slenderness ratio are given in Figs. 20–24. It appears that the reduction in strength at any level of temperature increases with increasing the b/t ratio and stress gradient coefficient. The numerical results presented show that the elevated temperature significantly reduces the critical local buckling stress of steel plates. The local buckling strength of steel plates at the ambient temperature with a b/t ratio of 60 subjected to uniform edge stress is about $0.61f_y$, while at a temperature of 600 °C is about $0.181f_{y,T}$. As illustrated in Figs. 20–24, the stress gradient ratio has a significant effect on the critical buckling strength of plates especially at higher temperatures. The critical buckling strength decreases with increasing the stress gradient ratio.

5. Proposed design formulas

5.1. Design formulas for critical local buckling strengths

The factors that affect the local buckling behavior of clamped steel

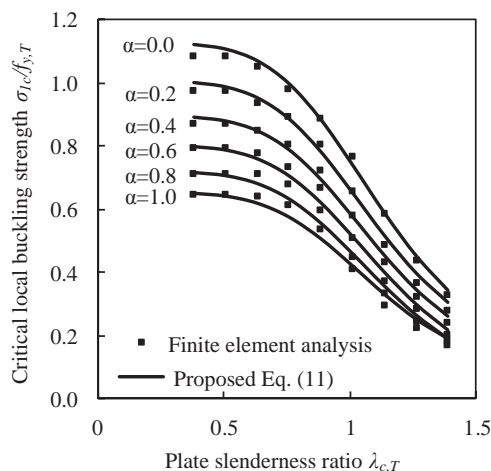


Fig. 20. Critical local buckling strengths of steel plates at ambient temperature.

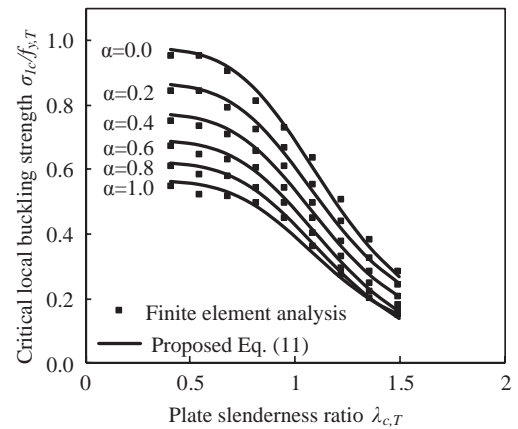


Fig. 21. Critical local buckling strengths of steel plates at temperature of 200 °C.

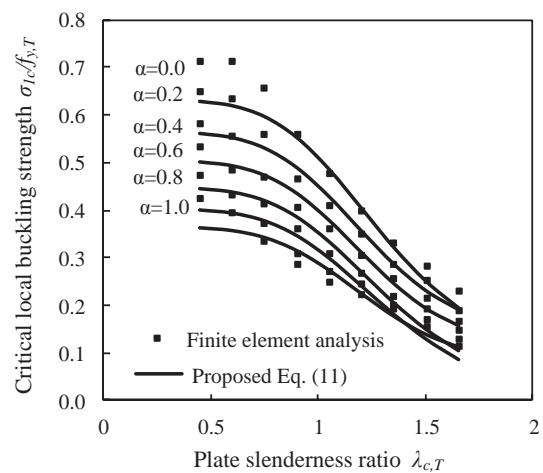


Fig. 22. Critical local buckling strengths of steel plates at temperature of 400 °C.

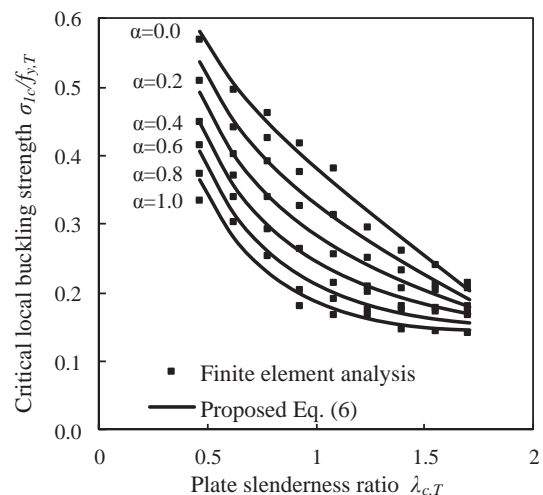


Fig. 23. Critical local buckling strengths of steel plates at temperature of 600 °C.

plates with an initial imperfection of $0.1t$ and residual stresses include the b/t ratio, stress gradient coefficient (α), and the yield strength of steel plate at ambient and elevated temperatures. It is worth to mention that the b/t ratio has been replaced with the non-dimensional slenderness ratio ($\lambda_{c,T}$) for comparison purposes. Based on the results

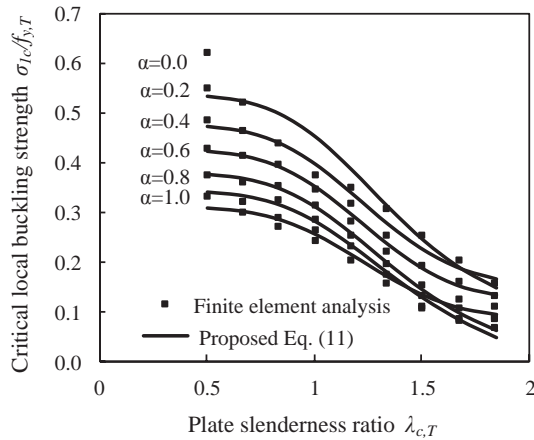


Fig. 24. Critical local buckling strengths of steel plates at temperature of 700 °C.

obtained from the nonlinear finite analyses, design formulas for determining the critical local buckling strengths of clamped steel plates under stress gradients have been proposed and presented herein.

For steel plates at temperature of 600 °C, the critical local buckling stresses of the plates is proposed as

$$\frac{\sigma_{1c,T}}{f_{y,T}} = (0.1916\lambda_{c,T}^{-0.7661} + 0.003889)(m_1\lambda_{c,T}^2 + m_2\lambda_{c,T} + m_3) \quad (6)$$

where $\sigma_{1c,T}$ is the critical local buckling strength of the steel plate at elevated temperatures, and $\lambda_{c,T}$ is the plate slenderness ratio at elevated temperature, which is expressed by

$$\lambda_{c,T} = \sqrt{\frac{12(1-\nu^2)(b/t)^2(k_{y,T}f_y)}{k\pi^2(k_{E,T}E)}} \quad (7)$$

in which ν is the Poisson's ratio, f_y is the steel yield strength at ambient temperature, $k = 9.95$ is the elastic local buckling coefficient and E is the Young's modulus of steel material at ambient temperature.

The coefficients m_1 , m_2 and m_3 in Eq. (6) are given as

$$m_1 = -1.0685\alpha^2 + 2.275\alpha - 0.8969 \quad (8)$$

$$m_2 = 2.3075\alpha^2 - 4.7791\alpha + 1.8475 \quad (9)$$

$$m_3 = -0.825\alpha^2 + 1.086\alpha + 1.0083 \quad (10)$$

For any other temperatures, the critical local buckling stress of steel plates is proposed as

$$\frac{\sigma_{1c,T}}{f_{y,T}} = (g_1\lambda_{c,T}^g + g_2) \frac{0.6566\lambda_{c,T}^{0.001521} \left(\frac{k_{p,T}}{k_{y,T}}\right)^{-0.1598}}{0.5415\lambda_{c,T}^{4.889} + \left(\frac{k_{p,T}}{k_{y,T}}\right)^{-0.8252}} \quad (11)$$

where the coefficients g , g_1 and g_2 are

$$g = -7.9339\alpha^2 + 11.29\alpha + 4.701 \quad (12)$$

$$g_1 = 0.0863\alpha^2 - 0.1248\alpha + 0.0431 \quad (13)$$

$$g_2 = 0.2656\alpha^2 - 0.9902\alpha + 1.719 \quad (14)$$

The critical buckling strengths of thin steel plates under stress gradients at various temperatures calculated using the proposed formulas are compared with those obtained from the nonlinear finite element analyses in Figs. 20–24. It can be observed that good agreement between these two solutions is obtained.

5.2. Design formulas for post-local buckling strengths

The post-local buckling strength of thin steel plates depends on the

plate slenderness ratio ($\lambda_{c,T}$), the stress gradient coefficient (α) and the level of temperature. Based on the results obtained from the finite element analyses, the design formula for determining the post-local buckling strengths of clamped thin steel plates in CFST columns is proposed as

$$\frac{\sigma_{1u,T}}{f_{y,T}} = (q_1\lambda_{c,T}^q) \frac{0.8418\lambda_{c,T}^{0.02368} \left(\frac{k_{p,T}}{k_{y,T}}\right)^{-0.3028} + 1.154 \left(\frac{k_{p,T}}{k_{y,T}}\right)}{2.055 + \lambda_{c,T}^{1.68}} \quad (15)$$

where $\sigma_{1u,T} \leq 1.25f_y$ for temperature less than 300 °C and q and q_1 are written as

$$q = 0.04007\alpha^2 - 0.05275\alpha + 0.03355 \quad (16)$$

$$q_1 = 0.1007\alpha^2 - 0.7027\alpha + 1.65 \quad (17)$$

The post-local buckling strengths of thin steel plates under stress gradients at various temperatures computed by using Eq. (15) are compared with those obtained from the nonlinear post-local buckling analyses in Figs. 13–17. The figures demonstrate that the proposed formula yields good predictions of the finite element results.

5.3. Effective width formulas

The effective width concept [36] is used to describe the post-local buckling behavior of thin steel plates in Eurocode 3 [35] and AISC [37] as illustrated in Fig. 25. In Eurocode 3, the effective width of steel plates at elevated temperatures is taken as that of the plates at ambient temperatures using the proof stress. Reduction factors are applied to the material properties due to high temperature effects. The AISC [37] uses a similar effective width approach to calculate the buckling strength of steel plates at elevated temperatures. The effective width formulas have been proposed for estimating the post-local buckling strengths of thin steel plates under different boundary conditions at ambient and elevated temperatures by various researchers. Liang et al. [20] proposed effective width formulas for clamped steel plates under stress gradients at ambient temperature. Quiel and Garlock [26] developed equations for computing the effective widths of steel plates under thermal loading where the two loaded edges were simply-supported. Couto et al. [25] presented an expression for determining the ultimate strengths of simply-supported steel plates at elevated temperatures. Effective width formulas can be implemented in the nonlinear analysis procedures to account for local buckling effects on the behavior of rectangular thin-walled CFST columns [21,22].

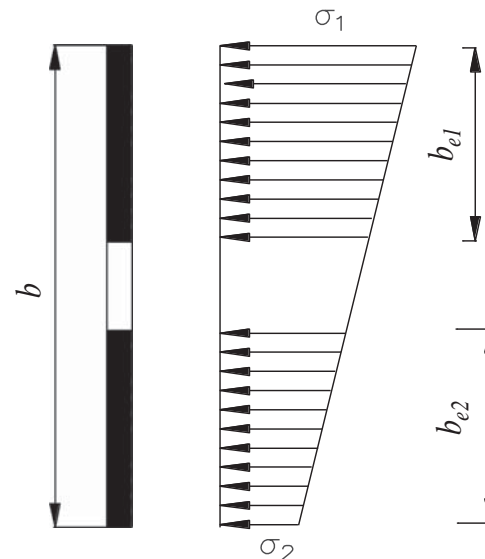


Fig. 25. Effective width of steel plate under stress gradient.

Based on the results obtained from the finite element analyses, the effective width formulas for clamped steel plate under stress gradients at any temperatures are proposed as follows:

$$\frac{b_{e1}}{b} = \frac{1}{2} (q_1 \lambda_{c,T}^q) \frac{0.8418 \lambda_{c,T}^{0.02368} \left(\frac{k_{p,T}}{k_{y,T}}\right)^{-0.3028} + 1.154 \left(\frac{k_{p,T}}{k_{y,T}}\right)}{2.055 + \lambda_{c,T}^{1.68}} \quad \text{for } \alpha > 0 \quad (18)$$

$$\frac{b_{e1}}{b} = \frac{1}{3} (q_1 \lambda_{c,T}^q) \frac{0.8418 \lambda_{c,T}^{0.02368} \left(\frac{k_{p,T}}{k_{y,T}}\right)^{-0.3028} + 1.154 \left(\frac{k_{p,T}}{k_{y,T}}\right)}{2.055 + \lambda_{c,T}^{1.68}} \quad \text{for } \alpha = 0 \quad (19)$$

$$\frac{b_{e2}}{b} = (1 + \phi) \frac{b_{e1}}{b} \quad (20)$$

in which b_{e1} and b_{e2} are the effective widths shown in Fig. 25, q and q_1 are defined in Eqs. (16) and (17) respectively, and $\phi = 1 - \alpha$.

6. Comparisons with existing formulas

The effective width formulas proposed in this study for steel plates at ambient and elevated temperatures are validated by comparisons of the predicted ultimate strengths with those computed using expressions provided by Liang et al. [20], Couto et al. [25] and Quiel and Garlock [26]. For clamped steel plates at ambient temperature, Liang et al. [20] proposed formulas for calculating the ultimate strength of steel plates in CFST columns under stress gradients as follow:

$$\frac{\sigma_{1u}}{f_y} = c_1 + c_2 \left(\frac{b}{t}\right) + c_3 \left(\frac{b}{t}\right)^2 + c_4 \left(\frac{b}{t}\right)^3 \quad (21)$$

where σ_{1u} is the ultimate strength corresponding to the maximum applied edge stress σ_1 and c_1, c_2, c_3 and c_4 are coefficients for every stress gradient ratio [20].

The expression for calculating the effective widths of steel plates at elevated temperatures presented by Quiel and Garlock [26] is written as

$$\frac{b_e}{b} = \frac{1.41}{\sqrt{\lambda_{c,T} \sqrt{k}}} \sqrt{\frac{k_{p,T}}{k_{y,T}}} \left(1 - \frac{0.96}{k \lambda_{c,T}^{0.5}}\right) < 1.0 \quad (22)$$

where k is taken as 4.0 for simply-supported plates and 7.0 for plates with two fixed unloaded edges and two simply-supported loaded edges [26].

Couto et al. [25] proposed an effective width formula for simply-supported steel plates at elevated temperatures as follow:

$$\frac{b_e}{b} = \frac{(\lambda_c + \alpha_T)^{\beta_T} - 0.055(3 + \alpha)}{(\lambda_c + \alpha_T)^{2\beta_T}} \leq 1.0 \quad (23)$$

where $\lambda_c = \sqrt{f_y / \sigma_{cr}}$ is the plate slenderness at ambient temperature, where σ_{cr} is the elastic local buckling of the plate at ambient temperature [5], and other parameters are defined as

$$\alpha_T = 0.9 - 0.315 \frac{k_{0.2p,T}}{\varepsilon_T} \quad (24)$$

$$\beta_T = 2.3 - 1.1 \frac{k_{0.2p,T}}{k_{y,T}} \quad (25)$$

$$\varepsilon_T = 0.85 \sqrt{235 / f_y} \quad (26)$$

The calculated ultimate strengths of thin steel plates under uniform edge compression at ambient temperature by using the proposed Eq. (15) are compared with those computed using formulas given by Liang et al. [20], and Quiel and Garlock [26] in Fig. 26. It can be observed that an excellent agreement between the strength curve computed by the proposed Eq. (15) and that given Liang et al. [20] is obtained. It

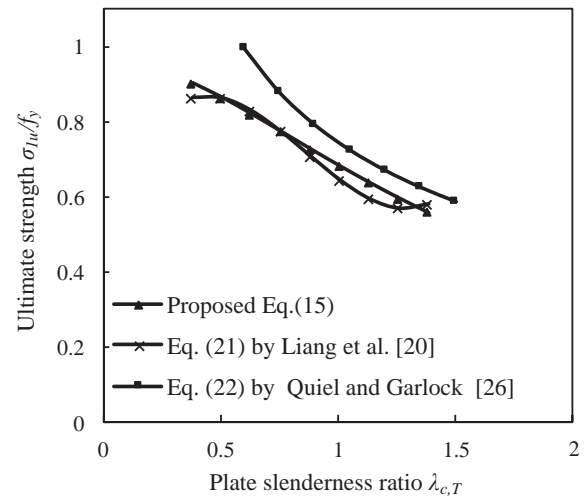


Fig. 26. Comparison of plate strength curves at ambient temperature predicted by the current proposed design formula with existing formulas.

should be noted that the effective width formulas for clamped steel plates proposed by Liang et al. [20] have been verified by experimental results on rectangular CFST columns. The strength curve predicted by the present study is conservative compared to the one given by Quiel and Garlock [26]. The reason for this is that the residual stresses are considered in the current model, but are not used in the model by Quiel and Garlock [26]. The comparison for elevated temperatures is depicted in Fig. 27. The post-local buckling strengths of steel plates predicted by the proposed formula are in good agreement with those given by Quiel and Garlock [26]. However, the results obtained by the formula of Couto et al. [25] are very conservative compared to the other two solutions as shown in Fig. 27. This is because the effective width formula given by Couto et al. [25] was developed for simply supported steel plates with initial geometric imperfections which were much larger than those incorporated in the finite element models in the present study.

7. Applications

The proposed effective width formulas for clamped steel plates at elevated temperatures can be used to account for local buckling effects on the ultimate axial loads of rectangular CFST short columns subjected

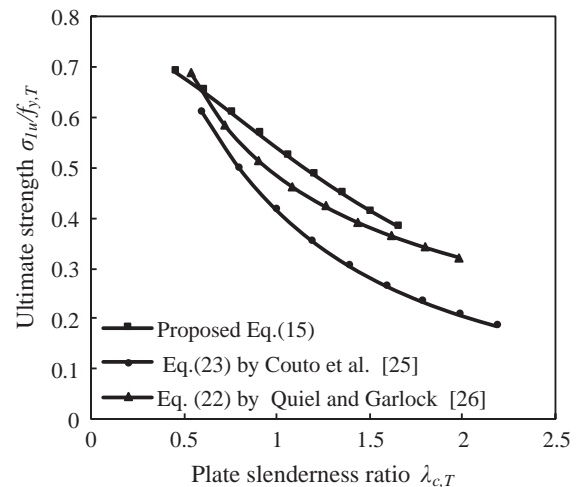


Fig. 27. Comparison of plate strength curves at temperature of 400 °C predicted by the current proposed design formula with those given by Couto et al. [25] Quiel and Garlock [26].

Table 1
Ultimate axial loads of rectangular CFST short columns at elevated temperatures.

Specimen	Dimensions $B \times D \times t$ (mm)	$P_{u,app} = 500$ kN				$P_{u,app} = 600$ kN			
		T_{max} (°C)	T_{min} (°C)	$P_{u,cal}$ (kN)	$\frac{P_{u,cal}}{P_{u,app}}$	T_{max} (°C)	T_{min} (°C)	$P_{u,cal}$ (kN)	$\frac{P_{u,cal}}{P_{u,app}}$
SHS	123 × 123 × 5	690	652	490.1	0.98	648	607	559.7	0.93
SHS1	118.9 × 118.9 × 5	712	678	431.7	0.86	644	605	534.6	0.89
SHS2	125.9 × 125.9 × 5	700	661	494.3	0.99	675	634	536.8	0.89
RHS	84.5 × 169 × 5	695	633	499	1.00	645	579	595.4	0.99
RHS1	79.3 × 158.5 × 5	687	628	460.4	0.92	632	570	560.1	0.93
RHS2	89.5 × 179 × 5	716	655	517.7	1.04	676	610	588.2	0.98
Mean					0.97				0.94

to standard fire. A simple expression for determining the ultimate axial load of a CFST short column at elevated temperatures is proposed as

$$P_{u,cal} = A_{se}f_{y,T} + A_c f_{c,T} \quad (27)$$

where $P_{u,cal}$ is the calculated ultimate axial load of the CFST short column, A_{se} is the effective cross-sectional area of the steel section computed using the proposed effective width formula Eq. (18), A_c is the concrete area of the section, and $f_{c,T}$ the compressive strength of concrete at elevated temperatures.

Dai and Lam [38] investigated the shape effects on the behavior of CFST short columns at elevated temperature using the commercial software package ABAQUS. Table 1 shows the geometric and material properties of square and rectangular CFST short columns provided by Dai and Lam [38]. The proposed effective width formulas and Eq. (27) were employed to calculate the ultimate axial loads of these columns and the results obtained are compared with those given by Dai and Lam [38] in Table 1. The reduction factors for the steel yielding strength and concrete at elevated temperatures given in Eurocode 3 [35] were adopted. As given in Table 1, the maximum temperature (T_{max}) appeared at the corner of the steel cross-section, while the minimum temperature (T_{min}) presented at the middle of the steel tube wall under consideration. It was assumed that the distribution of temperatures between the corner and the middle of the steel tube wall was linear. The concrete temperature was taken as 0.45 of the maximum temperature on the steel tube as suggested by Dai and Lam [38]. Local buckling of steel plates with b/t ratio greater than 20 was taken into account in the calculations of the ultimate axial loads. As demonstrated in Table 1, the calculated ultimate axial loads of CFST short columns at elevated temperatures are in good agreement with numerical results predicted using the finite element software ABAQUS. The mean ultimate axial loads computed by the proposed formulas are about 97% and 94% of those reported by Dai and Lam [38] for the applied loads ($P_{u,app}$) of 500 kN and 600 kN, respectively.

The above comparative study demonstrates that the effective width formulas developed for steel plates at elevated temperatures predict well the post-local buckling strengths of steel tube walls of CFST short columns exposed to fire. In addition, the assumed clamped boundary conditions for steel plates are able to simulate the boundary conditions of the steel tube walls of CFST columns at elevated temperatures.

8. Conclusions

The nonlinear critical local and post-local buckling behavior of thin steel plates under stress gradients in rectangular CFST columns at elevated temperatures has been investigated by using the finite element models developed. Geometric imperfections and residual stresses have been taken into account in the finite element models. The material stress-strain relationships for steels at elevated temperatures given in Eurocode 3 [35] have been adopted to simulate the material behavior. The critical local buckling and post-local buckling strength curves for clamped steel plates under compressive stress gradients at ambient and

elevated temperatures have been determined from the finite element analysis results. Based on the numerical results obtained, design formulas for determining the critical local buckling and post-local buckling strengths of steel plates at ambient and elevated temperatures have been proposed. The effective width formulas have also been developed for clamped steel plates in rectangular CFST columns subjected to elevated temperatures.

The proposed formulas have been utilized to account for local buckling effects on the ultimate axial loads of CFST short columns exposed to fire. The results obtained are in good agreement with numerical solutions predicted by the finite element analysis software ABAQUS. The effective width models developed in this study can be incorporated in nonlinear analysis procedures to account for progressive post-local buckling effects on the behavior of thin-walled rectangular CFST columns exposed to fire. Furthermore, the proposed formulas can be used directly in the design of CFST columns made of non-compact and slender steel sections at elevated temperatures.

References

- [1] Schneider SP. Axially loaded concrete-filled steel tubes. *J Struct Eng, ASCE* 1998;124(10):1125–38.
- [2] Sakino K, Nakahara H, Morino S, Nishiyama I. Behavior of centrally loaded concrete-filled steel-tube short columns. *J Struct Eng, ASCE* 2004;130(2):180–8.
- [3] Liang QQ, Patel VI, Hadi MNS. Biaxially loaded high-strength concrete-filled steel tubular slender beam-columns, Part I: multiscale simulation. *J Constr Steel Res* 2012;75:64–71.
- [4] Dundu M. Column buckling tests of hot-rolled concrete filled square hollow sections of mild to high strength steel. *Eng Struct* 2016;127:73–85.
- [5] Liang QQ. Analysis and design of steel and composite structures. Boca Raton and London: CRC Press, Taylor and Francis Group; 2014.
- [6] Wang YC. Steel and composite structures: behaviour and design for fire safety. London and New York: Spon Press; 2002.
- [7] Knobloch M. Local buckling behavior of steel sections subjected to fire. In: Fire safety science—proceedings of the ninth international symposium; 2008. p. 1239–54.
- [8] Albero V, Espinos A, Romero ML, Hospitaler A, Bihina G, Renaud C. Proposal of a new method in EN1994-1-2 for the fire design of concrete filled steel tubular columns. *Eng Struct* 2016;128:237–55.
- [9] Espinos A, Romero ML, Hospitaler A. Simple calculation model for evaluating the fire resistance of unreinforced concrete filled tubular columns. *Eng Struct* 2012;42:231–44.
- [10] Rush DI, Bisby LA, Jowsey A, Lane B. Residual capacity of fire-exposed concrete-filled steel hollow section columns. *Eng Struct* 2015;100:550–63.
- [11] Rodrigues JPC, Laim L. Fire response of restrained composite columns made with concrete filled hollow sections under different end-support conditions. *Eng Struct* 2017;141:83–96.
- [12] Rhodes J, Harvey JM. Effects of eccentricity of load or compression on the buckling and post-buckling behaviour of flat plates. *Int J Mech Sci* 1971;13(10):867–79.
- [13] Rhodes J, Harvey JM, Fok WC. The load-carrying capacity of initially imperfect eccentrically loaded plates. *Int J Mech Sci* 1975;17(3):161–72.
- [14] Usami T. Post-buckling of plates in compression and bending. *J Struct Div ASCE* 1982;108(3):591–609.
- [15] Usami T. Effective width of locally buckled plates in compression and Bending. *J Struct Eng ASCE* 1993;119(5):1358–73.
- [16] Shanmugam NE, Liew JYR, Lee SL. Thin-walled steel box columns under biaxial loading. *J Struct Eng ASCE* 1989;115(11):2706–26.
- [17] Uy B, Bradford MA. Elastic local buckling of thin steel plates in composite steel-concrete members. *Eng Struct* 1996;18(3):193–200.
- [18] Uy B, Bradford MA. Local buckling of thin steel plates in composite construction: experimental and theoretical study. *Proc Inst Civ Eng Struct Build* 1995;110:426–40.

- [19] Uy B. Strength of concrete-filled steel box columns incorporating local buckling. *J Struct Eng ASCE* 2000;126(3):341–52.
- [20] Liang QQ, Uy B, Liew JYR. Local buckling of steel plates in concrete-filled thin-walled steel tubular beam-columns. *J Constr Steel Res* 2007;63(3):396–405.
- [21] Liang QQ. Performance-based analysis of concrete-filled steel tubular beam-columns, Part I: theory and algorithms. *J Constr Steel Res* 2009;65:363–72.
- [22] Liang QQ. Performance-based analysis of concrete-filled steel tubular beam-columns, Part II: verification and applications. *J Constr Steel Res* 2009;65:351–62.
- [23] Ala-Outinen T, Myllymaki J. The local buckling of RHS members at elevated temperatures. VTT Research Notes 1672, Technical Research Centre of Finland (VTT), Espoo, Finland; 1995.
- [24] Heidarpour A, Bradford MA. Local buckling and slenderness limits for flange outstands at elevated temperatures. *J Constr Steel Res* 2007;63:591–8.
- [25] Couto C, Real PV, Lopes N, Zhao B. Effective width method to account for the local buckling of steel thin plates at elevated temperatures. *Thin-Walled Struct* 2014;84:134–49.
- [26] Quiel SE, Garlock MEM. Calculating the buckling strength of steel plates exposed to fire. *Thin-Walled Struct* 2010;48:684–95.
- [27] ANSYS R 16.1. Academic, 2015.
- [28] Feng M, Wang YC, Davies JM. A numerical imperfection sensitivity study of cold-formed thin-walled tubular steel columns at uniform elevated temperatures. *Thin-walled Struct* 2004;42:533–55.
- [29] Abambres M, Quach WM. Residual stresses in steel members; a review of available analytical expressions. *Int J Struct Integrity* 2016;7(1):70–94.
- [30] Chen, PS, Herman WA, Pense AW. Relaxation stresses in pressure vessels. Bulletin 302, February, Welding Research Council, New York, NY; 1985.
- [31] Stout RD. Postweld heat treatment of pressure vessels. Bulletin 302, February, Welding Research Council, New York, NY; 1985.
- [32] Zhou RJ, Pense AW, Basehore ML, Lyons DH. A study of residual stress in pressure vessel steels. Bulletin 302, February, Welding Research Council, New York, NY; 1985.
- [33] Tide RHR. Integrity of structural steel after exposure to fire. *AISC Eng J* 1998;35:26–38.
- [34] Diesner RW. The effect of elevated temperature exposure on residual stresses. Sundstrand Aviation, 710285.
- [35] Eurocode 3. Design of steel structures, Part 1. 2: General rules-structural fire design, CEN, Brussels, Belgium; 2005.
- [36] Von Karman T, Sechler EE, Donnell LH. The strength of thin plates in compression. *Trans Am Soc Mech Eng* 1932;54:53–7.
- [37] AISC. Steel construction manual, 13th ed. American Institute of Steel Construction; 2005.
- [38] Dai XH, Lam D. Shape effect on the behaviour of axially loaded concrete filled steel tubular stub columns at elevated temperature. *J Constr Steel Res* 2012;73:117–27.

3.4 CONCLUDING REMARKS

In this chapter, the critical local and post-local buckling behavior of thin steel plates in CFST rectangular columns subjected to stress gradients and various high temperatures has been investigated by conducting the material and geometric nonlinear finite element analyses on steel plates. The finite element results obtained have been utilized to develop a set of equations for quantifying the critical stresses at the onset of local buckling, the post-local buckling strength as well as effective widths of thin steel plates exposed to high temperatures. The proposed equations of effective widths have been employed to calculate the ultimate strengths of CFST rectangular columns, which have been shown to be in good agreement with test data. The equations proposed in this chapter can be incorporated in any nonlinear computer modeling procedures to account for the influences of gradual post-local buckling on the fire and post-fire responses of rectangular CFST columns loaded axially and eccentrically.

Chapter 4

CFST SHORT COLUMNS AT ELEVATED TEMPERATURES

4.1 INTRODUCTION

This chapter presents a computational model for determining the fire resistance and structural behavior of axially loaded short CFST columns of thin-walled rectangular sections under fire exposure including local buckling effects. The computer model incorporates the temperature-dependent material constitutive relations and thermal properties of concrete and steel. The formulation of the computer model utilizes the method of fiber elements, which discretizes the column cross-section into fine fiber elements. The equations proposed in Chapter 3 for local and post-local buckling predictions of steel plates at high temperatures are implemented in the computational model to include local and post-local buckling influences on structural and fire behavior. A sequentially coupled computational procedure is proposed for the thermal and stress analysis of CFST columns loaded axially, which predicts the temperature distribution in fiber elements, load-strain responses and fire resistance. The computer model verified is employed to undertake a parametric study on the fire and structural responses of CFST columns with various important parameters.

This chapter includes the following paper:

1. **Kamil, G. M.,** Liang, Q. Q. and Hadi, M. N. S. (2019) Numerical analysis of axially loaded rectangular concrete-filled steel tubular short columns at elevated temperatures, *Engineering Structures*, 180: 89-102.

GRADUATE RESEARCH CENTRE

DECLARATION OF CO-AUTHORSHIP AND CO-CONTRIBUTION: PAPERS INCORPORATED IN THESIS BY PUBLICATION

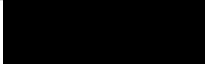
This declaration is to be completed for each conjointly authored publication and placed at the beginning of the thesis chapter in which the publication appears.

1. PUBLICATION DETAILS (to be completed by the candidate)

Title of Paper/Journal/Book:	Kamil, G. M., Liang, Q. Q. and Hadi, M. N. S. (2019) Numerical analysis of axially loaded rectangular concrete-filled steel tubular short columns at elevated temperatures. Engineering Structures, 180:89-102.		
Surname:	Kamil	First name:	Ghanim
College:	College of Engineering & Science	Candidate's Contribution (%):	70
Status:			
Accepted and in press:	<input type="checkbox"/>	Date:	
Published:	<input checked="" type="checkbox"/>	Date:	1 Feb. 2019

2. CANDIDATE DECLARATION

I declare that the publication above meets the requirements to be included in the thesis as outlined in the HDR Policy and related Procedures – policy.vu.edu.au.

	28/02/2019
Signature	Date

3. CO-AUTHOR(S) DECLARATION

In the case of the above publication, the following authors contributed to the work as follows:

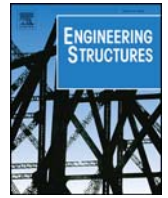
The undersigned certify that:

1. They meet criteria for authorship in that they have participated in the conception, execution or interpretation of at least that part of the publication in their field of expertise;
2. They take public responsibility for their part of the publication, except for the responsible author who accepts overall responsibility for the publication;
3. There are no other authors of the publication according to these criteria;
4. Potential conflicts of interest have been disclosed to a) granting bodies, b) the editor or publisher of journals or other publications, and c) the head of the responsible academic unit; and

5. The original data will be held for at least five years from the date indicated below and is stored at the following location(s):

<p>Location: College of Engineering and Science, Victoria University, Melbourne, Victoria, Australia.</p>
--

Name(s) of Co-Author(s)	Contribution (%)	Nature of Contribution	Signature	Date
Ghanim Mohammed Kamil	70	Developed and verified the model Conducted the parametric study Drafted the manuscript		28/02/ 2019
Qing Quan Liang	20	Provided initial concepts Provided critical revision of the article Final approval and submitting the manuscript		28/02/ 2019
Muhammad N. S. Hadi	10	Provided critical revision of the article Final approval of the manuscript		28/2/ 2019



Numerical analysis of axially loaded rectangular concrete-filled steel tubular short columns at elevated temperatures

Ghanim Mohammed Kamil^a, Qing Quan Liang^{a,*}, Muhammad N.S. Hadi^b

^a College of Engineering and Science, Victoria University, PO Box 14428, Melbourne, VIC 8001, Australia

^b School of Civil, Mining and Environmental Engineering, University of Wollongong, Wollongong, NSW 2522, Australia

ARTICLE INFO

Keywords:

Concrete-filled steel tubes
Elevated temperatures
Fire-resistance
Nonlinear analysis
Local buckling

ABSTRACT

Elevated temperatures significantly reduce the local buckling strengths of steel tubes and the ultimate strengths of rectangular concrete-filled steel tubular (CFST) columns exposed to fire. No fiber-based models have been developed that include local buckling effects on the fire-resistance of rectangular CFST columns. This paper presents a new fiber element model for the fire-resistance predictions of axially loaded rectangular CFST short columns at elevated temperatures considering local buckling. The thermal analysis problem of a CFST column is solved by the finite difference method to determine the temperature distribution within its cross-section including an air gap, concrete moisture content and the emissivity of exposure surfaces. The nonlinear stress analysis of axially loaded short CFST columns under fire recognizes the stress-strain behavior of concrete and steel at elevated temperatures. The expressions for initial local buckling and effective widths of steel plates are incorporated in the computational model to include the effects of local and post-local buckling on the fire responses of CFST columns. The existing experimental and numerical results are utilized to examine the accuracy of the fiber-based model. The fiber model developed is used to undertake parametric studies on the effects of local buckling, geometric and material properties and loading ratio on the thermal and structural responses of CFST short columns and the load distribution in steel tube and concrete. The numerical model proposed is demonstrated to simulate well the fire and structural performance of axially loaded CFST short columns under fire. Moreover, computational solutions presented provide a better understanding of the thermal and structural responses of CFST columns in fire.

1. Introduction

Rectangular concrete-filled steel tubular (CFST) columns have been widely used to resist heavy loads in high-rise composite buildings. Filling a rectangular hollow steel tube with concrete as illustrated in Fig. 1 not only remarkably increases the strength and stiffness of the hollow steel tube but also significantly improves its fire-resistance. The concrete infill is completely encased by the rectangular steel tube so that it exhibits improved ductility. In addition, the steel tube acts as longitudinal reinforcement and permanent formwork for the filled concrete, which greatly reduces the construction time and costs. Moreover, the concrete core delays the steel tube local buckling and forces it to buckle locally outward [1–9]. Some of the practical applications of circular and rectangular/square CFST columns in high-rise buildings include LDC Queen's Road Central in Hong Kong, Di Wang and The SEG Plaza in Shenzhen, the Sail in Singapore, the Petronas Tower in Kuala Lumpur and Two Union Square in Seattle. In AS 3600-

2009 [10], columns with a slenderness ratio (L/r) less than 22 are regarded as short columns. As shown in Table 1, the sizes of CFST columns used in the above mentioned high-rise buildings were very large and their slenderness ratios calculated by assuming the typical story height of 4.2 m ranged from 5.3 to 17.7. These CFST columns therefore were short columns whose strengths were governed by the section capacities. Rectangular CFST columns in tall composite structures may be exposed to extreme events such as fire in their design life. The elevated temperatures generated in a fire significantly reduce the stiffness and strength of concrete and steel materials as well as the local buckling resistance of steel tubes and therefore the ultimate strengths of CFST columns [11–13]. To accurately determine the fire-resistance of rectangular CFST columns, the influences of local buckling must be included in the nonlinear analysis procedures. However, no fiber-based modeling techniques have been proposed that included local buckling in the fire-resistance prediction of CFST short columns. Therefore, there is a need for the development of such a computational technique.

* Corresponding author.

E-mail address: Qing.Liang@vu.edu.au (Q.Q. Liang).

<https://doi.org/10.1016/j.engstruct.2018.11.037>

Received 10 July 2018; Received in revised form 9 October 2018; Accepted 13 November 2018

Available online 19 November 2018

0141-0296/ © 2018 Elsevier Ltd. All rights reserved.

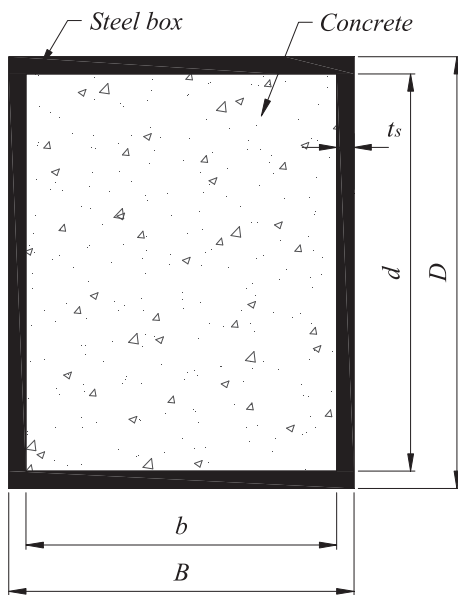


Fig. 1. Cross-section of rectangular CFST column.

Table 1
CFST columns utilized in high-rise buildings.

Name of building	City	Column section	Max. size (mm)	L/r
LDC queen's road central	Hong Kong	Square	2250 × 2250	6.5
Di Wang	Shenzhen	Square	1000 × 1000	14.5
Casselden place	Melbourne	Circular	950	17.7
The SEG Plaza	Shenzhen	Circular	1600	10.5
The sail	Singapore	Circular	2000	8.4
The petronas tower	Kuala Lumpur	Circular	2400	7.0
Two union square	Seattle	Circular	3200	5.3

Most of the experimental investigations on the fire-performance of CFST columns have focused on slender columns. Standard fire tests on square, rectangular and circular CFST slender columns subjected to constant axial load and increasing temperatures that followed the standard temperature-time curve given in design codes have been conducted by researchers, such as Lie and Chabot [14], Sakumoto et al. [15], Kodur and Lie [16], Han et al. [17], Choi et al. [18], Han et al. [19], Espinos et al. [20,21], and Dundu [22]. The temperatures on the surfaces and in the column cross-section, the axial deformation and the fire-resistance of the CFST column were recorded in the fire tests. The effects of important parameters were investigated, including the axial load ratio, loading eccentricity, column slenderness and size, types of concrete infill, material strengths and spray material thickness. Experimental results indicated that the typical failure mode associated with slender CFST columns in fire was overall column buckling. For CFST rectangular and square columns, however, the steel tube buckled locally outward.

Experimental studies on the responses of short square and rectangular CFST columns exposed to fire have been extremely scarce. Lu et al. [23] carried out fire tests on short CFST columns constructed by high-strength self-consolidating concrete to determine the temperature distributions, axial displacement-time relationships, limiting temperatures and fire-resistance. It was reported that the outward local buckling appeared on the four faces of each column while the concrete crushed at the column where the steel tube walls locally buckled. In addition, the axial load ratio had significant influences on the fire-performance of short square CFST columns. Moreover, the loading eccentricity was shown to have a minor effect on the fire-resistance of short CFST columns. Furthermore, it was observed that there was an

interaction between the steel tube and concrete infill during the fire exposure.

Although fire tests can be performed to determine the responses of CFST columns exposed to fire, these tests are highly time consuming and expensive. Therefore, mathematical models have been formulated for the fire-resistance predictions of CFST slender columns by researchers. The fiber-based numerical models for simulating the responses of slender CFST columns exposed to fire have been developed by Lie and Chabot [24], Lie and Irwin [25] and Kodur and Lie [26], Han [27], and Chung et al. [28]. In these fiber-based models, either the finite difference or the finite element method was utilized to calculate the distribution of temperatures in the column considering concrete and steel thermal properties. The numerical models considered the nonlinear stress-strain characteristics of concrete as well as steel at elevated temperatures, moisture in concrete, second order effects as well as geometric imperfections. Researchers have also employed commercial finite element software ABAQUS and ANSYS to create 3D models to investigate the responses of CFST slender columns in fire [29–33]. Ding and Wang [29] and Espinos et al. [30] examined the influences of the air gap, slip at the concrete and steel tube interface, tensile concrete strength and geometric imperfection on the fire-resistance of CFST columns. Hong and Varma [31] carried out extensive sensitivity analyses on the influences of material constitutive models, geometric imperfections, local buckling and the bond between the steel tube and concrete on the performance of square CFST columns.

Numerical studies on rectangular short CFST columns at elevated temperatures have been relatively limited. Yin et al. [34] presented an analytical model for the fire-performance predictions of square and circular CFST short column subjected to axial load and fire. It was reported that for the same concrete and steel cross-sectional areas, circular CFST short columns had slightly higher fire-resistance than square ones. The axial load-deformation responses of short CFST square and circular columns subjected to combined axial load and elevated temperatures including a cooling phase were investigated by Song et al. [35] using ABAQUS. The stress distributions and confinement stresses at different loading stages were also studied. The finite element results indicated that heating slightly increased the ultimate load of CFST circular columns but reduced that of square ones. Dai and Lam [36] utilized ABAQUS to examine the influences of the column sectional shape on the thermal and structural behavior of CFST short columns made of circular, elliptical, square or rectangular sections at elevated temperatures. The results obtained demonstrated that circular CFST short columns had higher fire performance than other sections. Increasing the axial load ratio remarkably reduced the critical temperatures and fire-resistance of CFST short columns regardless of sectional shape. The distribution of temperatures in CFST columns constructed by carbon or stainless steel tubes was investigated using ABAQUS by Tao and Ghannam [37], who reported that the thermal contact conductance at the interface of steel and concrete and concrete moisture content significantly influenced the temperature distribution. Xiong et al. [38] presented a modified finite difference method for computing the temperature distributions in circular and square CFST columns and in double-skin CFST columns exposed to fire. The numerical model presented was employed to undertake sensitivity analyses on the influences of important factors on the responses of CFST columns at elevated temperatures.

It appears from the above literature review that the existing fiber-based numerical models have not considered local buckling effects in the analysis of rectangular CFST columns under fire. Although local buckling could be included in the finite element analysis of rectangular CFST columns in fire, the development and computational cost of the finite element model is highly expensive compared to that of the fiber element model [31,39]. The comparative study conducted by Ahmed et al. [39] demonstrated that the total time for creating and analyzing the finite element model of a concrete-filled double steel tubular short column was 2640 s while the total time for creating and analyzing its

fiber element model was only 25 s. Moreover, there are relatively limited studies dealing with rectangular short CFST columns under fire loading. To address this knowledge gap, this paper describes a computationally efficient fiber-based numerical model for simulating the thermal and structural behaviors of axially-loaded short CFST rectangular columns subjected to elevated temperatures. The fiber model includes the influences of local and post-local buckling of steel tube, air gap, moisture content and emissivity of exposure surfaces on the fire performance of CFST columns. The mathematical formulations of the numerical model are described and its verification is followed. The fiber modeling technique is utilized to undertake a parametric study on the fire and structural responses of CFST columns with various important parameters.

2. The fiber element model for thermal problems

2.1. Discretization of cross-section

The present numerical model is developed using the fiber element method, which discretizes the cross-section of a CFST column into many small fiber elements but it does not require any discretization along the column length [40–44]. A typical fiber mesh of the column cross-section is depicted in Fig. 2 where the section is formed by welding four plates without the corner radius. The wall of the steel tube is discretized into layers through its thickness while its width is divided into square fiber elements according to the layer thickness. The filled concrete is discretized into square fiber elements and the size of the concrete fiber is twice the size of the steel fiber element as illustrated in Fig. 2. The temperature at the center of each fiber element is taken as its temperature. The material properties of steel or concrete are assigned to fibers. The uniaxial material stress-strain relationships of steel and concrete at elevated temperatures are employed to compute fiber stresses from axial fiber strains.

2.2. The sequential coupled analysis procedure

The nonlinear inelastic analysis of CFST short columns exposed to fire consists of sequential coupled thermal analysis and nonlinear stress analysis. In the thermal analysis, the temperatures on surfaces of the CFST column as a function of time are calculated first. The distribution of temperatures in the column cross-section is then computed by numerical techniques. The temperature is assigned to each fiber element based on the computed temperature distribution. The nonlinear stress

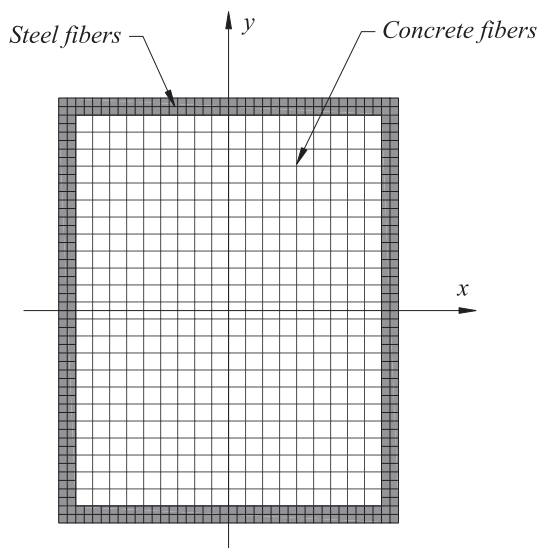


Fig. 2. Typical fibre element discretization.

analysis is carried out to simulate the structural responses of the axially loaded CFST short column under elevated temperatures determined in the thermal analysis. For a given time increment, the temperatures on the surfaces of the CFST column and within its cross-section are computed. The axial strain is incrementally increased and the corresponding axial load is computed as stress resultants in the section subjected to the computed temperature distribution. By repeating the above analysis process, the axial load-strain curves for the CFST short column for given time increments of fire exposure can be determined. The ultimate axial strength of the CFST column decreases as time increases. The fire-resistance of the CFST short column is determined as the time to reach the failure point of the column which has so low strength that it cannot support the axial load. A computer program implementing the fiber-based numerical model has been developed using MATLAB by the authors. The thermal and the nonlinear stress analyses are described in the following sections.

3. Thermal analysis

3.1. Fire temperature-time relationship

The standard temperature-time curve given in Eurocode 1 [45] as demonstrated in Fig. 3 is adopted in the present fiber model to determine the temperatures on the surfaces of the CFST column during fire exposure. This standard curve is expressed by

$$T(t) = 20 + 345 \log_{10}(8t + 1) \quad (1)$$

where T stands for the temperature in °C and t is the time of fire exposure in minutes.

3.2. Temperature distribution in the cross-section

The four sides of the rectangular CFST column are assumed to be exposed to uniform temperatures that follow the standard temperature-time curve represented by Eq. (1). To determine the temperature distribution at the fiber elements in the cross-section, the finite difference method is employed to solve the following heat transfer equation in two-dimensions [46]:

$$k \frac{\partial^2 T}{\partial x^2} + k \frac{\partial^2 T}{\partial y^2} = \rho c \frac{\partial T}{\partial t} \quad (2)$$

where ρ denotes the density in kg/m³, c is the specific heat in J/kg, and k is the thermal conductivity in W/m °C and q is the heat flux which is used to calculate the temperature distribution on the surfaces of the CFST column but is taken as zero for steel and concrete within the

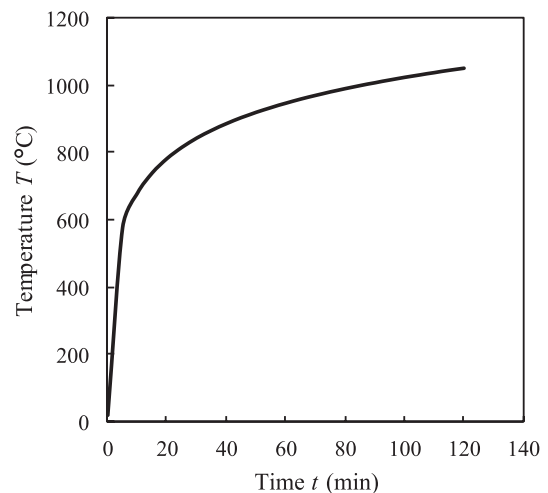


Fig. 3. Standard temperature-Time curve given in Eurocode 1 [43].

Table 2
Thermal properties of steel and concrete implemented in the numerical model.

Materials	Properties	Equations
Steel properties given in Eurocode 3 [48]	Thermal conductivity	$k_{s,T} = \begin{cases} 54 - 3.33 \times 10^{-2}T & \text{for } 20^\circ\text{C} \leq T \leq 800^\circ\text{C} \\ 27.3 & \text{for } 800^\circ\text{C} < T \leq 1200^\circ\text{C} \end{cases}$
	Specific heat	$c_{s,T} = 425 + 7.73 \times 10^{-1}T - 1.69 \times 10^{-3}T^2 + 2.2 \times 10^{-6}T^3$ for $20^\circ\text{C} \leq T \leq 600^\circ\text{C}$ $c_{s,T} = 666 + \frac{13002}{738 - T}$ for $600^\circ\text{C} \leq T \leq 735^\circ\text{C}$ $c_{s,T} = 545 + \frac{17820}{T - 731}$ for $735^\circ\text{C} \leq T \leq 900^\circ\text{C}$ $c_{s,T} = 650$ for $900^\circ\text{C} \leq T \leq 1200^\circ\text{C}$
	Thermal expansion strain	$\epsilon_{s,T} = 1.2 \times 10^{-5}T + 0.4 \times 10^{-8}T^2 - 2.416 \times 10^{-4}$ for $20^\circ\text{C} \leq T \leq 750^\circ\text{C}$ $\epsilon_{s,T} = 1.1 \times 10^{-2}$ for $750^\circ\text{C} \leq T \leq 860^\circ\text{C}$ $\epsilon_{s,T} = 2 \times 10^{-5}T - 6.2 \times 10^{-3}$ for $860^\circ\text{C} \leq T \leq 1200^\circ\text{C}$
	Concrete properties given by Lie and Chabot [24]	Thermal conductivity
	Thermal capacity	$\rho_c c_{c,T} = (0.005 \times T + 1.7) \times 10^6$ for $0 \leq T \leq 200^\circ\text{C}$ $\rho_c c_{c,T} = 2.7 \times 10^6$ for $200 < T \leq 400^\circ\text{C}$ $\rho_c c_{c,T} = (0.013 \times T - 2.5) \times 10^6$ for $400 < T \leq 500^\circ\text{C}$ $\rho_c c_{c,T} = (-0.013 \times T + 10.5) \times 10^6$ for $500 < T \leq 600^\circ\text{C}$ $\rho_c c_{c,T} = 2.7 \times 10^6$ for $T > 600^\circ\text{C}$
	Thermal expansion strain	$\epsilon_{c,T} = (0.008T + 6) \times 10^{-6}(T - 20)$

column.

The thermal properties of steel and concrete including the thermal conductivity, specific heats and thermal expansion coefficient need to be specified in the thermal analysis. The thermal properties of steel provided in Eurocode 3 [47] and the thermal properties of concrete given by Lie and Chabot [24] are employed in the fiber-based numerical model and are provided in Table 2 for convenience and completeness.

The nodes of fiber elements in the cross-section are schematically illustrated in Fig. 4. The distances between the adjacent two nodes in x and y directions are represented by dx and dy , respectively, and they are actually the size of the fiber element in x and y directions, respectively. As shown in Fig. 4, m and n denote the coordinates of the node in the y and x directions, respectively. Assume that the current temperature at the node (m, n) at the i th time increment is $T_{m,n}^i$. The next temperature $T_{m,n}^{i+1}$ at this node at the next time increment is calculated by solving the general heat transfer equation expressed by Eq. (2) using the forward finite difference method as follows:

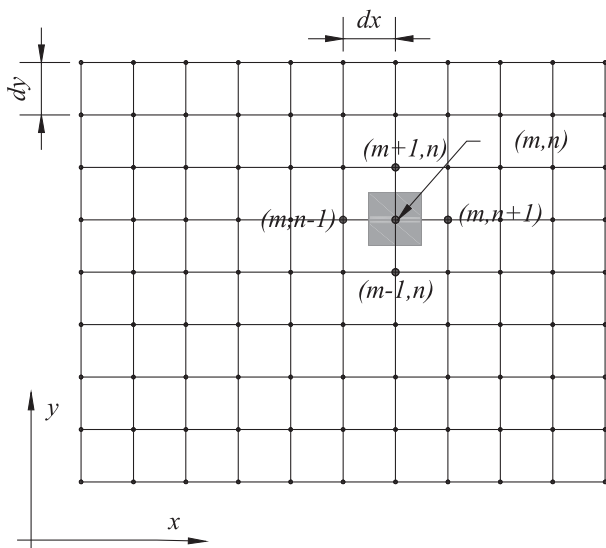


Fig. 4. Nodal grids for the finite difference for temperature analysis.

$$T_{m,n}^{i+1} = \frac{\alpha \Delta t}{(\Delta L)^2} (T_{m,n-1}^i + T_{m,n+1}^i + T_{m-1,n}^i + T_{m+1,n}^i) + \left(1 - \frac{4\alpha \Delta t}{(\Delta L)^2}\right) T_{m,n}^i \quad (3)$$

in which $1 - (4\alpha \Delta t / \Delta L)^2 \geq 0$; α is the diffusivity and is taken as $k/\rho c$; Δt is the time step in seconds; and the distance between two adjacent nodes is $\Delta L = dx = dy$.

It is assumed that an air gap between the steel tube and concrete during fire exposure exists because the steel tube expands more than the filled concrete does [29]. The temperatures at the contact nodes at the steel and concrete interface are computed by the following equation accounting for the effects of the air gap where the thermal contact resistance h_{tr} is taken as $100 \text{ W/m}^2\text{K}$ as suggested by other researchers [29]:

$$T_{1,1}^{i+1} = T_{1,1}^i + \frac{4\Delta t}{\rho c (d_c)^2} (h_{tr}(T_{3,3}^i - T_{1,1}^i) d_c + \lambda_c (T_{1,2}^i - T_{1,1}^i) + \lambda_c (T_{2,1}^i - T_{1,1}^i)) \quad (4)$$

where d_c and d_s are the concrete and steel fiber sizes, respectively, and the symbols that refer to the temperatures at nodes used in the above equation are illustrated in Fig. 5, which shows the interaction nodes between steel and concrete at the corner of the interface of steel and concrete as a typical case. The temperatures at the nodes of steel fibers at the boundaries can be calculated by using Eq. (4) with the heat

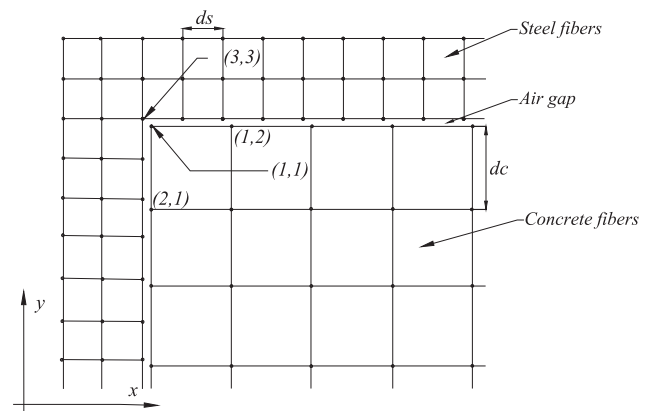


Fig. 5. Typical nodal grids for the interface of steel and concrete for the finite difference temperature analysis.

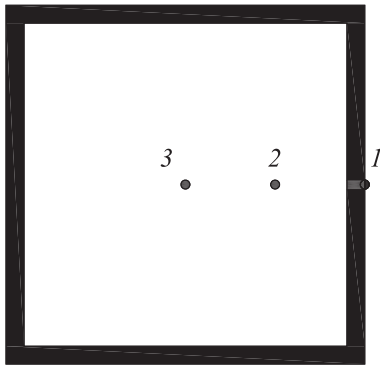


Fig. 6. Point positions in the square CFST column section for comparison purpose.

convection and thermal radiation coefficients. Research studies on the thermal analysis of CFST columns showed that the emissivity of the exposure surfaces and the moisture content in concrete had remarkable effects on the distribution of temperatures [30,31]. In the present numerical model, the emissivity of the exposure surface (ε) is taken as 0.7 and the Stephen–Boltzmann constant is taken as $5.67 \times 10^{-8} \text{ W/m}^2 \text{ K}^4$, while the moisture content is taken as 3%. These values have been used by other researchers and showed to give good predictions. The use of 3% moisture content is based on Eurocode 2 [48] that limits the moisture content to 3% and the research conducted by Espinos et al. [30]. The research conducted by Tao and Ghannam [37] indicated that the use of moisture content higher than 3% resulted in the over-estimation of the fire-resistance of CFST columns.

To validate the accuracy of the fiber modeling technique for thermal analysis on CFST rectangular columns, computed temperatures at various locations depicted in Fig. 6 are compared with experimentally measured ones provided by Lie and Chabot [14] in Figs. 7–9. The thermal analysis of three square CFST columns tested by Lie and Chabot [14] were undertaken by the proposed fiber model. The dimensions of the column cross sections were $152.4 \times 152.4 \text{ mm}$, $254 \times 254 \text{ mm}$ and $304 \times 304 \text{ mm}$ while the thickness of the steel tubes was 6.35 mm. It can be observed from these figures that the fiber model predicts well the temperatures at Point 1 on the surface of the column and at Point 2 within the column, but slightly underestimates the temperature at the center of the section. The steel temperature increased rapidly during the first 30 min exposure to fire as oppositely to the concrete core due to the direct contact between the steel and the fire source and because the

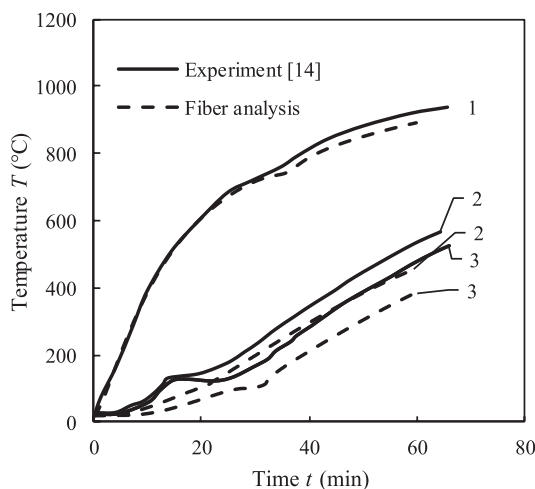


Fig. 7. Comparison of predicted temperatures with experimental results on square CFST column of $152.4 \times 152.4 \times 6.35 \text{ mm}$ tested by Lie and Chabot [14].

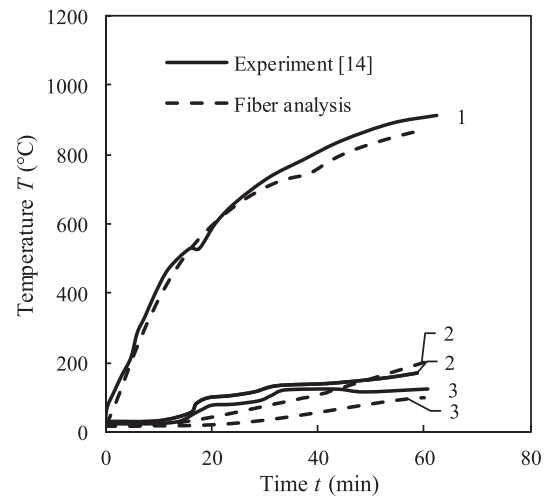


Fig. 8. Comparison of predicted temperatures with experimental results on square CFST column of $254 \times 254 \times 6.35 \text{ mm}$ tested by Lie and Chabot [14].

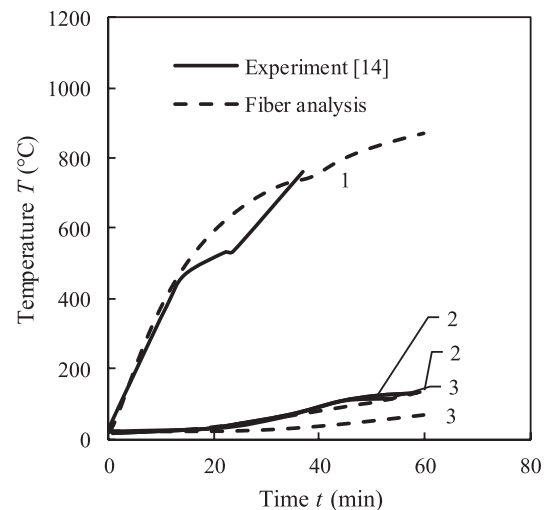


Fig. 9. Comparison of predicted temperatures with experimental results on square CFST column of $304.8 \times 304.8 \times 6.35 \text{ mm}$ tested by Lie and Chabot [14].

steel has a higher thermal conductivity than concrete, which was protected by steel. The discrepancy between the numerical predictions and measurements of the concrete temperatures was attributed to the uncertainty of the actual thermal properties of concrete. The plateau at concrete temperatures occurred after 30 min of fire exposure was caused by the slow rate defined by the standard fire curve and the position of core concrete and the low thermal conductivity of concrete. For the column with a larger cross-section, the Points 2 and 3 at the concrete were farther away from the fire source so that the concrete temperatures at Points 2 and 3 were lower and the curves look plateau as depicted in Figs. 6–8. The maximum temperatures on steel surface and at the core concrete computed by the proposed fiber model are compared against the finite element results obtained by Dai and Lam [36] using ABAQUS in Fig. 10. It appears that excellent agreement between these numerical predictions is obtained.

4. Nonlinear stress analysis

4.1. Axial strains

The short rectangular CFST column is under constant axial compression and increasing temperatures during fire exposure. The strain in

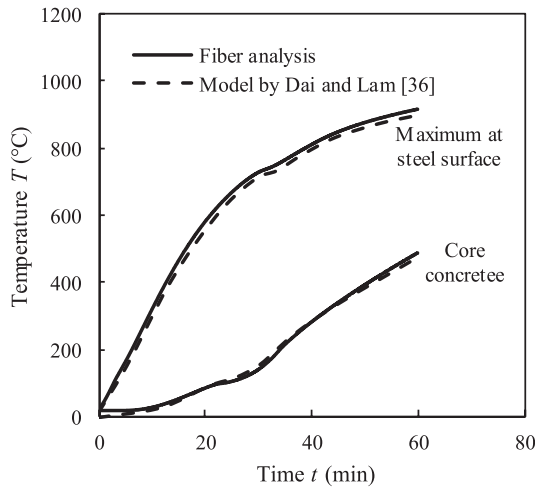


Fig. 10. Comparison of predicted temperatures with finite element results provided by Dai and Lam [36].

steel or concrete consists of axial strain caused by axial load and thermal strain due to thermal expansion. The concrete and steel components in a short CFST column are subjected to the same axial strain (ϵ). The strain in steel fibers (ϵ_s) is expressed by

$$\epsilon_s = \epsilon - \epsilon_{s,T} \quad (5)$$

The strain in concrete fibers (ϵ_c) is calculated as

$$\epsilon_c = \epsilon - \epsilon_{c,T} \quad (6)$$

In the nonlinear stress analysis, the axial strain ϵ is incrementally increased to determine the corresponding axial load that causes this axial deformation.

4.2. Stress-strain model for steel at elevated temperatures

The stress-strain model for structural steels at elevated temperatures provided in Eurocode 3 [47] is incorporated in the present mathematical model for steels exposed to fire. The stress-strain curves of steels are presented in Fig. 11 and expressed by the following equation:

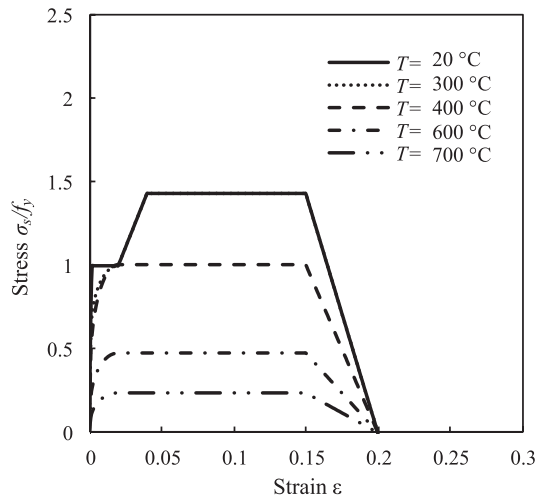


Fig. 11. Stress-strain curves for structural steels at elevated temperatures allowing for strain hardening based on Eurocode 3 [47].

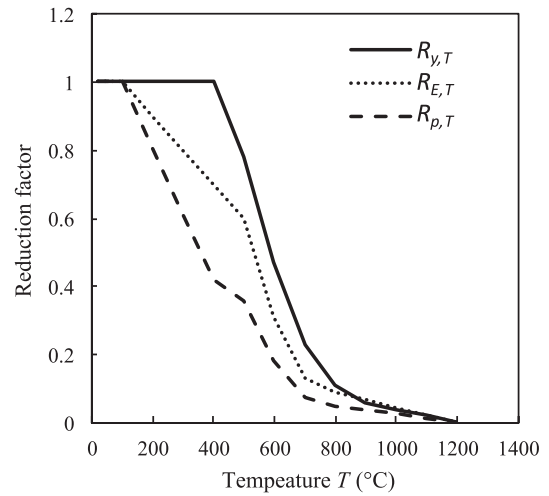


Fig. 12. Reduction factors for the mechanical properties of structural steels at elevated temperatures based on Eurocode 3 [47].

$$\sigma_{s,T} = \begin{cases} E_T \epsilon_s & \text{for } \epsilon_s \leq \epsilon_{p,T} \\ (f_{p,T} - h_3) + \frac{h_2}{h_1} \sqrt{h_1^2 - (\epsilon_{y,T} - \epsilon_s)^2} & \text{for } \epsilon_{p,T} < \epsilon_s \leq \epsilon_{y,T} \\ f_{y,T} & \text{for } \epsilon_{y,T} < \epsilon_s \leq \epsilon_{t,T} \\ f_{y,T} [1 - (\epsilon_s - \epsilon_{t,T}) / (\epsilon_{u,T} - \epsilon_{t,T})] & \text{for } \epsilon_{t,T} < \epsilon_s \leq \epsilon_{u,T} \\ 0 & \text{for } \epsilon_s > \epsilon_{u,T} \end{cases} \quad (7)$$

where the coefficients h_1 , h_2 , and h_3 are given as

$$h_1^2 = (\epsilon_{y,T} - \epsilon_{p,T})(\epsilon_{y,T} - \epsilon_{p,T} + h_3/E_T) \quad (8)$$

$$h_2^2 = E_T(\epsilon_{y,T} - \epsilon_{p,T})h_3 + h_3^2 \quad (9)$$

$$h_3 = \frac{(f_{y,T} - f_{p,T})^2}{E_T(\epsilon_{y,T} - \epsilon_{p,T}) - 2(f_{y,T} - f_{p,T})} \quad (10)$$

where E_T denotes the elastic modulus for steel, $f_{p,T}$ stands for the proportional limit, $f_{y,T}$ represents the yield stress, $\epsilon_{p,T}$ is the strain at $f_{p,T}$, $\epsilon_{y,T}$ denotes the yield strain, and $\epsilon_{u,T}$ stands for the ultimate strain at elevated temperatures. The reduction factors $R_{p,T}$ to the proportional limit, $R_{y,T}$ to the steel yield strength and $R_{E,T}$ to the modulus of elasticity of steels at elevated temperatures provided in Eurocode 3 [47] are used in the present study and are shown in Fig. 12.

The strain-hardening of steel at temperatures below 400 °C is taken into consideration by the following expression [47]:

$$\sigma_{s,T} = \begin{cases} 50[(f_{u,T} - f_{y,T})/0.02] + 2f_{y,T} - f_{u,T} & \text{for } 0.02 < \epsilon_s \leq 0.04 \\ f_{u,T} & \text{for } 0.04 < \epsilon_s \leq 0.15 \\ f_{u,T} [1 - 20(\epsilon_s - 0.15)] & \text{for } 0.15 < \epsilon_s \leq 0.2 \end{cases} \quad (11)$$

where $f_{u,T}$ denotes the ultimate strength of steel at elevated temperature, which is calculated as follows:

$$f_{u,T} = \begin{cases} f_u R_{y,T} & \text{for } T \leq 300^\circ\text{C} \\ f_{y,T} + 0.01(f_{u,T} - f_{y,T})(400 - T) & \text{for } 300 < T \leq 400^\circ\text{C} \end{cases} \quad (12)$$

4.3. Stress-strain model for concrete at elevated temperatures

For concrete at elevated temperatures, the stress-strain model given in Eurocode 2 [48] is incorporated in the numerical model and illustrated in Fig. 13. This model is represented by the following equation:

$$\sigma_{c,T} = \begin{cases} \frac{3\epsilon_c f'_{c,T}}{\epsilon'_{c,T} [2 + (\epsilon_c / \epsilon'_{c,T})^3]} & \text{for } \epsilon_c \leq \epsilon'_{c,T} \\ f'_{c,T} \left[\frac{\epsilon_{cu,T} - \epsilon_c}{\epsilon_{cu,T} - \epsilon'_{c,T}} \right] & \text{for } \epsilon_c > \epsilon'_{c,T} \end{cases} \quad (13)$$

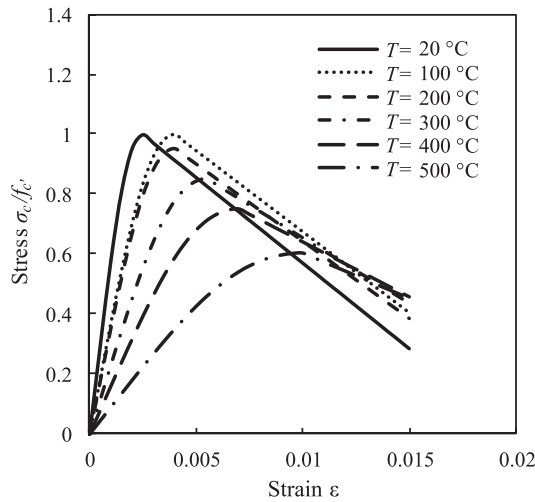


Fig. 13. Stress-strain curves for concrete at elevated temperatures based on Eurocode 2 [48].

where $f'_{c,T}$ represents the concrete compressive strength, $\epsilon'_{c,T}$ denotes the concrete strain at $f'_{c,T}$, and $\epsilon_{cu,T}$ is the concrete ultimate strain at elevated temperatures. The concrete strain values of $\epsilon'_{c,T}$ and $\epsilon_{cu,T}$ at elevated temperatures can be found in Eurocode 2 [48] for siliceous aggregates and appropriate values should be used for other types of aggregates.

4.4. Critical local buckling of steel tube

The steel tube of a rectangular CFST short column subjected to axial compression are under uniform compression and may undergo outward local buckling [40–42]. Expressions for computing the critical local buckling stress of clamped steel plates in CFST rectangular columns at room temperatures have been proposed by Liang et al. [49]. Liang [40,41] incorporated these expressions in the fiber-based computational model to include local buckling in the nonlinear modeling of CFST columns. The local buckling behavior of steel plates with imperfections at elevated temperatures in CFST rectangular columns was studied by Kamil et al. [50]. Design equations derived by Kamil et al. [50] are included in the present fiber modeling technique to compute the critical local buckling strength of steel tube in axially loaded CFST columns at elevated temperatures. These equations are applicable to steel tube walls with clear width-to-thickness ratio (b/t_s) ranging from 30 to 110.

For a steel tube wall exposed to temperatures ranging from 550 to 650 °C, its critical local buckling stress is calculated by [50]

$$\frac{\sigma_{1c,T}}{f_{y,T}} = (0.1916\lambda_{c,T}^{-0.7661} + 0.003889) (m_1\lambda_{c,T}^2 + m_2\lambda_{c,T} + m_3) \quad (14)$$

where $\sigma_{1c,T}$ stands for the plate critical local buckling stress at elevated temperatures, and $\lambda_{c,T}$ represents the relative slenderness of the plate at elevated temperatures, determined by

$$\lambda_{c,T} = \sqrt{\frac{12(1-\nu^2)(b/t_s)^2(R_{y,T}f_y)}{k\pi^2(R_{E,T}E)}} \quad (15)$$

where f_y denotes the steel yield stress at ambient temperature, ν represents the Poisson's ratio of steel, E is the Young's modulus of steel at ambient temperature, $k = 9.95$ stands for the coefficient of elastic local buckling. The four edges of the steel tube wall in a CFST column are assumed to be clamped as discussed by Liang et al. [49].

The coefficients m_1 , m_2 and m_3 in Eq. (14) are given as

$$m_1 = -1.0685\alpha_s^2 + 2.275\alpha_s - 0.8969 \quad (16)$$

$$m_2 = 2.3075\alpha_s^2 - 4.7791\alpha_s + 1.8475 \quad (17)$$

$$m_3 = -0.825\alpha_s^2 + 1.086\alpha_s + 1.0083 \quad (18)$$

where α_s is the stress gradient coefficient and defined as the ratio of the minimum stress to the maximum stress applied to the plate. For CFST columns in axial compression, the steel tube is under uniform edge stresses so that α_s is taken as 1.0.

Expression for predicting the critical local buckling stress of steel plates for any other temperatures given proposed by Kamil et al. [50] is

$$\frac{\sigma_{1c,T}}{f_{y,T}} = (g_1\lambda_{c,T}^{g_2} + g_2) \frac{0.6566\lambda_{c,T}^{0.001521} \left(\frac{R_{p,T}}{R_{y,T}}\right)^{-0.1598}}{0.5415\lambda_{c,T}^{4.889} + \left(\frac{R_{p,T}}{R_{y,T}}\right)^{-0.8252}} \quad (19)$$

where the coefficients g , g_1 and g_2 are

$$g = -7.9339\alpha_s^2 + 11.29\alpha_s + 4.701 \quad (20)$$

$$g_1 = 0.0863\alpha_s^2 - 0.1248\alpha_s + 0.0431 \quad (21)$$

$$g_2 = 0.2656\alpha_s^2 - 0.9902\alpha_s + 1.719 \quad (22)$$

4.5. Post-local buckling of steel tube

The effective width models developed by Liang et al. [49] were included in the fiber-based computational procedures to take into account the influences of post-local buckling on the performance of CFST columns at room temperatures by Liang [40,41]. The effective widths of a rectangular steel tube in CFST column in axial compression are schematically illustrated in Fig. 14. Kamil et al. [50] formulated effective width equations for computing the post-local buckling strengths of steel plates at elevated temperatures and are applicable to steel tube walls with clear width-to-thickness ratio (b/t_s) ranging from 30 to 110. The development of these formulas considered residual stresses and initial geometric imperfections for temperatures under 400 °C were considered in the development of these formulas. The formulas given by Kamil et al. [50] are coded in the computer program for the calculation of the effective widths of steel tube in axially-loaded steel tube in CFST columns in fire, which are expressed by

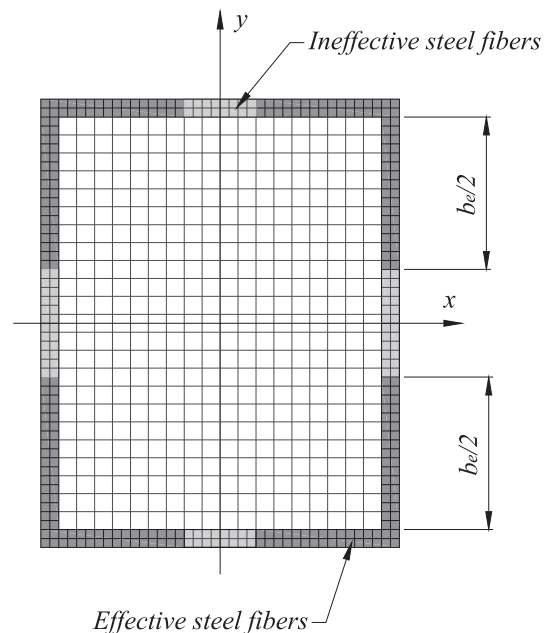


Fig. 14. Effective widths of steel tube walls in rectangular CFST column section.

$$\frac{b_e}{b} = (q_1 \lambda_{c,T}^q) \frac{0.8418 \lambda_{c,T}^{0.02368} \left(\frac{R_{p,T}}{R_{y,T}}\right)^{-0.3028} + 1.154 \left(\frac{R_{p,T}}{R_{y,T}}\right)}{2.055 + \lambda_{c,T}^{1.68}} \quad (23)$$

in which b_e and b represent the effective width and clear width of the steel tube wall, respectively; and q and q_1 are expressed by

$$q = 0.04007\alpha_s^2 - 0.05275\alpha_s + 0.03355 \quad (24)$$

$$q_1 = 0.1007\alpha_s^2 - 0.7027\alpha_s + 1.65 \quad (25)$$

After the critical local buckling occurs, the post-local buckling is associated with the redistribution of in-plane stresses in the thin steel plate as discussed by Liang [40,42]. Based on the effective width concept, the steel fiber stresses within the effective widths as illustrated in Fig. 14 are assigned to the steel yield stress while those located in the ineffective widths are set to zero. The simulation of the progressive post-local buckling is undertaken by the gradual redistribution of the in-plane stresses in the buckled steel plate. The effective width of the plate under edge stress greater than its critical buckling stress and less than its ultimate strength is computed by linear integration based on the stress level as suggested by Liang [40]. The modeling procedure given by Liang [40] is used to simulate the progressive post-local buckling of steel tube walls in CFST columns under axial load and fire.

5. Verification of the fiber element model

As discussed in the Introduction, computational and experimental research on the performance of axially-loaded rectangular CFST short columns subjected to fire loading has been very limited. Therefore, experimental data provided by Lu et al. [23] and numerical results presented by Yin et al. [34] and Dai and Lam [36] are utilized to verify the fiber element model developed. Lu et al. [23] conducted tests on square CFST short columns at elevated temperatures under constant axial compression. Table 3 provides the details of the specimens. The actual compressive strength of concrete in the tested CFST columns was unknown and usually varies from $0.8f'_{cd}$ to $1.0f'_{cd}$, where f'_{cd} is the compressive strength of concrete cylinder. In the numerical analyses, f'_c was taken as $0.82f'_{cd}$. Fig. 15 shows the predicted and experimentally measured axial deformation-time relationships. It can be seen that the numerical model generally predicts well the behavior of the tested specimens. However, as shown in Fig. 15a, b and d, experimental fire-resistances are lower than numerical predictions. This is because the actual thermal properties of steel and concrete and moisture content in the columns were not measured in the experiments and the fiber model employed idealized thermal properties of steel and concrete and 3% moisture content in the analyses.

The square CFST short column analyzed by Yin et al. [34] using their analytical model had the width of 443.12 mm and thickness of 17.72 mm. The steel yield strength at ambient temperature was 275 MPa and steel modulus of elasticity was 200000 MPa. The strength of the filled concrete in compression was 25 MPa. The concrete and steel thermal and mechanical properties given in Eurocode 3 [47] were used in the analyses. It was assumed that the contact at the interface of concrete and steel was perfect. The fiber element analysis of the column considered local buckling. The predicted ultimate axial load-exposure time relationship is compared against the solution given by Yin et al. [34] in Fig. 16. It is seen that good agreement between the two

Table 3
Dimensions and properties of CFST short columns tested by Lu et al. [23].

Specimen	$B \times D \times t_s$ (mm)	f_y (MPa)	f_u (MPa)	E_s (GPa)	Applied load (kN)
S1R2E0	150 × 150 × 5	486	558	197	486
S1R4E0	150 × 150 × 5	486	558	197	486
S3R3E0	200 × 200 × 6	467	544	199	1226
S2R4E0	200 × 200 × 6	467	544	199	1800

numerical solutions is achieved.

Dai and Lam [36] used analysis software ABAQUS to determine the responses of axially loaded short CFST rectangular and square columns under fire. The material and geometric properties of these columns as well as axial loads are provided in Table 4. The steel tube had the Young's modulus of 210000 MPa and yield stress of 350 MPa and filled with 30 MPa concrete. Both the concrete and steel thermal and mechanical properties provided in Eurocode 3 [47] were used. The air gap between the steel tube and concrete was not considered. The predicted fire-resistance of short CFST columns by the fiber model is compared against that obtained by Dai and Lam in Table 4. It can be observed that there is a good correlation between both numerical predictions. However, the fiber model slightly underestimates the fire-resistance of these CFST short columns. The computed axial displacements as a function of the maximum temperatures on steel tube walls are schematically presented in Figs. 17 and 18. The tube local buckling was not included in the finite element analyses conducted by Dai and Lam [36]. When local buckling was not included in the analyses, the predicted axial displacement-maximum temperature relations by the proposed computational procedure are in good correlation with finite element results. This demonstrates that the influence of local buckling on the fire responses of CFST rectangular short columns is significant.

6. Parametric study

A parametric study was undertaken to explore the behavior of rectangular CFST short columns under combined axial load and fire accounting for the local buckling of steel plates. The parameters examined included the concrete strength, the steel yielding strength, axial load ratio and width-to-thickness ratio. The modulus of elasticity for steel was taken as 210 GPa. The clear width-to-thickness ratios (b/t_s) of the CFST columns used in the following parametric study ranged from 38 to 98 so that the local buckling of these columns was considered in the numerical analyses. In the parametric study, the fiber-based modeling technique was employed to predict either the axial load-strain behavior of CFST short columns subjected to an elevated temperature by increasing the axial strain or the fire-resistance of CFST short columns under constant axial load by increasing the temperature.

6.1. Effects of local buckling

The computer program developed was used to study the influence of local buckling on the performance of short CFST rectangular columns at elevated temperatures. A short rectangular CFST column of 600×500 mm with thickness of 6 mm giving B/t_s and D/t_s ratios of 100 and 83, respectively was employed. The steel yield strength at ambient temperatures was 300 MPa while the concrete had a strength of 40 MPa. The fiber analyses were undertaken on the column exposed to standard fire by including local buckling and excluding its effect, respectively. Fig. 19 provides the axial load-strain responses of the CFST column subjected to fire exposure time of 10 min, where P_{10} is the ultimate axial strength of the column at 10 min of exposure fire. It is seen that the tube local buckling markedly reduces the column ultimate axial strength by 10.1%. The ultimate axial load-time curves are presented in Fig. 20. At ambient temperature, the reduction in the column ultimate load due to local buckling is 9.2%. At 20 min of fire exposure, the local buckling reduces the column ultimate load by 5.7%. This demonstrates that the effect of local buckling on the ultimate load-carrying capacity of CFST short columns within 20 min of fire exposure is significant and its effect diminishes as time increases further.

6.2. Effects of concrete strength

The influences of the concrete strength on the performance of CFST short columns under fire were studied using the fiber model incorporating local buckling. The concrete with compressive strengths of

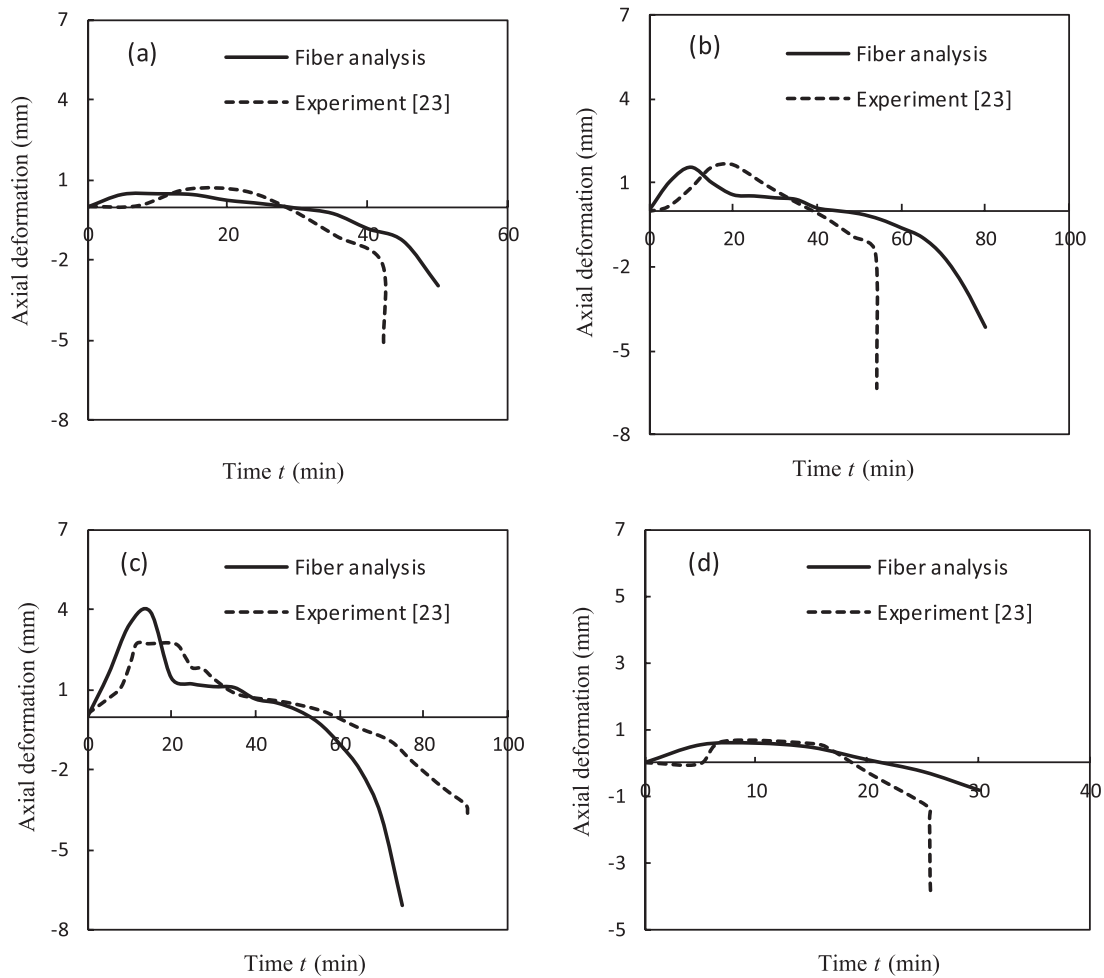


Fig. 15. Comparison of predicted axial displacement-maximum temperature at steel in square CFST short columns tested by Lu et al. [23]: (a) S2R4E0; (b) S2R3E0; (c) S1R2E0; and (d) S1R4E0.

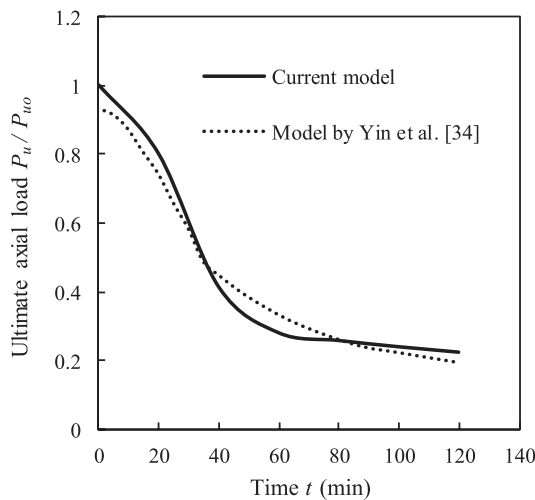


Fig. 16. Comparison of predicted ultimate axial loads with those given by Yin et al. [34].

25, 35, 45 and 55 MPa was used to fill the steel tubes, respectively. The cross-section of the square CFST column was $500 \times 500 \times 8.33$ mm with a b/t_s ratio of 58 and $f_y = 300$ MPa. Fig. 21 presents the axial load-strain responses of the short CFST column made of 35 MPa concrete. The column initial stiffness and ultimate strength and decrease significantly with increasing the temperatures. The reductions in the

Table 4

Comparisons of fire-resistance of CFST short columns.

Column	$B \times D \times t_s$ (mm)	Applied load			
		500 kN		600 kN	
		Dai and Lam [35] Fire time (min)	Fiber analysis Fire time (min)	Dai and Lam [35] Fire time (min)	Fiber analysis Fire time (min)
SHS	$123 \times 123 \times 5$	26.955	23.98	25.4	21.26
SHS1	$118.9 \times 118.9 \times 5$	28.984	22.57	24	20.31
SHS2	$125.9 \times 125.9 \times 5$	28.069	24.67	26.3	21.8
RHS	$169 \times 84.5 \times 5$	30.102	23.7	24.91	21.53
RHS1	$158.5 \times 79.3 \times 5$	26.18	22.43	23.35	20.33
RHS2	$179 \times 89.5 \times 5$	29.05	25.41	26.88	22.88

column ultimate strength are 24%, 36%, and 44% when the fire exposure time increases to 20, 40, and 60 min, respectively. The influences of the concrete strengths on the ultimate axial load-exposure time curves for CFST columns are shown in Fig. 22. The results show that increasing the strength of concrete significantly increases the column ultimate axial load regardless of the time exposure or temperatures. The column ultimate load could be increased by 24%, 48% and 72% by increasing the concrete strength from 25 MPa to 35 MPa, 45 MPa and 55 MPa, respectively. At fire exposure time of 10 min, the increases in strength of the CFST column are 26%, 53%, and 79% when the

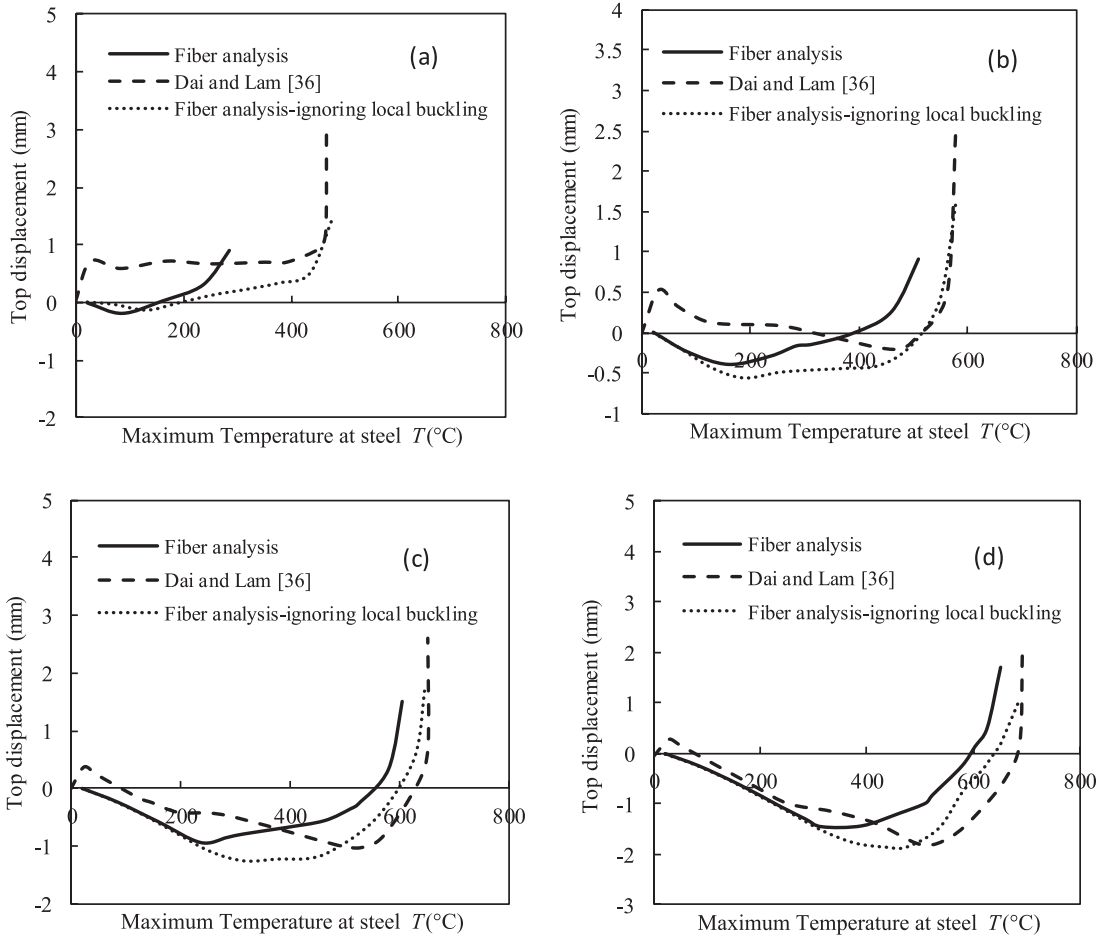


Fig. 17. Comparison of predicted axial displacement-maximum temperature at steel in square CFST short columns those given by Dai and Lam [36]: (a) Axial load=1000 kN; (b) Axial load=800 kN; (c) Axial load=600 kN; and (d) Axial load = 500 kN.

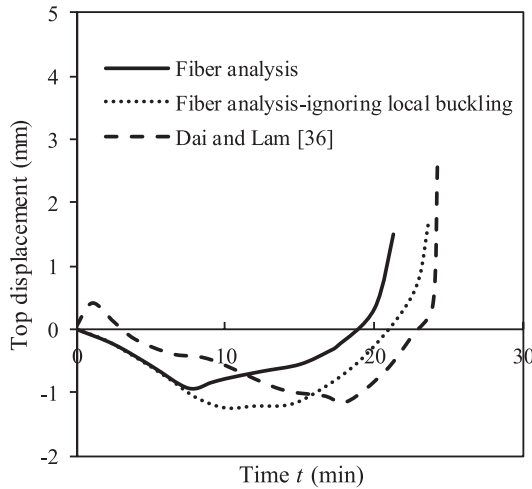


Fig. 18. Comparison of predicted axial displacement-maximum temperature at steel in square CFST short columns with results given by Dai and Lam [36] (axial load = 600 kN).

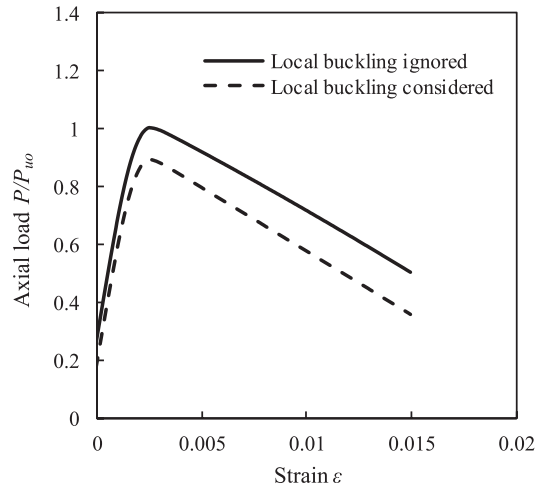


Fig. 19. Influences of local buckling on the axial load-strain behaviour of CFST column subjected to 10 min of standard fire.

compressive strength increases from 25 MPa to 35 MPa, 45 MPa and 55 MPa, respectively. At 20 min of fire exposure, the strength increases are 31%, 63, and 94% by increasing the concrete strength from 25 MPa to 35 MPa, 45 MPa and 55 MPa, respectively. This indicates that the steel tube loses its resistance to fire as time increases and the axial load is transmitted from the steel tube to the filled concrete.

6.3. Effects of steel yield strength

To examine the effects of steel yield strengths at ambient temperatures on the responses of CFST columns under fire, the short rectangular CFST column of 500 × 400 mm with B/t_s of 50 and D/t_s ratio of 40 was analyzed using the computer program developed. Steel tubes having the yield stresses of 250 MPa, 350 MPa and 450 MPa were

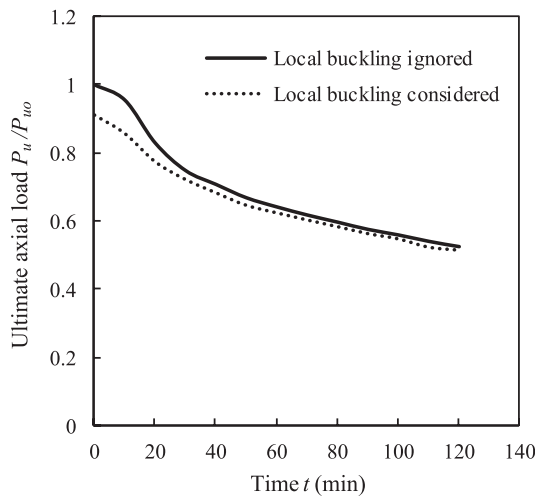


Fig. 20. Influences of local buckling on the ultimate axial strength of CFST column subjected to various time exposure to fire.

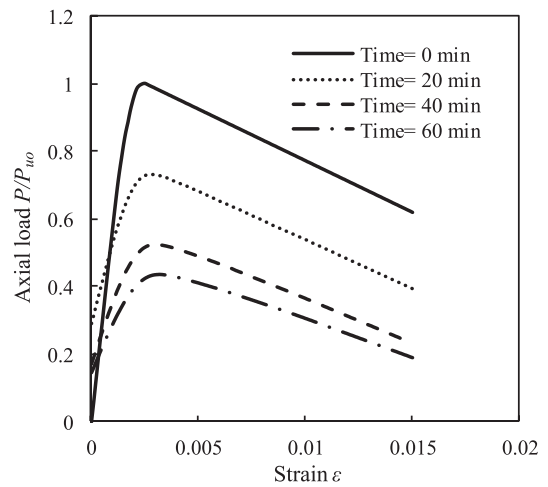


Fig. 23. Axial load-strain curves of rectangular short CFST column with yield strength of 450 MPa exposed to fire.

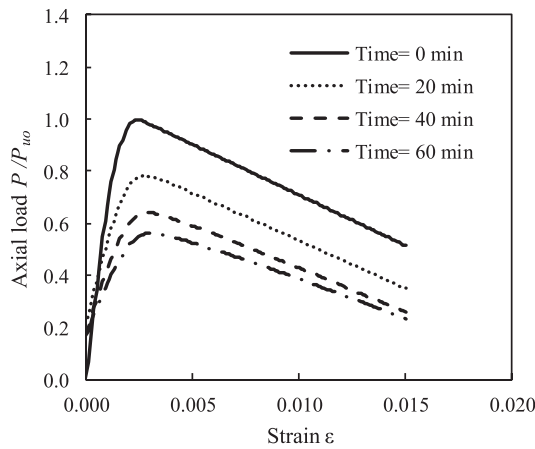


Fig. 21. Axial load-strain curves of square short CFST column with 30 MPa concrete and various fire time exposures.

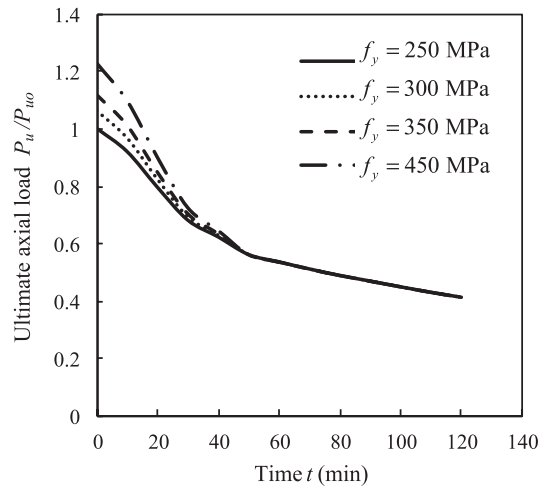


Fig. 24. Effects of the steel yield strength on the ultimate strength of rectangular short CFST columns under fire.

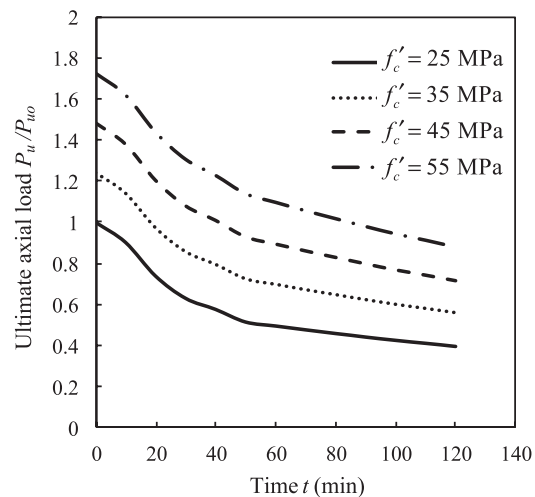


Fig. 22. Effects of concrete strengths on the ultimate strength and fire-resistance of square CFST columns.

considered. Fig. 23 shows the axial load–strain responses of the rectangular CFST short column with yield strength of 450 MPa at different fire exposures times. The column ultimate load-carrying capacity decreases with increasing the fire exposure time. The reductions in the

axial stiffness of the short rectangular CFST column are 27%, 48% and 57% when the time exposure increases to 20, 40 and 60 min, respectively. The column strength–exposure time curves of CFST columns that had different steel yield stress are provided in Fig. 24. The effect of the yield strength decreases with increasing the exposure fire time, and its effect vanishes after 40 min. At ambient temperature, the column ultimate strength increases by 6%, 12% and 23% respectively when the steel yield stress is increased from 250 MPa to 300 MPa, 350 MPa and 450 MPa. However, at the fire exposure time of 10 min, increasing the yield stress of steel from 250 MPa to 300 MPa, 350 MPa and 450 MPa leads to the column ultimate strength increase by 5%, 10% and 20%, respectively.

6.4. Effects of width-to-thickness ratio

The effects of width-to-thickness ratio on the fire behavior of CFST columns were examined herein. The fiber analyses of a CFST square column of 400 × 400 mm with B/t_s ratios of 40, 60, 80 and 100 were conducted. The steel tube had a yield stress of 300 MPa and filled with 40 MPa concrete. The axial load–strain–time relationships of the column with B/t_s ratio of 40 are provided in Fig. 25. When the fire exposure time increases to 20, 40 and 60 min, the percentage reductions in column ultimate axial strength are 24%, 44%, and 54%, respectively. Fig. 26 demonstrates the effect of B/t_s ratio on the column strength

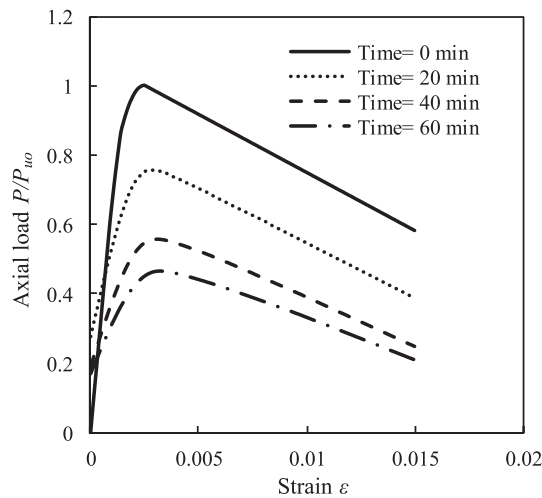


Fig. 25. Axial load-strain relationships of square short CFST column with B/t_s ratio of 60 with various exposure times.

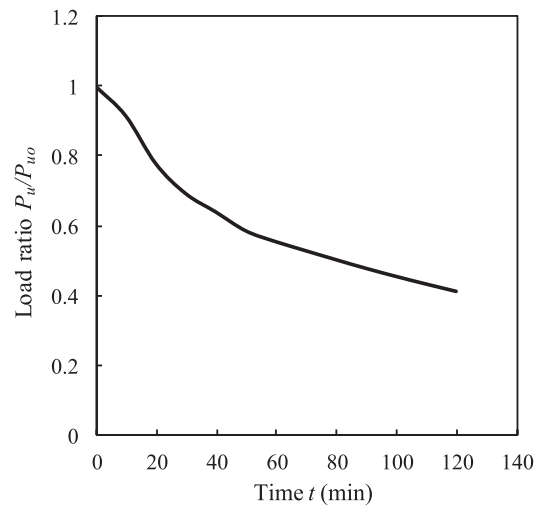


Fig. 27. Load ratio of square short CFST column with B/t_s ratio of 60 at different periods of exposure to standard fire.

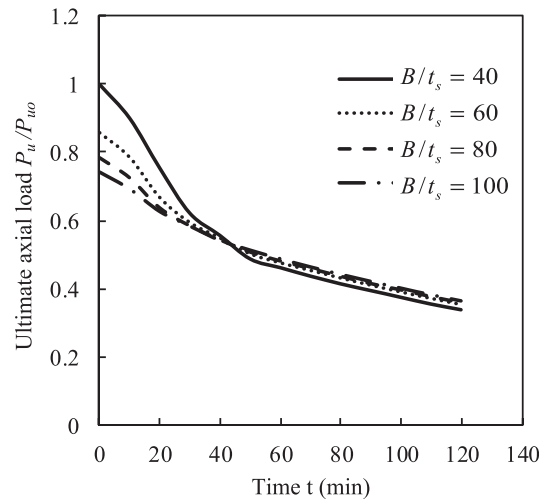


Fig. 26. Ultimate strength of square short CFST column with different B/t_s ratios at different periods of exposure to standard fire.

curves at elevated temperatures, where P_{u0} is the ultimate axial strength of the column at ambient temperature for B/t_s 40. It shows that the B/t_s ratio has the most pronounced effect on the column strength at ambient temperature. This effect decreases as the fire exposure time or temperature increases and diminishes after 40 min. The column strength at ambient temperature is reduced by 14%, 22% and 26% by increasing the B/t_s ratio from 40 to 60, 80 and 100, respectively. However, at the fire exposure time of 20 min, increasing the B/t_s ratio from 40 to 60, 80 and 100 reduces the column strength by 12%, 16%, and 17%, respectively. The smaller the thickness, the faster the heat transfers from the steel to the concrete.

6.5. Effects of axial load ratio

The axial load ratio is computed as the ratio of the applied axial load to the ultimate axial load of a CFST short column at ambient temperature. To study the influences of the loading ratio on fire-resistance of short CFST columns, the fiber model was employed to analyze a square CFST column of 400×400 mm with a B/t_s ratio of 60. The steel tube had a yield stress of 300 MPa was filled with concrete with strength of 40 MPa. The axial load ratio as a function of fire-resistance is given in Fig. 27, where P_{u0} is the ultimate axial strength of the column at ambient temperature. It would appear that the fire-resistance

increases significantly with decreasing the axial load ratio. In other words, the axial load has a significant effect on the column fire-resistance. As shown in Fig. 27, when the axial load ratio is 0.92, the fire-resistance obtained is 10 min. When the axial load ratio is reduced to 0.64, the fire-resistance increases to 40 min. The sharp decline of the column strength is because the steel loses its strength at high temperatures. After 40 min, the column strength decreases gradually with increasing the time and the axial load is mainly resisted by the concrete.

6.6. Load distribution

The analysis of a rectangular CFST column of 400×500 mm with thickness of 10 mm and a b/t ratio was carried out to examine the load distribution in the components of steel and concrete. The concrete with strength of 30 MPa was used to fill the steel tube with yield strength of 300 MPa. The axial loads resisted by the concrete, steel tube and the CFST column as a function of axial strain at the fire exposure time of 10 min are illustrated in Fig. 28. The results indicate that at this time of fire exposure, the steel has yielded and its value constant under the applied load. The concrete core shares a significant portion of the ultimate load. The computed contribution ratios for steel and concrete as a time function are given in Fig. 29. The contribution ratio is defined as $P_{u,s}/P_u$ and $P_{u,c}/P_u$ for steel and concrete, respectively, where $P_{u,s}$, $P_{u,c}$ and

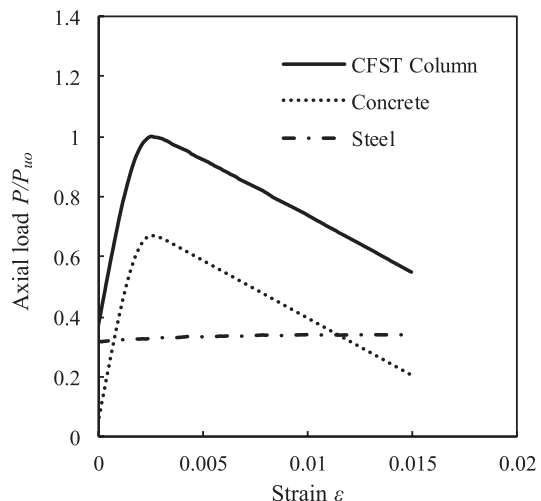


Fig. 28. Load distribution in steel tube and concrete in rectangular short CFST column subjected to 10 min fire exposure.

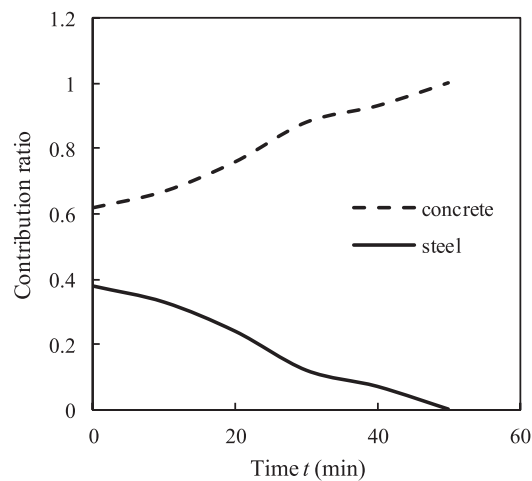


Fig. 29. Steel and concrete contribution ratio as a function of fire exposure time.

P_u are the ultimate axial loads carried by the steel, the concrete and the CFST section, respectively. It can be observed that the steel contribution ratio decreases with an increase in the time exposure or temperature and eventually the steel tube completely loses its strength. In contrast, the concrete contribution ratio increases with increasing the time exposure or temperature and the concrete carries the axial load alone after the steel tube completely loses its capacity.

7. Conclusions

This paper has presented an efficient fiber-based computational model for the fire-resistance simulation of axially-loaded short CFST rectangular columns subjected to fire. The important features including local and post-local buckling, air gap at the interface of concrete and steel tube, concrete moisture content and the emissivity of the exposure surfaces have been considered in the computational modeling technique. The progressive post-local buckling is simulated by the fiber stress redistribution within the buckled steel tube walls using effective width expression derived for steel plates exposed to elevated temperatures. A sequential coupled thermal and nonlinear stress analysis procedure has been developed that calculates the thermal and structural behaviors of CFST columns at elevated temperatures. The computer program implementing the sequential coupled computational procedure has been used to conduct a parametric study on the thermal and structural behavior of rectangular short CFST columns including local buckling effects at elevated temperatures.

The following conclusions are drawn from this research work:

- (1) The proposed fiber-based numerical model, which takes into consideration the effects of local buckling, air gap, moisture content and the emissivity of the exposure surfaces, is shown to capture well the fire-resistance of loaded rectangular CFST short columns under standard fire.
- (2) Local buckling remarkably reduces the ultimate axial loads of CFST rectangular columns at elevated temperatures and is recommended to be taken into account in numerical modeling techniques.
- (3) The ultimate axial load and initial stiffness of CFST short columns decreases significantly as fire exposure time increases.
- (4) The higher concrete strength, the higher the ultimate strength of short CFST columns regardless of the fire exposure time.
- (5) The steel yield strength has pronounced influences on the axial load-carrying capacities of CFST columns in the first 40 min fire exposure.
- (6) The B/t_s ratio has a pronounced effect on the column ultimate strengths in fire exposure time of 40 min, but its effect diminishes as the time increases.

- (7) As the fire exposure time increases, the axial load resisted by the steel tube decreases while the axial load carried by the concrete increases.

References

- [1] Furlong RW. Strength of steel-encased concrete beam-columns. *J Struct Div ASCE* 1967;93(5):113–24.
- [2] Knowles RB, Park R. Strength of concrete-filled steel tubular columns. *J Struct Div ASCE* 1969;95(12):2565–87.
- [3] Uy B, Bradford MA. Elastic local buckling of thin steel plates in composite steel-concrete members. *Eng Struct* 1996;18(3):193–200.
- [4] Schneider SP. Axially loaded concrete-filled steel tubes. *J Struct Eng ASCE* 1998;124(10):1125–38.
- [5] Hajjar JF, Schiller PH, Molodan A. A distributed plasticity model for concrete-filled steel tube beam-columns with interlayer slip. *Eng Struct* 1998;20(8):663–76.
- [6] Uy B. Strength of concrete-filled steel box columns incorporating local buckling. *J Struct Eng ASCE* 2000;126(3):341–52.
- [7] Susantha KAS, Ge HB, Usami T. Uniaxial stress-strain relationship of concrete confined by various shaped steel tubes. *Eng Struct* 2001;23(10):1331–47.
- [8] Shanmugam NE, Lakshmi B, Uy B. An analytical model for thin-walled steel box columns with concrete in-fill. *Eng Struct* 2002;24(6):825–38.
- [9] Mollazadeh MH, Wang YC. New insights into the mechanism of load introduction into concrete-filled steel tubular column through shear connection. *Eng Struct* 2014;75:139–51.
- [10] AS 3600-2009. Australian standard for concrete structures. Sydney, New South Wales, Australia: Standards Australia; 2009.
- [11] Wang YC. Steel and composite structures: Behaviour and design for fire safety. London and New York: Spon Press; 2002.
- [12] Quiel SE, Garlock MEM. Calculating the buckling strength of steel plates exposed to fire. *Thin-Wall Struct* 2010;48:684–95.
- [13] Couto C, Real PV, Lopes N, Zhao B. Effective width method to account for the local buckling of steel thin plates at elevated temperatures. *Thin-Wall Struct* 2014;84:134–49.
- [14] Lie TT, Chabot M. Experimental studies on the fire resistance of hollow steel columns filled with plain concrete. Internal report, National Research Council Canada, Institute for Research in Construction, 1992-01.
- [15] Sakumoto Y, Okada T, Yoshida M, Takasa S. Fire resistance of concrete-filled, fire-resistat steel-tube columns. *J Mat in Civil Eng ASCE* 1994;69(2):169–84.
- [16] Kodur VKR, Lie TT. Fire performance of concrete-filled hollow steel columns. *J Fire Prot Eng* 1995;79(3):89–98.
- [17] Han LH, Yang YF, Xu L. An experimental study and calculation on the fire resistance of concrete-filled SHS and RHS columns. *J Constr Steel Res* 2003;59:427–52.
- [18] Choi SM, Kim DK, Kim JH, Chung KS, Park SH. Experimental study on fire resistance of concrete-filled steel tube column under constant axial loads. *Steel Struct* 2005;5(4):305–13.
- [19] Han LH, Chen F, Liao FY, Tao Z, Uy B. Fire performance of concrete filled stainless steel tubular columns. *Eng Struct* 2013;56:165–81.
- [20] Espinos A, Romero ML, Serra E, Hospitaler A. Circular and square slender concrete-filled tubular columns under large eccentricities and fire. *J Constr Steel Res* 2015;110:90–100.
- [21] Espinos A, Romero ML, Serra E, Hospitaler A. Experimental investigation on the fire behavior of rectangular and elliptical slender concrete-filled tubular columns. *Thin-Wall Struct* 2015;93:137–48.
- [22] Dundu M. Column buckling tests of hot-rolled concrete filled square hollow sections of mild to high strength steel. *Eng Struct* 2016;127:73–85.
- [23] Lu H, Zhao XL, Han LH. Fire behaviour of high strength self-consolidating concrete filled steel tubular stub columns. *J Constr Steel Res* 2009;65:1995–2010.
- [24] Lie TT, Chabot M. A method to predict the fire resistance of circular concrete filled hollow steel columns. *J Fire Prot Eng* 1990;2(4):111–26.
- [25] Lie TT, Irwin RJ. Fire resistance of rectangular steel columns filled with bar-reinforced concrete. *J Struct Eng ASCE* 1995;121(5):797–805.
- [26] Kodur VKR, Lie TT. Evaluation of fire resistance of rectangular steel columns filled with fibre-reinforced concrete. *Can J Civil Eng* 1997;24:339–49.
- [27] Han LH. Fire performance of concrete filled steel tubular beam-columns. *J Constr Steel Res* 2001;57:695–709.
- [28] Chung K, Park S, Choi S. Fire resistance of concrete filled square steel tube columns subjected to eccentric axial load. *Steel Struct* 2009;9:67–76.
- [29] Ding J, Wang YC. Realistic modelling of thermal and structural behaviour of unprotected concrete filled tubular columns in fire. *J Constr Steel Res* 2008;64:1086–102.
- [30] Espinos A, Romero ML, Hospitaler A. Advanced model for predicting the fire response of concrete filled tubular columns. *J Constr Steel Res* 2010;66:1030–46.
- [31] Hong SD, Varma AH. Analytical modeling of the standard fire behavior of loaded CFT columns. *J Constr Steel Res* 2009;65:54–69.
- [32] Schaumann P, Kodur V, Bahr O. Fire behaviour of hollow structural section steel columns filled high strength concrete. *J Constr Steel Res* 2009;65:1794–802.
- [33] Wang K, Young B. Fire resistance of concrete-filled high strength steel tubular columns. *Thin-Wall Struct* 2013;71:46–56.
- [34] Yin J, Zha XX, Li LY. Fire resistance of axially loaded concrete filled steel tube columns. *J Constr Steel Res* 2006;62:723–9.
- [35] Song TY, Han LH, Tu HX. Concrete filled steel tube columns under combined temperature and loading. *J Constr Steel Res* 2010;66:369–82.
- [36] Dai XH, Lam D. Shape effect on the behaviour of axially loaded concrete filled steel

- tubular stub columns at elevated temperature. *J Constr Steel Res* 2012;73:117–27.
- [37] Tao Z, Ghannam M. Heat transfer in concrete-filled carbon and stainless steel tubes exposed to fire. *Fire Safety J* 2013;61:1–11.
- [38] Xion MX, Wang YH, Liew JYR. Evaluation on thermal behaviour of concrete-filled steel tubular columns based on modified finite difference method. *Adv in Struct Eng* 2016;19(5):746–61.
- [39] Ahmed M, Liang QQ, Patel VI, Hadi MNS. Nonlinear analysis of rectangular concrete-filled double steel tubular short columns incorporating local buckling. *Eng Struct* 2018;175:13–26.
- [40] Liang QQ. Performance-based analysis of concrete-filled steel tubular beam-columns. Part I: Theory and algorithms. *J Constr Steel Res* 2009;65(2):363–73.
- [41] Liang QQ. Performance-based analysis of concrete-filled steel tubular beam-columns. Part II: Verification and applications. *J Constr Steel Res* 2009;65(2):351–62.
- [42] Liang QQ. Analysis and design of steel and composite structures. Boca Raton and London: CRC Press, Taylor and Francis Group; 2014.
- [43] Liang QQ. Nonlinear analysis of circular double-skin concrete-filled steel tubular columns under axial compression. *Eng Struct* 2017;131:639–50.
- [44] Liang QQ. Numerical simulation of high strength circular double-skin concrete-filled steel tubular slender columns. *Eng Struct* 2018;168:205–17.
- [45] Eurocode 1. 1991-1-2, Actions on structures, Part 1.2: General actions- Actions on structures exposed to fire, CEN, Brussels, Belgium; 2002.
- [46] Incropera FP, Dewitt DP, Bergman TL, Lavine AS. *Fundamental of heat and mass transfer*. 6 USA: John Wiley & Sons; 2005.
- [47] Eurocode 3. Design of steel structures, Part 1.2: General rules-structural fire design, CEN, Brussels, Belgium; 2005.
- [48] Eurocode 2. Design of concrete structures, Part 1.2: General rules-structural fire design, CEN, Brussels, Belgium; 2004.
- [49] Liang QQ, Uy B, Liew JYR. Local buckling of steel plates in concrete-filled thin-walled steel tubular beam-columns. *J Constr Steel Res* 2007;63(3):396–405.
- [50] Kamil GM, Liang QQ, Hadi MNS. Local buckling of steel plates in concrete-filled steel tubular columns at elevated temperatures. *Eng Struct* 2018;168:108–18.

4.4 CONCLUDING REMARKS

A computer modeling technique has been described in this chapter, which simulates the fire and structural behaviors of short CFST columns having thin-walled rectangular cross-sections loaded concentrically when exposed to fire defined by standard temperature-time curve. The important features including gradual post-local buckling, air gap at the interface of steel and concrete and moisture content have been considered in the formulation based on the approach of fiber discretization. The thermal simulator proposed has been shown to predict well the temperatures in cross-sections. The computer simulation procedure developed has been demonstrated to produce numerical results that are in good correlations with standard fire test data and finite element solutions reported by other researchers. The computational results obtained from the parametric studies are valuable for developing design guides for the fire resistance design of CFST columns in tall composite buildings.

Chapter 5

CFST SLENDER COLUMNS UNDER FIRE EXPOSURE

5.1 INTRODUCTION

As discussed in Chapter 2, standard fire tests indicated that axially or eccentrically loaded thin-walled rectangular CFST slender columns exposed to fire failed by the local-global interaction buckling, which markedly reduced their fire resistance and strengths. This chapter describes a computational model developed by the theory of fiber analysis for computing the fire resistance and responses of slender CFST columns of thin-walled rectangular sections loaded axially and eccentrically to failure. The computer model accounts for the influences of various important features, including local-global interaction buckling, temperature-dependent material responses, concrete tensile behavior, deformations caused by preloads, initial geometric imperfection, and air gap between the concrete and steel tube. The temperatures in fiber elements are calculated by using the thermal simulator proposed in Chapter 3. Computer simulation procedure and solution algorithms are developed, which compute the load-deflection responses and fire resistance of eccentrically loaded slender CFST columns exposed to standard fire defined by the temperature-time curve. Comparative studies are conducted to validate the computer model. The computational model is then used to demonstrate the significance of various parameters on the fire behavior of loaded CFST slender columns.

This chapter includes the following papers:

1. **Kamil, G. M.**, Liang, Q. Q. and Hadi, M. N. S. (2019) Interaction behavior of local and global buckling of axially loaded rectangular thin-walled concrete-filled steel tubular slender columns under fire exposure, *Thin-Walled Structures* (currently under review).
2. **Kamil, G. M.**, Liang, Q. Q. and Hadi, M. N. S. (2019) Fire-resistance of eccentrically loaded rectangular concrete-filled steel tubular slender columns incorporating interaction of local and global buckling, *International Journal of Structural Stability and Dynamics*,19(8): 1950085.

GRADUATE RESEARCH CENTRE

DECLARATION OF CO-AUTHORSHIP AND CO-CONTRIBUTION: PAPERS INCORPORATED IN THESIS BY PUBLICATION

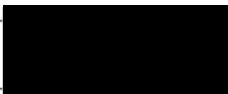
This declaration is to be completed for each conjointly authored publication and placed at the beginning of the thesis chapter in which the publication appears.

1. PUBLICATION DETAILS (to be completed by the candidate)

Title of Paper/Journal/Book:	Kamil, G. M., Liang, Q. Q. and Hadi, M. N. S. (2019) Interaction behavior of local and global buckling of axially loaded rectangular thin-walled concrete-filled steel tubular slender columns under fire exposure, Thin-Walled Structures (currently under review).		
Surname:	Kamil	First name:	Ghanim
College:	College of Engineering & Science	Candidate's Contribution (%):	70
Status:			
Accepted and in press:	<input type="checkbox"/>	Date:	<input type="text"/>
Published:	<input type="checkbox"/>	Date:	<input type="text"/>

2. CANDIDATE DECLARATION

I declare that the publication above meets the requirements to be included in the thesis as outlined in the HDR Policy and related Procedures – policy.vu.edu.au.

	15/04/2019
Signature	Date

3. CO-AUTHOR(S) DECLARATION

In the case of the above publication, the following authors contributed to the work as follows:

The undersigned certify that:

1. They meet criteria for authorship in that they have participated in the conception, execution or interpretation of at least that part of the publication in their field of expertise;
2. They take public responsibility for their part of the publication, except for the responsible author who accepts overall responsibility for the publication;
3. There are no other authors of the publication according to these criteria;
4. Potential conflicts of interest have been disclosed to a) granting bodies, b) the editor or publisher of journals or other publications, and c) the head of the responsible academic unit; and

5. The original data will be held for at least five years from the date indicated below and is stored at the following location(s):

<p>Location: College of Engineering and Science, Victoria University, Melbourne, Victoria, Australia.</p>
--

Name(s) of Co-Author(s)	Contribution (%)	Nature of Contribution	Signature	Date
Ghanim Mohammed Kamil	70	Developed and verified the model Conducted the parametric study Drafted the manuscript		28/02/ 2019
Qing Quan Liang	20	Provided initial concepts Provided critical revision of the article Final approval and submitting the manuscript		28/02/ 2019
Muhammad N. S. Hadi	10	Provided critical revision of the article Final approval of the manuscript		28/2/ 2019

GRADUATE RESEARCH CENTRE

DECLARATION OF CO-AUTHORSHIP AND CO-CONTRIBUTION: PAPERS INCORPORATED IN THESIS BY PUBLICATION

This declaration is to be completed for each conjointly authored publication and placed at the beginning of the thesis chapter in which the publication appears.

1. PUBLICATION DETAILS (to be completed by the candidate)

Title of Paper/Journal/Book:	Kamil, G. M., Liang, Q. Q. and Hadi, M. N. S. (2019) Fire-Resistance of Eccentrically Loaded Rectangular Concrete-Filled Steel Tubular Slender Columns Incorporating Interaction of Local and Global Buckling, International Journal of Structural Stability and Dynamics (accepted).		
Surname:	Kamil	First name:	Ghanim
College:	College of Engineering & Science	Candidate's Contribution (%):	70
Status:			
Accepted and in press:	<input checked="" type="checkbox"/>	Date:	11 April 2019
Published:	<input type="checkbox"/>	Date:	

2. CANDIDATE DECLARATION

I declare that the publication above meets the requirements to be included in the thesis as outlined in the HDR Policy and related Procedures – policy.vu.edu.au.

			15/04/2019
Signature			Date

3. CO-AUTHOR(S) DECLARATION

In the case of the above publication, the following authors contributed to the work as follows:

The undersigned certify that:

1. They meet criteria for authorship in that they have participated in the conception, execution or interpretation of at least that part of the publication in their field of expertise;
2. They take public responsibility for their part of the publication, except for the responsible author who accepts overall responsibility for the publication;
3. There are no other authors of the publication according to these criteria;
4. Potential conflicts of interest have been disclosed to a) granting bodies, b) the editor or publisher of journals or other publications, and c) the head of the responsible academic unit; and

5. The original data will be held for at least five years from the date indicated below and is stored at the following location(s):

<p>Location: College of Engineering and Science, Victoria University, Melbourne, Victoria, Australia.</p>
--

Name(s) of Co-Author(s)	Contribution (%)	Nature of Contribution	Signature	Date
Ghanim Mohammed Kamil	70	Developed and verified the model Conducted the parametric study Drafted the manuscript		28/02/ 2019
Qing Quan Liang	20	Provided initial concepts Provided critical revision of the article Final approval and submitting the manuscript		28/02/ 2019
Muhammad N. S. Hadi	10	Provided critical revision of the article Final approval of the manuscript		28/2/ 2019

Interaction behavior of local and global buckling of axially loaded rectangular thin-walled concrete-filled steel tubular slender columns under fire exposure was published as Fiber element simulation of interaction behavior of local and global buckling in axially loaded rectangular concrete-filled steel tubular slender columns under fire exposure

Fiber element simulation of interaction behavior of local and global buckling in axially loaded rectangular concrete-filled steel tubular slender columns under fire exposure by G.M. Kamil, Q.Q. Ling, and M.N.S. Hadi was published in the peer review journal, *Thin-Walled Structures*, 145, 2019.

The published version is available at <https://doi.org/10.1016/j.tws.2019.106403>

Manuscript prepared for

Thin-Walled Structures

April 2019

Interaction behavior of local and global buckling of axially loaded rectangular thin-walled concrete-filled steel tubular slender columns under fire exposure

Ghanim Mohammed Kamil^a, Qing Quan Liang^{a,*}, Muhammad N. S. Hadi^b

^a College of Engineering and Science, Victoria University, PO Box 14428,
Melbourne,
VIC 8001, Australia

^b School of Civil, Mining and Environmental Engineering, University of
Wollongong, Wollongong, NSW 2522, Australia

Corresponding author:

Associate Professor Qing Quan Liang
College of Engineering and Science
Victoria University
PO Box 14428
Melbourne VIC 8001
Australia
Phone: +61 3 9919 4134
E-mail: Qing.Liang@vu.edu.au

Interaction behavior of local and global buckling of axially loaded rectangular thin-walled concrete-filled steel tubular slender columns under fire exposure

Ghanim Mohammed Kamil^a, Qing Quan Liang^{a,*}, Muhammad N. S. Hadi^b

^a *College of Engineering and Science, Victoria University, PO Box 14428, Melbourne, VIC 8001, Australia*

^b *School of Civil, Mining and Environmental Engineering, University of Wollongong, Wollongong, NSW 2522, Australia*

Abstract

Slender rectangular thin-walled concrete-filled steel tubular (CFST) columns in composite building structures exposed to fire may experience the interaction of local and global buckling. Numerical investigations on the interaction buckling responses of such columns under fire exposure have been rarely reported. This paper describes a fiber-based computational model for the prediction of the fire-resistance and interaction responses of local and global buckling of concentrically-loaded slender CFST columns made of rectangular sections exposed to fire. The thermal analysis is undertaken to calculate the distribution of temperatures in the column cross-section considering the effects of the air gap between concrete and steel, exposure surface emissivity as well as moisture content in concrete. The local and post-local buckling models proposed previously for steel tube

* Corresponding author. Tel.: 61 3 9919 4134.
E-mail address: Qing.Liang@vu.edu.au (Q. Q. Liang)

walls at elevated temperatures are incorporated in the inelastic analysis of cross-sections to model the progressive post-local buckling. The global buckling analysis of slender CFST columns exposed to fire accounts for the effects of material and geometric nonlinearities as well as local buckling. Efficient computational procedure and solution algorithms are developed to solve the nonlinear equilibrium dynamic functions of loaded slender CFST columns exposed to fire. Independent experimental and numerical results on slender CFST columns are utilized to validate the computational model. The interaction behavior of local and global buckling and fire-resistance of slender rectangular CFST columns are investigated. It is shown that the developed computational model provides a reasonably accurate and efficient method for the prediction of the interaction buckling responses as well as the fire-resistance of slender CFST columns subjected to axial loading and fire.

Keywords: Concrete-filled steel tubes; Elevated temperatures; Fire-resistance; Nonlinear analysis; Interaction of local and global buckling.

1. Introduction

Thin-walled square and rectangular concrete-filled steel tubular (CFST) slender columns as illustrated in Fig. 1 have been used widely in subway stations, bridges, industrial buildings and tall buildings to support heavy loads [1]. The CFST columns possess not only high strength, stiffness, ductility and seismic resistance but also high fire-resistance. The behavior of short and slender CFST columns at room temperatures has been investigated experimentally and numerically by researchers [2-8]. In design codes [9], a

column having a member slenderness ratio (L/r) greater than 22 is treated as a slender column. The design of slender CFST columns for the fire limit state is one of the important design criteria that must be considered in practice [10]. To achieve economical designs, thin-walled steel tubes are often used to construct rectangular CFST columns. However, slender rectangular CFST columns where steel cross-sections are non-compact or slender exposed to fire may undergo the interaction of local and global buckling, which is complex and has not been fully understood [6, 11]. Although fire tests on such composite columns can be conducted, they are highly expensive and time-consuming. Computer simulation programs are cost-effective numerical techniques that compute the fire-resistance of CFST columns. However, computational research on the interaction of local and global buckling of rectangular CFST slender columns exposed to fire has been extremely limited [12]. Therefore, an efficient computer simulation model for the prediction of concentrically loaded rectangular slender CFST columns exposed to fire considering coupled instability is much needed.

When CFST columns in engineering structures are exposed to fire, they are subjected to constant axial or eccentric loads. The behavior of a CFST column during various stages of the fire exposure can be described as follows: (1) in the initial phase, the temperature of the steel section rises rapidly and the column load is mainly carried by the steel tube; (2) when the temperature of the steel tube is high enough, the stiffness and resistance of the tube reduce considerably and the load of the column is transferred to the concrete core; (3) during this development, the axial and bending stiffness of the composite section are reduced due to the local buckling of the steel tube, leading to rapidly growing lateral displacement of the column. Standard fire tests have been conducted to determine the

fire-responses of loaded CFST slender columns under increasing temperatures by researchers [13-21]. The axial and lateral deformations, temperatures on the column, and fire-resistance were measured in a standard fire test. Lie and Chabot [13] and Kodur and Lie [15] performed fire tests on the fire responses of circular and square CFST slender columns made of plain or reinforced concrete under axial loads. The influences of sectional dimension, section type, column slenderness, applied load ratio, and loading eccentricity on the fire behavior were examined. Square columns had the length of 3810 mm and the width-to-thickness ratios ranging from 24 to 48. It was observed that slender square CFST columns failed by the interaction of local and global buckling. Han et al. [16] undertook experiments on the fire-performance of CFST columns made of square and rectangular sections with and without fire protection loaded either axially or eccentrically. It was reported that the fire resistance of CFST columns was moderately affected by the material strengths, steel ratio and load eccentricity, but significantly influenced by the cross-sectional area, protection thickness and column slenderness. Moreover, the interaction of local and global buckling caused the failure of slender columns.

Experimental results on seven square CFST slender columns loaded axially and subjected to increasing temperatures were reported by Kim et al. [17]. The tested columns had the width-to-thickness ratios of 33.3 and 38.9 and a length of 3500 mm. However, only part of the column length was heated in the furnace. Espinos et al. [18] performed tests to examine the influences of large loading eccentricities on the fire-resistance of slender CFST columns constructed by circular or square sections reinforced with steel bars. Test results showed that square columns failed by global buckling due to their small width-to-

thickness ratios of 18.75 and 22. In addition, the fire resistance of CFST columns was remarkably reduced by increasing the loading eccentricity. Espinos et al. [19] undertook further tests on the fire behavior of slender CFST columns of rectangular and elliptical sections loaded concentrically or eccentrically. The aforementioned fire tests have shown that loaded slender thin-walled CFST rectangular columns with the width-to-thickness ratios of 15, 25 and 35 exposed to fire fail by the interaction local and global buckling. The load is transferred from the buckled steel tube to the concrete core, causing crushing of concrete.

Researchers have employed the nonlinear computational procedures to investigate the responses of slender CFST columns subjected to standard fire defined by the standard temperature-time curve [22-29]. A mathematical model using the fiber approach was proposed by Lie and Irwin [23] for computing the temperature distributions as well as the load-deflection behavior of CFST rectangular columns with longitudinal reinforcing bars subjected to concentric loads and elevated temperatures. The thermal analysis considered the effect of water content in the concrete. However, the tensile behavior of concrete, deflection caused by preload and the interaction of local and global buckling were not taken into account in the mathematical model. Han [24] developed a fiber-based theoretical model to determine the fire-resistance as well as the strength of slender CFST beam-columns of square and circular sections loaded eccentrically. The temperature fields in column cross-sections were calculated by the finite element method. The theoretical model by Han [24] has not incorporated the interaction of local and global buckling and the deformations induced by preloads in the fire-resistance simulations of slender square CFST columns. The fire-performance of slender square CFST columns

subjected to either concentric or eccentric loads was investigated by Chung et al. [25, 26] by employing the fiber-based numerical models. The limitations of their numerical models are that the models have not considered the effects of local buckling, initial geometric imperfection and air gap at the concrete-steel interface on the fire responses.

Ding and Wang [27] and Espinos et al. [28] used commercial finite-element programs to determine the effects of the air-gap and slip between the steel tube and concrete as well as concrete tensile strength on the fire performance of loaded slender CFST square columns with initial geometric imperfections. It was found that the effect of the slip between the steel and concrete on the fire behavior was minor while the inclusion of an air gap improved the accuracy of numerical simulations. Hong and Varma [29] developed a sequentially coupled finite element (FE) model using ABAQUS to determine the fire behavior of slender CFST square columns. The FE model was used to examine the sensitivities of the fire performance of CFST columns to local buckling, geometric imperfections, and material constitutive models. The numerical results confirmed that the stress-strain models for concrete and steel at high temperatures had marked effects on the predicted fire responses. However, it was found that the cracking behavior of concrete in tension could not be accurately simulated by the finite element model.

Numerical investigations performed by Kamil et al. [12] demonstrated that local buckling considerably reduces the fire-resistance of loaded short CFST thin-walled rectangular columns. However, the existing computational procedures based on the fiber element approach have not taken into consideration the effects of the interaction of local and global buckling on the responses of slender rectangular CFST columns during the

exposure of fire. This paper extends the mathematical model proposed by Kamil et al. [12] to slender CFST columns of rectangular sections exposed to standard fire loading considering the interaction of local and global buckling. The simulation scheme of the local and post-local buckling is incorporated in the global buckling computation of slender CFST columns under fire. The computer simulation procedure for the ultimate strength and fire-resistance of slender CFST columns accounting for material and geometric nonlinearities at elevated temperatures is described. Numerical algorithms are developed that solve the nonlinear equilibrium dynamic functions for CFST columns at elevated temperatures. The independent experimental and numerical results are employed to validate the numerical model. The responses due to the interaction of local and global buckling of CFST rectangular columns under fire are investigated by using the developed computational model.

2. Cross-sectional analysis incorporating local buckling

2.1. Discretization of cross-section

The cross-section of a rectangular CFST column is divided into fiber elements by using the fiber element approach [5, 11, 30]. A typical fiber mesh used for both the stress and thermal analyses is illustrated in Fig. 2, where the size of the steel fiber is half of that of the concrete fiber. However, the discretization of the column along its length is not required in the fiber approach, which significantly reduces the computational time in comparison with the finite element method. Both the mechanical and thermal properties are assigned to steel and concrete fibers. In the thermal analysis, temperatures at the nodes

of fiber elements are computed. The temperature at an element is taken as the average temperature at its nodes. Stresses at fibers are calculated from axial strains by means of using the uniaxial temperature-dependent stress-strain models for steel and concrete.

The assumptions made in the formulation of the mathematical model are: (1) the rectangular CFST slender column is subjected to uniform temperatures along its length; (2) there is a perfect bond between the concrete infill and steel tube; (3) after deformation, the plane section remains plane; (4) the effects of local and post-local buckling of thin-walled steel tubes are included; (5) an air gap between the concrete core and steel tube is considered; (6) the concrete tensile strength is ignored; (7) the shrinkage and creep of concrete are not taken into account.

2.2. Temperature distributions

The calculations of temperatures on a rectangular CFST column exposed to fire involve the determinations of temperatures on its outer surfaces and temperatures within its cross-section. The temperatures on the column surfaces are computed by using the standard temperature-time relationship provided in Eurocode 1 [31], which is written as

$$T(t) = 20 + 345 \log_{10}(8t + 1) \quad (1)$$

in which T represents the temperature in $^{\circ}\text{C}$ and t stands for the fire exposure time in minutes.

The distribution of temperatures within the column cross-section is determined by means of solving the following heat equation [32]:

$$k \frac{\partial^2 T}{\partial x^2} + k \frac{\partial^2 T}{\partial y^2} + q = \rho c \frac{\partial T}{\partial t} \quad (2)$$

where the density ρ is in kg/m^3 , c denotes the specific heat in J/kg , k represents the thermal conductivity in $\text{W/m}^\circ\text{C}$ and q stands for the heat flux. The concrete properties at elevated temperatures provided by Lie and Chabot [22] and the steel properties at elevated temperatures specified in Eurocode 3 [33] are used in the present mathematical model and details can also be found in the paper by Kamil et al. [12].

The heat equation in 2D space with time expressed by Eq. (2) is solved by means of employing the finite difference method. The nodal temperatures of fiber elements as illustrated in Fig. 3 are computed by the forward finite difference method of the heat equation expressed by

$$T_{m,n}^{i+1} = \frac{\alpha \Delta t}{(\Delta L)^2} (T_{m,n-1}^i + T_{m,n+1}^i + T_{m-1,n}^i + T_{m+1,n}^i) + \left(1 - \frac{4\alpha \Delta t}{(\Delta L)^2}\right) T_{m,n}^i \quad (3)$$

where $1 - (4\alpha \Delta t / \Delta L)^2 \geq 0$; $\alpha = k / \rho c$; Δt stands for the time increment in seconds; and the element length is $\Delta L = dx = dy$.

Ding and Wang [27] reported that the predictions of structural and thermal responses of CFST columns were found to improve by introducing an air gap between the concrete and steel tube. Therefore, such an air gap is included in the temperature calculations in which the thermal contact resistance (h_r) of $100 \text{ W/m}^2\text{K}$ is specified for the air gap. In the present formulation, a constant value of 0.7 is adopted for the emissivity of exposed surfaces (ε), the Stephan-Boltzmann constant is taken as $5.67 \times 10^{-8} \text{ W/m}^2\text{K}^4$, and the moisture content of 3% is used [27, 34]. By taking the effects of the air gap into account, the temperatures at the contact nodes at the corner of the steel-concrete interface are calculated by

$$T_{1,1}^{i+1} = T_{1,1}^i + \frac{4\Delta t}{\rho c d_c^2} \left[h_r (T_{3,3}^i - T_{1,1}^i) d_c + \lambda_c (T_{1,2}^i - T_{1,1}^i) + \lambda_c (T_{2,1}^i - T_{1,1}^i) \right] \quad (4)$$

in which $T_{1,1}$ is the nodal temperature at the node of the corner concrete fiber; $T_{1,2}$ and $T_{2,1}$ are the nodal temperatures of the concrete fiber nodes adjacent to the corner respectively; $T_{3,3}$ is the nodal temperature of the corner node of the steel fiber; d_c denotes the size of concrete fibers; λ_c is the thermal conductivity of concrete as a function of the averaged temperature of two adjacent nodes [12, 35]. Equation (4) is used to compute the nodal temperatures at fibers at the boundaries with the thermal radiation and heat convection coefficients. The numerical model proposed for the thermal analysis has been verified by comparisons with experimental data as well as numerical solutions by Kamil et al. [12].

2.3. Strain distribution

The linear strain distribution in the column cross-section is shown in Fig 2. As demonstrated in Fig. 2, the strain at any fiber is determined by multiplying the curvature by the distance measured from the element centroid to the neutral axis. In the analysis, compressive strains are treated as positive and tensile strains as negative. For a CFST slender column with rectangular section subjected to concentric loading, the column will buckle about the weak axis. The fiber strains are calculated as follows:

$$y_{n,i} = \frac{D}{2} - d_n \quad (5)$$

$$d_{e,i} = |y_i - y_{n,i}| \quad (6)$$

$$\varepsilon_i = \begin{cases} \phi d_{e,i} - \varepsilon_T & \text{for } y_i \geq y_{n,i} \\ -\phi d_{e,i} - \varepsilon_T & \text{for } y_i < y_{n,i} \end{cases} \quad (7)$$

where d_n denotes the distance of the neutral axis from the edge fiber in the composite section, $d_{e,i}$ represents the perpendicular distance from the neutral axis to the centroid of each element, y_i stands for coordinates of the fiber i , ε_i denotes the strain of the element i ; ϕ represents the curvature; and ε_T is the thermal strain of steel or concrete [12].

2.4. Modeling of critical local buckling

Elevated temperatures cause a significant reduction in the steel tube stiffness and strength of a CFST column with rectangular sections subjected to axial compression and bending.

This increases the possibility of the local buckling of steel plates [10, 12]. Expressions for determining the critical local-buckling stresses of steel tube walls of CFST rectangular columns subjected to non-uniform stresses at elevated temperatures were proposed by Kamil et al. [36]. These expressions accounted for the residual stresses in the steel plates at temperatures below 400°C and initial geometric imperfection and can be applied to plates having clear width-to-thickness ratios (b/t_s) in the range of 30 to 110. The formulas derived by Kamil et al. [36] are utilized in the proposed computational procedures to calculate the critical local-buckling stresses of steel tube walls in rectangular CFST slender columns under fire. For temperatures from 550 to 650°C, the critical local buckling stress of plates [36] is calculated by

$$\frac{\sigma_{1c,T}}{f_{y,T}} = (0.1916\lambda_{c,T}^{-0.7661} + 0.003889) (m_1\lambda_{c,T}^2 + m_2\lambda_{c,T} + m_3) \quad (8)$$

where $\sigma_{1c,T}$ is the critical local-buckling stress of plate at elevated temperatures, $f_{y,T}$ is the temperature-dependent steel yield stress, and $\lambda_{c,T}$ represents the temperature-dependent relative slenderness of a steel plate, written as

$$\lambda_{c,T} = \sqrt{\frac{12(1-\nu^2)(b/t_s)^2(R_{y,T}f_y)}{k\pi^2(R_{E,T}E)}} \quad (9)$$

In Eq. (9), f_y is the steel yield strength at room temperature, ν is the Poisson's ratio of steel, E is the Young's modulus of steel at room temperature, $k = 9.95$ is the elastic local buckling coefficient of steel plates with clamped boundary conditions as reported by

Liang et al. [37]. The parameters $R_{y,T}$ and $R_{E,T}$ are reduction factors applied to the steel yield strength and Young's modulus due to elevated temperatures, respectively, and are given in Eurocode 3 [33] and shown in Fig. 4.

The coefficients m_1 , m_2 and m_3 in Eq. (7) are determined from

$$m_1 = -1.0685\alpha_s^2 + 2.275\alpha_s - 0.8969 \quad (10)$$

$$m_2 = 2.3075\alpha_s^2 - 4.7791\alpha_s + 1.8475 \quad (11)$$

$$m_3 = -0.825\alpha_s^2 + 1.086\alpha_s + 1.0083 \quad (12)$$

where the coefficient of stress gradient α_s is determined as the ratio of the minimum edge stress to the maximum edge stress on the plate.

For any other temperatures, Kamil et al. [36] proposed the following equation for the determination of the critical local buckling stresses of steel plates:

$$\frac{\sigma_{lc,T}}{f_{y,T}} = (g_1 \lambda_{c,T}^g + g_2) \frac{0.6566 \lambda_{c,T}^{0.001521} \left(\frac{R_{p,T}}{R_{y,T}} \right)^{-0.1598}}{0.5415 \lambda_{c,T}^{4.889} + \left(\frac{R_{p,T}}{R_{y,T}} \right)^{-0.8252}} \quad (13)$$

where $R_{p,T}$ is the reduction factor to the proportional limit $f_{p,T}$ given in Fig. 4, and the coefficients g , g_1 and g_2 are expressed as

$$g = -7.9339\alpha_s^2 + 11.29\alpha_s + 4.701 \quad (14)$$

$$g_1 = 0.0863\alpha_s^2 - 0.1248\alpha_s + 0.0431 \quad (15)$$

$$g_2 = 0.2656\alpha_s^2 - 0.9902\alpha_s + 1.719 \quad (16)$$

2.5. Modeling of post-local buckling

The effective width method can be employed to calculate the post-local buckling strengths of steel plates in CFST columns with rectangular sections as discussed by Liang [11] and Liang et al. [37]. The effective width equations were given by Kamil et al. [36] for steel tube walls of CFST rectangular columns at any temperatures. Figure 5 illustrates the ineffective and effective widths of a rectangular steel cross-section subjected to axial compression as well as uniaxial bending. The present fiber technique incorporates the following expressions of effective width by Kamil et al. [36] to model the post-local buckling of slender CFST columns exposed to fire:

$$\frac{b_{e1}}{b} = \frac{1}{2}(q_1\lambda_{c,T}^q) \frac{0.8418\lambda_{c,T}^{0.02368} \left(\frac{R_{p,T}}{R_{y,T}}\right)^{-0.3028} + 1.154 \left(\frac{R_{p,T}}{R_{y,T}}\right)}{2.055 + \lambda_{c,T}^{1.68}} \quad (\alpha_s = 1.0) \quad (17)$$

$$\frac{b_{e1}}{b} = \frac{1}{3}(q_1\lambda_{c,T}^q) \frac{0.8418\lambda_{c,T}^{0.02368} \left(\frac{R_{p,T}}{R_{y,T}}\right)^{-0.3028} + 1.154 \left(\frac{R_{p,T}}{R_{y,T}}\right)}{2.055 + \lambda_{c,T}^{1.68}} \quad (\alpha_s = 0) \quad (18)$$

$$\frac{b_{e2}}{b} = (2 - \alpha_s) \frac{b_{e1}}{b} \quad (19)$$

where b_{e1} and b_{e2} denote the effective widths depicted in Fig. 5, b is the clear width of the steel plate, q and q_1 are expressed as

$$q = 0.04007\alpha_s^2 - 0.05275\alpha_s + 0.03355 \quad (20)$$

$$q_1 = 0.1007\alpha_s^2 - 0.7027\alpha_s + 1.65 \quad (21)$$

The progressive post-local buckling behavior of a thin steel plate is developed due to the gradual redistribution of in-plane stresses in the buckled plate. The numerical scheme for simulating the progressive post-local buckling proposed by Liang [5] is implemented in the present computational model. The full details of the scheme can be found in the work by Liang [5, 11].

2.6. Axial force and bending moment

The internal axial force (P) and bending moment (M_x) in the cross-section of a CFST rectangular column under combined axial compression and uniaxial bending are computed as stress resultants by the following equations:

$$P = \sum_{j=1}^{ns} \sigma_{s,j} A_{s,j} + \sum_{k=1}^{nc} \sigma_{c,k} A_{c,k} \quad (22)$$

$$M_x = \sum_{j=1}^{ns} \sigma_{s,j} A_{s,j} y_j + \sum_{k=1}^{nc} \sigma_{c,k} A_{c,k} y_k \quad (23)$$

in which subscripts j and k denotes the fibers in the concrete and steel tube, respectively; subscripts s and c represent steel and concrete, respectively; σ is the longitudinal fiber stress; A denotes the area of a fiber element; y is the coordinate of the fiber element; nc and ns are the total element numbers in the concrete and steel tube, respectively.

3. Global buckling analysis

3.1. Theoretical formulation

A mathematical model is formulated for the global buckling analysis of concentrically-loaded CFST rectangular columns exposed to fire. Both ends of the slender column are pin-supported. The concentrically-loaded slender column at elevated temperatures is subjected to single curvature bending about its minor principal axis. The half-sine wave shape function has been used by a number of researchers and shown to predict well the deformed shape of pin-ended slender columns [38-41]. Therefore, the half-sine wave shape function is used to model the column deformed shape, which is expressed by

$$u = u_m \sin\left(\frac{\pi z}{L}\right) \quad (24)$$

in which u_m denotes the lateral displacement at the mid-length of the column, and L represents the column effective length.

The curvature at the column mid-length can be determined from the displacement function as

$$\phi_m = u_m \left(\frac{\pi}{L} \right)^2 \quad (25)$$

The constant axial load acting on the CFST column before being exposed to fire induces initial stresses and deflections within the column. This constant axial load is treated as a preload on the column as suggested by Patel et al. [41]. The mid-height lateral deflection caused by the preload is calculated using the load-deflection computational procedure and is used as an additional initial geometric imperfection (u_{po}) in the fire-resistance simulation. The initial geometric imperfection (u_o) and lateral displacement (u_m) at the column mid-length are also included in the formulation. The external bending moment at the column mid-length is therefore

$$M_{ext} = P(u_{po} + u_o + u_m) \quad (26)$$

To determine the complete axial load-lateral deflection responses of slender CFST columns exposed to fire, the method of deflection control is adopted in the formulation. The lateral deflection at the column mid-length is incremented in steps. The method calculates the axial load on the column that causes the given lateral displacement. The internal axial force in the column satisfying the moment equilibrium at the mid-height is treated as the external applied axial load. The complete axial load-lateral displacement responses of the slender CFST column are determined by means of repeating this

computational procedure. The residual moment function in the calculation is expressed as

$$r_M = M_x - P(u_{po} + u_o + u_m) \quad (27)$$

The moment equilibrium condition is achieved if $|r_M| < \varepsilon_k = 10^{-4}$ in the numerical calculations.

3.2. Numerical solution algorithms

To determine the true internal axial force corresponding to a specified lateral deflection, the neutral axis depth (d_n) needs to be iteratively adjusted. It should be noted that the residual moment function is a dynamic nonlinear function which is not derivative with respect to the design available. Therefore, Muller's method [42] is utilized to determine the neutral axis depth in the cross-section [6, 30, 40]. The method requires three initial neutral axis depths $d_{n,1}$, $d_{n,2}$ and $d_{n,3}$ to begin the iterative computation process. The new neutral axis depth $d_{n,4}$ is calculated by means of applying the following equations:

$$d_{n,4} = d_{n,3} + \frac{-2c_m}{b_m \pm \sqrt{b_m^2 - 4a_m c_m}} \quad (28)$$

$$a_m = \frac{(d_{n,2} - d_{n,3})(r_{M,1} - r_{M,3}) - (d_{n,1} - d_{n,3})(r_{M,2} - r_{M,3})}{(d_{n,1} - d_{n,2})(d_{n,1} - d_{n,3})(d_{n,2} - d_{n,3})} \quad (29)$$

$$b_m = \frac{(d_{n,2} - d_{n,3})^2(r_{M,2} - r_{M,3}) - (d_{n,2} - d_{n,3})^2(r_{M,1} - r_{M,3})}{(d_{n,1} - d_{n,2})(d_{n,1} - d_{n,3})(d_{n,2} - d_{n,3})} \quad (30)$$

$$c_m = r_{M,3} \quad (31)$$

The above equations are employed to iteratively adjust the location of the neutral axis until the condition of moment equilibrium is satisfied.

3.3. Computational procedure

A sequential coupled computational procedure is developed to determine the ultimate axial resistance and fire-resistance of concentrically-loaded slender CFST rectangular columns exposed to fire, including the influences of interaction of local and global buckling. For a given fire exposure time, the column ultimate axial strength is determined by employing the method of load-deflection analysis [39]. The computation is repeated until the complete ultimate axial load-fire exposure time curve is obtained. The ultimate axial load of the CFST slender column decreases gradually as the fire exposure time increases. The fire exposure time for reaching the failure point in the load-displacement curve of the CFST column is the computed fire resistance.

The computer flow chart for calculating the ultimate axial strength and fire-resistance of a loaded CFST column exposed to standard fire is depicted in Fig. 6 and the main computational steps are described as follows:

1. Input data.
2. Divide the column cross-section into fine fibers.
3. Compute the lateral deformation of the slender column under constant axial load.
4. Initialize the fire exposure time as $t = \Delta t$.

5. Calculate temperatures on column surfaces and at fiber elements in its cross-section.
6. Initialize the lateral displacement at the column mid-length as $u_m = \Delta u_m$.
7. Calculate the curvature ϕ_m at the column mid-length.
8. Adjust the neutral axis depth d_n using Müller's method.
9. Calculate element stresses from strains using the temperature-dependent stress-strain models for steel and concrete.
10. Simulate the initial local and post-local buckling behavior of the steel tube walls.
11. Determine the internal axial force P and moment M_x .
12. Compute the residual moment function r_M .
13. Repeat Steps 8 to 12 until $|r_M| < \varepsilon_k = 10^{-4}$.
14. Increase the mid-height deflection by $u_m = u_m + \Delta u_m$.
15. Repeat Steps 7 to 14 until $P < 0.5P_u$ or the deflection exceeds the specified limit (u_l).
16. Increase the fire exposure time by $t = t + \Delta t$.
17. Repeat Steps 5 to 16 until the fire-resistance of the CFST column is obtained.

4. Constitutive relationships for materials at elevated temperatures

4.1. Structural steels

The temperature-dependent stress-strain relations of structural steels given in Eurocode 3 [33] is implemented in the computational algorithms developed. The stress-strain

relations of steels as a function of temperatures are plotted in Fig. 7, and are determined by:

$$\sigma_{s,T} = \begin{cases} E_T \varepsilon_s & \text{for } \varepsilon_s \leq \varepsilon_{p,T} \\ (f_{p,T} - h_3) + \frac{h_2}{h_1} \sqrt{h_1^2 - (\varepsilon_{y,T} - \varepsilon_s)^2} & \text{for } \varepsilon_{p,T} < \varepsilon_s \leq \varepsilon_{y,T} \\ f_{y,T} & \text{for } \varepsilon_{y,T} < \varepsilon_s \leq \varepsilon_{t,T} \\ f_{y,T} \left[1 - (\varepsilon_s - \varepsilon_{t,T}) / (\varepsilon_{u,T} - \varepsilon_{t,T}) \right] & \text{for } \varepsilon_{t,T} < \varepsilon_s \leq \varepsilon_{u,T} \\ 0 & \text{for } \varepsilon_s > \varepsilon_{u,T} \end{cases} \quad (32)$$

where

$$h_1^2 = (\varepsilon_{y,T} - \varepsilon_{p,T})(\varepsilon_{y,T} - \varepsilon_{p,T} + h_3 / E_T) \quad (33)$$

$$h_2^2 = E_T (\varepsilon_{y,T} - \varepsilon_{p,T}) h_3 + h_3^2 \quad (34)$$

$$h_3 = \frac{(f_{y,T} - f_{p,T})^2}{E_T (\varepsilon_{y,T} - \varepsilon_{p,T}) - 2 (f_{y,T} - f_{p,T})} \quad (35)$$

in which E_T is the temperature-dependent Young's modulus for the steel, $\varepsilon_{p,T}$ is the strain at the proportional limit $f_{p,T}$, $\varepsilon_{y,T}$ is the yield strain, and $\varepsilon_{u,T}$ is the temperature-dependent ultimate strain.

Structural steels exhibit strain-hardening at temperatures below 400°C, which is considered in the formulation by [33]:

$$\sigma_{s,T} = \begin{cases} 50 \left[(f_{u,T} - f_{y,T}) / 0.02 \right] + 2f_{y,T} - f_{u,T} & \text{for } 0.02 < \varepsilon_s \leq 0.04 \\ f_{u,T} & \text{for } 0.04 < \varepsilon_s \leq 0.15 \\ f_{u,T} [1 - 20(\varepsilon_s - 0.15)] & \text{for } 0.15 < \varepsilon_s \leq 0.2 \end{cases} \quad (36)$$

in which $f_{u,T}$ is the temperature-dependent tensile strength of steel, which is computed

by

$$f_{u,T} = \begin{cases} f_u R_{y,T} & \text{for } T \leq 300^\circ C \\ f_{y,T} + 0.01(f_{u,T} - f_{y,T})(400 - T) & \text{for } 300 < T \leq 400^\circ C \end{cases} \quad (37)$$

4.2. Concrete

Eurocode 2 [34] provides a temperature-dependent stress-strain model for concrete, which is adopted in the proposed computational procedure. Figure 8 depicts the stress-strain-curves as a function of temperatures determined by means of applying the model given in Eurocode 2. These curves are expressed by

$$\sigma_{c,T} = \begin{cases} \frac{3\varepsilon_c f'_{c,T}}{\varepsilon'_{c,T} \left[2 + (\varepsilon_c / \varepsilon'_{c,T})^3 \right]} & \text{for } \varepsilon_c \leq \varepsilon'_{c,T} \\ f'_{c,T} \left[\frac{\varepsilon_{cu,T} - \varepsilon_c}{\varepsilon_{cu,T} - \varepsilon'_{c,T}} \right] & \text{for } \varepsilon_c > \varepsilon'_{c,T} \end{cases} \quad (38)$$

where $f'_{c,T}$ denotes the concrete compressive strength, $\varepsilon'_{c,T}$ represents the concrete strain at $f'_{c,T}$, and $\varepsilon_{cu,T}$ is the temperature-dependent ultimate concrete strain. The values of $\varepsilon'_{c,T}$ and $\varepsilon_{cu,T}$ for concrete with siliceous aggregates are given in Eurocode 2 [34].

5. Verification of the fiber-based computational model

The test and computational results on the fire-resistance of loaded slender CFST square and rectangular columns made of plain concrete reported by Lie and Chabot [13], Kim et al. [17], Han [24], Chung et al. [26], and Ding and Wang [27] were utilized to validate the proposed computational model formulated by the fiber approach. These columns had the dimensions and ambient temperature material properties given in Table 1, where the effective lengths of these columns and the applied constant axial loads are also shown. The clear width-to-thickness ratios (b/t_s) of CFST columns shown in Table 1 range from 14 to 46. The local buckling effect was included in the global buckling simulations for cross-sections with b/t_s ratios greater than 30.

The tested fire-resistance times of CFST columns with square sections reported by Lie and Chabot [13] and Kim et al. [17] are compared with predictions by the fiber-based computational procedure in Fig. 9. It is demonstrated that there are good correlations between predictions and test data. The computational model generally produces conservative fire-resistance of tested columns. The discrepancy between tested and computed fire-resistance is likely due to the uncertainties in the steel and concrete properties at elevated temperatures, and water contents in concrete. Particularly, the

concrete properties and water contents in the actual specimens are unknown. Moreover, in the standard fire test, only part of the column length is exposed to fire. This implies that the measured fire-resistance time of the column is generally longer than the computed result.

Figure 10 gives the axial load-lateral displacement curves for a slender square CFST column during various fire-exposure times determined by the present computational programs and the theoretical model given by Han [24]. It appears that both numerical models produce almost the same load-deflection curve for the column at ambient temperature. However, the load-deflection curve at elevated temperatures given by Han slightly differs from the one simulated by the present computational model. The reason for this is that both numerical models employed different temperature-dependent material constitutive laws for steel and concrete. As demonstrated in Fig. 11, the ultimate axial strengths of a slender CFST square column as a function of fire exposure time calculated by the present fiber simulation technique are in excellent agreement with those given by Chung et al. [26]. As illustrated in Fig. 12, the evaluated fire resistances of CFST columns computed with the developed calculation procedure based on the fiber approach are in good agreement with the results obtained by the finite element model presented by Ding and Wang [27]. The fiber model generally yields slightly conservative fire-resistances of CFST columns compared to finite element results.

6. Interaction behavior of local and global buckling

A computer program written by the authors implements the numerical model presented in the preceding sections. The computer program was utilized to quantify the sensitivities of the interaction of local and global buckling responses of concentrically loaded slender CFST rectangular columns under fire to the tube local buckling, concrete strength, steel yield strength, member slenderness and width-to-thickness ratio of steel tube. In the parametric studies, the Young's modulus of steel at ambient temperature was 200 GPa. The initial geometric-imperfection at the mid-length of the columns was specified as $L/1000$. The columns used in the parametric studies had the member slenderness ratio (L/r) of 40, except where indicated otherwise.

6.1. Effects of local buckling

The local buckling effects on the global buckling behavior as well as the fire-resistance of a slender CFST column having a square section were investigated by means of using the computational program. The column cross-section considered was $600 \times 600 \times 6$ mm having a B/t_s ratio of 100. The steel tube having a yield strength of 300 MPa was filled with 35 MPa concrete. The responses of the CFST column exposed to fire was simulated by means of considering local buckling or ignoring it, respectively. Figure 13 shows the axial load-lateral displacement curves of the column at 20 min fire-exposure time. The reduction in ultimate axial load of the column caused by local buckling at exposure time of 20 min is 8%. The ultimate axial strength-fire resistance curves for the column are provided in Fig. 14. It is found from Fig. 14 that the local buckling effect on the ultimate load decreases as the time of fire exposure increases. The reductions in the column

ultimate strength caused by local buckling at fire exposure times 0 min, 20 min, 40 min and 60 min are 11%, 8%, 5% and 2%, respectively.

6.2. Effects of column slenderness ratio

The effect of the column slenderness ratio (L/r) on the fire behavior of CFST columns was examined by means of analyzing five slender CFST square columns by the computer programs developed. The cross section used was 500×500 mm with 10 mm thickness. The steel tube at ambient temperature had a yield strength of 300 MPa and was filled with 40 MPa concrete. The column slenderness ratios of 22, 40, 50 and 60 were determined by varying the length. The predicted global buckling responses of these columns at the fire exposure time of 20 min are given Fig. 15. It is discovered that increasing the L/r ratio results in a significant decrease in the column ultimate load but a significant increase in the lateral displacement at the peak load. Figure 16 shows the effect of the L/r ratio on the ultimate load-fire exposure time relations of CFST square columns. At the fire exposure time of 20 min, when the L/r ratio increases from 22 to 40, 50 and 60, the ultimate load of the CFST column decreases by 12 %, 23% and 35%, respectively. However, at time of 60 min, the column ultimate strength decreases by 19%, 34%, and 48%, respectively. This implies that the longer the fire exposure time, the lower the ultimate strength of the more slender column.

6.3. Effects of concrete strength

The infill concrete of the CFST columns plays a significant role in resisting the fire loading. The sensitivities of the interaction of local and global buckling responses and fire performance of rectangular CFST columns to the concrete strength were studied. Four grades of concrete strengths were used, namely 25 MPa, 35 MPa, 45 MPa and 55 MPa. The columns had the same steel cross-section of 450×650×7 mm and the steel yielding strength of 300 MPa. The computed axial load-lateral displacement curves for these columns made of different concrete strengths are shown in Fig. 17. Both the ultimate axial load and initial stiffness of the columns are found to increase by the increase in the concrete strength. Figure 18 shows the sensitivities of the ultimate load-fire exposure time curves to the concrete strength. At the ambient temperature, the column ultimate strengths are found to increase by 27%, 53% and 80%, respectively, when the concrete strength is increased from 25 MPa to 35 MPa, 45 MPa and 55 MPa. At fire time of 20 min, the increases in the ultimate strengths are 35%, 71% and 106 %, respectively. This is owing to the fact that the mechanical properties and the steel tube local buckling strength are significantly reduced by high temperatures, and the axial load is transferred from the buckled steel tube to the concrete infill. The use of higher strength concrete leads to the higher ultimate axial strengths of the columns when exposed to the same fire time.

6.4. Effects of steel yield strength

Investigations on the influences of steel yield stress on the interaction of local and global buckling of CFST rectangular columns exposed to fire were conducted by using the computer program developed. The rectangular steel sections had the dimensions of 500×600×7 mm but with different yield stresses of 250 MPa, 300 MPa, 350 MPa and 450

MPa, respectively. The filled concrete had the strength of 40 MPa. The predicted the interaction responses of local and global buckling of the columns at the 20 min fire exposure time are given in Fig. 19. It is apparently shown that at this level of temperatures, the steel yield stress has only minor effect on the column behavior. During the first 20 min fire exposure, the temperature on the steel tube surfaces increases significantly, which causes yielding in the steel tubes regardless of their yield strengths at room temperature. Figure 20 shows the ultimate axial strength-fire exposure time curves as a function of the yield stress of steel. The steel yield stress is found to have a pronounced influence on the column ultimate load exposed to room temperature and its influence diminishes as the time of fire exposure increases. At 20 min fire exposure time, the increase in the steel yield stress from 250 MPa to 450 MPa leads to a slight increase in the column strength by 3%. This suggests that high strength steel tubes are not effective in resisting high temperatures in a fire situation.

6.5. Effects of width-to-thickness ratio

The influences of the B/t_s ratios on the interaction responses of local and global buckling of CFST square columns were investigated. The cross-section of 600×600 mm was considered. The B/t_s ratios of 40, 60, 80 and 100 were calculated by means of varying only the tube thickness. The yield stress of the steel tube was 300 MPa and the concrete had a compressive strength of 50 MPa. Figure 21 presents the buckling responses of the columns with various B/t_s ratios at 20 min fire exposure time. Reducing the tube thickness markedly decreases the ultimate load of the column. The ultimate load-fire exposure time relationships of the columns are demonstrated in Fig. 22. The B/t_s ratio is shown to have

a pronounced influence on the ultimate strength of the columns exposed to room temperature. Its influence decreases with increasing the time of fire exposure. At ambient temperature, when increasing the B/t_s ratio from 40 to 100, the reduction in the ultimate strength is 24%. However, at exposure time of 20 min, the strength reduction is only 15%. As depicted in Fig. 22, after the columns have been exposed to fire for 40 min, the effect of the B/t_s ratio on the column strength could be ignored. This is because after 40 min fire exposure, the axial load is mainly carried by the concrete core.

6.6 Effects of preloads

The computer model proposed was employed to analyze a square CFST column that had the dimensions of 400×400 mm and a B/t_s ratio of 80 under various preloads and fire loading to ascertain the significance of preloads on the fire behavior. The preload ratios (β) of 0.0, 0.4 and 0.6 were considered. The column had the slenderness ratio of 60, loading eccentricity ratio of 0.1, steel yield strength of 350 MPa and concrete compressive strength of 45 MPa. The Young's modulus for steel was 210 GPa. The tensile behavior of concrete was considered. The predicted column ultimate strength-fire exposure time curves as a function of preload ratio are presented in Fig. 23. It is evident that regardless of the fire exposure time, increasing the preload ratio decreases the column ultimate strength. When the column is in room temperature, increasing the preload ratio from 0.0 to 0.4 and 0.6 leads to a reduction in the column strength by 4% and 6%, respectively. As depicted in Fig. 23, the column has the most pronounced strength reduction at the fire exposure time of 20 min. At this time, the reductions in the column strength were obtained as 12% and 21%, respectively, when changing the preload ratio from 0.0 to 0.4 and 0.6.

7. Conclusions

The computational model formulated by the fiber approach has been presented in this paper for predicting the fire-resistance and the interaction behavior of local and global buckling in concentrically-loaded slender rectangular CFST subjected to fire loading. A sequential coupled computational procedure incorporating nonlinear thermal and stress analyses for CFST columns exposed to fire has been developed and described. The computational model has taken into account the important features associated with CFST slender columns made of rectangular sections exposed to fire, including the interaction of local and global buckling, air gap between the concrete and steel tube, water contents in concrete, emissivity of exposed surfaces, temperature-dependent material and geometric nonlinearities, initial geometric imperfections and preloads in the simulation. Comparisons with the existing results of the standard fire tests and numerical solutions have been made to validate the fiber model proposed. The fire-resistance and interaction behavior of local and global buckling of CFST columns with rectangular sections exposed to standard fire have been investigated. The computational model presented in this paper can be used in the structural fire engineering design of rectangular CFST slender columns under fire. However, further research should be undertaken to develop simple design equations for estimating the fire resistance of CFST columns exposed to fire.

The concluding remarks are given as follows:

- (1) The fiber-based computational model proposed predicts well the fire-resistances of CFST rectangular columns which are in good agreement with standard fire test and numerical results available in the literature.

- (2) The effect of the tube local buckling on the column ultimate axial strength decreases as the fire exposure time increases.
- (3) Regardless of the fire exposure time, the ultimate axial resistance of CST columns reduces significantly when the member slenderness increases. This effect increases as the time of fire exposure increases.
- (4) Significant increases in the ultimate load of CFST columns are obtained by using higher strength concrete at any fire-exposure time.
- (5) The yield stress of steels has a minor influence on the column ultimate load at elevated temperatures. Therefore, it is not effective to use high strength steels in CFST columns in resisting high temperatures in a fire situation.
- (6) At ambient temperature, the B/t_s ratio has a considerable influence on the ultimate resistance of the column, but its influence decreases during fires when the exposure time increases.
- (7) Increasing the preload ratio generally decreases the ultimate strength and fire-resistance of slender CFST columns.

References

- [1] Han LH, Li W, Bjorhovde R. Developments and advanced applications of concrete-filled steel tubular (CFST) structures: Members. *J Constr Steel Res* 2014; 100: 211-228.
- [2] Hajjar JF, Schiller PH, Molodan A. A distributed plasticity model for concrete-filled steel tube beam-columns with interlayer slip. *Eng Struct* 1998; 20(8):663-676.

- [3] Susantha KAS, Ge HB, Usami T. Uniaxial stress-strain relationship of concrete confined by various shaped steel tubes. *Eng Struct* 2001; 23(10):1331-1347.
- [4] Shanmugam NE, Lakshmi B, Uy B. An analytical model for thin-walled steel box columns with concrete in-fill. *Eng Struct* 2002; 24(6):825-838.
- [5] Liang QQ. Performance-based analysis of concrete-filled steel tubular beam-columns. Part I: Theory and algorithms. *J Constr Steel Res* 2009; 65(2):363-373.
- [6] Liang QQ, Patel VI, Hadi MNS. Biaxially loaded high-strength concrete-filled steel tubular slender beam-columns. Part I: Multiscale simulation. *J Constr Steel Res* 2012; 75:64-71.
- [7] Mollazadeh MH, Wang YC. New insights into the mechanism of load introduction into concrete-filled steel tubular column through shear connection. *Eng Struct* 2014; 75:139–151.
- [8] Xiong MX, Xiong DX, and Liew JYR. Axial performance of short concrete filled steel tubes with high-and ultra-high-strength materials. *Eng Struct* 2017; 136:494-510.
- [9] AS 3600-2009, Australian Standard for Concrete structures, Standards Australia, Sydney, NSW, Australia, 2009.
- [10] Wang, YC. *Steel and Composite Structures: Behaviour and Design for Fire Safety*. London and New York: Spon Press, 2002.
- [11] Liang QQ. *Analysis and Design of Steel and Composite Structures*, CRC Press, Taylor and Francis Group, Boca Raton and London, 2014.
- [12] Kamil GM, Liang QQ, Hadi, MNS. Numerical analysis of axially loaded rectangular concrete-filled steel tubular short columns at elevated temperatures. *Eng Struct* 2019; 180:89-102.

- [13] Lie TT, Chabot M. Experimental studies on the fire resistance of hollow steel columns filled with plain concrete. Internal report, National Research Council Canada, Institute for Research in Construction, 1992-01.
- [14] Sakumoto Y, Okada T, Yoshida M, Tasaka S. Fire resistance of concrete-filled, fire-resistant steel-tube columns. *J Mat in Civil Eng ASCE* 1994; 69(2):169-184.
- [15] Kodur VKR, Lie TT. Fire performance of concrete-filled hollow steel columns. *J Fire Prot Eng* 1995; 79(3):89-98.
- [16] Han LH, Yang YF, Xu L. An experimental study and calculation on the fire resistance of concrete-filled SHS and RHS columns. *J Constr Steel Res* 2003; 59:427-452.
- [17] Kim DK, Choi SM, Kim JH, Chung KS, Park SH. Experimental study on fire resistance of concrete-filled steel tube column under constant axial loads. *Int J Steel Struct* 2005; 5(4):305-313.
- [18] Espinos A, Romero ML, Serra E, Hospitaler A. Circular and square slender concrete-filled tubular columns under large eccentricities and fire. *J Constr Steel Res* 2015; 110:90-100.
- [19] Espinos A, Romero ML, Serra E, Hospitaler A. Experimental investigation on the fire behavior of rectangular and elliptical slender concrete-filled tubular columns. *Thin-Wall Struct* 2015; 93:137-148.
- [20] Han LH, Chen F, Liao FY, Tao Z, Uy B. Fire performance of concrete filled stainless steel tubular columns. *Eng Struct* 2013; 56:165-181.
- [21] Yang YF, Zhang L, Dai X. Performance of recycled aggregate concrete-filled square steel tubular columns exposed to fire. *Advances in Struct Eng* 2017; 20(9):1340-1356.

- [22] Lie TT, Chabot M. A method to predict the fire resistance of circular concrete filled hollow steel columns. *J Fire Prot Eng* 1990; 2(4):111-126.
- [23] Lie TT, Irwin RJ. Fire resistance of rectangular steel columns filled with bar-reinforced concrete. *J Struct Eng ASCE* 1995; 12(5):797-805.
- [24] Han LH. Fire performance of concrete filled steel tubular beam-columns. *J Constr Steel Res* 2001; 57:695-709.
- [25] Chung K., Park S, Choi S. Material effect for predicting the fire resistance of concrete-filled square steel tube column under constant axial load. *J Constr Steel Res* 2008; 64:1505-1515.
- [26] Chung K, Park S, Choi S. Fire resistance of concrete filled square steel tube columns subjected to eccentric axial load. *Int J Steel Structures* 2009; 9:69-76.
- [27] Ding J, Wang YC. Realistic modelling of thermal and structural behaviour of unprotected concrete filled tubular columns in fire. *J Constr Steel Res* 2008; 64:1086-1102.
- [28] Espinos A, Romero ML, Hospitaler A. Advanced model for predicting the fire response of concrete filled tubular columns. *J Constr Steel Res* 2010; 66:1030-1046.
- [29] Hong SD, Varma AH. Analytical modeling of the standard fire behavior of loaded CFT columns. *J Constr Steel Res* 2009; 65:54-69.
- [30] Liang QQ. Numerical simulation of high strength circular double-skin concrete-filled steel tubular slender columns. *Eng Struct* 2018; 168:205-217.
- [31] Eurocode 1. 1991-1-2, Actions on structures, Part 1.2: General actions- Actions on structures exposed to fire, CEN, Brussels, Belgium, 2002.
- [32] Incropera FP, Dewitt DP, Bergman TL, Lavine AS. Fundamentals of heat and mass transfer. John Wiley & Sons, 6th Edition, USA 2005.

- [33] Eurocode 3. Design of steel structures, Part 1.2: General rules-structural fire design, CEN, Brussels, Belgium, 2005.
- [34] Eurocode 2. Design of concrete structures, Part 1.2: General rules-structural fire design, CEN, Brussels, Belgium, 2004.
- [35] Xiong MX, Wang YH, Liew JYR. Evaluation on thermal behaviour of concrete-filled steel tubular columns based on modified finite difference method. *Adv in Struct Eng* 2016; 19(5): 746-761.
- [36] Kamil GM, Liang QQ, Hadi MNS. Local buckling of steel plates in concrete-filled steel tubular columns at elevated temperatures. *Eng Struct* 2018; 168: 108-118.
- [37] Liang QQ, Uy B, Liew JYR. Local buckling of steel plates in concrete-filled thin-walled steel tubular beam-columns. *J Constr Steel Res* 2007; 63(3):396-405.
- [38] Shakir-Khalil H, Zeghiche J. Experimental behaviour of concrete-filled rolled rectangular hollow-section columns. *The Structural Engineer* 1989; 67(19): 346–53.
- [39] Liang QQ. High strength circular concrete-filled steel tubular slender beam-columns, Part I: Numerical analysis. *J Constr Steel Res* 2011; 67(2):164-171.
- [40] Patel VI, Liang QQ, Hadi MNS. High strength thin-walled rectangular concrete-filled steel tubular slender beam-columns. Part I: Modeling. *J Constr Steel Res* 2012; 70:377-384.
- [41] Patel VI, Liang QQ, Hadi MNS. Behavior of biaxially-loaded rectangular concrete-filled steel tubular slender beam-columns with preload effects. *Thin-Wall Struct* 2014; 79:166-177.
- [42] Müller DE. A method for solving algebraic equations using an automatic computer. *MTAC* 1956; 10:208-15.

Figures and Tables

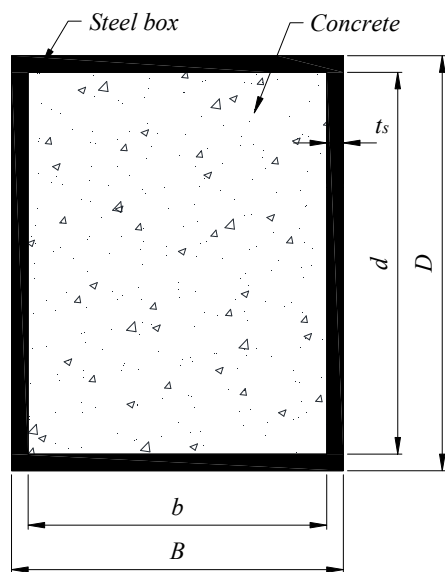


Fig. 1. Cross-section of rectangular CFST column.

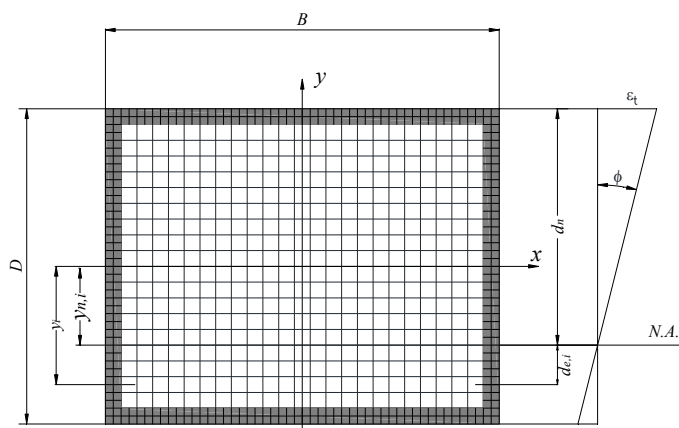


Fig. 2. Typical fiber mesh and strain distribution in a rectangular column cross-section

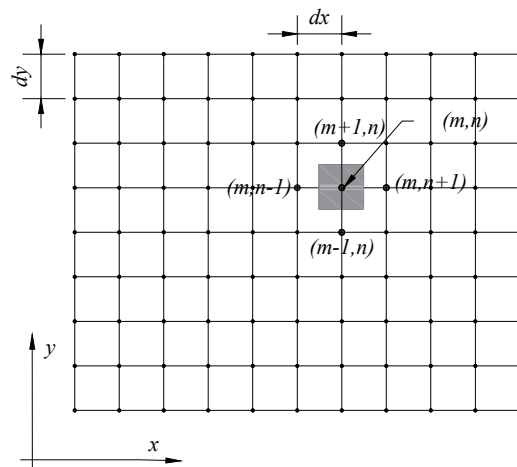


Fig. 3. Nodal grid for the temperature calculations using the method of finite differences

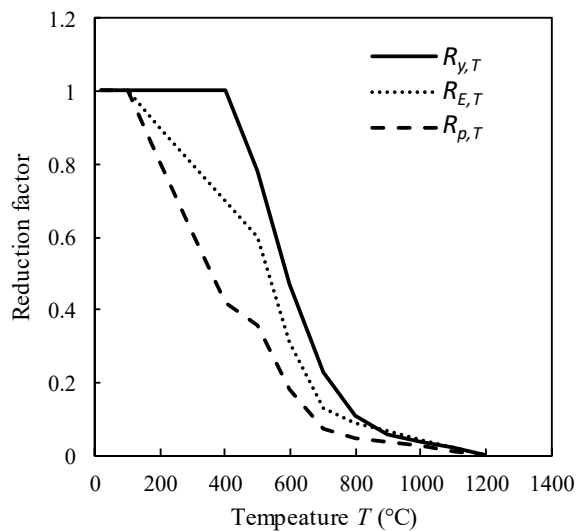


Fig. 4. Reduction factors for the mechanical properties of structural steels at elevated temperatures based on Eurocode 3 [33].

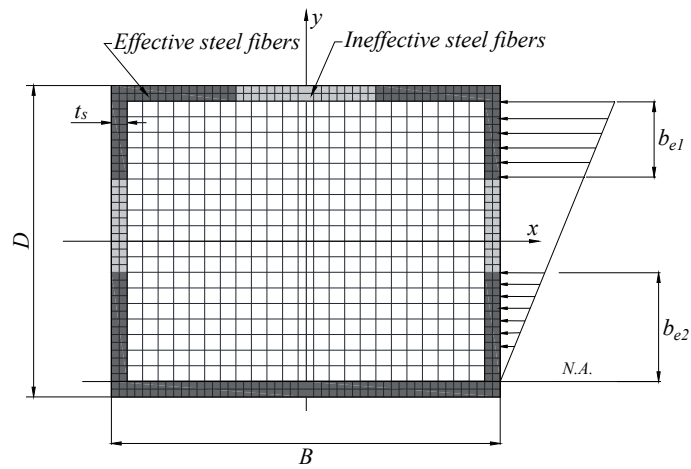


Fig. 5. Effective and ineffective widths of steel tube walls in rectangular CFST column section under uniaxial bending

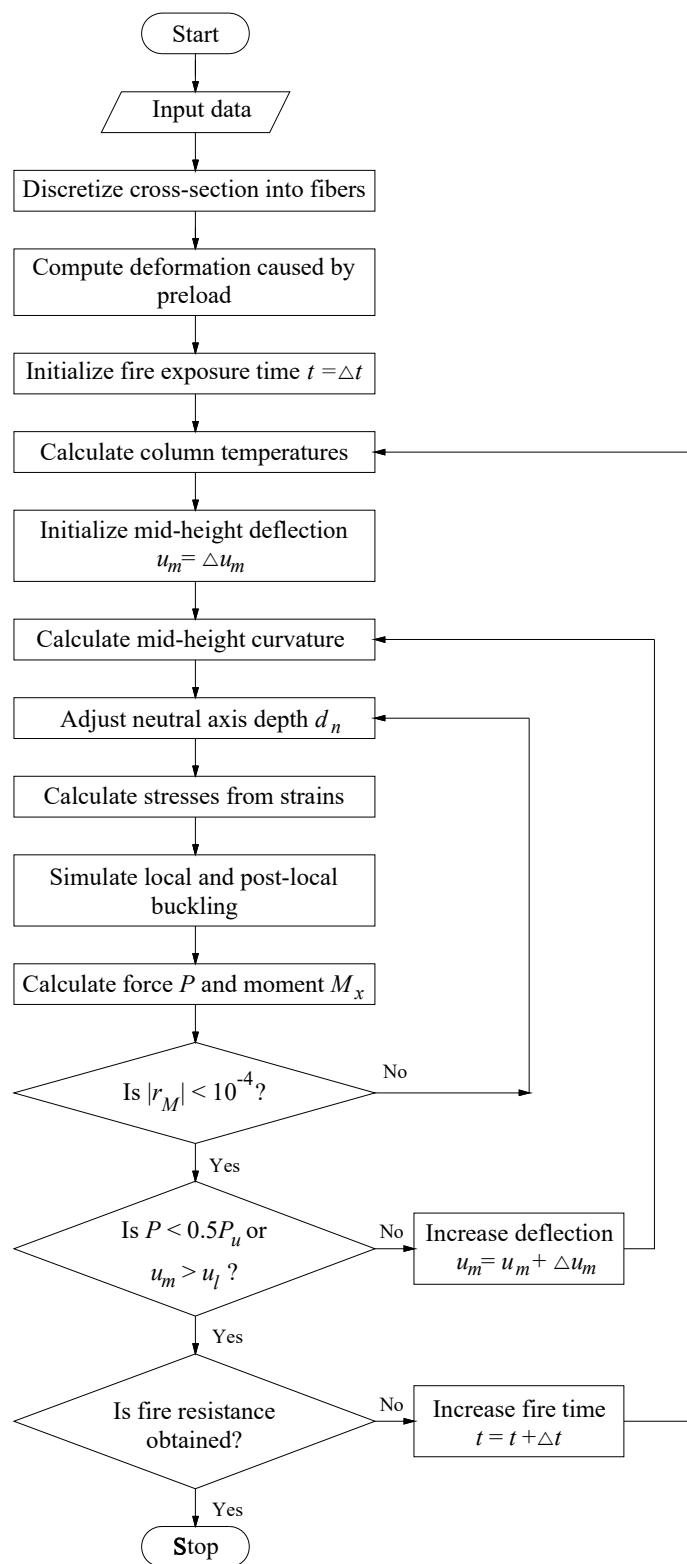


Fig. 6. Computer flow chart for calculating the fire resistance of axially loaded rectangular CFST slender columns exposed to fire

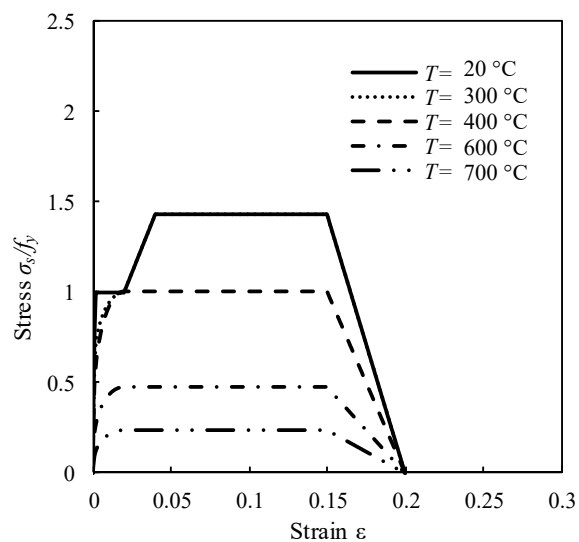


Fig. 7. Stress-strain curves for structural steels at elevated temperatures allowing for strain hardening based on Eurocode 3 [33].

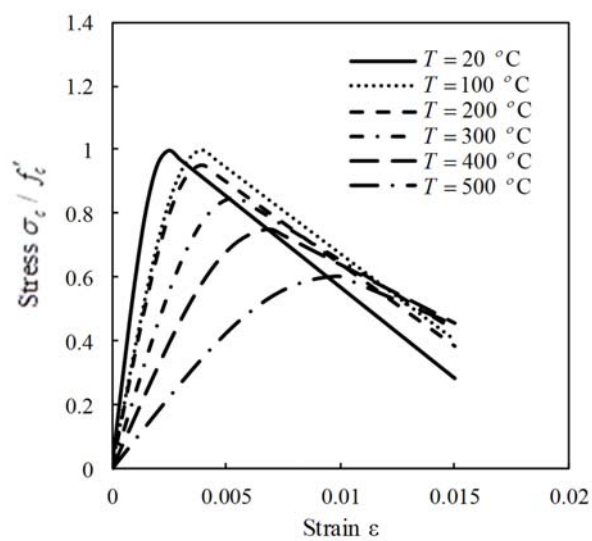


Fig 8. Stress-strain curves for concrete at elevated temperatures based on Eurocode 2 [34].

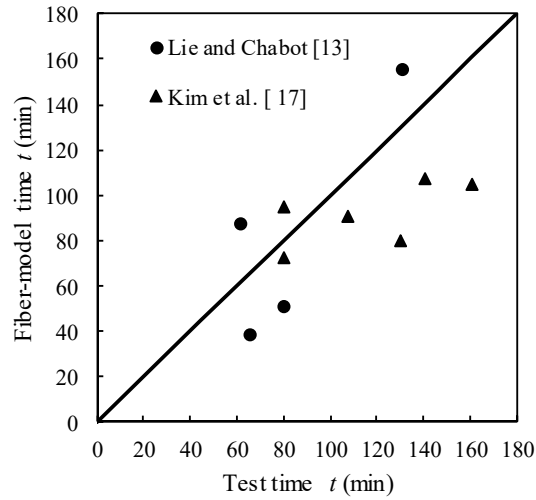


Fig. 9. Comparison of predicted fire-resistances of slender square CFST columns with test results given by Lie and Chabot [13] and Kim et al. [17].

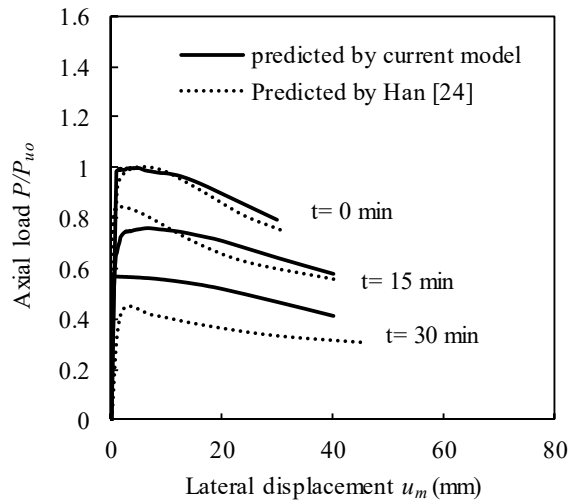


Fig. 10. Comparison of the axial load-lateral displacement curves for a square CFST columns in fire computed by the proposed computational model and the model by Han [24].

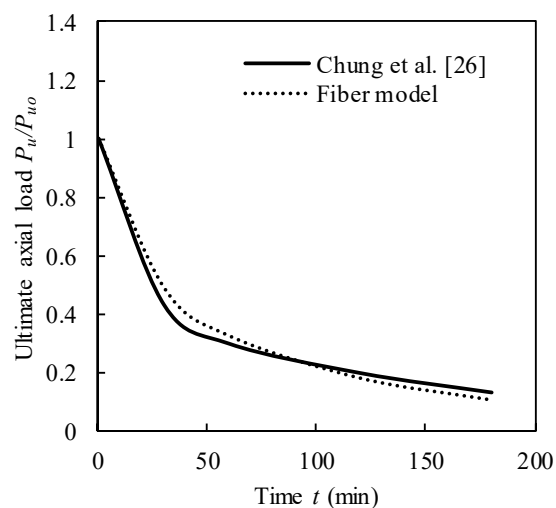


Fig. 11. Comparison of the ultimate strength-fire exposure time curves for a square CFST column calculated by the proposed fiber model and the model by Chung et al. [26].

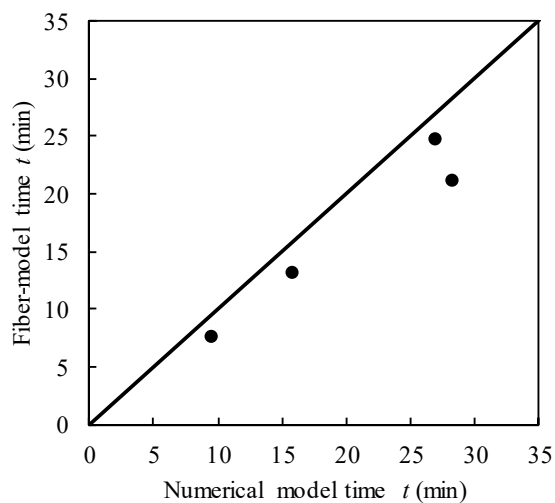


Fig. 12. Comparison of fire-resistances of CFST columns predicted by the proposed fiber-based computational model with the finite element results given by Ding and Wang [27].

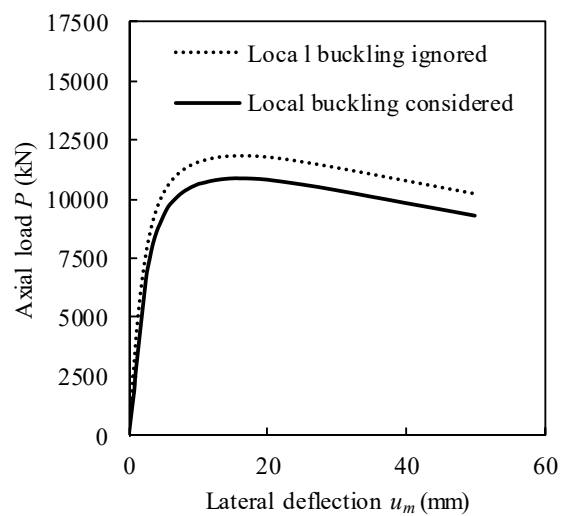


Fig. 13. Influences of local buckling on the axial load-lateral deflection behavior of slender square CFST column at fire-exposure time of 20 min.

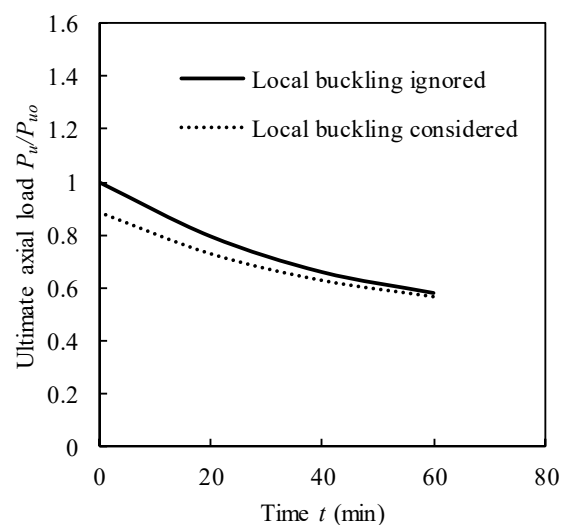


Fig. 14. Influences of local buckling on the ultimate axial strength-fire exposure time curve for slender CFST column.

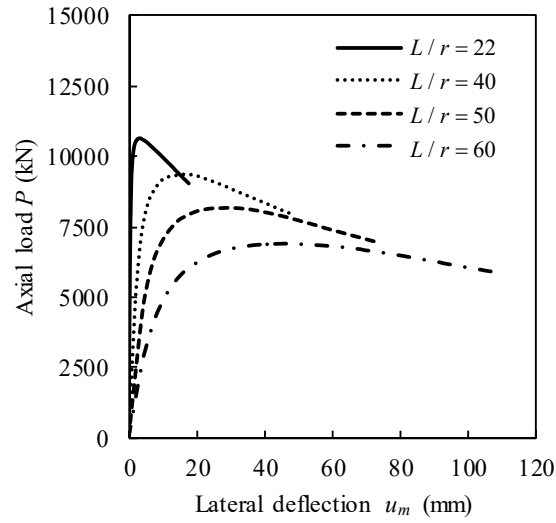


Fig. 15. Axial load-lateral displacement curves of square slender CFST columns with various slenderness ratio at fire-exposure time of 20 min.

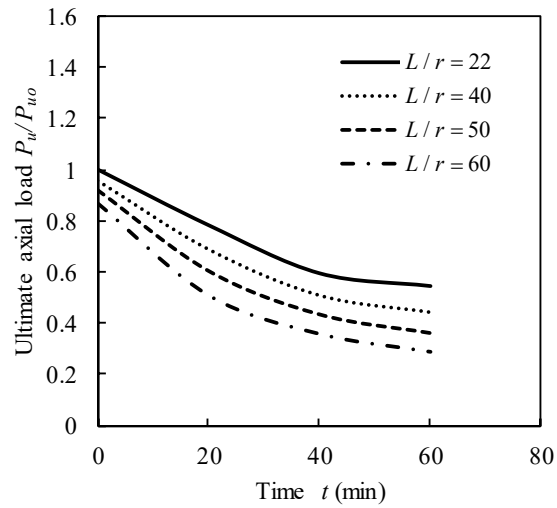


Fig. 16. Effects of the column slenderness ratio on the ultimate strength-fire exposure time curves of square slender CFST columns.

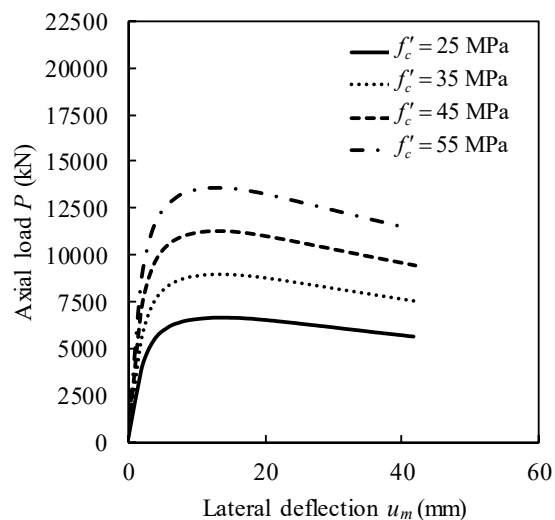


Fig. 17. Axial load-lateral displacement curves of rectangular slender CFST columns with various concrete strengths at fire-exposure time of 20 min

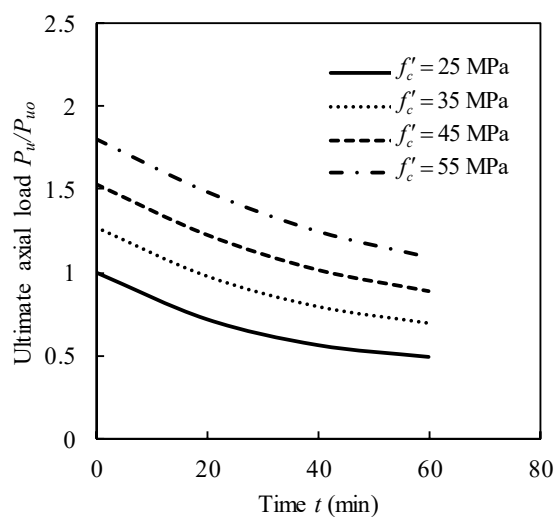


Fig. 18. Effects of the concrete strength on the ultimate strength-fire exposure time curves of rectangular slender CFST columns.

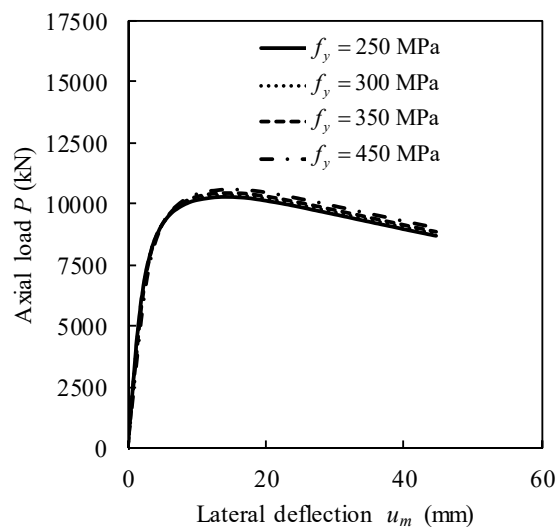


Fig. 19. Axial load-lateral displacement curves of rectangular slender CFST columns with different yield strengths at fire-exposure time of 20 min

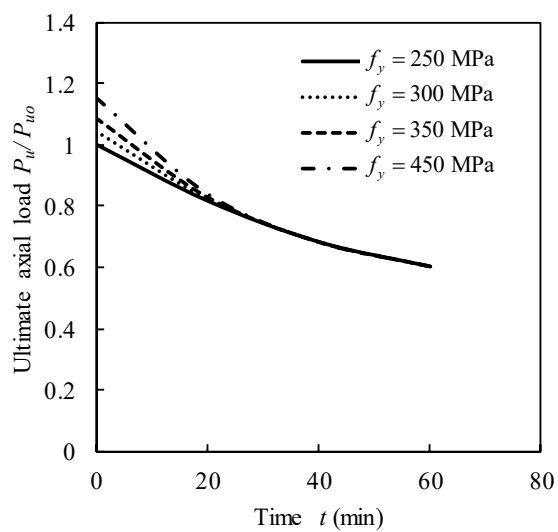


Fig. 20. Effects of the steel yield strength on the ultimate strength-fire exposure time curves of rectangular slender CFST columns.

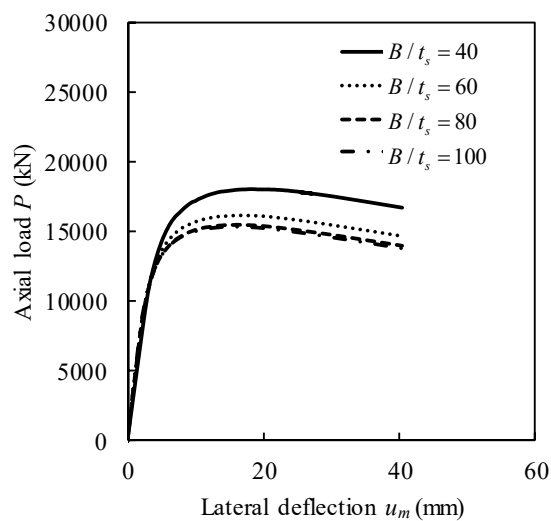


Fig. 21. Axial load-lateral displacement curves of square slender CFST columns with various B/t_s ratios at fire-exposure time of 20 min

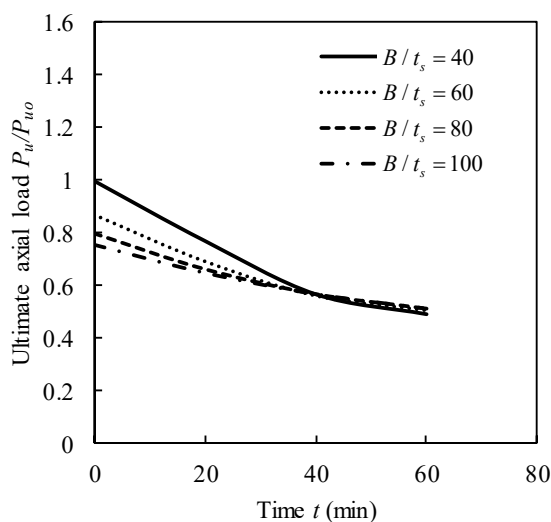


Fig. 22. Effects of B/t_s ratios on the ultimate strength-fire exposure time curves of square slender CFST columns.

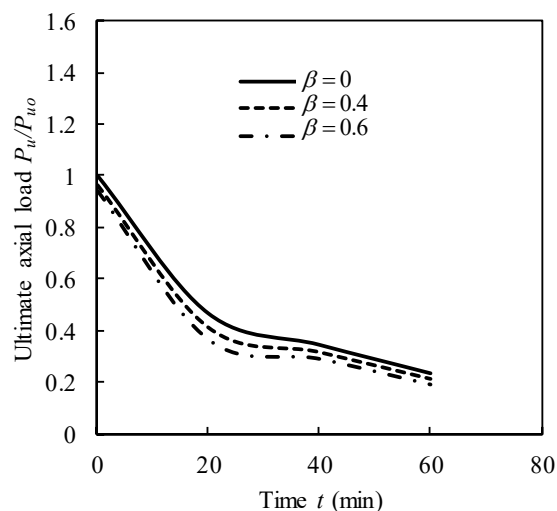


Fig. 23. Effects of preload ratios on the column strength-fire exposure time curves.

Table 1. Dimensions and properties of CFST slender columns used in the verifications

Specimen	$B \times D \times t_s$ (mm)	B/t_s	L (mm)	f_y (MPa)	f'_c (MPa)	Applied load (kN)	Ref.
SQ-01	152.4×152.4×6.35	24	1905	350	58.3	376	[13]
SQ-7	177.8×177.8×6.35	28	1905	350	57	549	
SQ-17	254×254×6.35	40	1905	350	58.3	1096	
SQ-24	304.8×304.8×6.35	48	1905	350	58.8	1130	
SAL1	300×300×9	33.3	3500	363	27.5	842.8	[17]
SAL2	300×300×9	33.3	3500	363	27.5	744.8	
SAH1	300×300×9	33.3	3500	363	37.8	1401.4	
SBL1	350×350×9	38.9	3500	363	27.5	1293.6	
SBL2	350×350×9	38.9	3500	363	27.5	1038.8	
SBH1	350×350×9	38.9	3500	363	37.8	1940.4	
SBH2	350×350×9	38.9	3500	363	37.8	1558.2	
A1b	200×100×5	40	3000	275	30	268	[27]
B1b	200×200×6.3	31.7	3000	275	30	660	
C1b	200×200×12.5	16	3000	275	30	969	
C3b	200×200×12.5	16	3000	275	30	2261	
SC1	400×400×12	33.3	4000	345	50	-	[24]
SC2	350×350×9	38.9	3000	363	27.5	-	[26]

Fire-Resistance of Eccentrically Loaded Rectangular Concrete-Filled Steel Tubular Slender Columns Incorporating Interaction of Local and Global Buckling by G.M. Kamil, Q.Q. Ling, and M.N.S. Hadi was published in the peer review journal, *International Journal of Structural Stability and Dynamics*, 19/8, 2019.

The full-text of this article is subject to copyright restrictions, and cannot be included in the online version of the thesis.

It is available at <https://doi.org/10.1142/S0219455419500858>

5.4 CONCLUDING REMARKS

This chapter has described a computational modeling technique, which has been proposed for quantifying the load-deflection responses and fire resistance of rectangular CFST slender columns subjected to concentric and eccentric loads when exposed to fire. The computational model is innovative as it has explicitly incorporated the local and global interaction buckling, deflections induced by preloads and concrete tensile behavior in the theoretical formulation. These important features have not been considered in the fiber-based nonlinear modeling procedures presented by other researchers. Experimental verifications have demonstrated that the computational model produces realistic load-deflection responses and fire resistance of slender CFST columns, which are in good correlations with test data. The model has been employed to undertake parametric studies on the fire behavior of CFST slender columns and the results obtained can be used to develop design guides for the structural fire engineering design of slender CFST columns.

Chapter 6

PERFORMANCE OF CFST SHORT COLUMNS AFTER BEING EXPOSED TO FIRE

6.1 INTRODUCTION

Rectangular CFST columns in a tall building after being exposed to fire have been damaged but might not collapse. Their residual strength and stiffness must be assessed in order to develop an efficient and economical post-fire repair solution. A nonlinear post-fire computational model formulated by the theory of fiber elements is developed in this chapter, which can predict the post-fire structural behavior as well as the residual strengths of rectangular CFST tube columns subjected to concentric loads. The mathematical model utilizes the post-fire material constitutive relations of concrete and steel that are available in the published literature. The gradual local and post-local buckling of steel tubes is considered in the mathematical model, which generates the load-axial strain responses of CFST columns after fire exposure. After experimental verification, the computer model is used to demonstrate the significance of local buckling, geometric parameters and material strengths on the post-fire behavior of CFST short columns.

This chapter includes the following paper:

1. **Kamil, G. M.**, Liang, Q. Q. and Hadi, M. N. S. (2019) Nonlinear post-fire simulation of concentrically loaded rectangular thin-walled concrete-filled steel tubular short columns accounting for progressive local buckling, *Thin-Walled Structures* (currently under review).

GRADUATE RESEARCH CENTRE

DECLARATION OF CO-AUTHORSHIP AND CO-CONTRIBUTION: PAPERS INCORPORATED IN THESIS BY PUBLICATION

This declaration is to be completed for each conjointly authored publication and placed at the beginning of the thesis chapter in which the publication appears.

1. PUBLICATION DETAILS (to be completed by the candidate)

Title of Paper/Journal/Book:	Kamil, G. M., Liang, Q. Q. and Hadi, M. N. S. (2019) Nonlinear post-fire simulation of concentrically loaded rectangular thin-walled concrete-filled steel tubular short columns accounting for progressive local buckling, Thin-Walled Structures (currently under review).		
Surname:	Kamil	First name:	Ghanim
College:	College of Engineering & Science	Candidate's Contribution (%):	70
Status:			
Accepted and in press:	<input type="checkbox"/>	Date:	<input type="text"/>
Published:	<input type="checkbox"/>	Date:	<input type="text"/>

2. CANDIDATE DECLARATION

I declare that the publication above meets the requirements to be included in the thesis as outlined in the HDR Policy and related Procedures – policy.vu.edu.au.

	15/04/2019
Signature	Date

3. CO-AUTHOR(S) DECLARATION

In the case of the above publication, the following authors contributed to the work as follows:

The undersigned certify that:

1. They meet criteria for authorship in that they have participated in the conception, execution or interpretation of at least that part of the publication in their field of expertise;
2. They take public responsibility for their part of the publication, except for the responsible author who accepts overall responsibility for the publication;
3. There are no other authors of the publication according to these criteria;
4. Potential conflicts of interest have been disclosed to a) granting bodies, b) the editor or publisher of journals or other publications, and c) the head of the responsible academic unit; and

5. The original data will be held for at least five years from the date indicated below and is stored at the following location(s):

Location: College of Engineering and Science, Victoria University, Melbourne, Victoria, Australia.

Name(s) of Co-Author(s)	Contribution (%)	Nature of Contribution	Signature	Date
Ghanim Mohammed Kamil	70	Developed and verified the model Conducted the parametric study Drafted the manuscript	[Redacted Signature]	28/02/2019
Qing Quan Liang	20	Provided initial concepts Provided critical revision of the article Final approval and submitting the manuscript	[Redacted Signature]	28/02/2019
Muhammad N. S. Hadi	10	Provided critical revision of the article Final approval of the manuscript	[Redacted Signature]	28/2/2019

Nonlinear post-fire simulation of concentrically loaded rectangular thin-walled concrete-filled steel tubular short columns accounting for progressive local buckling by G.M. Kamil, Q.Q. Liang, M.N.S. Hadi was published in a peer review journal, *Thin-Walled Structures*, 145, 2019.

The published version is available at <https://doi.org/10.1016/j.tws.2019.106423>

Manuscript prepared for

Thin-Walled Structures

April 2019

Nonlinear post-fire simulation of concentrically loaded rectangular thin-walled concrete-filled steel tubular short columns accounting for progressive local buckling

Ghanim Mohammed Kamil^a, Qing Quan Liang^{a,*}, Muhammad N. S. Hadi^b

^a College of Engineering and Science, Victoria University, PO Box 14428, Melbourne, VIC 8001, Australia

^b School of Civil, Mining and Environmental Engineering, University of Wollongong, Wollongong, NSW 2522, Australia

Corresponding author:

Associate Professor Qing Quan Liang
College of Engineering and Science
Victoria University
PO Box 14428
Melbourne VIC 8001
Australia
Phone: +61 3 9919 4134
E-mail: Qing.Liang@vu.edu.au

Nonlinear post-fire simulation of concentrically loaded rectangular thin-walled concrete-filled steel tubular short columns accounting for progressive local buckling

Ghanim Mohammed Kamil^a, Qing Quan Liang^{a,*}, Muhammad N. S. Hadi^b

^a *College of Engineering and Science, Victoria University, PO Box 14428, Melbourne, VIC 8001, Australia*

^b *School of Civil, Mining and Environmental Engineering, University of Wollongong, Wollongong, NSW 2522, Australia*

Abstract

The repair of fire-damaged thin-walled rectangular concrete-filled steel tubular (CFST) columns in engineering structures after fire exposure requires the assessment of their residual strength and stiffness. Existing numerical models have not accounted for the effects of unilateral local buckling on the post-fire behavior of CFST columns with rectangular thin-walled sections. This paper describes a nonlinear post-fire simulation technique underlying the theory of fiber analysis for determining the residual strengths and post-fire responses of concentrically loaded short thin-walled rectangular CFST columns accounting for progressive local buckling. The post-fire stress-strain laws for concrete in rectangular CFST columns are proposed based on available test data and implemented in the theoretical model. An innovative numerical scheme for modeling the progressive local and post-local buckling of CFST thin-walled columns is discussed. The

* Corresponding author. Tel.: 61 3 9919 4134.
E-mail address: Qing.Liang@vu.edu.au (Q. Q. Liang)

nonlinear post-fire simulation model is verified by experimental data and then used to show the significance of local buckling, material strengths and width-to-thickness ratio on the post-fire responses of CFST stub columns. The proposed post-fire computer model is shown to be capable of predicting well the residual stiffness and strength of concentrically loaded thin-walled CFST columns after fire exposure. A design formula is proposed that estimates well the post-fire residual strengths of CFST columns. Computational results presented provide a better understanding of the post-fire behavior of CFST columns fabricated by thin-walled sections incorporating unilateral local and post-local buckling.

Keywords: Concrete-filled steel tubes; Local and post-local buckling; Nonlinear post-fire analysis; Residual strength.

1. Introduction

Rectangular concrete-filled steel tubular (CFST) columns fabricated with thin-walled sections as shown in Fig. 1 are widely used in tall buildings to support heavy compressive loads. In the design life of a tall composite building, the building as well as CFST columns may be under fire exposure. The fire responses of loaded rectangular and circular CFST short and slender columns exposed to fire have been studied by many researchers experimentally [1-8] and numerically [9-15]. Standard fire tests indicated that the use of steel bar-reinforced concrete or fiber-reinforced concrete instead of plain concrete improved the fire performance of CFST columns. It was reported that CFST short columns of rectangular and square thin-walled sections failed by the outward local

buckling coupled with concrete crushing while slender rectangular and square CFST columns failed by local and global interaction buckling. The air gap at the concrete-steel interface, concrete tensile strength, deformations induced by preloads, and local buckling have been shown to have marked influences on the structural responses of CFST columns to fire effects, which must be incorporated in the nonlinear fire response simulations of CFST columns to yield realistic fire resistance [12, 15].

After fire exposure, CFST columns in a composite building have been damaged in some degrees by fire effects, but they might not collapse. Therefore, the fire-damaged CFST columns must be repaired, which requires the assessment of their residual strength and stiffness in order to develop an economical solution to the post-fire repair. After being exposed to fire, the steel material could restore much of its strength while the strength of concrete has been significantly degraded [16]. Experiments could be conducted to determine the residual stiffness and strength of CFST columns after fire exposure. In a post-fire experiment, the CFST column is gradually loaded to failure in a room temperature environment [16-22]. Post-fire tests were performed on the residual strengths of rectangular and square CFST short and slender columns by Han et al. [16-18], circular CFST stub columns by Huo et al. [19], square and circular CFST slender columns by Rush et al. [20], and short CFST circular columns made of steel bar-reinforced concrete by Liu et al. [21, 22]. The post-fire experiments conducted by Han et al. [16] on rectangular CFST stub columns having the depth-to-thickness ratios of 35 and 45.5 indicated that these columns failed by the local buckling. In addition, increasing the exposure temperature resulted in earlier and more serious unilateral local-buckling of rectangular steel sections. Moreover, the maximum exposure temperature had a

remarkable influence on the residual stiffness and strength of CFST columns. Han et al. [17] and Rush et al. [20] reported that slender square CFST columns failed by the local and global interaction buckling.

Although post-fire tests on CFST columns could be conducted, the tests are highly time-consuming and expensive. It is impossible to undertake post-fire tests on CFST columns in real buildings to determine their residual strength and stiffness. Consequently, the assessment of the post-fire structural responses of CFST columns in real buildings mainly relies on the use of nonlinear inelastic post-fire analysis techniques. Han et al. [16, 17] proposed analytical models for ascertaining the residual stiffness and strength of CFST short and slender columns after exposure to elevated temperatures. The stress-strain laws of confined concrete at ambient temperature provided by Han et al. [23] was modified by using the expressions given by Li and Guo [24] for estimating the residual strength and strain of compressive concrete exposed to a maximum temperature and had cooled down to the room temperature. However, the unilateral local-buckling of thin-walled steel sections was not included in the analytical models presented by Han et al. [16, 17]. Yang et al. [25] proposed a finite element model using the fiber discretization for calculating the post-fire performance of loaded CFST slender columns. The finite element program ABAQUS was employed to investigate the residual strengths of short and slender CFST columns that considered various material and geometric parameters by Huo et al. [19], Liu et al. [21, 22], Song et al. [26], Yao and Hu [27] and Ibanez et al. [28].

The unilateral local-buckling of rectangular thin-walled steel sections, which markedly reduces the strength and stiffness of CFST columns with or without fire exposure [15, 16,

29-33], has not been considered in the existing theoretical models for post-fire simulations. To overcome this limitation, this paper presents a new fiber-based nonlinear post-fire simulation technique for quantifying the residual strength and stiffness of concentrically loaded short CFST column with rectangular thin-walled sections after exposure to fire accounting for progressive local buckling. The post-fire material laws for concrete in rectangular CFST columns are developed and incorporated in the proposed post-fire simulation model. The existing post-fire experimental results are utilized to verify the computer post-fire modeling procedure. A parametric study is performed that investigates the post-fire load-axial strain responses of thin-walled CFST stub columns after being exposed to high temperatures. A design formula is derived for estimating the residual strengths of CFST columns after being exposed to fire.

2. The fiber-based nonlinear post-fire simulation

2.1. Fiber element formulation

The present method of nonlinear post-fire analysis employs the fiber approach to mesh the cross-sections of rectangular CFST columns. The method of fiber analysis has shown to be an accurate and computationally efficient numerical technique for simulating the inelastic behavior of composite columns as it does not require the meshing of the column along its length [31-35]. The typical fiber mesh of a CFST column is shown in Fig. 2, in which the steel fiber size is equal to half of that of the concrete fiber. Each element in the cross-section represents either a steel fiber or concrete fiber running longitudinally. The post-fire material properties can be assigned to steel and concrete fibers. The nonlinear

post-fire simulation model is formulated by means of the following assumptions: (1) the CFST column has been exposed to elevated temperature; (2) the slip between the concrete core and steel tube is zero; (3) the unilateral progressive local buckling of thin-walled steel sections is taken into account; (4) the shrinkage and creep of concrete are ignored.

The strain compatibility requires that the steel tube and concrete in a CFST column loaded concentrically have the same axial strain. To determine the softening post-peak responses of CFST columns, the method of strain control is used in the computational procedure. In this method, the axial strain is gradually increased and the stresses in fiber elements are calculated from the given axial strain by means of employing the uniaxial material post-fire constitutive laws of concrete and steel. The numerical schemes given in Sections 2.4 and 2.5 are utilized to model the post-local buckling in addition to the initial local-buckling of thin-walled steel sections and update stresses of steel fibers in accordance with the effective width method. The internal axial force (P) is then computed by integrating the fiber stresses over the entire cross-section. By means of repeating the above computation process, the load-axial strain curve of the CFST stub column can be completely quantified. The incremental numerical analysis process is terminated when either the specified ultimate concrete strain is exceeded or the axial load falls to 50% of the column ultimate load [34].

2.2. Post-fire stress-strain laws for structural steels

The idealized elastic-plastic post-fire stress-strain curve with strain-hardening for structural steels given by Cheng [36] is shown in Fig. 3, which is implemented in the

present nonlinear post-fire analysis technique. This stress-strain relationship of steel after exposure to elevated temperatures is expressed as

$$\sigma_s = \begin{cases} E_s \varepsilon_s & \text{for } \varepsilon_s \leq \varepsilon_{yp} \\ f_{yp}(T) + E_{st} [\varepsilon_s - \varepsilon_{yp}(T)] & \text{for } \varepsilon_s > \varepsilon_{yp} \end{cases} \quad (1)$$

where σ_s , ε_s denote the longitudinal stress and strain in steel fibers, respectively; E_s the Young's modulus of steel that is exposed to room temperature, ε_{yp} the yield strain at post-fire, E_{st} the tangent modulus at strain hardening taken as $E_{st} = 0.01E_s$, T the maximum exposure temperature in °C, and f_{yp} the yield strength of steel tube after being exposed to elevated temperature and was given by Cheng [36] as

$$f_{yp} = \begin{cases} f_y & \text{for } T \leq 400^\circ\text{C} \\ f_y [1 + 2.33 \times 10^{-4} (T - 20) - 5.88 \times 10^{-7} (T - 20)^2] & \text{for } T > 400^\circ\text{C} \end{cases} \quad (2)$$

in which f_y stands for the yield stress of steel in room temperature without exposure to elevated temperatures.

2.3. Post-fire stress-strain laws for concrete

The high temperatures significantly degrade the maximum compressive strength of concrete. The available post-fire stress-strain relationships for concrete in CFST rectangular columns have been extremely limited due to the difficulty in testing the

concrete in CFST columns after being exposed to fire. The stress-strain relationships for concrete at ambient temperature has been modified by utilizing the post-fire material properties of concrete and the modified model has been employed to model the material post-fire behavior of concrete in CFST columns by Han et al. [16] and Yang et al. [25]. In the present computer simulation technique, the stress-strain laws for compressive concrete at room temperature suggested by Mander et al. [37] is modified by using the post-fire material properties of concrete proposed by the authors in the present study to simulate the material responses of concrete in rectangular CFST columns after fire exposure as follows:

$$\sigma_{cp} = \frac{f'_{cp} \lambda (\varepsilon_{cp} / \varepsilon'_{cp})}{\lambda - 1 + (\varepsilon_{cp} / \varepsilon'_{cp})^\lambda} \quad (3)$$

$$\lambda = \frac{E_{cp}}{E_{cp} - (f'_{cp} / \varepsilon'_{cp})} \quad (4)$$

where σ_{cp} and ε_{cp} represent the post-fire concrete stress and strain in compression, respectively; f'_{cp} and ε'_{cp} the post-fire compressive strength and corresponding strain of concrete, respectively; E_{cp} is the post-fire modulus of elasticity of concrete, which is calculated by the following equation given by ACI Committee 363 [38] with the post-fire compressive strength of concrete:

$$E_{cp} = 3320 \sqrt{f'_{cp}} + 6900 \text{ (MPa)} \quad (5)$$

The maximum post-fire strength of compressive concrete in rectangular CFST columns and the corresponding strain were determined based on the experimental results on axially loaded short rectangular CFST columns tested by Han et al. [16]. In the computations of the post-fire ultimate strengths of CFST columns, the post-fire steel yield strengths defined by Eq. (2) were used and the local buckling of steel sections was taken into account. The computed post-fire compressive strengths and corresponding strains of concrete in the tested CFST rectangular columns presented in Table 1 are provided in Figs. 4 and 5, respectively. Based on the nonlinear regressive analyses, expressions for determining the post-fire maximum compressive strength and corresponding strain of concrete in rectangular CFST columns are proposed as follows:

$$f'_{cp} = (-6 \times 10^{-7} T^2 - 2 \times 10^{-4} T + 0.952) f'_c \quad (6)$$

$$\varepsilon'_{cp} = (2.14 \times 10^{-6} T^2 + 3.66 \times 10^{-3} T + 1) \varepsilon'_c \quad (7)$$

in which T is the maximum temperature to which the CFST column has been exposed; f'_c and ε'_c the compressive strength and corresponding strain of the concrete cylinder at room temperature. The strain ε'_c of concrete at room temperature can be computed by the following expressions suggested by Liang [31]:

$$\varepsilon'_c = \begin{cases} 0.002 & \text{for } f'_c \leq 28 \text{ MPa} \\ 0.002 + \frac{f'_c - 28}{54000} & \text{for } 28 < f'_c \leq 82 \text{ MPa} \\ 0.003 & \text{for } f'_c > 82 \text{ MPa} \end{cases} \quad (8)$$

The post-fire compressive strengths and corresponding strains of concrete in rectangular CFST columns calculated by the proposed Eqs. (6) and (7) are compared with those obtained from the experiments conducted by Han et al. [16] in Figs. 4 and 5, respectively. The figures demonstrate that the proposed formulas predict well the post-fire compressive strengths and corresponding strains of concrete. The typical post-fire stress-strain curves of concrete CFST columns with rectangular steel sections based on the proposed material constitutive models are presented in Fig. 6.

2.4. Modeling of initial local buckling

After exposure to high temperatures, the steel tube in a CFST column with rectangular thin-walled section loaded gradually at ambient temperature will undergo the progressive unilateral buckling from the onset of initial local buckling to the post-local buckling. Kamil et al. [33] proposed equations for the calculations of the initial local-buckling stress of steel plates subjected to stress gradients in rectangular CFST columns exposed to room temperature as well as elevated temperatures. When a steel plate has been cooled down from elevated temperatures, it can restore much of its strength. For the post-fire analysis, CFST columns have been cooled down to the room temperature so that the equations developed by Kamil et al. [33] for thin steel plates at ambient temperature can be applied to the determination of the initial local-buckling stress of the steel tube walls in a CFST column after fire exposure. This can be done by means of replacing the yield strength of steel at room temperature with its post-fire yield strength.

The critical stress ($\sigma_{1c,p}$) that causes initial local buckling of the thin-walled steel walls in a CFST column subjected to uniform compression after fire exposure can be calculated by the following equation given by Kamil et al. [33]:

$$\frac{\sigma_{1c,p}}{f_{yp}} = (g_1 \lambda_{c,p}^g + g_2) \frac{0.6566 \lambda_{c,p}^{0.001521}}{0.5415 \lambda_{c,p}^{4.889} + 1} \quad (9)$$

where $\lambda_{c,p}$ stands for the relative slenderness ratio of the column at post-fire, expressed by

$$\lambda_{c,p} = \sqrt{\frac{12(1-\nu^2)(b/t_s)^2 f_{yp}}{k\pi^2 E_s}} \quad (10)$$

where b , t_s represent the clear width and thickness of steel section, respectively; ν the Poisson's ratio of steel; and k the coefficient for the elastic local buckling of clamped plates, taken as 9.95 [33].

The coefficients g , g_1 and g_2 in Eq. (9) are calculated by

$$g = -7.9339\alpha_s^2 + 11.29\alpha_s + 4.701 \quad (11)$$

$$g_1 = 0.0863\alpha_s^2 - 0.1248\alpha_s + 0.0431 \quad (12)$$

$$g_2 = 0.2656\alpha_s^2 - 0.9902\alpha_s + 1.719 \quad (13)$$

where α_s denotes the stress-gradient coefficient, which is equal to 1.0 for a steel plate subjected to uniform edge compressive stresses.

2.5. Modeling of post-local buckling

The method of effective width is usually employed to determine the post-local buckling strengths of thin steel plates that fabricate a rectangular CFST column [30, 31, 34]. Figure 7 illustrates the ineffective and effective widths of a rectangular steel cross-section filled with concrete subjected to axial compression. Kamil et al. [33] proposed effective width formulas for calculating the strengths of post-local buckling of thin steel plates exposed to various temperatures. Their formulas are incorporated in the fiber-based post-fire model to ascertain the effective widths of steel sections in CFST columns after fire exposure, which are written as

$$\frac{b_e}{b} = (q_1 \lambda_{c,p}^q) \frac{0.8418 \lambda_{c,p}^{0.02368} + 1.154}{2.055 + \lambda_{c,p}^{1.68}} \quad (14)$$

in which b_e denotes the effective width of a steel tube wall depicted in Fig. 5, q and q_1 are expressed as

$$q = 0.04007 \alpha_s^2 - 0.05275 \alpha_s + 0.03355 \quad (15)$$

$$q_1 = 0.1007 \alpha_s^2 - 0.7027 \alpha_s + 1.65 \quad (16)$$

The method of effective width assumes that steel fibers within the effective widths are stressed to the yield strength of the steel material while steel fibers within the ineffective widths withstand zero stress. This method determines the ultimate strength of a thin steel plate under compression. A thin steel plate has the capacity of undergoing the progressive buckling from initial local buckling to the post-local buckling until attains its ultimate limit state. In this gradual buckling process, the in-plane stresses in the heavily buckled regime are redistributed to the edge strips of the plate [34]. After the onset of initial local buckling, the ineffective width of the steel plate increases with increasing the loading until its ultimate strength is attained. The computer modeling technique developed by Liang [31] is adopted in the post-fire analysis procedure to model the gradual post-local buckling of steel sections after fire exposure.

3. Experimental verification

The post-fire ultimate loads of rectangular and square CFST short columns obtained by the computational model are compared against experimentally measured data given by Han et al. [16, 39] to verify its accuracy. The details of the CFST columns tested are listed in Table 1. It is seen from Table 1 that D/t_s ratio of square sections was 20 while rectangular sections had the D/t_s ratio of 43. Therefore, the local buckling of rectangular CFST columns shown in Table 1 was considered in the nonlinear post-fire analysis. It is noted that the cross-sectional dimensions of all columns listed in Table 1 are smaller than those of concrete cubes that were employed to estimate the compressive strength of concrete in tested specimens. As a result of this, the actual compressive strength of

concrete in these specimens was conservatively taken as the average compressive strength of concrete cubes in the post-fire simulations of these columns. The predicted post-fire ultimate axial strengths ($P_{u, fib}$) of CFST columns and corresponding experimentally measured values ($P_{u, exp}$) are given in Table 1. The comparison indicates that good agreement between predictions and experimental data is generally obtained. The mean value of the $P_{u, fib} / P_{u, exp}$ ratios is 0.961. The discrepancy between the theory and post-fire tests is likely caused by the fact that the measurements on the post-fire stress-strain relations for concrete and steel were not undertaken and might be different from those implemented in the computer model.

The predicted post-fire load-axial strain responses of Specimens S-20-1, S-200, S-300, S-600, S-800, S900, R2-200, R2-400, R2-800 and R2-900 are compared with experimentally measured data reported by Han et al. [16, 39] in Figs. 8 and 9. It would appear that the experimental post-fire load-axial strain responses of square CFST short columns are captured reasonably well by the nonlinear post-fire simulation technique. It is confirmed that the post-peak responses of CFST columns after being exposed to temperatures up to 400 °C are characterized by the descending stress-strain behavior while columns after being exposed to temperatures higher than 400 °C experience strain-hardening behavior in the post-yield regime.

4. Post-fire behavior of CFST columns

The nonlinear post-fire modeling technique proposed was utilized to examine the significance of the outward local buckling, concrete strength, steel yield strength and the width-to-thickness ratio on the post-fire structural behavior of short CFST columns with thin-walled rectangular sections. In the parametric studies, the modulus of elasticity of steel at room temperature was specified as 210 GPa. The effect of local buckling was taken into consideration in the nonlinear post-fire analyses of CFST columns having clear width-to-thickness ratios ranging from 30 to 100.

4.1. Effects of unilateral local buckling

The nonlinear post-fire simulation technique proposed was used to examine the significance of unilateral local buckling on the post-fire ultimate strengths of stub CFST columns. For this purpose, square steel columns with 500×500 mm, the B / t_s ratio of 100, and yield strength of 300 MPa filled with 40 MPa concrete were analyzed by means of including and excluding local buckling, respectively. These columns had been exposed to the maximum temperatures ranging from 20 °C to 800 °C and cooled down to the ambient temperature. The post-fire load-axial strain curves of the CFST columns after exposure to the temperature of 600 °C have been plotted in Fig. 10. It is demonstrated that the load-strain curve computed by considering local buckling departs from the one without considering local buckling. The unilateral local buckling causes a significant reduction in the column ultimate load by 14% after being exposed to 600 °C temperature. Figure 11 provides the column strength-maximum exposure temperature curves. The figure demonstrates that the strength reduction caused by local buckling increases as the maximum exposure temperature rises. The percentage reductions in the ultimate loads of

CFST columns due to local buckling after being heated to 400°C, 700°C and 800°C are 12%, 16% and 18%, respectively. It would appear that local buckling causes more reductions in the ultimate strengths of CFST columns after exposure to high temperatures in comparison with CFST columns without exposure to fire [32]. This is mainly caused by the fact that after being cooled down from an elevated temperature, the steel can restore an immense magnitude of its strength while the concrete suffers a sustainable degradation in its strength. Consequently, the contribution of steel tube after fire exposure to the column strength is relatively more than that of the one without fire exposure due to the lower post-fire concrete strength.

4.2. Effects of concrete strength

The sensitivities of the post-fire responses of CFST rectangular columns to the concrete compressive strength were examined by conducting nonlinear fiber analyses on the steel columns of 500×600×6 mm filled with concrete having compressive strengths ranging from 25 MPa to 55 MPa. The yield stress of steel tubes at room temperature was 350 MPa. The calculated post-fire load-axial strain responses of the CFST columns after being heated to the temperature of 600°C are given in Fig. 12. It is illustrated that the column initial axial stiffness is not sensitive to the change of concrete strength, but at higher load levels, increasing the concrete strength leads to a remarkable improvement in the column axial stiffness. The post-fire column ultimate load is shown to have a significant increase when increasing the concrete strength. Figure 13 depicts the significance of concrete strength on the column strength-maximum exposure temperature curves. Increasing the concrete strength markedly improves the column ultimate load, but this effect decreases

when rising the maximum exposure temperature. When changing the concrete strength from 25 MPa into 35 MPa, 45 MPa and 55 MPa after being heated to the temperature of 400 °C, the percentage increases in the column ultimate load are 27%, 53% and 80%, respectively. After the columns were heated to the temperature of 600 °C, however, the column ultimate load is reduced by 25%, 50% and 75%, respectively, if the concrete strength is changed from 25 MPa to 35 MPa, 45 MPa and 55 MPa.

4.3. Effects of steel yield strength

The post-fire simulation model was employed to analyze rectangular CFST columns fabricated by thin-walled steel tubes with yield strengths varying from 250 MPa to 450 MPa. The columns under investigation had the cross-sectional dimensions of 450×550×10 mm and a B/t_s ratio of 45 and was constructed by concrete with compressive strength of 45 MPa. The post-fire load-axial strain responses of these columns with various steel yield strengths after being exposed to the temperature of 600 °C have been plotted in Fig. 14. It is clearly demonstrated that the column initial stiffness is not affected by the steel yield strength. The higher of the steel yield strength, the higher of the post-fire ultimate load of the CFST column. Figure 15 gives the post-fire ultimate strengths of CFST columns that were made of steel tubes having different yield strengths after being experienced different temperatures. It is discovered that using steel tubes with higher yield strength results in a considerable increase in the column strength regardless of the exposure temperature. However, the effect of steel yield strength on the column post-fire ultimate load is shown to increase with rising the exposure temperature. After exposure to the temperature of 400 °C, changing the steel yield strength from 250 MPa

to 300 MPa, 350 MPa and 450 MPa leads to the increase in the column post-fire strength by 6%, 11% and 22%, respectively; if the columns were exposed to the temperature of 800 °C, the corresponding strength increase is 8%, 16% and 31%, respectively.

4.4. Effects of width-to-thickness ratio

The B/t_s ratio has a marked influence on the post-fire strengths of CFST columns. To investigate this effect, the computer model was utilized to analyze square CFST columns that had the cross-section of 600×600 mm. The B/t_s ratios of 40, 60, 80 and 100 were determined by varying only the thickness of the steel tubes. The steel yield strength of 350 MPa and the concrete compressive strength of 35 MPa were specified in the analyses. Figure 16 depicts the post-fire load-axial strain curves for CFST columns after exposure to 700 °C temperature. It is clearly shown that the use of a larger B/t_s ratio in CFST columns leads to a remarkable reduction in the column post-fire initial axial stiffness. The relationships between the column post-fire strength, the maximum exposure temperature and the B/t_s ratio are explicitly illustrated in Fig. 17. The computational solutions indicate that increasing the B/t_s ratio greatly decreases the column post-fire ultimate loads for all levels of exposure temperatures. However, the influence of the B/t_s ratio on the post-fire ultimate load increases as the exposure temperature rises. When changing the B/t_s ratio from 40 into 60, 80 and 100 for CFST columns being exposed to the temperature of 600 °C, the reduction in the post-fire ultimate load is 22%, 33% and 40%, respectively; for columns being heated to the temperature of 800 °C, however, the strength reduction is 25%, 37% and 45%, respectively. This implies that the larger the

B / t_s ratio and the higher exposure temperature, the greater reduction in the column post-fire strength.

5. Proposed design formula

Although the computer post-fire simulation technique developed can be used directly in the assessment of the residual stiffness and strength of CFST columns after being exposed to fire, a simple design formula is needed for use in design practice. The design formula for estimating the post-fire ultimate axial load of rectangular CFST short columns loaded concentrically is proposed as

$$P_u = A_{se}f_{yp} + A_c f'_{cp} \quad (17)$$

where P_u is the post-fire ultimate axial load of the short CFST column, A_{se} the effective cross-sectional area of the steel section that is computed by Eq. (14), and A_c the cross-sectional area of the concrete infill.

The post-fire ultimate axial loads of CFST columns calculated by the proposed formula are compared against experimental data in Table 1, where $P_{u,cal}$ is the column ultimate axial strength computed by the proposed Eq. (17). It can be observed from Table 1 that the calculated results are in good agreement with test data. The mean value of $P_{u,cal} / P_{u,exp}$ ratios is 0.941. The statistical analysis gives that the standard deviation is 0.055 and the coefficient of variation is 0.058. The proposed design formula generally yields

conservative results compared with the computer simulation model. This is due to the fact that the post-fire steel yield strength was used in the simple calculations while the computer simulation model considered the strain-hardening of steel. The comparative study shows that the simple design formula proposed can be used in practice to assess the residual strengths of fire-damaged thin-walled CFST columns.

6. Conclusions

A fiber-based nonlinear post-fire simulation technique has been described in this paper, which calculates the post-fire structural responses of concentrically loaded short CFST columns of rectangular thin-walled sections after being exposed to high temperatures. The computational model for post-fire simulations of CFST columns has incorporated the important feature of the progressive local and post-local buckling of non-compact and slender steel sections, which has not been included in other theoretical post-fire models. The post-fire stress-strain models for concrete in rectangular CFST columns has been proposed based on experimental data and have been used in the numerical studies. The proposed post-fire modeling technique generally gives good predictions of the post-fire responses of short CFST columns loaded concentrically. The post-fire behavior of short rectangular CFST columns with various parameters has been studied by utilizing the computer simulation program developed. A design formula has been proposed for quantifying the post-fire ultimate strengths of axially loaded short CFST rectangular columns considering post-local buckling.

The concluding remarks are provided as follows:

- (1) The unilateral local buckling markedly reduces the post-fire ultimate loads of CFST columns fabricated with rectangular thin-walled sections, and its effect increases as the maximum exposure temperature increases.
- (2) Using high strength concrete greatly improves the post-fire ultimate strength of CFST short columns, but its influence decreases when the maximum exposure temperature rises.
- (3) The post-fire ultimate load of CFST columns is increased considerably by means of using higher yield strength steel tubes. The influence of steel yield strength increases as the exposure temperature increases.
- (4) Increasing the B/t_s ratio sustainably decreases the post-fire stiffness and strength of CFST columns, and its influence increases when increasing the exposure temperature.
- (5) The design formula proposed is demonstrated to give good prediction of the post-fire ultimate strengths of CFST columns.

References

- [1] T.T. Lie and M. Chabot, Experimental studies on the fire resistance of hollow steel columns filled with plain concrete, Internal report, National Research Council Canada, Institute for Research in Construction, 1992-01.
- [2] Y. Sakumoto, T. Okada, M. Yoshida and S. Tasaka, Fire resistance of concrete-filled, fire-resistant steel-tube columns, J. Mat. in Civil Eng. ASCE 69 (2) (1994) 169-184.

- [3] V.K.R. Kodur and T.T. Lie, Fire performance of concrete-filled hollow steel columns, *J. Fire Prot. Eng.* 79 (3) (1995) 89-98.
- [4] L.H. Han, Y.F. Yang and L. Xu, An experimental study and calculation on the fire resistance of concrete-filled SHS and RHS columns, *J. Constr. Steel Res.* 59 (2003) 427-452.
- [5] D.K. Kim, S.M. Choi, J.H. Kim, K.S. Chung and S.H. Park, Experimental study on fire resistance of concrete-filled steel tube column under constant axial loads, *J. Steel Struct.* 5 (4) (2005) 305-313.
- [6] A. Espinos, M.L. Romero, E. Serra and A. Hospitaler, Experimental investigation on the fire behavior of rectangular and elliptical slender concrete-filled tubular columns, *Thin-Walled Struct.* 93 (2015) 137-148.
- [7] L.H. Han, F. Chen, F.Y. Liao, Z. Tao and B. Uy, Fire performance of concrete filled stainless steel tubular columns, *Eng. Struct.* 56 (2013) 165-181.
- [8] Y.F. Yang, L. Zhang and X. Dai, Performance of recycled aggregate concrete-filled square steel tubular columns exposed to fire, *Adv. in Struct. Eng.* 20 (9) (2017) 1340-1356.
- [9] T.T. Lie and R.J. Irwin, Fire resistance of rectangular steel columns filled with bar-reinforced concrete, *J. Struct. Eng. ASCE* 12 (5) (1995) 797-805.
- [10] L.H. Han, Fire performance of concrete filled steel tubular beam-columns, *J. Constr. Steel Res.* 57 (2001) 695-709.
- [11] K. Chung, S. Park and S. Choi, Material effect for predicting the fire resistance of concrete-filled square steel tube column under constant axial load, *J. Constr. Steel Res.* 64 (2008) 1505-1515.

- [12] J. Ding and Y.C. Wang, Realistic modelling of thermal and structural behaviour of unprotected concrete filled tubular columns in fire, *J. Constr. Steel Res.* 64 (2008) 1086-1102.
- [13] A. Espinos, M.L. Romero and A. Hospitaler, Advanced model for predicting the fire response of concrete filled tubular columns, *J. Constr. Steel Res.* 66 (2010) 1030-1046.
- [14] S.D. Hong and A.H. Varma, Analytical modeling of the standard fire behavior of loaded CFT columns, *J. Constr. Steel Res.* 65 (2009) 54-69.
- [15] G.M. Kamil, Q.Q. Liang and M.N.S. Hadi, Numerical analysis of axially loaded rectangular concrete-filled steel tubular short columns at elevated temperatures, *Eng. Struct.* 180 (2018) 89-102.
- [16] L.H. Han, H. Yang and S.L. Cheng, Residual strength of concrete filled RHS stub columns after exposure to high temperatures, *Adv. in Struct. Eng.* 5 (2002) 123-133.
- [17] L.H. Han and J.S. Huo, Concrete-filled structural steel columns after exposure to ISO-834 fire standard, *J. Struct. Eng. ASCE* 129 (1) (2003) 68-78.
- [18] L.H. Han, J.S. Huo and Y.C. Wang, Compressive and flexural behavior of concrete filled steel tubes after exposure to standard fire, *J. Constr. Steel Res.* 61 (2005) 882-901.
- [19] J. Huo, G. Huang and Y. Xiao, Effects of sustained axial load and cooling phase on post-fire behavior of concrete-filled steel tubular stub columns, *J. Constr. Steel Res.* 65 (2009) 1664-1676.
- [20] D.I. Rush, L. Bisby, A. Jowsey and B. Lane, Residual capacity of fire-exposed concrete-filled steel hollow section columns, *Eng. Struct.* 100 (2015) 550-563.

- [21] F. Liu, L. Gardner and H. Yang, Post-fire behaviour of reinforced concrete stub columns confined by circular steel tubes, *J. Constr. Steel Res.* 102 (2014) 82-103.
- [22] F. Liu, H. Yang and L. Gardner, Post-fire behaviour of eccentrically loaded reinforced concrete columns confined by circular steel tubes, *J. Constr. Steel Res.* 122 (2016) 495-510.
- [23] L.H. Han, X.L. Zhao and Z. Tao, Tests and mechanics model of concrete-filled SHS stub columns, columns and beam-columns, *Steel and Comp. Struct.* 1 (1) (2001) 51-74.
- [24] W. Li and Z.H. Guo, Experimental investigation of strength and deformation of concrete at elevated temperatures, *Build. Struct.* 14 (1) (1993) 8-16 (in Chinese).
- [25] H. Yang, L.H. Han and Y.C. Wang, Effects of heating and loading histories on post-fire cooling behaviour of concrete-filled steel tubular columns, *J. Constr. Steel Res.* 64 (5) (2008) 556-570.
- [26] T.Y. Song, L.H. Han and H.X. Yu, Concrete filled steel tube stub columns under combined temperature and loading, *J. Constr. Steel Res.* 66 (2010) 369-384.
- [27] Y. Yao and X.X. Hu, Cooling behavior and residual strength of post-fire concrete filled steel tubular columns, *J. Constr. Steel Res.* 112 (2015) 282-292.
- [28] C. Ibanez, L. Bisby, D. Rush, M.L. Romero and A. Hospitaler, Analysis of concrete-filled steel tubular columns after fire exposure, *The 12th Int. Conf. on Adv. in Steel-Concrete Compos. Struct.* (2018) 795-802.
- [29] Q.Q. Liang, B. Uy and J.Y.R. Liew, Nonlinear analysis of concrete-filled thin-walled steel box columns with local buckling effects, *J. Constr. Steel Res.* 62 (2006) 581-591.

- [30] Q.Q. Liang, B. Uy and J.Y.R. Liew, Local buckling of steel plates in concrete-filled thin-walled steel tubular beam-columns, *J. Constr. Steel Res.* 63 (3) (2007) 396-405.
- [31] Q.Q. Liang, Performance-based analysis of concrete-filled steel tubular beam-columns. Part I: Theory and algorithms, *J. Constr. Steel Res.* 65 (2) (2009) 363-373.
- [32] Q.Q. Liang, Performance-based analysis of concrete-filled steel tubular beam-columns, Part II: Verification and applications, *J. Constr. Steel Res.* 65 (2) (2009) 351-362.
- [33] G.M. Kamil, Q.Q. Liang and M.N.S. Hadi, Local buckling of steel plates in concrete-filled steel tubular columns at elevated temperatures, *Eng. Struct.* 168 (2018) 108-118.
- [34] Q.Q. Liang, *Analysis and design of steel and composite structures*, Boca Raton and London: CRC Press, Taylor and Francis Group; 2014.
- [35] Q.Q. Liang, Nonlinear analysis of circular double-skin concrete-filled steel tubular columns under axial compression, *Eng. Struct.* 131 (2017) 639-650.
- [36] S.L. Cheng, Behaviors of concrete-filled rectangular steel tubes subjected to axial compression after high temperatures, ME Thesis, School of Civil Engineering, Harbin Institute of Technology, Harbin, China (in Chinese).
- [37] J.B. Mander, M.N.J. Priestly and R. Park, Theoretical stress-strain model for confined concrete, *J Struct. Eng. ASCE* 114 (8) (1998) 1804-1826.
- [38] ACI Committee 363, *State of the Art Report on High-Strength Concrete*, ACI Publication 363R-92, Detroit, MI: American Concrete Institute, 1992.

- [39] L.H. Han, H. Yang and S.L. Chen, Tests on the residual strength of concrete filled steel tubes after high temperatures, Proc. of the First Int. Conf. on Steel and Compos. Struct. Pusan, Korea, 14-16 June 2001; 1709-1716.

Figures and Tables

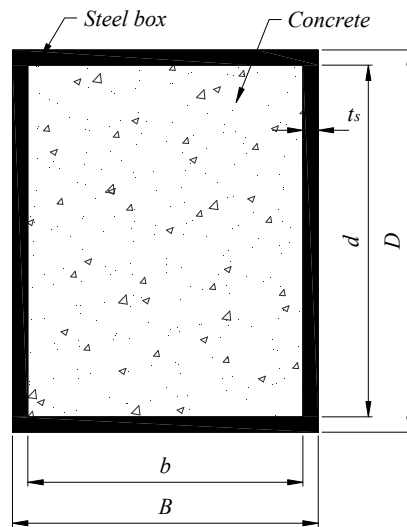


Fig. 1. Cross-section of rectangular CFST column.

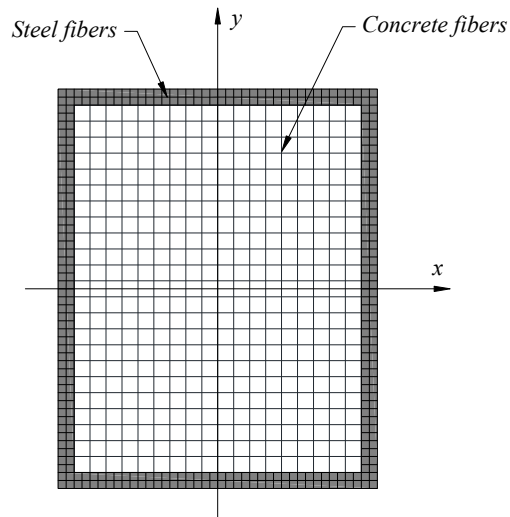


Fig. 2. Typical fibre element discretization.

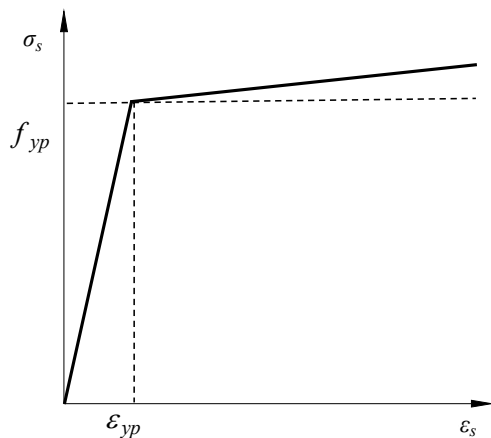


Fig. 3. Idealized post-fire stress-strain curve for structural steels.

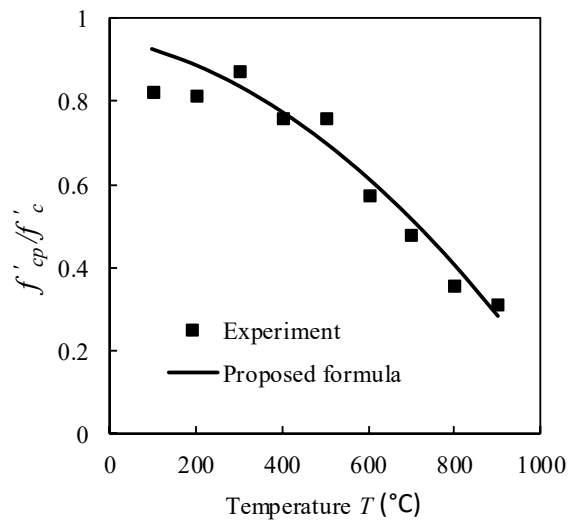


Fig. 4. Comparison of the post-fire maximum compressive strengths of concrete in rectangular CFST columns obtained from experiments and by the proposed formula

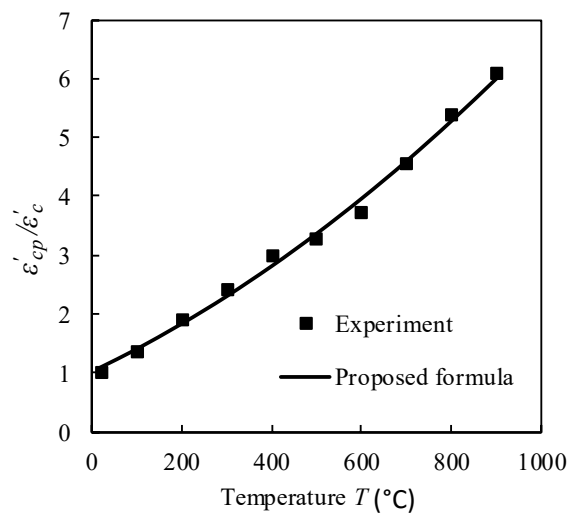


Fig. 5. Comparison of the post-fire strains ϵ'_{cp} of concrete in rectangular CFST columns obtained from experiments and by the proposed formula

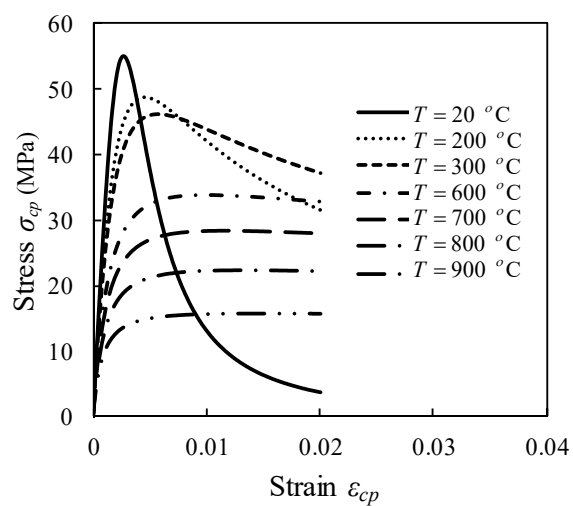


Fig. 6. Typical post-fire stress-strain curves for concrete in rectangular CFST columns

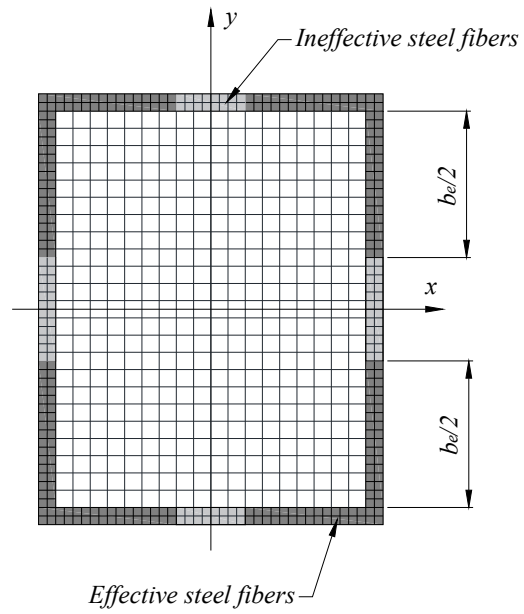


Fig. 7. Effective widths of steel tube walls in rectangular CFST column section.

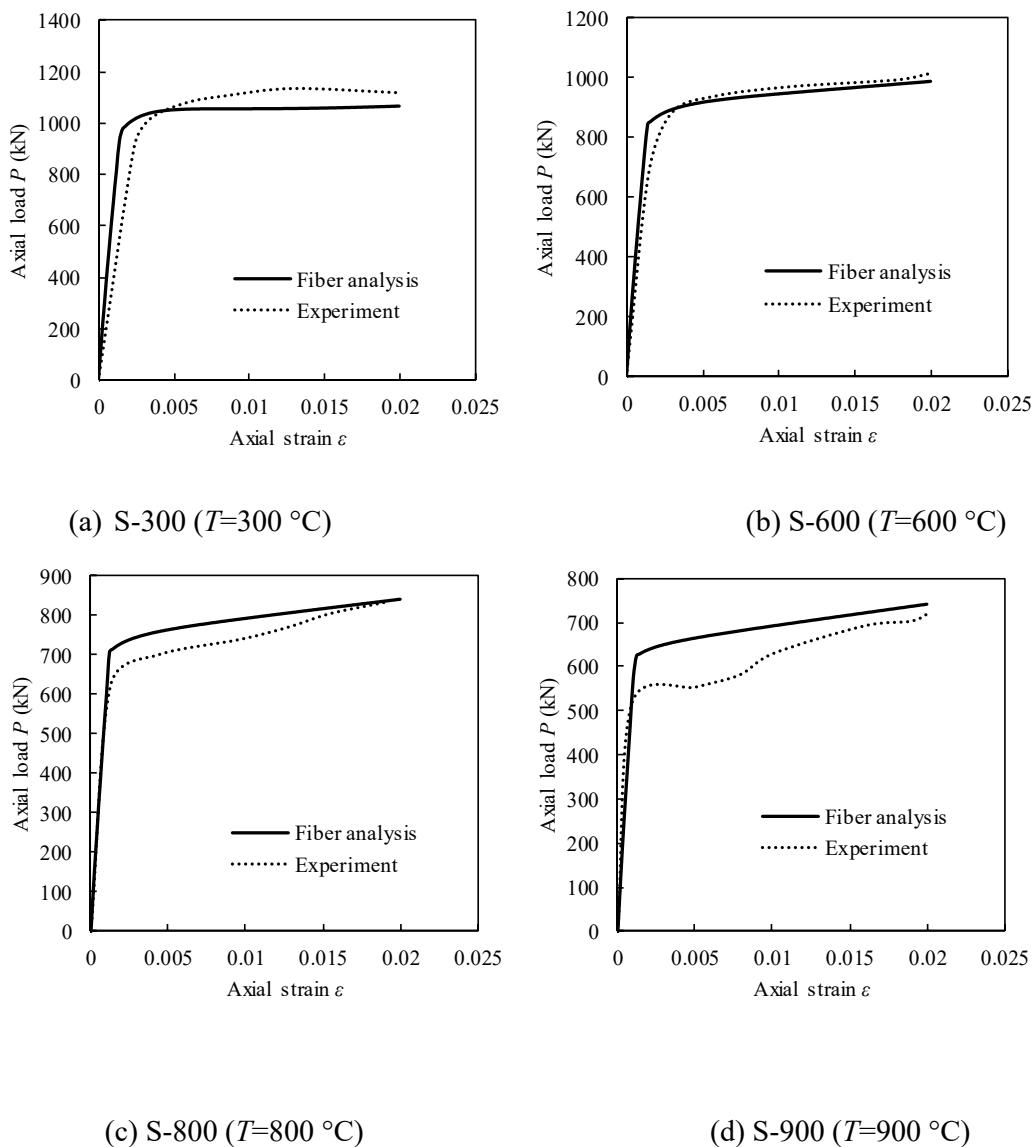


Fig. 8. Comparison of predicted and experimental post-fire axial load-strain responses of square CFST columns after exposure to high temperatures.

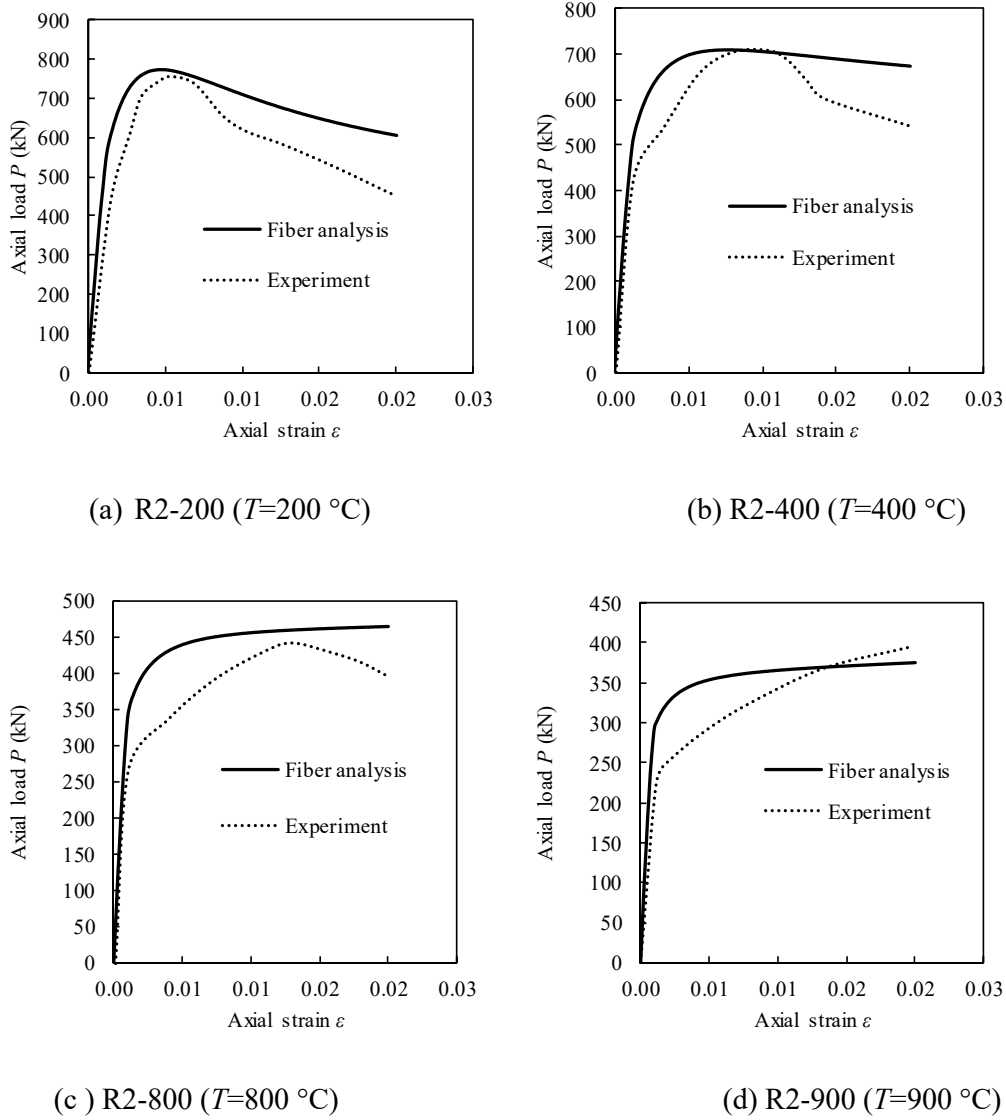


Fig. 9. Comparison of predicted and experimental post-fire axial load-strain responses of rectangular CFST columns after exposure to high temperatures.

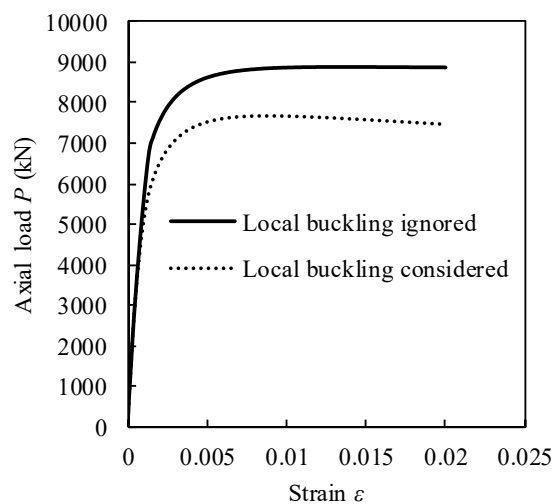


Fig. 10. Influences of local buckling on the post-fire axial load-strain behavior of square CFST column after being exposed to temperature of 600 °C.

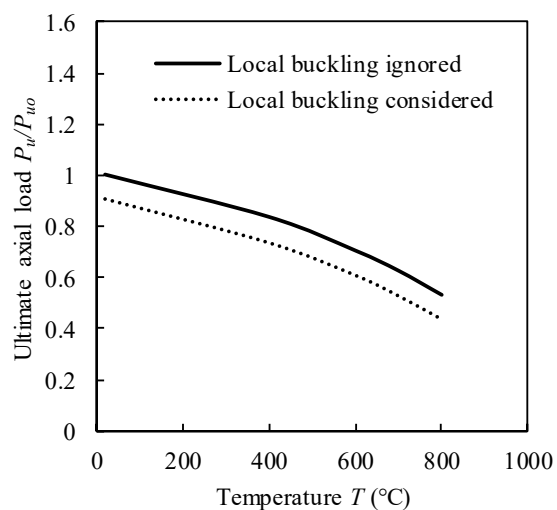


Fig. 11. Influences of local buckling on the post-fire ultimate axial strengths of square CFST column.

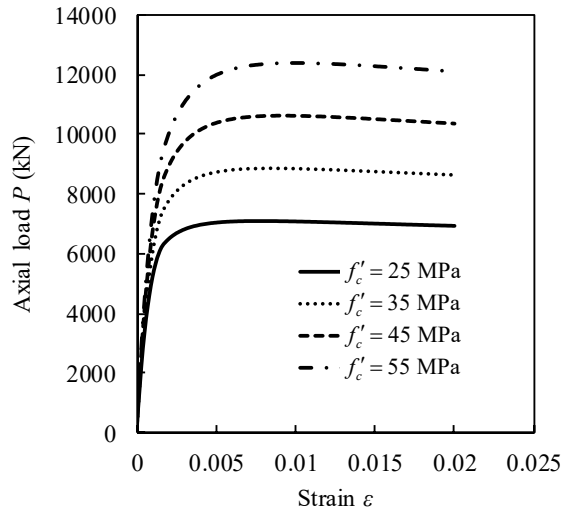


Fig. 12. Post-fire axial load-strain curves of rectangular CFST columns with various concrete strengths after being exposed to temperature of 600 °C.

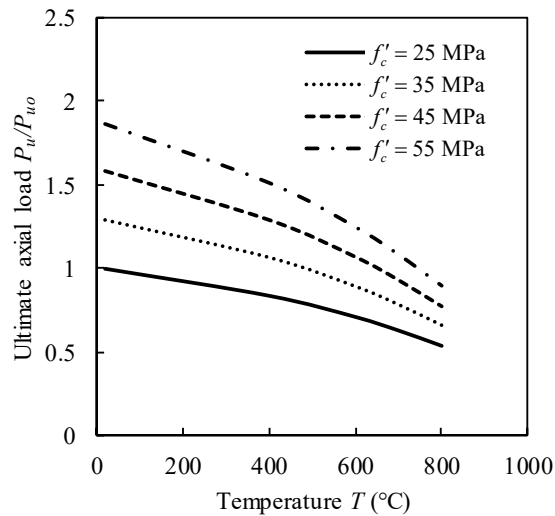


Fig. 13. Effects of concrete strength on the post-fire ultimate strength-exposure temperature curves for rectangular CFST columns.

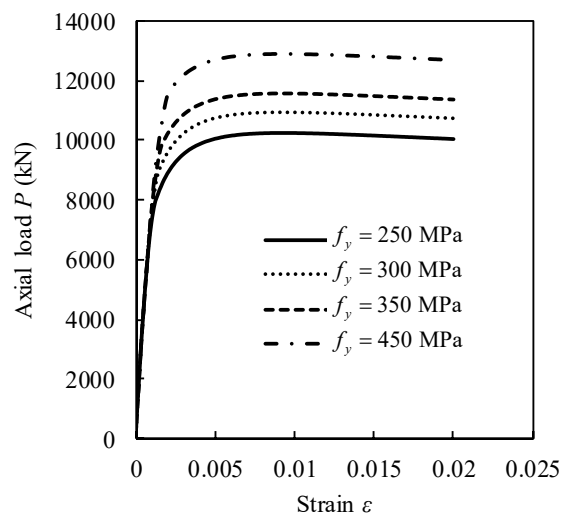


Fig. 14. Effects of steel yield strength on the post-fire axial load-strain curves of rectangular CFST columns after being exposed to temperature of 600 °C.

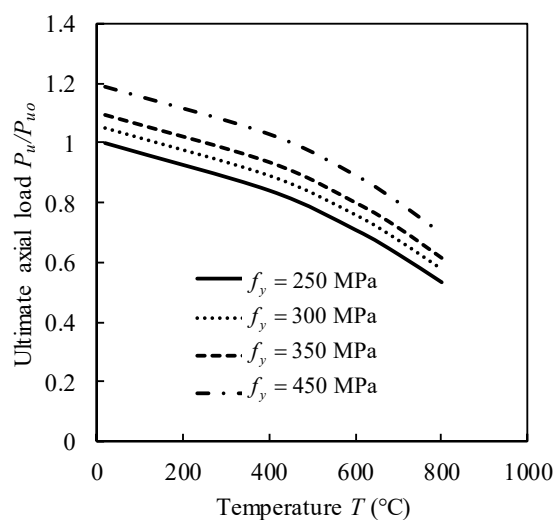


Fig. 15. Effects of steel yield strength on the post-fire ultimate strength-exposure temperature curves for rectangular CFST columns.

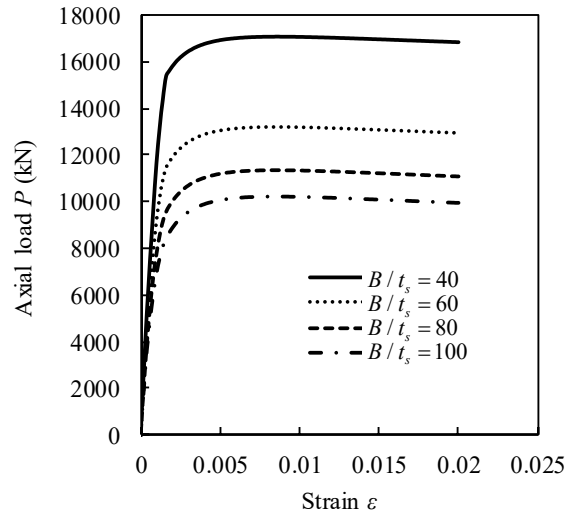


Fig. 16. Effects of B/t_s ratios on the post-fire axial load-strain responses of square CFST columns after being exposed to temperature of 600 °C.

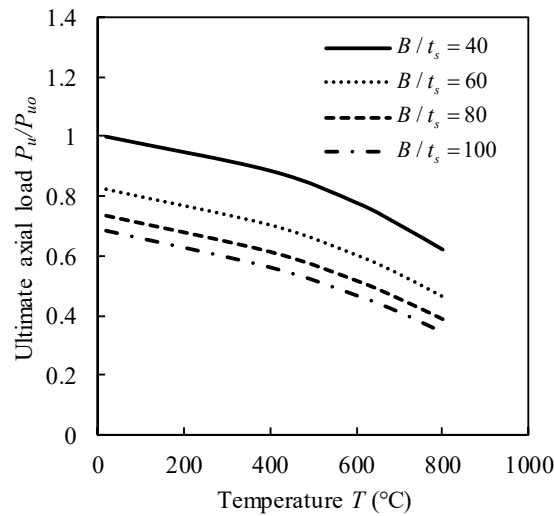


Fig. 17. Effects of B/t_s ratios on the post-fire ultimate strength-exposure temperature curves for square CFST columns.

Table 1. Post-fire ultimate axial loads of rectangular and square CFST short columns under axial compression

Specimen	T (°C)	$B \times D \times t_s$ (mm)	f_y (MPa)	f_{cu} (MPa)	$P_{u,exp}$ (kN)	$P_{u,fib}$ (kN)	$P_{u,cal}$ (kN)	$\frac{P_{u,fib}}{P_{u,exp}}$	$\frac{P_{u,cal}}{P_{u,exp}}$	Ref.
R2-20-1	20	85×130×2.86	228	59.3	825.2	835.56	834.62	1.013	1.011	[16]
R2-100	100	85×130×2.86	228	59.3	761.3	793.19	791.44	1.042	1.04	
R2-200	200	85×130×2.86	228	59.3	757.5	772.03	769.24	1.019	1.015	
R2-300	300	85×130×2.86	228	59.3	793.2	744	740.02	0.938	0.933	
R2-400	400	85×130×2.86	228	59.3	725.6	709.15	703.80	0.977	0.97	
R2-500	500	85×130×2.86	228	59.3	725.6	665.32	654.96	0.917	0.903	
R2-600	600	85×130×2.86	228	59.3	603.4	607.23	595.45	1.006	0.987	
R2-700	700	85×130×2.86	228	59.3	537.6	540.88	526.07	1.006	0.979	
R2-800	800	85×130×2.86	228	59.3	445.5	463.56	446.79	1.041	1.003	
R2-900	900	85×130×2.86	228	59.3	398.5	374.56	357.53	0.940	0.897	
S-20-1	20	120×120×6	265	31.5	1115.82	1096.15	1092.46	0.982	0.979	[39]
S-200	200	120×120×6	265	31.5	1183.6	1064.22	1051.34	0.899	0.888	
S-300	300	120×120×6	265	31.5	1140	1064.96	1032.97	0.934	0.906	
S-400	400	120×120×6	265	31.5	1190	1069.85	1010.19	0.899	0.849	
S-500	500	120×120×6	265	31.5	1129.9	1041.24	965.87	0.922	0.855	
S-600	600	120×120×6	265	31.5	1016.9	990.25	905.97	0.974	0.891	
S-700	700	120×120×6	265	31.5	850	922.42	833.14	1.085	0.98	
S-800	800	120×120×6	265	31.5	833.33	839.45	747.38	1.007	0.897	
S-900	900	120×120×6	265	31.5	723.2	742.34	648.67	1.026	0.897	
Mean								0.961	0.941	
Standard deviation (SD)								0.052	0.055	
Coefficient of variation (COV)								0.053	0.058	

6.4 CONCLUDING REMARKS

A fiber-based technique has been developed in this chapter to simulate the nonlinear post-fire behavior of concentrically loaded rectangular CFST short columns after being experienced elevated temperatures. The local buckling of steel tubes has been incorporated in the post-fire simulation model. The available nonlinear post-fire stress-strain models for steel and concrete have been used in the computer program. The proposed computer model allows the residual stiffness and strength of fire-damaged CFST columns fabricated by slender, non-compact or compact steel sections in composite buildings to be determined. The model can be used by practicing engineers to assess the post-fire performance of fire-damaged CFST columns.

Chapter 7

CONCLUSIONS

7.1 SUMMARY

The systematic development of computer simulation techniques underlying the theory of fiber element analysis for determining the fire and post-fire responses of rectangular and square CFST short and slender columns loaded axially and eccentrically has been presented in this thesis. Design equations for estimating the initial local and post-local buckling strengths of thin-walled steel sections in eccentrically loaded CFST columns exposed to high temperatures have been proposed. These equations can be employed in numerical models to consider local and post-local buckling effects on the fire and post-fire behavior. The sequentially coupled procedures of nonlinear thermal and stress analysis have been proposed that compute the load-deformation responses and fire resistance of loaded short and slender CFST columns under fire exposure. The computer simulation techniques have incorporated the salient features associated with thin-walled rectangular CFST columns at high temperatures, including local buckling, interaction local-global buckling, air gap between concrete and steel, concrete tensile strength, initial deflection, second order, and deformations caused by preloads. Numerical solution algorithms underlying Müller's method have been programmed to solve highly nonlinear dynamic functions produced in an incremental-iterative analysis process. A nonlinear

post-fire computer model has also been developed, which evaluates the post-fire behavior of axially loaded CFST short columns accounting local buckling influences.

The computer simulation techniques developed have been verified by experimental and numerical solutions available in the published literature. It has been shown that the computational models developed are accurate and efficient computer simulation and design tools for assessing the structural responses of rectangular CFST columns exposed to fire and after fire exposure. These advanced computational technologies can be used by practicing engineers in the structural fire engineering design of CFST columns in steel and composite buildings.

The advantages of the developed fiber-based computational model are its simplicity in mathematical formulation, computational efficiency, and its ability in simulating the interaction behavior of local and global buckling. Its disadvantage is that the equilibrium is maintained only at the column mid-height. The fiber-based computational model proposed has incorporated important features, such as the interaction of local and global buckling, deflections caused by preloads and initial geometric imperfections, which have not been considered in the fiber-based models proposed by other researchers [Lie and Chabot (1990), Lie and Irwin (1995), Han (2001), Yang et al. (2008), and Ibanez et al (2013)]. The fiber-based numerical model developed is computationally more efficient than the 3D finite element models presented by other researchers [Ding and Wing (2008), Espinos et al. (2010), Hong and Varma (2009)].

7.2. ACHIEVEMENTS

This thesis has made remarkable contributions to the field of structural fire engineering.

These significant achievements are summarized as follow:

- (1) Developed design equations for ascertaining the local buckling stresses, post-local buckling strength and effective widths of steel tube walls of rectangular CFST columns exposed to high temperatures. These equations can be employed in inelastic modeling techniques to model gradual local buckling.
- (2) Developed a thermal simulator that calculates the temperature distribution in column cross-sections discretized into fiber elements.
- (3) Developed a fiber-based numerical model for the predictions of the nonlinear fire behavior of rectangular short CFST columns loaded axially at elevated temperatures incorporating local buckling effects.
- (4) Developed a computational modeling technique for ascertaining the fire performance slender rectangular CFST loaded axially under fire exposure accounting for local-global interaction buckling.
- (5) Developed a mathematical model for determining the fire resistance of rectangular CFST slender columns loaded eccentrically with local-global interaction buckling.
- (6) Developed a nonlinear post-fire computer model to study the post-fire performance of rectangular CFST short columns after being exposed to fire.
- (7) Presented numerical results on the fire and post-fire behavior of CFST columns including local and global interaction buckling. These numerical results provide a better understanding of the fire and post-fire behavior of CFST columns.

7.3. FURTHER RESEARCH

This thesis focuses on developing computational techniques for modeling the fire and post-fire behavior of short and slender rectangular CFST columns made of normal strength materials loaded axially and eccentrically. Further studies are recommended as follow:

- (1) The computational models proposed can be extended to CFST rectangular columns made of high strength concrete and steel at high temperatures.
- (2) The research work presented can be extended to study the fire behavior of double-skin rectangular tubular steel sections filled with concrete incorporating the local buckling influence.
- (3) The computer models proposed can be extended to the simulation of fire performance of rectangular CFST columns constructed by fiber-reinforced concrete and rebar-reinforced concrete.
- (4) The mathematical models can be extended to the predictions of fire responses of biaxially loaded rectangular CFST columns.
- (5) Extend the nonlinear post-fire computer procedure to slender rectangular CFST columns.
- (6) The computer models developed can be extended to the simulations of the fire performance of stainless steel rectangular tubular columns filled with concrete at elevated temperatures.

REFERENCES

AIJ (1997) *Recommendations for design and construction of concrete-filled steel tubular structures*, Architectural Institute of Japan, Japan.

AISC360-05 (2005) *Specifications for Structural Steel Buildings*, Chicago.

AISC (2005) *Steel construction manual*, 13th edn, Chicago.

Anderberg, Y. and Thelandersson, S. (1976) Stress and deformation characteristics of concrete, 2-experimental investigation and material behaviour model, *Bulletin 54*, University of Lund, Sweden.

ASTM E119-83 (1985) *American Society for Testing and Materials, Standard Methods of Fire Tests of Building Construction and Materials*, Philadelphia.

ASTM E119 (1988) *American Society for Testing and Materials, Standard Methods of Fire Tests on Building Construction and Materials*, Philadelphia, PA.

Azhari, M. and Bradford, M. A. (1991) Inelastic initial local buckling of plates with and without residual stresses, *Engineering Structures*, 15(1):31-39.

Bedair, O. (2009) Stability of web plates in W-shape columns accounting for flange/web interaction, *Thin-walled Structures*, 47, 768-775.

Bridge, R. Q. (1976) *Concrete Filled Steel Tubular Columns*, Research Report No. R283, School of Civil Engineering, The University of Sydney, Sydney, Australia.

Bridge, R. Q. and O'Shea, M. D. (1998) Behaviour of thin-walled steel box sections with or without internal restraint, *Journal of Constructional Steel Research*, 47(1-2):73-91.

Bulson, P. S. (1970) *The Stability of Flat Plates*, Chatto and Windus, London, England.

CANIULC-SIOI-M89 (1982) *Standard Methods of Fire Endurance Tests of Building Construction and Materials*, Underwriters' Laboratories of Canada, Canada.

Chabot, M. and Lie, T. T. (1992) *Experimental Studies on the Fire Resistance of Hollow Steel Columns Filled with Bar-reinforced Concrete*, IRC Internal Report No. 628, National Research Council of Canada, Institute for Research in Construction, Ottawa, Ontario, Canada.

Cheng, S. L. (2001) *Behaviors of Concrete-Filled Rectangular Steel Tubes Subjected to Axial Compression after High Temperatures*, ME Dissertation, School of Civil Engineering, Harbin Institute of Technology, Harbin, China (in Chinese).

Choi, S. M., Kim, D. K., Kim, J. H., Chung, K. S. and Park, S. H. (2005) Experimental study on fire resistance of concrete-filled steel tube column under constant axial loads, *Steel Structures*, 5(4): 305–313.

Couto, C. Real, P. V., Lopes, N. and Zhao, B. (2014) Effective width method to account for the local buckling of steel thin plates at elevated temperatures, *Thin-Walled Structures*, 84: 134–49.

Dai, X. H. and Lam, D. (2012) Shape effect on the behaviour of axially loaded concrete filled steel tubular stub columns at elevated temperature, *Journal of Construction Steel Research*, 73: 117–27.

Ding, J., and Wang, Y. C. (2008) Realistic modelling of thermal and structural behaviour of unprotected concrete filled tubular columns in fire, *Journal of Constructional Steel Research*, 64: 1086-1102.

Espinós, A., Hospitaler, A. and Romero, M. L. (2009) Fire Resistance of Axially Loaded Slender Concrete Filled Steel Tubular Columns. Development of a Three-Dimensional Numerical Model and Comparison with Eurocode 4, *Acta Polytechnica*, 49(1): 39-43.

Espinós, A., Romero, M. L., and Hospitaler, A. (2010) Advanced model for predicting the fire response of concrete filled tubular columns, *Journal of Constructional Steel Research*, 66(8–9): 1030–1046.

Espinós, A., Romero, M. L., Serra, E. and Hospitaler, A. (2015a) Experimental investigation on the fire behaviour of rectangular and elliptical slender concrete-filled tubular columns, *Thin-walled Structures*, 93: 137-148.

Espinós, A., Romero, M. L., Serra, E. and Hospitaler, A. (2015b) Circular and square slender concrete-filled tubular columns under large eccentricities and fire, *Journal of Constructional Steel Research*, 110: 90-100.

Eurocode 1. 1991-1-2 (2002) *Actions on structures, Part 1.2: General actions- Actions on structures exposed to fire*, CEN, Brussels, Belgium.

Eurocode 4 (1992) *Design of composite steel and concrete structures, part 1.1—General rules and rules for building*, CEN, Brussels, Belgium.

Eurocode 4 (1994) *Design of composite steel and concrete structures, Part 1.2: Structural fire design*, CEN, Brussels, Belgium.

Eurocode 4 (2003), *Part 1.2. Structural fire design. ENV 1994-1-*, London, British Standards Institution, European Committee for Standardization.

Eurocode 2 (2004) *Design of concrete structures, Part 1.2: General rules-structural fire design*, Brussels, Belgium.

Eurocode 4 (2004) *Design of composite steel and concrete structures. Part 1-1, General rules and rules for buildings*, Brussels, Belgium.

Eurocode 3 (2005) *Design of steel structures, Part 1.2: General rules-structural fire design*, CEN, Brussels, Belgium.

Eurocode 4 (2005) *Design of composite steel and concrete structures—part 1–1: general rules and rules for buildings*, Brussels, Belgium.

Furlong, R. W. 1967 Strength of steel-encased concrete beam columns, *Journal of the Structural Division*, ASCE, 93(5), 113-124.

Fujimoto, T., Mukai, A., Nishiyama, I and Sakino, K 2004 Behavior of eccentrically loaded concrete-filled steel tubular columns, *Journal of Structural Engineering*, ASCE, 130(2): 203-212.

Han L. H. (2001) Fire performance of concrete filled steel tubular beam–columns, *Journal of Constructional Steel Research*, 57: 695–709.

Han, L. H. (2002), “Tests on stub columns of concrete-filled RHS sections, *Journal of Constructional Steel Research*, 58(3): 353-372.

Han, L. H. , Chen, F., Liao, F. Y., Tao, Z. and Uy, B. (2013) Fire performance of concrete filled stainless steel tubular columns, *Engineering Structures*, 56: 165–181.

Han, L. H., and Huo, J. S. (2003) Concrete-filled structural steel columns after exposure to ISO-834 fire standard, *Journal of Structural Engineering*, ASCE, 129 (1): 68-78.

Han, L. H., Huo, J. S. and Wang, Y. C. 2005 Compressive and flexural behavior of concrete filled steel tubes after exposure to standard fire, *Journal Construction Steel Research*, 61: 882-901.

Han, L. H., Lam, D. and Nethercot, D. A. (2018) *Design Guide for Concrete-Filled Double Skin Steel Tubular Structures*, Boca Raton and London: CRC Press, Taylor and Francis Group.

Han, L. H. and Yang, Y. F. (2003) Analysis of thin-walled steel RHS columns filled with concrete under long-term sustained loads, *Thin-Walled Structures*, 41 (9): 849–70.

Han, L. H., Yang, H., and Cheng, S. L. (2002) Residual strength of concrete filled RHS stub columns after exposure to high temperatures, *Advances in Structural Engineering*, 5: 123-133.

Han, L. H., Yang, Y. F. and Xu, L. (2003a) An experimental study and calculation on the fire resistance of concrete-filled SHS and RHS columns, *Journal of Constructional Steel Research*, 59: 427-452.

Han, L. H., Zhao, X. L. and Yang, Y. F. (2003b) Experimental study and calculation of fire resistance of concrete-filled hollow steel columns, *Journal of Structures Engineering*, ASCE, 129(3): 346–356.

Heidarpour, A. and Bradford, M. A. (2007) Local buckling and slenderness limits for flange outstands at elevated temperatures, *Journal of Constructional Steel Research*, 63: 591–8.

Hong, S. and Varma, A. H. (2009) Analytical modelling of the standard fire behavior of loaded CFT columns, *Journal of Constructional Steel Research*, 65 (1): 54–69.

Hu, H. T., Huang, C.S., Wu, M. H. and Wu, Y. M. (2003) Nonlinear analysis of axially loaded concrete-filled tube columns with confinement effect, *Journal of Structural Engineering*, ASCE, 129(10): 1322-1329.

Huo J., Huang, G., and Xiao, Y. (2009) Effects of sustained axial load and cooling phase on post-fire behavior of concrete-filled steel tubular stub columns, *Journal of Constructional Steel Research*, 65: 1664-1676.

Ibáñez, UC, Bisby, L., Rush D., Romero, M. L. and Hospitaler, A (2018) Analysis of concrete-filled steel tubular columns after fire exposure *12th International Conference on Advanced in Steel-Concrete Composite Structures*, 795-802.

Ibáñez, U. C., Romero, M and Hospitaler, A (2013) Fiber beam model for fire response simulation of axially loaded concrete filled tubular columns, *Engineering Structures*, 56: 182–193.

ISO (International Standards Organization) (1980) *Fire Resistance Tests, Elements of Building Construction*, Switzerland.

Jiang S.F., Wu, Z. Q., and Niu, D. S. (2010) Experimental study on fire-exposed rectangular concrete-filled steel tubular (CFST) columns subjected to bi-axial force and bending, *Advances in Structural Engineering*, 13: 551-560.

Klöppel, V. K., and Goder, W. (1957) An investigation of the load carrying capacity of concrete filled steel tubes and development of design formula, *Der Stahlbau*, 26(2): 44-50.

Knobloch, M. and Fontana, M. (2006) Strain-based approach to local buckling of steel sections subjected to fire, *Journal of Constructional Steel Research*, 62 (1-2): 44-67,

Knowles, R. B. and Park, R. (1969) Strength of concrete-filled steel tubular columns, *Journal of Structural Division*, ASCE, 95(12): 2565-2587.

Kodur, V. K. R. (1999) Performance-based fire resistance design of concrete-filled steel columns, *Journal of Constructional Steel Research*, 51(1): 21-36.

Kodur, V. K. R. and Lie, T. T. (1995) Fire performance of concrete-filled hollow steel columns, *J. of Fire Prot. Eng.*, 79(3): 89-98.

Kodur, V. and Sultan, M. (2003) Effect of Temperature on Thermal Properties of High-Strength Concrete, *Journal of Materials in Civil Engineering*, 15(2): 101-107.

Kodur V. K. R., Wang T. C., Cheng F. R. (2004) Predicting the fire resistance behavior of high strength concrete columns, *Cement and Concrete Composites*, 26: 141–53.

Li, G., Chen, B., Yang, Z. and Feng, Y. (2018) Experimental and numerical behaviour of eccentrically loaded high strength, *Thin-Walled Structures*, 127: 483-499.

Li, W. and Guo, Z .H. (1993) Experimental investigation of strength and deformation of concrete at elevated temperature, *China Journal of Building Structures*, 14 (1): 8-16. (in Chinese)

Liang, Q. Q. (2009a) Performance-based analysis of concrete-filled steel tubular beam–columns, Part I: Theory and algorithms, *Journal of Constructional Steel Research*, 65(2): 363-372.

Liang, Q. Q. (2009b) Performance-based analysis of concrete-filled steel tubular beam–columns, Part II: Verification and applications, *Journal of Constructional Steel Research*, 65(2): 351-362.

Liang, Q. Q. (2011a) High strength circular concrete-filled steel tubular slender beam columns, Part I: Numerical analysis, *Journal of Constructional Steel Research*, 67(2): 164-171.

Liang, Q. Q. (2011b) High strength circular concrete-filled steel tubular slender beam-columns, Part II: Fundamental behavior, *Journal of Constructional Steel Research*, 67(2): 172-180.

Liang, Q. Q. (2014) *Analysis and Design of Steel and Composite Structures*, Boca Raton and London: CRC Press, Taylor and Francis Group.

Liang, Q. Q., Patel, V. I. and Hadi, M. N. S. (2012) Biaxially loaded high-strength concrete-filled steel tubular slender beam-columns, Part I: Multiscale simulation, *Journal of Constructional Steel Research*, 75: 64–71.

Liang, Q. Q. and Uy, B. (1998) Parametric study on the structural behaviour of steel plates in concrete-filled fabricated thin-walled box columns, *Advances in Structural Engineering*, 2(1): 57-71.

Liang, Q. Q. and Uy, B. ((2000)) Theoretical study on the post-local buckling of steel plates in concrete-filled box columns, *Computers and Structures*, 75(5): 479-490.

Liang, Q. Q., Uy, B. and Liew, J. Y. R. (2006) Nonlinear analysis of concrete-filled thin-walled steel box columns with local buckling effects, *Journal of Constructional Steel Research*, 62(6): 581-591.

Liang, Q. Q., Uy, B. and Liew, J. Y. R. (2007) Local buckling of steel plates in concrete-filled thin-walled steel tubular beam-columns, *Journal of Constructional Steel Research*, 63(3): 396-405.

Liang, Q. Q., Uy, B., Wright, H. D. and Bradford, M. A. (2004) Local buckling of steel plates in double skin composite panels under biaxial compression and shear, *Journal of Structural Engineering*, ASCE, 130 (3): 443-451.

Lie, T. T. (1984) A procedure to calculate fire resistance of structural members, *Fire and Materials*, 8(1): 40–48.

Lie, T. T. (1992) *Structural fire protection Manual and reports on engineering practice*, ASCE, vol. 78, New York.

Lie, T. T. (1994) Fire resistance of circular steel columns filled with bar-reinforced concrete, *Journal of Structural Engineering*, ASCE, 120(5): 1489–1509.

Lie, T. T. and Chabot, M. (1990) A method to predict the fire resistance of circular concrete filled hollow steel columns, *Journal of Fire Protective Engineering*, 2(4): 111–126.

Lie, T. T. and Chabot, M (1992) *Experimental studies on the fire resistance of hollow steel columns filled with plain concret*, Internal report No. 611. Ottawa, Canada: Institute for Research in Construction, National Research Council of Canada (NRCC).

Lie, T. T. and Irwin, R. J. (1995) Fire resistance of rectangular steel columns filled with bar-reinforced concrete, *Journal of Structural Engineering*, ASCE, 121(5): 797–805.

Lie, T. T. and Stringer, D. C. (1994) Calculation of the fire resistance of steel hollow structural section columns filled with plain concrete, *Canadian Journal of Civil Engineering*, 21(3): 382-385.

Liew, J. Y. R. and Xiong, M. X. (2015) *Design Guide for Concrete Filled Tubular Members with High Strength Materials to Eurocode 4*, Singapore: Research Publishing.

Liu, D. (2006) Behaviour of eccentrically loaded high-strength rectangular concrete filled steel tubular columns, *Journal of Constructional Steel Research*, 62(8): 839-846.

Liu, F., Gardner, L. and Yang, H. (2014) Post-fire behaviour of reinforced concrete stub columns confined by circular steel tubes, *Journal of Constructional Steel Research*, 102: 82-103.

Liu, F., Yang, H. and Gardner, L. (2016) Post-fire behaviour of eccentrically loaded reinforced concrete columns confined by circular steel tubes, *Journal of Constructional Steel Research*, 122: 495-510.

Lu, H, Zhao, X. L. and Han, L. H. (2009) Fire behaviour of high strength self-consolidating concrete filled steel tubular stub columns *Journal of Constructional Steel Research*, 65(10–11): 1995-2010.

Lue, D, Liu, J.-L. and Yen, T. (2007) Experimental study on rectangular CFT columns with high-strength concrete, *Journal of Constructional Steel Research*, 63: 37-44.

O'Shea, M. D. and Bridge, R. Q. (2000) Design of circular thin-walled concrete filled steel tubes, *Journal of structural engineering*, ASCE, 126(11): 1295-1303.

Park, S., Choi, S., and Chung, K. (2008) A study on the fire-resistance of concrete-filled steel square tube columns without fire protection under constant central axial loads, *Steel and composite Structures*, 8(6): 491-510.

Patel, V. I., Liang Q. Q. and Hadi M. N. S. (2012a) High strength thin-walled rectangular concrete filled steel tubular slender beam-columns, Part I: Modelling, *Journal of Constructional Steel Research*, 70: 377–384.

Patel, V. I., Liang, Q. Q. and Hadi, M. N. S. (2012b) High strength thin-walled rectangular concrete-filled steel tubular slender beam-columns, Part II: Behavior, *Journal of Constructional Steel Research*, 70: 368–376.

Patel, V. I., Liang, Q. Q. and Hadi, M. N. S. (2015a) *Nonlinear Analysis of Concrete-Filled Steel Tubular Columns*, Germany: Scholar's Press.

Patel, V. I., Liang, Q. Q. and Hadi, M. N. S. (2015b) Biaxially loaded high-strength concrete-filled steel tubular slender beam-columns, Part II: Parametric study, *Journal of Constructional Steel Research*, 110: 200–207.

Patel, V. I., Liang, Q. Q. and Hadi, M. N. S. (2018) *Concrete-Filled Stainless Steel Tubular Columns*, Boca Raton and London: CRC Press, Taylor and Francis Group.

Qu, X., Chen, Z. and Sun, G. (2013) Experimental study of rectangular CFST columns subjected to eccentric loading, *Thin-Walled Structures*, 64: 83–93.

Quiel, S. E. and Garlock, M. E. M. (2010) Calculating the buckling strength of steel plates exposed to fire, *Thin-Walled Structural*, 48: 684–95.

Ragheb, W. (2010) Local buckling analysis of pultruded FRP structural shapes subjected to eccentric compression, *Thin-Walled Structures*, 48: 709-717.

Ragheb, W. (2015) Local buckling of welded steel I-beams considering flange–web interaction, *Thin-Walled Structures*, 97: 241-249.

Ragheb, W. (2016) Estimating the local buckling capacity of structural steel I-section columns at elevated temperatures, *Thin-Walled Structures*, 107: 18-27.

Rodrigues, J. P. and Laím, L. (2017) Fire resistance of restrained composite columns made of concrete filled hollow sections, *Journal of Constructional Steel Research*, 133: 65-76.

Romero, M. L., Moliner, V., Espinós, A., Ibañez, C. and Hospitaler, A. (2011) Fire behavior of axially loaded slender high strength concrete-filled tubular columns, *Journal of Constructional Steel Research*, 67(12): 1953-1965.

Rush, D., Bisby, L. A., Jowsey, A. and Lane, B. (2015) Residual capacity of fire-exposed concrete-filled steel hollow section columns, *Engineering Structures*, 100: 550-563.

Sakumoto, Y., Okada, T., Yoshida, M. and Tasaka, S. (1994) Fire Resistance of Concrete-Filled, Fire-Resistant Steel-Tube Columns, *Journal of Materials in Civil Engineering*, 6(2): 169-184.

Schaumann, P., Kodur, V. and Bahr, O. (2009) Fire behaviour of hollow structural section steel columns filled with high strength concrete, *Journal of Constructional Steel Research*, 65: 1794-1802.

Schneider, S.P. (1998) Axially loaded concrete-filled steel tubes, *Journal of Structural Engineering*, ASCE, 124(10): 1125-1138.

Shakir-Khalil, H. and Mouli, M. (1990) Further Tests on Concrete-Filled Rectangular Hollow-Section Columns, *The Structural Engineer*, 68(20): 405-413.

Shakir-Khalil, H. and Zeghiche, J. (1989) Experimental behavior of concrete-filled rolled rectangular hollow-section columns, *The Structural Engineer*, 67(3): 346-53.

Song, T. Y., Han, L. H. and Yu, H. X. (2010) Concrete filled steel tube stub columns under combined temperature and loading, *Journal of Constructional Steel Research*, 66: 369-384.

Tao, Z., Ghannam, M., Song, T. and Han, L. H. (2016) Experimental and numerical investigation of concrete-filled stainless steel columns exposed to fire, *Journal of Constructional Steel Research*, 118: 120-134.

Tao, Z., Uy, B., Han, L. H. and Wang, Z. B. (2009) Analysis and design of concrete-filled stiffened thin-walled steel tubular columns under axial compression, *Thin-Walled Structures*, 47: 1544-1556.

Tao, Z., Uy, B., Liao, F. Y. and Han, L. H. (2011) Nonlinear analysis of concrete-filled square stainless steel stub columns under axial compression, *Journal of Constructional Steel Research*, 67: 1719-1732.

Timoshenko, S. and Gere, J. (1963) *Theory of Elastic Stability*, 2nd Edition, New York: McGraw-Hill.

Usami, T. 1982 post-buckling of plates in compression and bending, *Journal of the Structural Division*, ASCE, 108(3): 591-609.

Usami, T. (1993) Effective width of locally buckled plates in compression and bending, *Journal of Structural Engineering*, ASCE, 119(5): 1358-1373.

Uy, B., (2000) Strength of concrete filled steel box columns incorporating local buckling, *Journal of Structural Engineering*, ASCE, 126(3): 341-352.

Vrcelj, Z. and Uy, B. (2002) Strength of slender concrete-filled steel box columns incorporating local buckling, *Journal of Constructional Steel Research*, 58(2): 275-300.

Wang, Y. C. (2002) *Steel and Composite Structures: Behaviour and design for fire safety*, London: Spon Press.

Wang, Y. C. and Kodur, V. R. (1999) An approach for calculating the failure loads of unprotected concrete, *Structural Engineering and Mechanics*, 7(2): 127-145.

Wang, X. Q., Tao, Z., Song, T. Y. and Han, L. H. (2014) Stress-strain model of austenitic stainless steel after exposure to elevated temperatures, *Journal of Constructional Steel Research*, 99: 129-139.

Wang, K. and Yong, B. (2013) Fire resistance of concrete-filled high strength steel tubular columns, *Thin-Walled Structures*, 71: 46-56.

Wright, H. (1993) Buckling of plates in contact with a rigid medium, *The Structural Engineer*, 71(12): 209-215.

Wright, H. D. (1994) Local Buckling of Filled Sections, *International Specialty Conference on Cold Formed Steel Structures, 12th International Specialty Conference on Cold-Formed Steel Structures*, 421-436.

Yang, H., Han, .L H. and Wang, Y. C. (2008) Effects of heating and loading histories on post-fire cooling behaviour of concrete-filled steel tubular columns, *Journal of Constructional Steel Research*, 64(5): 556-570.

Yang, Y. F, Zhang, L. and Dai, X. (2017) Performance of recycled aggregate concrete-filled square steel tubular columns exposed to fire, *Advances in Structural Engineering*, 20(9): 1340-1356.

Yao, Y. and Hu X. X. (2015) Cooling behavior and residual strength of post-fire concrete filled steel tubular columns, *Journal of Constructional Steel Research*, 112: 282-292.

Yao, Y., Li, H. , Hongcun, G and Tan, KH (2016) Fire resistance of eccentrically loaded slender concrete-filled steel tubular columns, *Thin-Walled Structures*, 106: 102-112.

Yin, J., Zha, X. X. and Li, L. Y. (2006) Fire resistance of axially loaded concrete filled steel tube columns, *Journal of Constructional Steel Research*, 62: 723-729.

Zhang, S., Guo, L. and Tian, H. (2003) Eccentrically loaded high strength concrete filled square steel tubes, *Proceedings of the International Conference on Advances in Structures, Sydney, Australia*, 2, 987-993.

Zhao, X.-L., Han, L.-H. and Lu, H. (2010) *Concrete-Filled Tubular Members and Connections*, London and New York: Spon Press, Taylor and Francis Group.